DEVELOPMENT OF HEMP FABRIC REINFORCED COMPOSITES

A thesis submitted by

Mohd Iqbal Misnon

For the award of

DOCTOR OF PHILOSOPHY

University of Southern Queensland
Faculty of Health, Engineering and Sciences
School of Mechanical and Electrical Engineering

Australia
2016

Abstract

One of the activities producing a destructive impact on the environment is uncontrolled or illegal timber harvesting. It is a response to high market demand due to the modernisation of lifestyles. The awareness of world's population of the global environmental problems related to this issue has increased the popularity of natural fibre reinforced composites. Its availability and the data available on its properties tend to provide assurance for its application in many fields. The main objective of this project is to develop material using woven hemp fabric (WHF) and vinyl ester resin as a potential alternative to the utilisation of woods or engineered wood products. Apart from the composite development, fire retardant, water absorption and fatigue properties of the WHF reinforced composite are investigated.

Some characterisations of the fabric properties were undertaken to verify the data given by the supplier as well as to collect more data about the fabric since the data given by the supplier is usually more general and inadequate for technical purposes. Investigation was done on the properties of two batches of a similar nominal quality which were obtained within a three month time interval. The weight of fabric was found to be lower than what was provided by the supplier. Other properties measured were fabric densities, yarn sizes, yarn crimp percentage, cloth cover factors, chemical composition, thermal properties as well as fabric strength. It was concluded that the properties of the two batches are most likely not only identical from a textile point of view, but are also similar from an engineering point of view. Characterisation on the composite made of WHF with different layering orientations and vinyl ester (HVE) were found to have consistent density and fibre volume fraction due to properties of WHF. In terms of tensile, flexural and impact properties, depending on the layer orientation, their properties were slightly different. Inferential statistical analysis confirmed layering orientation affected the mechanical properties of the fabricated composite. Nevertheless, the differences among them less than 10% which suggests that any layering of this fabric can be used for composite fabrication. The properties of fabricated composites were comparable to some wood and engineered wood product. However, their densities were found to be higher than those of woods.

When the WHFs were treated with sodium hydroxide (NaOH), fire retardant chemical (FR) and combination of both (NaOH+FR), their densities and shrinkage properties increased due to the swollen fibres. The fire retardant properties of treated fabric also increased and this were proven by the burning, themogravimetry analysis and limiting oxygen index tests. However, all the treatments decreased the mechanical strength of WHFs. All these treated fabric were then utilised to reinforce vinyl ester using $[0, 90]_{10}$ layering orientation. The changes in the WHFs's physical properties increased the density (ranging from 1.1 to 1.21g/cm^3) and fibre volume fraction (ranging from 33 to 37.12%) of HVEs. Although the mechanical properties of HVEs made of treated WHFs were found to be decreased due to poor adhesion between hemp fibres and vinyl ester, they are still comparable to woods and engineered wood products. The improvements in fire retardant properties for treated fabrics were also proven to enhance their HVEs' fire retardant properties. HVE made of WHF treated with FR was found to be the best against the fire and its mechanical properties were still suitable for use as an alternative to woods and engineered wood products. This kind of HVE was then used to analyse it degradation properties (mechanical and fire retardant properties) when subjected to water absorption.

In terms of HVEs' water absorption properties, the maximum water uptake and time to reach saturation point were 3.27% and 552 hr respectively. The diffusion coefficient calculated using Fick's law, which is 4.71E-06 mm^2/s and this was found lower than wood products. In terms of mechanical properties, the presence of water reduced the tensile strength and modulus up to 24% and 39% respectively due to the penetration of water which weakened the adhesion between the fibres and resin. The flexural properties was increased after 2688 hr of water immersion due to the swollen fibres which is attributed to high amount of water infiltration thus fill the gaps between the fibre and the matrix. The presence of water also degraded its fire retardant performance. It was found that the durability or fastness of fire retardant chemical treatment on this HVE composite was between 168 hr and 840 hr of water immersion. In terms of fatigue properties, the fatigue strength coefficient, b, was found to be 0.12 and these HVEs were tested under low load cycle with higher stress level ranging from 50% up to 80%. As suggested by other worker, the safety limits for sample HVE-UT (untreated WHF) and HVE-FR (FR treated WHF) are defined to be 30 and 24MPa respectively.

At the end of this study, a ‘material selection guide’ was established for the use by relevant stake holders when producing WHF reinforced vinyl ester. This selection guide is important which can be related in many ways such as in product life cycle, determination of cost/energy, identification of suitable application etc.

Certification of Thesis

I certify that the ideas, experimental work, results, analysis and conclusions reported in this dissertation are entirely my own effort, except where otherwise acknowledged. I also certify that the work is original and has not been previously submitted for any award, except where otherwise acknowledged.

---------- / /

Signature of Candidate

Endorsed:

---------- / / ---------- / /

Signature of Supervisor/s Signature of Supervisor/s

---------- / / ---------- / /

Signature of Supervisor/s Signature of Supervisor/s

Acknowledgements

First of all, I would like to express my deepest gratitude to the Ministry of Higher Education, Malaysia for providing me with a scholarships to carry out this study. The financial support from this organisation is very much appreciated. I am also thankful to Universiti Teknologi MARA, Malaysia for providing a family allowance. Without the allowance, it might have been difficult for me and my family to live peacefully here in Toowoomba.

Many thanks are also extended to my principal supervisor, Dr. Mainul Islam for his valuable ideas, advice, comments and encouragement. His effort in ensuring this study is completed in a reasonable time is appreciated. I would also like to extend my gratitude to all my associate supervisors, Dr. Jayantha Epaarachchi, Prof. Hao Wang and Prof. Kin Tak Lau for their suggestions and support in filling the gaps throughout this study.

I want to thank Ms. Sandra Cochrane for her critique and proofreading. Special thanks are also due to Mr. Wayne Cornell and Mr. Martin Geach, technical and laboratory assistants, CEEFC, University of Southern Queensland, Australia for their kindness in providing instruments, technical advice and information during my experimental and laboratory work.

Finally, my sincere gratitude is due to my wife, Amilin Abdul Jalil and my children Insyirah, Isaura and Iril Muhammad for their patience and support. This study might not be as it is today without their continuous encouragement. Also to my parents and parents in law for their continuous prayers for me. Thanks are also due to all of my friends and those who are directly or indirectly related to this study.

Associated Publications

Journals

Misnon M.I., Islam M.M., Epaarachchi J.A., Lau K.T. Analyses of woven hemp fabric characteristics for composite reinforcement. Materials and Design. 2015;66, Part A:82-92. (This paper has won **"USQ Publication Excellence Award"** during the period July – September 2014).

Misnon MI, Islam MM, Epaarachchi JA, Lau K.T. Potentiality of utilising natural textile materials for engineering composites applications. Materials and Design. 2014;59:359-68. (This paper has won **"USQ Publication Excellence Award"** during the period January – March 2015).

Misnon M.I., Islam M.M., Epaarachchi J.A., Lau K.T. Fabric Parameter Effect on the Mechanical Properties of Woven Hemp Fabric Reinforced Composites as an Alternative to Wood Products. Journal of Industrial Textile (*Under review*).

Misnon M.I., Islam M.M., Epaarachchi J.A., Chen H., Wang H., Lau K.T. Flammability Characteristics of Chemical Treated Woven Hemp Fabric. Fire and Materials (*Under review*).

Misnon M.I., Islam M.M., Epaarachchi J.A., Chen H., Wang H., Lau K.T. (*In progress*). Flammability Characteristics of Chemical Treated Woven Hemp Fabric Reinforced Vinyl Ester Composites. Journal of Composite Materials (*Under review*).

Refereed Conference Proceedings

Misnon M. I., Islam M. M., and Epaarachchi J., and Lau K.T., (2013). Textile Material Forms for Reinforcement Materials: A Review. In: 3rd Malaysian Postgraduate Conference (MPC 2013), 4-5 Jul 2013, Sydney, Australia.

Misnon M.I., Islam M.M., Epaarachchi J. and Lau, K.T., (2014) Selection of Hemp Fabric as Reinforcement in Composite Materials. In: 3rd International Conference on Mechanical, Industrial and Energy Engineering (ICMIEE 2014), 26-27 Dec 2014, Khulna, Bangladesh.

Misnon M.I., Islam M.M., Epaarachchi J.A., Chen H, Wang H., (2016) Woven Hemp Fabric Reinforced Vinyl Ester Composite Treated With Fire Retardant. In: 44th International Conferences on Metallurgy Technology and Materials (ICMTM 2016), 13-14 May 2016, Auckland, New Zealand.

Misnon M.I., Islam M.M., Epaarachchi J.A., Wang H., Lau K.T., (2016) Woven Hemp Fabric Reinforced Vinyl Ester Composite: Effect of Water Absorption on the Mechanical Properties Degradation. In: 44th International Conferences on Metallurgy Technology and Materials (ICMTM 2016), 13-14 May 2016, Auckland, New Zealand.

Table of Contents

List of Figures

List of Tables

Chapter 1 Introduction

1.1 Background

Recently, in some developing countries, the issues surrounding uncontrolled or illegal timber harvesting and logging have become more serious [1, 2]. This situation will have a destructive impact on the environment in the long run because of an imbalance between harvesting and cultivating trees. The reason that leads to these circumstances is the high demand for particular kinds of wood-based material due to the modernisation of living quality without considering the volume of high-value timber in the forest [2, 3]. For example, the demand of rainforest products in a developing country such as Malaysia can be seen in Figure 1.1. A total of RM 10.5 billion (approximately AU$ 3.46 billion) worth of wood products was exported abroad in just a half year of 2015 (January-June) only and a similar trend can be observed in 2014 [4]. These trends will keep growing or at least stagnant in the future, and Malaysian's timber deposit is depleting due to the high demand for wood products. Replanting is the most common method used to replace trees however, it takes several decades to yield high-quality timber before it can be harvested again.

Malaysia exports timber for international demand while importing timber products for domestic utilization. Most of the wood products imported are used in building infrastructure construction and these include wooden furniture, chipboard, fibreboard and plywood (Figure 1.2). A total of RM 1.6 billion (approximately AU$ 0.53 billion) were spent to import timber products from overseas in 2015 (January-June only) and this is a significant amount for something that could be produced domestically [4]. Based on the two figures, something has to be done to reduce the logging (or timber harvesting) in order to preserve the rainforest before its loss affects the environment.

Research and development of new material should be increased and strengthened to replace wood based products and this will generate new businesses and create more jobs thus enhancing Malaysia's economy. This will also create healthier circumstances which lead to more control over logging activities thus saving more timber deposits and reducing the risk of negative environmental effects. Another benefit that comes from this shift is that the country could reduce the imports because there will be a strong supply of non-load bearing material (bio-based composite) that could satisfy the local demand and at the same time, provide bio-based composite products to replace wood based products.

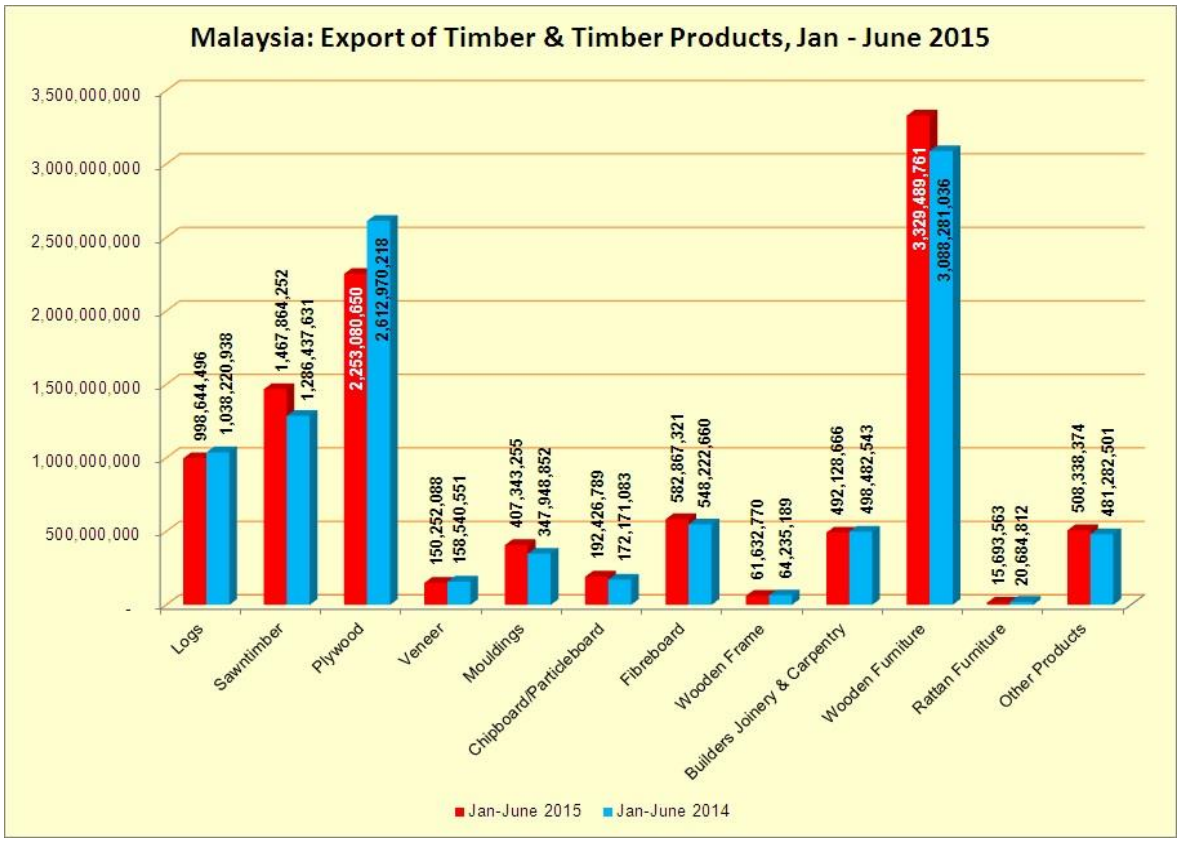

*Currency - RM (Ringgit Malaysia); (1 RM = Approximately 0.33 AUD)

Figure 1.1 The export of timber products in Malaysia in 2015 [4].

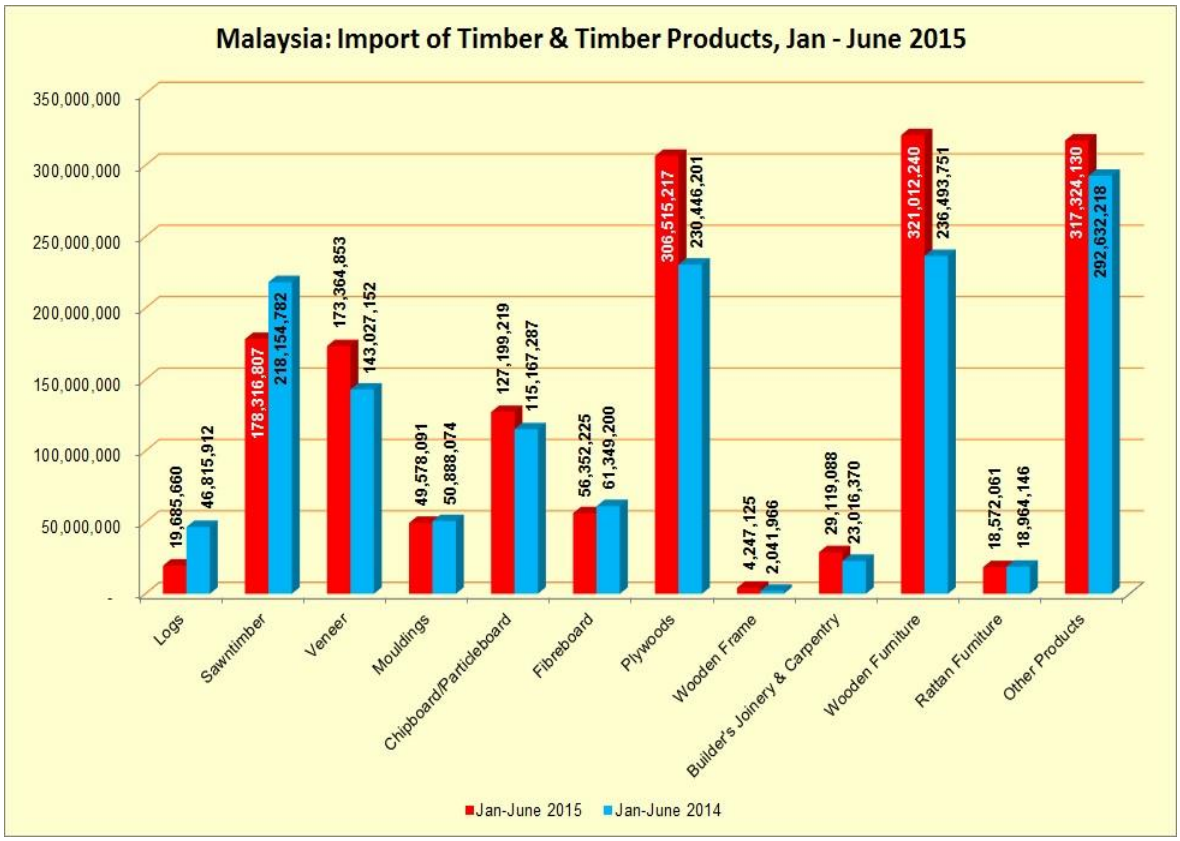

Figure 1.2 The import of timber products in Malaysia from January to June 2015 [4].

Therefore, there is an urgent need for new material to reduce or replace the utilization of wood-based products, enhance the preservation of timber and contribute to a new sector within the national country. Related to these issues, are efforts to search for new high-performance materials at affordable costs focused on developing, creating and innovating eco-friendly materials. This effort began at least 30 years ago and since then it has been categorized as bio-based composites [5-8]. The motivation for bio-based composites development is not only about uncontrolled timber harvesting, but also the drawbacks possessed by traditional composite materials which are high cost, non-recyclable, non-biodegradable, require high energy consumption and over performance. On the other hand, natural fibres offer advantages such as low cost, low density, light weight, renewable, flexible during processing, highly specific stiffness

and biodegradable. Furthermore, up until now, its availability and the data available on its properties tend to provide assurance for this natural fibre to be used in many fields [9].

One of the fields where bio-based composite can be used is civil infrastructure especially in non-load bearing applications. The growth of the world's population has led to an increased need for housing, and this situation has led to increasing cost in housing material [10]. Therefore, the utilisation of bio-based composites as housing materials could reduce the cost of house construction. Particleboard, fibreboard and plywood are all materials used for non-load bearing applications in the housing industry. Particleboard and fibreboard are commonly used for furniture such as cupboards, table tops, wardrobes etc. while plywood is more versatile and can be applied in many fields such as aircraft, marine and building/housing. They are also in the class of bio-based composite but the main resource of these materials is wood or timber, thus they are called reengineered wood products. The advantages possessed by bio-based composite seemingly overwhelm reengineered wood products [11, 12].

1.2 Natural Fibres

Natural fibres can be clustered into their physical forms which are fibre, yarn and fabric. Much work addresses the use of fibre forms as reinforcement for composite material. Flax, jute, sisal and hemp fibres are types of well-known fibres used due to their long existence and the application of extraction methods which are almost prefect. The fibres that are used for composites are clean and fine [5, 13-21]. That is why they can be found not only in fibre but also in yarn and fabric forms. Whereas coir, kenaf and baggase are kind of new fibres and need research on their extraction focusing on fibre fineness and cleanliness [22-24]. One of the real challenges of using

fibre forms is dealing with the dispersion and distribution of fibres which are difficult to control. This limits the producers or manufacturer to design the material properties using established fabrication method such as resin transfer moulding and vacuum infusion.

Unlike fibre, yarn can give more control to fibre distribution, at least in one longitudinal direction. Several works on using natural yarn particularly flax, jute and hemp showed good mechanical properties for composite material [25-30]. Nevertheless, yarn is always utilised in producing circular and hollow composites and this is due the limitation on fabrication method. The established method for producing composite using yarn form is filament winding. Some other works try to use other methods by winding this yarn onto a metal plate which imitates filament winding technique to produce flat material. However, this method is difficult to apply for the production of bigger panel sizes and usually perform well in longitudinal but not in transverse direction.

There are numerous works reported on using fabrics as reinforcement material, especially high performance fabrics such as carbon, glass and aramid. These are the most preferred form of reinforcement material because they are easy to handle and it have good dimensional stability which is very important during composite fabrication [31, 32]. All fibres in the fabric are designed according to specific arrangement and alignment (known as fabric structure), hence the fibres are interconnected with each other and create some kind of synergistic effect. Thus, by looking at fabric contribution, neither fibre nor yarn reinforcement can surpass fabric reinforcement in terms of overall performances (the most isotropic can be achieved) [31, 32].

Textile fabric form can be the most suitable material from which to fabricate composites for replacing material such as particleboard, fibreboard and plywood for several reasons. The homogenous distribution of fibre can be achieved because the fibre is fabricated in accordance with designed fabric structure. This makes the utilisation of this reinforcement easy to handle due to good dimensional stability during composite manufacture. Fabric is manufactured using either a weaving loom, knitting or nonwoven machine and this allows the fabric to be produced at least 114 inches in width by the desired length. Some machines can manufacture fabric up to 250 cm and this fabric is quite promising in producing bigger sized composites. It is more justifiable to use natural textile fabric composite as an alternative material for plywood and particleboard. Compared with wood based products, using natural textile fabric can produce thinner products at similar cost with improved properties.

1.3 Problem Statement

Utilization of traditional high-performance reinforcement is preferred in fabric form rather than fibre and yarn [31-34]. Apart from this, it is easier to handle and could maintain its dimensional stability during the composite fabrication, the distribution of fibres in a specific area covered by fabric, which is far more consistent as compared to fibre and yarn forms. As far as natural fibre is concerned, there are only several types of natural fibre that can be found in fabric form and these include jute, flax, ramie, hemp and recently, bamboo.

Hemp is a type of natural fibre in use for a very long time and is very well known in the textile industry. It is one of the primary materials in the production of heavy and medium-weight fabric in linen production. Based on the literature, there are a number of works on hemp fibre as reinforcement in composite material. The properties of this

material, especially hemp reinforced composites, are varied according to the different fibre forms, fibre volume fraction, chemical treatment, resin types and fabrication methods [20, 21, 27, 28, 33, 35-38]. Only by utilising fabric forms, overall performance of a bio-based composite can be achieved because fabric is easier to handle and can maintain its dimensional stability during the composite fabrication [32, 33, 39].

Nevertheless, when utilising natural textile fabric, most works only discusses fibre volume fraction as the important property that contributes to composite material. Work undertaken by Christian and Billington [35] and Song et al. [33] which use hemp fabric in their composites have proved that the fabric properties (density and weave structure of fabrics) do influence the properties of composite materials. Therefore, there is less work discussed on other properties such as fabric density, fabric weight, fabric's yarn crimp, yarn linear density and fabric strength that might affect composite properties and behaviour. This is because the properties and characteristic of a hemp fabric are not well determined. Therefore, fabric properties should be determined in order to understand why a fabricated composite behaves in the ways that it does.

Enhancing the compatibility between reinforcement and matrix can be done using chemical treatment. However, utilising chemical treatment on the materials will increase the cost of production. Except if the chemical treatment is necessary to improve certain properties of material for certain applications, it would be wise just to apply basic chemical treatment in the fabrications. A study by Kabir et al. [36] showed that alkalisation treatment is good enough to produce a material with acceptable quality and any post-treatment with acetylation and siloxane tends to reduce material properties. More importantly, any treatment applied to a bio-based composite should

be fire retardant as, unlike high performance reinforcements, natural reinforcement is flammable in nature. Recent works proved the enhancement of fire retardant bio-based composite by incorporating fire retardant treatment in the composite fabrication process. However, so far less work has applied fire retardant directly to the reinforcement material, particularly to hemp fabric.

The moisture and water absorption properties of material are important criteria for defining materials' durability. Works by Dhakal et al. [38], Ramezani Kakroodi et al. [40] and Christian and Billington [41] showed that the water and moisture absorption behaviours of hemp fibre composites are different based on the surrounding temperatures. However, one common thing is that the mechanical properties of hemp fibre composites decreased with the presence of water or moistures. It is believe that the fastness of fire retardant treatment will be degraded as water or moisture penetrates into the composite. Nevertheless, no work has studied the effect of water or moisture presence on the fastness of fire retardant treatment for the hemp fibre composite.

Fatigue behaviour is another criterion that can be used to define the durability of material. Non-woven hemp fabric is proven to have fatigue properties comparable with glass fibre composite [42]. Alkali treatment to the non-woven fabric doest enhance the fatigue properties of the non-woven fabric composite [43]. Work by Shah et al. [44] provides very extensive knowledge on the fatigue behaviour of natural fibre composite with regard to types of fibre, fibre volume fraction, textile architecture and stress ratio. However, his study was limited only to yarn and roving form reinforcements. A study by de Vasconcellos et al. [45] emphasised the effect of fibre loading orientation on the fatigue behaviour of hemp fabric composites. Based on the literature review, there is still lack of knowledge about the fatigue behaviour of treated hemp fabric composites

especially on the effect of fire retardant and alkalisation treatment on the fatigue behaviour of woven hemp fabric composite.

1.4 Research Question

Bio-based composite can be used as a non-load bearing and infrastructure material. In terms of mechanical properties, it is comparable with wood and engineered wood products. However, there remains a lack of knowledge regarding its performance over time, especially in utilising hemp fabric as reinforcement. A bio-based composite should be fully explored before it is used in the infrastructure field. The criteria highlighted by Dittenber and GangaRao [10] can be used as guidance to develop and design new material for replacing wood and engineered wood products.

Based on the discussion in the previous section, there are gaps in current knowledge. This study aims to address the following research questions:

1. How the hemp fabric properties (e.g. yarn size, yarn crimp, fabric density, fabric weight, fabric strength etc.) can influence the hemp fabric composite?

2. How the fire retardant treated woven hemp fabric affects the fire retardant performance of the composites?

3. What is the effect of water absorption on the mechanical and fire retardant performances the composite?

1.5 Objectives

The main objective of this research is to develop material as a potential alternative to the utilisation of wood-based or engineered wood products. Apart from the composite development, fire retardant, water absorption and fatigue properties of the hemp fabric

reinforced composite will be investigated. Also, the possibility of applying this material as an infrastructure product will be explored. Towards achieving the above primary objective, the related aims associated with it are identified as follows:

1. To characterise the woven hemp fabric properties (e.g. yarn size, yarn crimp, fabric density, fabric weight, fabric strength, etc.) to relate with the woven hemp fabric composite properties
2. To characterise the properties of woven hemp fabric composite with different layer orientation to analyse its suitability as a potential infrastructure material
3. To characterize the effect of fire retardant treatments on the woven hemp fabric and its composites
4. To examine the degradability of woven hemp fabric composites with respect to water absorption and the fatigue loading as part of identifying material selection guidelines.

1.6 Structure of the Dissertation

This dissertation consists of eight chapters. A brief outline for each chapter is given as follows:

Chapter 1 Provides a background of the study, the statement of the problem as well as the objectives of this research.

Chapter 2 Literature review on the natural fibre composites.

Chapter 3 Characterisation of woven hemp fabric properties.

Chapter 4 Characterisation of woven hemp fabric composite properties.

Chapter 5 Improvement of fire retardant properties on woven hemp fabric for composite applications .

Chapter 6 Mechanical and fire retardant properties of woven hemp fabric composites

Chapter 7 Degradability of woven hemp fabric composite with respect to water absorption and fatigue loading.

Chapter 8 Conclusions which can be drawn from this research and recommendation for future research.

Chapter 2 Literature Review

2.1 Composite Materials

Composite can be defined in different ways. Akovali and Uyanik [31] defined composite as a combination of two or more distinctive components in composition on a macroscale, with two or more different phases having recognisable interfaces between them. While Britnell et al. [46], defined composite as a material that contains

a chemically and/or physically distinct phase distributed within another continuous phase and exhibits properties that are different from both of these and Rowell [47], defined a composite as a reconstituted product made from a combination of two or more substances using some kind of mastic to hold the components together. All the definitions established the existence of two major substances, reinforcement and matrix parts which have specific internal and external structures to achieve unique mechanical properties and superior performance characteristics that are not possible with any of the component materials alone.

Bio-based composite is another term of composite material which utilises, partly or fully a natural substance in the composite system. This kind of material has gained most popularity due to the growing awareness of world's population of global environmental issues [5, 48, 49]. Therefore, bio-based composite can be defined as materials formed by a combination of matrix (resin) and fibres, in which the fibres are mainly formed by natural fibres normally originating from plants [46, 50].

The application of textile materials for composite reinforcement is not new. There are several definitions that to acknowledge the existence of this reinforcement material in the composite materials. Scardino [32] defined the textile composite as a combination of textile fibre, yarn, or fabric embedded in a resin system and Long [51] defined a textile composite as a material that is composed of textile reinforcements combined with binding matrix (usually polymeric). The definition, especially by Long [51] is very general considering the large family of materials used for various applications within a number of industrial sectors. Textile composite can be created in the form of flexible or quite rigid materials. Examples of flexible composite are tyres or conveyor belts, while inflexible textile composite are found in a variety of products and

sometimes referred to as a fibre reinforced plastic system. These products can be manufactured by established modern machinery producing textile materials such as weaving, knitting and braiding machines which are capable of delivering high-quality textile material at production rates up to thousand kilograms per hour.

It is important to note that, with the recognition of textile material via the definition above, in bio-based composites, the existence of textile material cannot be denied. This is because the definition of textile materials covered from the basic form which is fibres.

2.2 Textile Materials

A very generic definition of textile material is 'any material that involved fibrous material' [51]. This term applies to product forms (fibre, yarn and fabric) whether they are originated from natural or synthetic sources as well as products derived from them. The term also includes all types of yarn or ropes, all types of fabrics, hosiery, household textiles, furnishing and upholstery, industrial and technical textiles. The definition of textile gives the understanding of the types and forms of textile materials as well as acknowledging and appreciating their existence not only in apparel and garments, but also in the technical industries such as automotive, aeronautic, infrastructure, composite, etc. [52].

Basically, textile fibres can be clustered into two big families which are natural and synthetic/man-made fibres. Under natural fibre, the classifications can be further extended to animal, vegetable/plant and mineral groups. Silk and wool are some examples of fibre coming from the animal group whereas asbestos is the only fibre which comes from a mineral. Fibres from plants are grouped according to whether they are extracted from seed (e.g. cotton, kapok and coir), leaf (eg. manila, henequen, sisal

and phormium tenax) and bast (flax, hemp, jute, kenaf and ramie). Another family in textile fibre is man-made fibre and it can be further clustered into three main groups which are synthetic (eg. polyester, nylon, aramid and modacrylic), natural polymer (alginate, rubber, regenerated protein, regenerated cellulose and cellulose ester) and other (eg. carbon, glass, metal and ceramic) [53, 54]. For composite materials, carbon, kevlar and glass are high performance fibres that are usually utilised for high performance applications. Whilst in semi-structural and non-load bearing application, natural fibres, especially from the bast group (such as ramie, jute, and hemp) have always been used for that particular purpose.

From the broad definition of 'textile', Lomov et al. [52] introduced three important notions to characterize textile materials. First, it states that textile is a fibrous material made from fibres which are characterized by flexibility, fineness and high ratio of length (usually greater than 100). 'Continuous' fibre is called filament and is usually made and produced from synthetic material, while 'discontinues' is a type of short fibres having length from a few millimetres to a centimetres long and are called staple fibre (can be natural or chopped fibres in man-made fibres). These fibres, regardless their lengths, are assembled into yarn and fibrous plies (yarn, roving or sliver) before being transformed into textiles (woven, knitted or non-woven).

The hierarchical nature is the second important feature of textiles. At this point, the distinguishing of textile can be made from three hierarchicies on top of associated scales (characterized normally by a length) which are; (1) fibres at the microscopic scale, say 0.01 mm; (2) yarns, repeating unit cells and plies at the microscopic scale (0.5–10 mm for yarn diameters and repeating unit cells) and (3) fabrics at the macroscopic scale (1–10 m and above for textiles and textile structures). Another usual

characterization is also made by dimensionality, where fibres and yarns are mostly referred as one-dimensional, while fabrics are two or three-dimensional [52].

Lastly, a textile can be recognized by referring to it as structured material. For instance, a synthetic fibre can be possibly represented as reinforcement by thinking of a textile substance as an entity and making an abstraction of its internal structure. Therefore, the fibre stiffness attribution in composite material can be studied, provided that the internal structure as well as its properties is taken into account. This last feature is very important and very useful when utilizing textile material in technical applications [52].

2.3 Utilisation of Textile Material in Composite

The simplest categorisation of textile materials is by clustering it in the form of fibre, yarn and fabric. They are widely used in many fields, especially in composite materials. The properties of the textile composite are strongly influenced by the properties of their distribution and the interactions among them [32]. Therefore, utilisation of textile material in the different forms will result in distinct properties and behaviours of the composite fabricated. Thus, this section discusses the composite material properties emphasising the basic mechanical properties according to different forms of textile material as reinforcement, and with more focus given to the natural textile material which is suits the purpose of this work.

2.3.1 Fibres

Fibre is the basic unit of the fibrous material in textile material. Basically, fibre can be clustered into two categories; synthetic or man-made and natural fibre. Synthetic or man-made fibres are made chemically usually by polymerization processes using an extrusion machine called a spinneret. Commercial natural fibres used for composite

materials are flax, jute, hemp and ramie, which have conventionally taken a secondary role in terms of consumption, functional and technical requirements [17, 20, 21]. They are considered coarse, durable and traditionally used for making rope and agricultural packaging fabric except for flax which is smoother and usually used for producing linen. Therefore, their acceptance and preference in composite material between the composite scientists cannot be denied above and beyond what other natural fibres could give. Figure 2.1 provides some examples of textile fibres.

The properties of a composite made from natural fibre varies based on the type of fibre, chemical treatment and volume fractions as well as fabrication methods. Table 2.1 shows the mechanical properties of resin reinforced with natural fibres. From the table, jute can be seen to have a wider range of tensile as well as flexural properties in comparison with all other natural fibres, while kenaf and baggase can be said to have lowest mechanical properties. Jute, flax, sisal and hemp can be considered as a senior fibre and their utilization in composite material began nearly a thousand years ago. Their production also varied from rough fibre to be used as rope, mat and geotextile, to a very fine fibre intended for textile in heavy fabric and garments. As for kenaf and baggase, their existence is still new, beginning as early as 30 years ago. Therefore, they are still new and need more researches to extract their fibres because so far their fibres can be said to be rough, there are lots of impurities and voids which lead to lower properties in composite materials.

(a) (b) (c)

(d) (e) (f)

Figure 2.1 Examples of textile fibre; (a) Aramid, (b) Glass, (c) Wool, (d) Hemp, (e) Jute and (f) Flax [53].

Utilization of natural textile fibres in composite material has been established for quite sometimes, even the utilization of high-performance fibre alone is meant for medium load bearing applications. The distribution and contribution of natural fibre form are small even with high-performance [51]. Thus, if the natural fibres are used in composite material, it usually caters for low and medium load bearing applications. A factor that could lead to this scenario is that the dispersion and distribution of fibre in composite material are not easy to control. The method of fabrication usually does not take the alignment of fibre into account, thus they are not interconnected. Fabrication methods such as; resin transfer moulding, mixing and blending a thermoplastic with fibre, and vacuum infusion normally result in low fibre volume fraction. It is also difficult to control the uniformity of fibres' distribution, which could lead a failure when a less concentrated fibre point is subjected to any destruction force. Research is

still being carried out to improve the properties of natural fibres as well as enhancing the method of fabrications for improving composite materials' properties so they can be used in many applications.

Table 2.1 Mechanical properties of composite reinforced with natural fibre forms.

Fibre Types	**Tensile Properties**			**Flexural Properties**		**Impact Resistance**	**Ref./ Sources**
	Tensile Strength (MPa)	**Tensile Modulus (GPa)**	**Elongation at Break (%)**	**Flexural Strength (MPa)**	**Flexural Modulus (GPa)**	**(kJ/m^2)**	
Flax	25.0-99.0	1.8-9.6	1.2-2.4	-	-	64.0-138	[13-15]
jute	23.6-216.0	0.48-7	5.15-6.42	37.9-241	2.2-15.0	37-60	[16, 17, 55]
Sisal	12.2-75.0	0.17-0.37	10.0-69	79-89	-	-	[5, 19]
Hemp fibre	39.3-54.6	7.0-8.4	1.34-2.25	75.6-102.6	3.7-5.3	-	[20, 21]
Coir	34.0-53.0	1.4-2.5	6.0-6.1	53.0-68.0	0.8-1.3	-	[22]
Kenaf	15.0-58.0	2.0-8.8	-	-	-	-	[23]
Baggase	16.5-26.8	-	-	31.19-50.86	1.1-2.6	4.12-11.27	[24]

*All figures are subjected to different fabrication methods, volume fractions and chemical treatments.

2.3.2 Yarn

A group of fibres with or without twist is called yarn, which has a substantial length and relatively small cross-section. Monofilament is yarn containing only one fibre, for example, nylon. Untwisted, thick yarns are termed tows and these terms are usually applied to high-performance yarn such as glass, aramid and carbon. A twist is introduced to continuous filament in the process of 'twisting' and to staple fibres in the process called 'spinning' involving a long chain of preparatory operations. There are different yarn spinning processes (ring spinning, open-end spinning, friction spinning) leading to yarns, each with a distinctive internal distributions of fibres. Figure 4 shows some example of textile yarns (natural and man-made) available on the market. The common composite fabrication method of applying yarn is called

‘filament winding’ which usually to produces hollow, generally circular or oval materials; and thermoset resin is the most preferred matrix.

(a) (b)

Figure 2.2 Example of yarn, (a) Carbon tows and (b) Cotton yarns [53].

Table 2.2 shows some of the mechanical properties of textile natural yarns reinforced resin and common natural yarns such as flax, hemp and jute which have good coverage regarding their contribution as a reinforcement material [25-30]. The wide range in their mechanical properties depends on the type of chemical treatments, fibre volume fractions, resins and fabrication techniques. As discussed earlier, these kinds of material were established a long time ago thus the development in yarn processing can be said to be mature.

There are several criteria for a fibre to be neatly converted into good yarns. The cleanliness, length, diameter and colour of fibres are the important properties that should be taken into account when converting fibres into yarns. This is to ensure that the spinning machine can handle the fibre smoothly and thus produce good quality yarns. Therefore, good fibre extraction is required to ensure that extracted fibres have good properties suited to spinning processing. This is an opportunity for researchers

to work on producing good fibres such as kenaf, baggase and coir because, so far, these kinds of fibre are coarse, inconsistent in length, possess unattractive colours and are too unclean to be used in spinning process. The rapid development of bamboo extraction has recently produced not only good fibre, but also yarns and fabric.

The utilization of textile yarn provides more control over the properties of composite materials as compared to the textile fibre form. This is because the scattered fibres are combined and aligned in a group with or without twist given. At this rate, the properties of this material can be designed based on how the yarn is wound around the base. Even though the design of material is limited, at least it is more versatile and easier to control compared to fibre form.

This type of reinforcement is really useful to manufacture circular and hollow material. At this rate, the properties of this material can be designed based on how the yarn is wound around the base. Even though the design of material is limited, at least it is more versatile compared to fibre form due to the fabrication method for reinforcement material [25-30]. Some other works have tried to use methods other than filament winding, which is winding yarn onto a metal plate. However, this method is basically similar in principle to the existing method. Therefore, further work is needed to vary the processing methods of composite material using textile natural yarn (even for high-performance yarn) in order to enhance the potential of this kind of reinforcement to its optimum performances.

Table 2.2 Mechanical properties of textile natural yarns reinforced resin.

Fibre Types	Tensile			Flexural		Impact Resistance (kJ/m^2)	References/ Sources
	Strength (MPa)	E-Modulus (GPa)	Elongation (%)	Strength (MPa)	Modulus (GPa)		

Flax	246.0-298.2	3.8-4.3	12.8-13.2	42-145.6	4.4-15.26	19-110	[25-27]
Hemp	253.3-277.0	6.54-6.61	7.73-9.70	114.7-127.2	9.27-11.23	-	[27, 28]
Jute	53-78.9	2.5-8.4	-	63-110	2.6-8.6	16-23	[29, 30]

*All figures are subjected to different fabrication methods, volume fractions, resin and chemical treatments.

2.3.3 Fabric

Scardino [32] divided the textile structures or reinforcement forms into four categories including simple fabrics (2-D) and advanced fabrics (3-D) systems. These kinds of reinforcement are preferably used by manufacturer or researcher because basically, they are easy to handle. Figure 2.3 shows some common textile fabric forms used as composite reinforcement [52]. Utilizing 2-D as well as 3-D fabrics made of high-performance fibres have been well-known and discussed by many material scientists for various application and purposes. However, so far, when a natural fabric is concerned, only simple fabric (2-D) is well known to be utilised for composite materials [52].

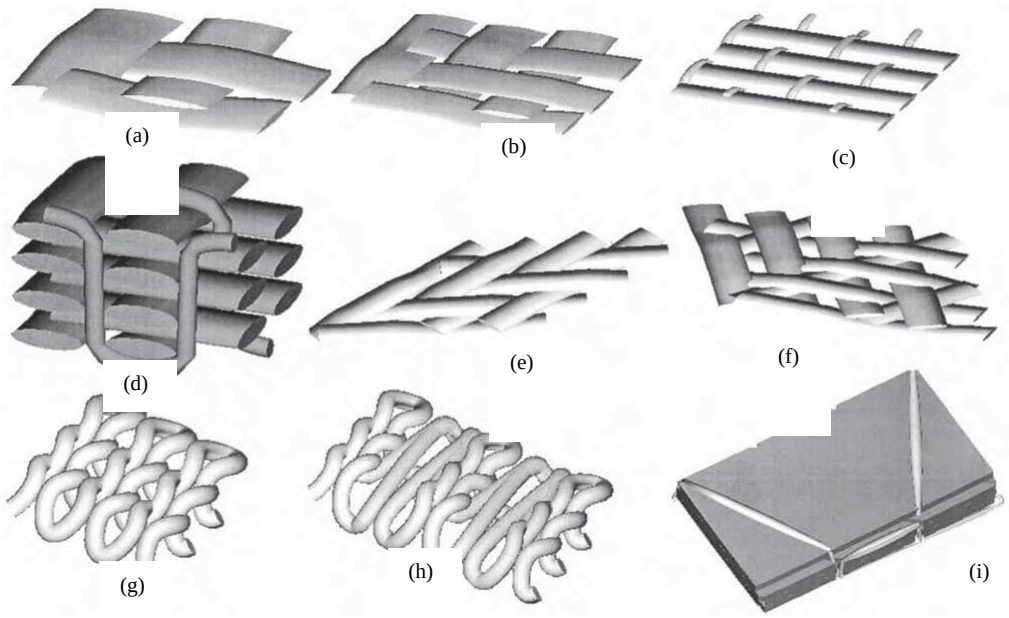

Figure 2.3 Structure of textile fabric; (a-c) 2-D woven fabrics, (d) 3-D fabric, (e-f) braided fabrics, (g-h) knitted fabric and (i) multiaxial multiply warp-knitted fabric[52].

Table 2.3 shows some mechanical properties of composite made from textile fabrics. The wide ranges in properties result in different fabric structures, chemical treatment, fibre volume fraction, resins and fabrication method in producing the composite materials. From the table, it in case be seen that the mechanical strengths of composite made of woven fabric are higher than those made of nonwoven fabric. The reason is because the fibre is better arranged than the nonwoven fabric [31-33]. The fibre in woven fabric is, firstly converted into yarn (first degree of arrangement) and then interlaced into a woven fabric (second degree of arrangement). Yarn in a woven fabric is arranged based on set design (woven fabric structure) created by the weavers, and this yarn arrangement should enable consistent fibre distribution on fabric [31, 32]. Unlike woven fabric, nonwoven fabric has no specific alignment on the fibre. The fibre is basically scattered before the bonding or interlocking process takes place. Therefore, the properties of nonwoven fabric can be said to be lower than woven fabric.

Table 2.3 Mechanical properties of a resin reinforced with textile fabrics.

Fibre Types	Tensile			Flexural Strength		Impact Resistance		Ref./ Sources
	Strength (MPa)	E-Modulus (GPa)	Elongation (%)	Strength (MPa)	Modulus (GPa)	J/m	kJ/m^2	
Woven flax	54.6-81.9	0.9-1.8	7.7-19.1	20.9-75	0.75-7.5	-	-	[26, 56]
Nonwoven flax	25-39	4-8.5	1.4-1.8	-	-	66-138		[13]
Woven jute	22.6-92	2.23-7.2	-	86-134	5.5-6.5	-	-	[57, 58]
Nonwoven Jute	22.4-35.6	0.714-1.04	5.8-10.2	21.9-38.4	0.68-1.12	-	-	[59]
Woven Hemp	63-69	3-4.3	4.2-7.1	41.7-94.5	3.2-4.4	30-210	-	[35-37]
Nonwoven hemp	24-63	0.56-1.27	5.9-11	54-110	4.2-7.3	-	-	[38]
Woven ramie	31-44	-	-	67-92	4.2-6.2	-	6.0-18.0	[60]
Woven bamboo	48.72-77.58	0.983-1.75	9.8-14.59	104.8-149.3	1.2-2.29	-	13.44-26.93	[61]
Nonwoven kenaf	22-58	1.4-3.1	-	30-59	-	-	-	[62]

*All figures are subjected to different fabric structures, fabrication methods, volume fractions, resin and chemical treatments.

The properties of a composite material are easier to design by varying the properties of the fabric properties. For instance, jute fibre is supposed to have far higher mechanical properties than flax (Table 2.1); however, the gap can be narrowed by using it in fabric forms (Table 2.3). This is an example on how fabrics can offer more flexible design and how we want the material properties to be.

2.3.4 Comparison of Natural Textile Materials in Composites

When comparing all reinforcement forms (Table 2.1, 2.2 and 2.3), utilization of traditional high-performance reinforcements are preferred in fabric form rather than fibre and yarn [31-33]. Normally, neither fibre nor yarn reinforcements can surpass the composite reinforced with the fabric form in terms of overall performance (the most isotropic can be achieved). Fabric is easier to handle and can maintain its dimensional

stability during the composite fabrication in comparison with the other two forms. All fibres in the fabric are arranged and aligned according to specific designs (also known as fabric structure) hence the fibres are interconnected with each other and thus perform a kind of a synergistic effect.

Unlike fabric, yarn is formed by a group of aligned fibres, and then some twists are given until the direction of fibre becames 10-80° in yarn longitudinal direction. Yet, layering yarn for composite fabrication usually does not connect them with each other [52, 63]. Some yarn composites could surpass the strength of the fabric composite in the longitudinal direction however, they are weaker in the transverse or 45° directions [39]. Therefore, the performance of composites reinforced with yarn is dependent on how the yarns are layered.

Based on the discussion of this topic, in order to achieve the optimal performance of composite material for specific applications, justification should be made regarding the selection of textile structures because some applications might not need very high strength or superior performances. However, when seeking overall performances, fabric form is the best solution for this requirement. Therefore, hemp in the form of fabric will be utilised as the reinforcement for composite fabrication in this project.

2.4 Natural Fibres

The popularity of natural fibres todays is strongly influenced by the growing sensitivity of the world's population to environmental issues. Again, it is worth mentioning the advantages of natural fibres such as low cost, low density, renewability, flexibility during processing, high specific stiffness and biodegradability. Their availability, complete data and sustainability are other reasons that strengthen the preferences for natural fibres [9].

The fibres commonly used to produce composites are bamboo, ramie, abaca, sisal, kenaf, baggase, hemp, flax, jute and grass [49]. Table 2.4 shows the world production of natural fibre used as composite reinforcements. The figures are quite promising for ensuring the sustainability of supplies for the bio-based composite industry, especially for bamboo that has recently been produced in China due to the success development of the fibre extraction method.

Table 2.4 World fibre production [49].

Fibre Source	World Production (10^3 ton)
Bamboo	30000
Jute	2300
Kenaf	970
Flax	830
Sisal	378
Hemp	214
Coir	100
Ramie	100
Abaca	70
Sugar cane baggase	75000
Grass	700

2.4.1 Mechanical Properties of Natural Fibres

In normal practice, the selection of natural fibre by many researchers is dependent on the fibres' mechanical properties above and beyond the types of polymer and end products. A product designer will scrutinize the properties of several natural fibres before coming to a decision on what type of natural fibre they are going to utilize for the end product. Table 2.5 presents some important physical and mechanical properties of commercial natural fibres [10, 49, 64]. As a reference, the mechanical properties of some high-performance fibres were also included in the table.

The range of characteristic values is normally caused by the environmental conditions it experienced during the growth of the natural fibres. The range of conditions can be considered one of the drawbacks for all natural products. However, certain properties of some natural fibres can be considered at par, or sometimes to exceed the high-performance fibres. For instance, Young's modulus of hemp is similar to e-glass and could be higher than aramid. Therefore hemp can replace E-glass and aramid for those applications which place a crucial emphases on the material's stiffness.

Table 2.5 Mechanical and physical properties of natural fibres[10, 49, 64].

Fibre	Density (g/cm^3)	Tensile Strength (MPa)	Young's Modulus (GPa)	Elongation at Break (%)	Length (mm)	Diameter (μm)
Bamboo	0.6–1.1	140–800	11–32	2.5-3.7	1.5-4	25-40
Jute	1.3-1.49	320–800	8-78	1.5–1.8	1.5-200	20-200
Kenaf	1.4	223-930	14.5-53	1.5-2.7	-	-
Flax	1.4-1.5	345–2000	27.6-103	1.2–3.3	5-900	12-600
Sisal	1.33-1.5	363–700	9.0–38	2.0–7.0	900	8-200
Hemp	1.4-1.5	270-900	23.5-90	1.0-3.5	5-55	25-500
Coir	1.15-1.46	95-230	2.8–6	15-51.4	20-150	10-460
Ramie	1.0-1.55	400-1000	24.5-128	1.2-4.0	900-1200	20-80
Abaca	1.5	400-980	6.2-20	1-10	-	-
Baggase	1.25	222-290	17-27.1	1.1	10-300	10-34
Cotton	1.5 – 1.6	287 – 800	5.5 – 12.6	3.0 – 10.0	10-60	10-45
E-glass	2.5-2.59	2000 – 3500	70	2.5	-	-
Aramid	1.4	3000 – 3150	63.0 – 67.0	3.3 – 3.7	-	-
Carbon	1.4	4000	230.0 – 240.0	1.4 – 1.8	-	-

Besides environment conditions mentioned before, the variation of the natural fibres' properties are found due to different fibres, different moisture conditions, and different testing methods employed. At a micro level, the natural fibre reinforced polymer composites' performance also depends on several factors including the fibre's

chemical composition, cell dimensions, microfibrillar angle, defects, structure, physical properties, mechanical properties, and the interaction of the fibre with the polymer. To expand the use of natural fibres for composites and improve their performance, it is essential to know the fibre characteristics before any decision is taken regarding design and production.

2.4.2 Chemical Composition

Understanding the chemical composition of natural fibre is necessary to comprehend how the fibre reacts and how each component could influence the fibre properties and characteristics. In each typical natural fibre, there is a primary cell on the outer layer of fibre consisting of disorderly arranged crystalline cellulose microfibrils, and three secondary walls comprising of helically arranged crystalline cellulose microfibrils as shown in Figure 2.4.

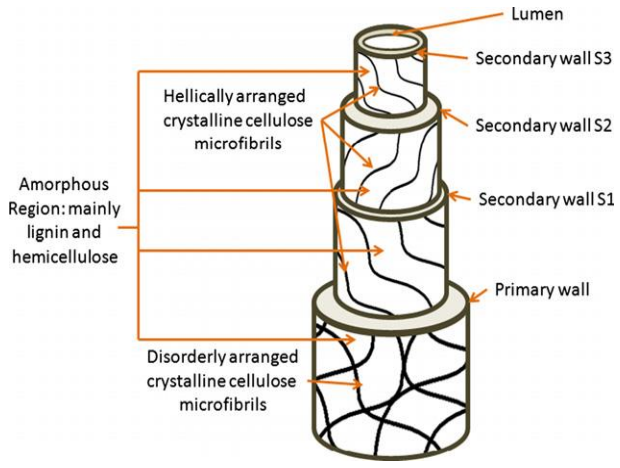

Figure 2.4 Typical structure of natural fibres, adapted from [65].

Cellulose is the most important structure in many natural fibres. As in Figure 2.5, it is a natural polymer with each repeating unit containing three hydroxyl groups. These groups are responsible to the hydrophilic characteristic of cellulose. Cellulose is

resilient to hydrolysis, strong alkali as well as oxidizing agents [66]. Nevertheless, degradation can occur when it is exposed to some chemical treatments.

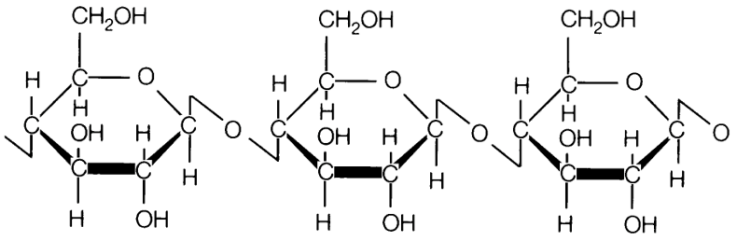

Figure 2.5 Typical chemical structure of cellulose.

Hemicellulose is totally different from cellulose and some works claims that the name of hemicellulose is an unfortunate one [64]. Hemicellulosic are lower in molecular weight comprising a group of polysaccharides that act as adhesive as well as chain branching between cellulose microfibrils. Lignin is a composition that is responsible for transporting water and gives rigidity to plant. Its combination with hemicellulose became a matrix for long chain cellulose molecules (microfibrils) [10, 65, 66]. Lignin is hydrophobic, resists acid hydrolysis and most microorganism attacks, soluble in hot alkali, readily oxidised, and easily condensable with phenol [65, 67, 68]. Pectin gives plants flexibility and it can be removed it in water after neutralization with ammonium hydroxide or alkali by retting or scotching processes [64, 69]. Waxes make up the last part of the fibres and they consist of different types of alcohols that can be extracted with organic solutions [65]. Wax is a substance on the fibre surface that functions to protect the fibre.

Table 2.6 shows chemical composition of commercial natural fibres. Their moisture content ranges from 5 to 14% except for ramie and sisal, which can be considered to possess the highest values of 17 and 22% respectively. Even 10% of moisture content

is considerably high for becoming a composite reinforcement because the major issue with using natural fibres in composite material is the compatibility between natural fibres' hydrophilic surfaces and the hydrophobic nature of polymer resin. Nevertheless, so far, a number of works have been putting their effort into resolving the issue chemically, mechanically and thermally.

Table 2.6 Some examples of chemical compositions of various natural fibres [10, 49, 67].

Fibre	Cellulose (wt.%)	Hemicellulose (wt.%)	Lignin (wt.%)	Pectin (wt.%)	Waxes (wt.%)	Microfibrillar angle (deg)	Moisture Content (wt.%)
Bamboo	22-65	30	5-31	-	-	-	
Jute	59-71	13.6-20.4	11.8-13	0.2-0.4	0.5	8.0	12.5-13.7
Kenaf	31-72	20.3-21.5	8-19	3-5	-	-	-
Flax	62-72	18.6-20.6	2-5	2.3	1.5-1.7	5-10	8-12
Sisal	60-78	10-14.2	8-14	10	2	10-22	10-22
Hemp	68-74.4	15-22.4	3.7-10	0.9	0.8	2-6.2	6.2-12
Coir	32-43.8	0.15-20	40-45	3-4	-	30-49	8
Ramie	68.6-85	13-16.7	0.5-0.7	1.9	0.3	7.5	7.5-17
Abaca	56-63	20-25	7-13	1	3	-	5-10
Baggase	32-55.2	16.8	19-25.3				
Cotton	82.7-90	5.7	<2	0-1	0.6	-	7.85-8.5

Generally, for those natural fibres which possess higher mechanical strength, there is as higher cellulose content with a higher degree of polymerisation, longer length of cell but lower microfibrillar angle. Therefore, some traditional fibres such as cotton, jute, flax, hemp, sisal and ramie can be considered to be strong fibres. We can tell this by looking at the composition of the cellulose percentage in the fibre (Table 2.6). Kenaf, bamboo, coir and baggase are considered as new fibres which possess lower strength. Hence, it is usual for the researcher to consider important variables such as

fibre structure, microfibrillar angle and chemical composition on top of defects when determining overall properties of fibres.

2.5 Natural Fibre Composites in Building Industry

Some advantages of textile composites in a construction industry are the reduction of weight, possible overall cost reduction, reduction in construction time, and production of multifunctional components. Other than these, from an architectural point of view, textile composites offer a variety of appearances: translucency, colour, surface texture, finish quality, etc. Glass, carbon and aramid reinforced epoxy/polyester are the materials most commonly used in the construction industry [70, 71]. Even though they still do not hold a prominent position in building, they have attracted the attention of architects and engineers for many years [70].

One of of the long-term benefits to infrastructure especially from an ecological perspective, is the potential to create large-volume and biodegradable structural components which result in reduced quantities of construction waste embodied energy. The use of natural fibre composites also reduces and increases energy efficiency which provides a solution to immediate infrastructure needs while promoting the concept of sustainability [10]. The integration of natural fibres such as flax, jute, sisal, ramie, hemp, etc. in composite material have been proven to increase the mechanical properties of the polymeric matrix [14]. Most of the bio-based composites have maximum tensile strengths and stiffness in the ranges of 100-200MPa and 1- 4GPa respectively [72]. These figures are too low to be used for primary applications yet are good enough to be an alternative for low-load bearing or semi-structural applications.

Some other types of material used in construction or infrastructure under low-load bearing applications are wood and engineered wood products, and bio-based

composites are reported to have comparable properties to these materials. Wood products that are commonly used in the construction industry are Douglas Fir, Western Hemlock, Ponderosa Pine etc., while engineered wood products are plywood, oriented strand board, particleboard, fibreboard and glue laminated timber (glulam) [35, 73]. Table 2.7 shows the mechanical strength of wood and engineered wood products. Some mechanical properties of natural composites (Table 2.3) can be said to be comparable with wood and engineered wood products; and have the potential to be used to be an alternative for wood and engineered wood products.

Table 2.7 Mechanical properties of biocomposites, wood and engineered wood products [35].

Material	Tensile strength (MPa)	Tensile modulus (GPa)	Shear strength (MPa)	Flexural strength (MPa)	Flexural modulus (GPa)
Douglas-Fir(coast)	-	-	7.8	85	13.4
Weatern-Hemlock	-	-	8.6	78	11.3
Ponderosa Pine	-	-	7.8	65	8.9
Plywood (B-B Class1)	27	10.3	1	27	10.3
Oriented Strand Board	-	-	1.2	21.2	5.25
Glulam	-	-	-	26-72	10.6

Dittenber and GangaRao [10] highlighted several important criteria for a bio-based composite to be used as a civil infrastructure and building construction material. First, the mechanical properties of bio-based composites should be well determined in order to give an idea of the type of application this material is suitable for. Second, since the natural fibre is hydrophilic in nature, some modification and treatment should be made to increase its hydrophobicity thus enhancing the incompatibility with polymer. Third, fibre reinforced polymer composites can lose strength and stiffness at elevated

temperatures. Depending on the application and necessity, the fire resistance of bio-based composite should be evaluated in order to determine the material's resistivity against fire. Fourth, less work has been carried out on natural fibre composite fatigue. Last, the manufacturing/processing method is a very important criteria for a material to be applied in infrastructure fields as this will ensure that the material can be produced consistently and persistently. Therefore, it is concluded that these criteria will be a necessary area of research before natural fibres are accepted in the infrastructure field.

2.6 Previous Investigation of Hemp Fabric Composites

Based on the discussion above (2.2 Comparison of Natural Textile Material in Composite Material), it is concluded that natural textile fabric is the most preferred form to achieve overall performance of the composite; due to it is easy to handle results to good dimensional properties, good distribution of fibre due to fabric design and ease of manufacture into a composite. Hemp is a well-known fibre in the textile industry. It is one of the primary materials used in the production of heavy and medium-weight fabrics in linen production. It is composed of 68-74.4% of cellulose, 15 - 22.4% of lignocellulosic, is lower in lignin, pectin and waxes [10, 49, 67] and this reflects its mechanical properties, with the density of 1.4-1.5g/cm^3 , its tensile strength, young's modulus; elongation at break, length and diameter are 270-900MPa, 23.5-90GPa 1.0-3.5%, 5-55mm and 25-500μm respectively [10, 49, 64] which make it relatively strong.

The Young's modulus of hemp can be said to be comparable with and even higher and its availability in the forms of fibre, yarn and fabric make it suitability versatile for use in a variety applications. The production of hemp fabric is quite promising to ensure

the sustainability and availability of supplies for composite material (Table 2.4). This is the main factor to ensure that a composite material can survive and be continuously available in the market. Using hemp fabric in a composite material can ensure the consistency of material properties as well as achieve overall performance of the composite material. So far, there are few natural fibres available in woven fabric form. Hemp is one of the fibres that can satisfy the need for technical application, is available in fabric form and is easy to obtain.

2.6.1 Effect of Fabric Properties

As discussed in the Section 2.5, hemp composite can be used as an alternative material or replace some wood and engineered wood product. This can be achieved by taking advantage of hemp fibre in the form of fabric. Christian and Billington [35] used a plain weave hemp fabric which had the fabric density of 45 warp yarns and 42 weft yarns. They found that the hemp composites fabricated were comparable with some wood and wood products. Song et al. [33] used a woven hemp fabric in their study comparing two different kind of weave structures (plain and twill structure) fabric to reinforce polylactic acid (PLA) resin. They found that the composite made of twill fabric had better results than the plain weave fabric in terms of mechanical, thermal and viscoelastic properties. Table 2.8 shows the mechanical properties of hemp fabric composites.

However, both studies did not mention any fabric properties such as density of fabric, yarn size, yarn crimp in fabric and fabric strength. Comparing composite materials made of fabric with particular wood and engineered wood products such as particleboard, plywood and glue laminated is more valuable if the fabric properties used in the fabricated composites' mechanical properties is known. This information

is very important, especially when designing and manufacturing natural fabric composites for ensuring the consistency of composite performances.

Table 2.8 Some mechanical properties of hemp fabric composites.

Materials	Tensile Strength (MPa)	Tensile Modulus (GPa)	Flexural Strength (MPa)	Flexural Modulus (GPa)	Shear strength (MPa)	Shear Modulus (GPa)	Impact strength (J/m)	References
Hemp/PHB	44.5-55.9	3.6-5.47	48.2-64.8	2.7-5.05	9.85	0.88	-	Christian and Billington [35]
Hemp/CA	54.2-54.4	4.8-5.4	80.7-94.5	6.56-5.98	12.3	1.09	-	Christian and Billington [35]
Hemp/PLA (Plain weave)	63-65	3-3.3	-	-	-		30-190	Song et al. [33]
Hemp/PLA (Twill weave)	67-69	3.1-3.5	-	-			35-210	Song et al. [33]

*Subject to different fibre volume fraction

2.6.2 Chemical Treatment and Moisture/Water Absorption

Chemical treatment is a common method used to enhance the adhesion between reinforcement and matrix, especially for bio-based composites. The presence of water will lead to poor adhesion between reinforcement and matrix since most of the matrix is naturally hydrophobic, and this will decrease the performance of the composite.

Kabir et al. [36] used hemp fabric as a skin for a hemp fibre core in order to fabricate a sandwich structure. They formulated several chemical treatments to treat the fibre to enhance the adhesion of resin and reinforcement. By applying unsaturated polyester resin, the mixture between resin and catalyst performed with the ratio of 1:0.015 and the technique they used to fabricate the composite was hand lay-up. The effect of the chemical treatment was confirmed by using SEM, FTIR, DSC and TGA analyses. Flexural and compression test was conducted to determine the mechanical properties of the treated composite. They found that the sample of fibre treated only with an alkali solution is good enough to produce a material with acceptable quality. Table 2.9 shows

the results of their work on hemp composites. Any post-treatment with acetylation and siloxane tended to reduce the mechanical properties of the material and increase the cost of manufacturing.

Table 2.9 Effect of chemical treatment on the hemp reinforced composites [36].

Sample	Tensile Strength (MPa)	Tensile Modulus (GPa)	Compressive Strength (MPa)	Compressive Modulus (GPa)
Alkalised	47.50-60.50	1.60-4.44	84.06-111.05	2.2-2.65
Acetylated	44.46-53.30	1.37-1.78	87.81-95.59	2.4-2.67
Silanised	41.65-54.95	3.2-4.31	88.53-97.71	2.27-2.58

Another important treatment to be considered is fire/flame retardant. Since this composite material is purposely used and designed for infrastructure application, safety issues should be considered, particularly its ability to inhibit flame. Dorez et al. [74] studied the thermal and fire behavior of natural fibres (hemp, flax, sugar cane and bamboo) reinforced polybutylene succinate (PBS) biocomposites. According to them, the maximum rate of heat emission (MARHE) is a good parameter to determine the effect of fire retardant treatment, which imitate the real situation. They found that the incorporation of fibres in PBS reduced thermal stability as well as the time to ignition of composites, but increased the mass residue corresponding to the formation of a char barrier. Later, the addition of a fire retardant agent, ammonium polyphosphate (APP) in flax/s lead to a hot hydrolysis of PBS, and the phosphorylation of fibre thus retarded the fire by the formation of a barrier layer on the biocomposites due to the charring of the matrix and preservation of the fibre skeleton. Kandare et al. [75] studied the fire reaction properties on flax/epoxy laminates and balsa as a core in sandwich composites. Incorporation of ammonium phosphate as a fire retardant agent improved the fire retardant properties of their composites. Lazko et al. [76] studied the effect of several kinds of fire retardant agents (melamine phosphate (MMP), melamine borate

(MMB), zinc borate (ZB) and aluminium trihydroxide (ATH)) on the semi-rigid panel. The semi-rigid panels were composed of flax short fibre and pea protein binder. They found that the treatments improved flame resistance and the best result were obtained by incorporating melamine borate (heat released was reduced up to 50% and ignition time increased six times from the reference sample). However, the addition of the fire retardant agent (ammonium polyphosphate) could reduce the mechanical properties of the composite [76]. Table 2.10 exhibits the fire retardant properties of natural fibre before and after fire retardant treatments.

Table 2.10 Effect of fire retardant treatment on the natural fibre composites.

Materials	Fire retardant agent	Before Treatment, MARHE (Maximum rate of Heat Emission), (kW/m^2)	After Treatment, MARHE (Maximum rate of Heat Emission), (kW/m^2)	References
PBS	-	238.7	213.8	[74]
Cellulose	-	91.2	91.2	
Flax	-	60.5	60.5	
Hemp	-	58.1	58.1	
Flax/PBS	Ammonium polyphosphate (APP)	178.8	127.4	
Flax/Epoxy	APP	419	307	[75]
Balsa-Flax/Epoxy	APP	393	286	
Flax/Pea Protein	Aluminium tri-hydroxide	126	86	[76]
Flax/Pea Protein	Zinc Borate	126	94	

Flax/Pea Protein	Melamine Phosphate	126	80	
Flax/Pea Protein	Melamine Borate	126	61-107	

Another quantitative measurement used to evaluate fire retardant of a material is by the limiting oxygen index test (LOI). It shows the minimum amount of oxygen in oxygen–nitrogen mixture required to support complete combustion of a vertically held sample that burns downward. The higher the LOI value, the more effective the flame-retardant treatment [77, 78]. Shukor et al. [77] used ammonium polyphosphate in different concentrations in their kenaf/PLA mixture and they found that the LOI value increased with the increment of ammonium polyphosphate concentrations. Xu et al. [78] treated hemp fibre with various solutions (nitrogen, phosphorus and boron) and mixture percentages. They found that the LOI of treated samples were increased as compared to untreated and the values were different among treated samples. All the composites treated with fire retardant exceed or surpass the LOI minimum value of 28 which is generally classified as a fire retardant material [79]. Thus, a composite materials which has higher LOI value than 28 indicates better fire retardant properties.

A common method of incorporating a fire retardant agent is by adding it during the mixing process. Most researchers highlighted a concern about the greater flammable nature of natural fibres more than the resin. There are few works applying fire retardant agent to the reinforcement directly (especially on hemp fabric) and assessing the effect of this treated reinforcement in composite materials. There is also less work reporting the fastness of this treatment for long term testing (water absorption and fatigue). Therefore, there is a need to study the short and long-term effects of reinforcement treated with a fire retardant agent in composite material application.

Moisture and water absorption of the material is an important criteria for defining material's life cycle [10]. Table 2.11 shows the effect of water/moisture penetration on the hemp reinforced composites for long-term exposure of several works. Dhakal et al. [38] studied the effect of water absorption on the mechanical properties of hemp non-woven fabric reinforced unsaturated polyester at 25ºC and 100ºC in a de-ionised water bath. When immersed in boiling temperature, water induces the degradation of composite more significantly. Ramezani Kakroodi et al. [40] studied the water uptake of hemp reinforced maleated polyethylene (MAPE) with the addition of ground tyre rubber (GTR). They found that, with the maleic anhydride treatment, water uptake in the fabricated composite increased with the increment of fibre content. A study undertaken by Christian and Billington [41] emphasized on the characteristic of moisture absorption properties when exposed to different moisture and temperature conditions. They found that the rate of diffusion for the composites increased with increasing temperature and depended on the types of matrix used in the material.

All the water/moisture absorption works above emphasized composites made of hemp fibre and non-woven hemp. It is obvious that the presence of water and moisture could reduce the mechanical and physical properties of fabricated material. Since there are fewer works studying the moisture or water absorption of composite made of woven hemp fabric, the water absorption should be tested to identifying its behaviour and characteristic when dealing with water occurrence. It is also believed that the fastness of fire retardant treatment will be degraded as water/moisture penetrates into a composite. Nevertheless, there is no work studying for the effect of water/moisture presence on the fastness of fire retardant treatments for the hemp fibre composite.

Table 2.11 Effect of water/moisture absorption on the hemp reinforced composites.

Materials	Water/Moisture Uptake (%)	Diffusion Coefficient, D		References
Hemp/Polyester	3.441	1.551 to 4.367 × 10-6 mm^2/s	Water absorption in room temp. up to 888 hrs	Dhakal et al. [38]
Hemp/ Polyester	13.533	48 to 67 × 10-3 mm^2/s	Water absorption in 1000C up to 31 hrs	
Hemp/Polyester	16	8.7 × 10-13 m^2/s	Room temp.	Shahzad [80]
Hemp/ MAPE (different volume of fibre)	1.34 – 6.85	1.442 – 1.543 × 10-13 m^2/s	Water absorption for 23 wks	Ramezani Kakroodi et al. [40]
Hemp/MAPE/GTR (different volume of fibre)	4.54-4.83	1.511-1.525 × 10-13 m^2/s (	Water absorption for 23 wks	
Hemp/Cellulose Acetate	11.20-11.5	1.30-2.76 x 10-5 mm^2/s	Moisture absorption until saturation for 30, 40, 50°C	Christian and Billington [41]
Hemp/PHB	6.83-8.13	1.14-9.57 x 10-5 mm^2/s	Moisture absorption until saturation for 30, 40, 50°C	

2.6.3 Durability

A major concern with bio-based composites is their long-term behaviour when exposed to continuous loading as well as the prediction of lifetimes. The long-term behaviour of material will define its durability and serviceability. Consensus from the literature is that very little fatigue work has been carried out on natural fibre composites [10, 42, 44, 81].

Yuanjian and Isaac [42] investigated the fatigue behaviour of hemp mat (fibre density 720g/m^2) reinforced polyester. Glass reinforced polyester were also fabricated purposely for the comparison. Based on their static mechanical results, hemp mat could replace glass fibre composites when the ultimate tensile strengths of the composites were 53 and 43MPa respectively. Fatigue testing indicated that, even though hemp composites show longer lifetimes, its steeper S-N slope suggests a higher rate of reduction in fatigue strength compared to the glass fibre composite. Steady decreases of modulus during fatigue cycling were observed for the glass composite whilst for hemp composites, throughout fatigue cycling, the modulus suddenly drops like a brittle material. There was a crossover point at high cycle of about 10^6 cycles for both hemp and glass composites even hemp composite showed superior fatigue strength at the low cycle.

Shahzad [43] studied the effect of alkalisation on the fatigue behaviour of hemp fibre composites. The composites were made of hemp mat treated with various NaOH solution concentrations reinforced unsaturated polyester. However, he did not mention any parameter or properties of fibre used for the fabrication. Fatigue results in his work showed that all the samples reached their endurance limit after 10^6 cycles. The alkalised samples showed an improvement of about 30MPa at the endurance limit

point as compared to the untreated sample. By plotting a normalised stress versus cycle to failure, he compared the fatigue sensitivity coefficient. From these curves, he found that the alkalization improved the fatigue sensitivity of composites. However, based on the S-N curve, the data plot for each type of composite is rather scattered and maybe due to the inconsistent fibre distribution in the composites. Based on the static strength properties, there is a little inconsistent data plotted, and standard error bar gaps were quite wide over all of the samples indicating an inconsistency of data. Therefore, it can be implied that the material used for this work had inhomogeneous fibre distribution.

An extensive study by Shah et al. [44] provides very good information about fatigue behaviour of bio-based composites. In their work, five types of yarn/roving involving jute, hemp and flax were used to reinforce unsaturated polyester. They studied the fatigue behaviour of composites based on four experimental variables, which were fibre type, fibre volume fraction, textile architecture and stress ratio. Based on the S-N curve, all samples met the endurance limit at 10^7 cycles in a similar trend indicating a similar rate of fatigue strength degradation. The fatigue strength coefficient of glass fibre composite was found to be comparable ($b \approx -0.074$), and in some cases lower than bio-based composite (-0.0739 to -0.0623) indicating that damage development, fatigue strength degradation and damage accumulation rate were higher than for the bio-based composites. An increase in fibre volume fraction (Vf from 17 up to 40%) was found, improving fatigue performance where S-N curves did not converge into each other for at least 10^{10} cycles. In terms of textile architecture effect on the fatigue behaviour, even though off-axis loading direction resulted in a significant drop in fatigue loading capacity throughout their fatigue life; in terms of fatigue strength degradation rate, it was better than the uniaxial of other bio-based composites in this work and biaxial and triaxial lay-up of glass fibre composites at least up to 10^8 cycles under the normalised

stress versus cycles curves. This is based on the higher fatigue strength coefficient (b value) and lower fatigue strength degradation. Last, in terms of the different stress ratios, it was found that increasing the stress ratio R substantially reducing the fatigue life at high stress. It can be explained from the S-N curves, when the stress ratio increasing; it will lead to a flatter curve thus resulting in slower fatigue degradation as well as damage accumulation rates.

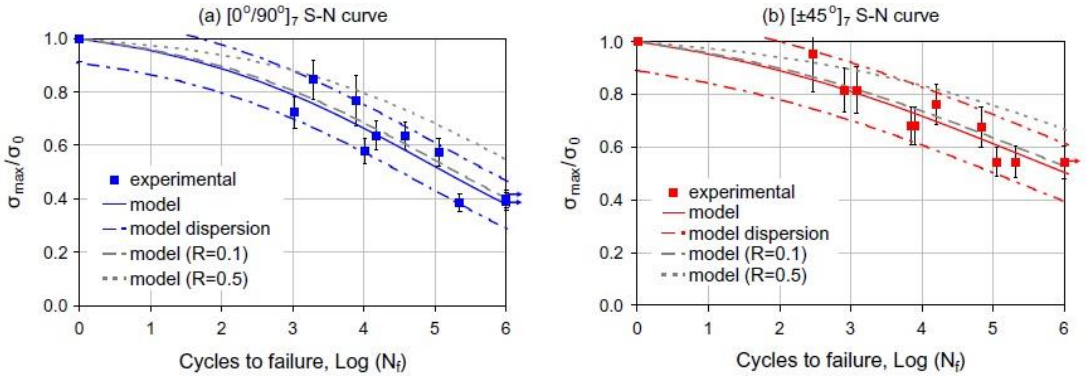

(a) (b)

Figure 2.6 Experimental and calculated S-N curves for (a) [0º/90º]7 and (b) [±45º]7 hemp/epoxy composites [45].

de Vasconcellos et al. [45] studied the tensile-tensile fatigue behaviour of a woven hemp fibre reinforced epoxy. Two different fibre orientations are compared: [0º/90º]7 and [±45º]7. Based on static tensile strength, a fatigue test was set up at the frequency of 1 Hz with a stress ratio of 0.01. This testing was stopped at specimen failure or when 10^6 cycles were reached. The small stress ratio was chosen to approach 'zero load', enabling a correct measurement of the minimum strain value. In this study, they found that the sample [±45º]7 possessed better fatigue strength in comparison with sample [0º/90º]7 under normalised stress terms. From the S-N curves, [±45º]7 sample curve was stopped at 10^6 cycles at a higher normalised stress ratio, which was about 0.5 as

compared to [0º/90º]7 samples, which were about 0.4 and stopped at similar cycles. Similar trends were found for both S-N curves indicating similar fatigue strength degradation. However, in this work, they did not provide any fatigue strength coefficient for comparison thus it is quite difficult to observe the fatigue degradation rate for both samples. Figure 2.6 shows the results of a fatigue test of hemp/epoxy. On a review of the literature, there still lack of knowledge about the fatigue behaviour of treated hemp fabric composites, especially on the effect of fire retardant on the fatigue behaviour of woven hemp fabric composites.

2.7 Summary of Literature

Based on the literature, there are numbers of work on hemp fibre as reinforcement in composite material. The properties of this material, especially hemp reinforced composite are varied depends on the different fibre volume fraction, chemical treatment, resin types and fabrication methods (refer Table 2.1, 2.2 and 2.3). Only by utilising fabric forms, overall performance of a bio-based composite can be achieved because fabric is easier to handle and could maintain its dimensional stability during the composite fabrication [31, 32, 33].

When utilising natural textile fabric, many workers are most likely only considered fibre volume fraction as an important parameter that contributes to composite material. The works done by Christian and Billington [35] and Song et al. [33] which use hemp fabric in their composite have proven that the fabric parameters (density and weave structure of fabrics) do influence the properties of composite materials. Therefore, there is less work emphasising on fabric properties such as fabric density, fabric weight, fabric's yarn crimp, yarn linear density and fabric strength that might be

contributed to composite materials and how these fabric properties would affect its properties behaviour.

Enhancing the compatibility between reinforcement and matrix can be done using chemical treatment. However, utilising chemical treatment on the materials will increase the cost of production. Except if the chemical treatment is necessary to improve certain properties of a material for certain applications, it would be wise just to apply basic chemical treatment in the fabrications. Study by Kabir et al. [36] showed that alkalisation treatment is good enough to produce a material with acceptance quality, and any post-treatment with acetylation and siloxane tend to reduce material properties. More important treatment should be done on the bio-based composite is fire retardant because, unlike high-performance reinforcement, natural reinforcement is flammable in nature. Recent works proved the enhancement of fire retardant of bio-based composite by incorporating fire retardant treatment in the composite fabrication process. However, so far there is no work done on applying fire retardant directly on the reinforcement material especially for hemp fabric.

Moisture and water absorption properties of a material are important criteria to define material's' durability. Several works showed that water or moisture absorption behaviours of hemp fibre composites are different based on the surround temperatures [35, 38, 40]. One thing in common is that the mechanical properties of hemp fibre composites decreased in the presence of water/moisture. It is believed that the fastness of fire retardant treatment will be degraded as water/moisture penetrates into a composite. Nevertheless, there is no work studied for the effect of water/moisture presence on the fastness of fire retardant treatment for the hemp fibre composite.

Fatigue behaviour is another criterion that can be used to define the durability of a material. Non-woven hemp fabric is proven to have comparable fatigue properties with glass fibre composite [42]. On the literature review, there still lack of knowledge about the fatigue behaviour of treated hemp fabric composite, especially on the effect of fire retardant and alkalisation treatment on the fatigue behaviour of woven hemp fabric composite. Therefore, this research attempts to measure and enhance the addressed issues above in order to develop a good hemp fabric reinforced composites.

Chapter 3 Characterisation of Woven Hemp Fabric

3.1 Introduction

Utilisation of natural textile fabric as reinforcement for composite material is well established. Nevertheless, as mentioned in Section 2.6.1, there is limited work considering fabric properties contribution to the properties' of composite materials [34]. Understanding some major properties such as fabric density, weight, thickness, yarn size and yarn crimp percentage will give a better understanding of how the fabric will behave and latter influence the behaviour of composite materials.

These analyses are also important to ensure the consistency of the natural woven fabric because even in one quality, fabric properties can be varied due to dissimilar quality of fibres, dissimilar weathering conditions experienced by the growing plants and irregularities of materials during spinning and weaving processes. Therefore, in this chapter, two fabric properties with similar quality are measured. Their properties have then been analysed with respect to (i) physical properties, (ii) thermal and chemical composition analysis, (iii) fibre density, (iv) fabric appearance structure, and (v) mechanical properties. Descriptive and inferential statistical analysis using analysis of variance (ANOVA) were also conducted in order to seek the significant differences between the average results and the suitability of both fabrics in composite fabrication.

3.2 Materials and Method

3.2.1 Hemp Fabric Materials

Two batches of commercial woven hemp fabric (WHF) were investigated and supplied by Hemp Wholesale Australia. These batches were bought within a time interval of about three months. According to the specifications provided by the supplier, the two fabrics had equal nominal properties. The weight of the fabrics was 271g/m^2 and can be categorized as 'heavy fabric' in textile terms.

According to the specifications given by the supplier, the fabrics were produced by 100% yarn hemp in both warp and weft with the similar yarn linear density (yarn size) of 100 tex (g/1000m) for each direction respectively. The yarns were converted from cleaned hemp fibre into yarn through spinning processes and the twist given was 430 twists per meter. These yarns were then converted into fabric via weaving processes and the fabrics were woven by employing a loose plain weave (taffeta) structure. Figure 3.1 shows a schematic diagram of plain weave fabric structure. As referred to plan view, the vertical yarn is known as warp while the other direction is weft. The plain weave structure can be categorized by observing the warp yarn which alternately and repeatedly goes over and under the weft yarn.

Plan view Cross-section

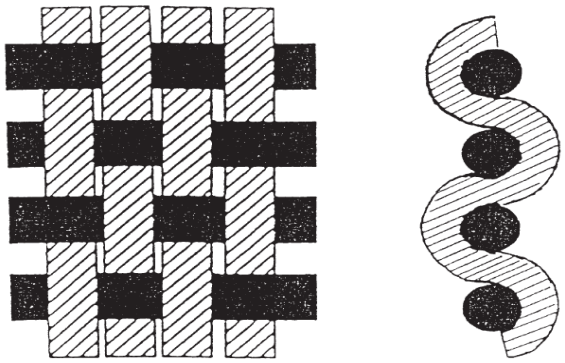

Figure 3.1 The plain weave fabric structure in plan and cross-section views [82].

Other than this, not much data was provided by the supplier. Therefore, further investigation was needed to characterise these two batches of hemp fabric. For comparison purposes, the two batches of hemp fabrics will be denoted as Fabric A and Fabric B (the batch bought after three months). Figure 3.2 shows the heavy weight 100% plain WHF used in this work.

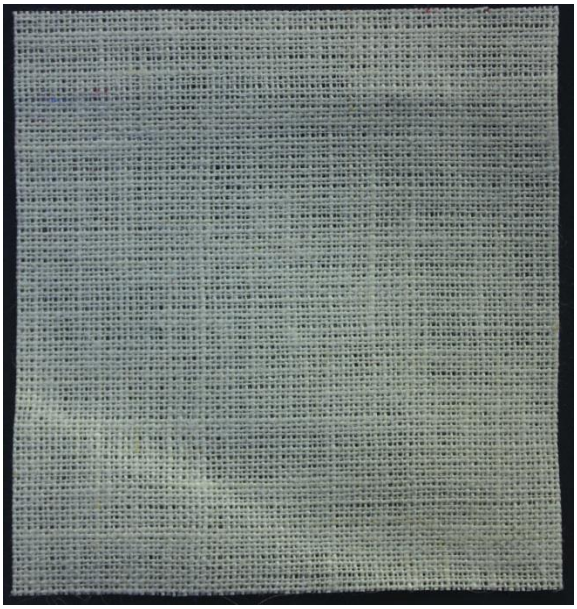

Figure 3.2 WHF used for this work.

3.2.2 Physical Properties Characterisation

WHFs are characterised for their weight, thickness, fabric density or fabric count while their yarn is characterised for its yarn size (linear density) and crimp (for warp and weft). All tests were done employing several textile materials standard methods with some alterations. These standard methods are commonly used in the textile industry for characterization as well as product quality determination purposes. Table 3.1 shows the standard methods used to characterise both WHFs.

Table 3.1 Standard methods used to determine fabric properties.

Properties	Testing	Standard Method
Fabric Density	Warp (end) and filling (pick) count of woven fabrics	ASTM D3775 [83]
Fabric Weight	Mass per unit area (weight) of fabric	ASTM D3776 [84]
Fabric Thickness	Thickness of Textile Materials	ASTM D1777 [85]
Yarn Size	Yarn number (linear density)	ASTM D1907 [86]
Yarn Crimp	Yarn crimp and yarn take-up in woven fabrics	ASTM D3883 [87]

Yarn spacing is normally related to the fabric compactness and this can affect the fabric properties significantly. Yarn density in fabric is generally known as ‘fabric density’ or ‘fabric count’. By employing ASTM D3775 standard method, fabric was placed on a smooth surface and the number of warp and filling yarns were counted using a pick counter in a 2cm length and the result was pronounced as; total warp yarn × total weft yarn, per 2cm.

Fabric weight was analysed in accordance to ASTM D3776. Five specimens were needed for this analysis and three readings were taken from each specimen to obtain an average of fabric weight. The weight was measured in gram per square meter (g/m^2).

Fabric thickness was measured according to ASTM D1777. Twenty randomly selected locations were used to obtain the average value. This is to make sure that this precision value represents the thickness of a sample, because the sample has a lot of thick and thin places all around. The thickness values were taken in millimetres (mm).

ASTM D 3883 was followed to measure yarn crimp. Parallel lines were marked in the warp direction 20cm apart (this is the distance of the yarn in the fabric, Y1 = 20cm). A cut of 30cm was made along the filling yarn, which crossed the parallel lines. Several yarns from one edge were unraveled. The next ten yarns were carefully unravelled for measurement. Each yarn was pulled taut without exerting extreme force and the extended length between the two marks was measured as Y2. The yarn crimp, C, is calculated as shown below in Equation (3.1):

$$Yarn\ crimp\ (\%), \qquad C\ = \frac{Y_2 - Y1_1}{Y1_1} \times 100 \tag{3.1}$$

Yarn linear density was measured in accordance with ASTM D1907. Yarn was unravelled from the fabric and then cut to 1 m length before it was weighed using a weighing balance. Ten specimens were measured and the average weight, w, in grams, was used for calculating the yarn linear density using Equation (3.2):

$$Yarn\ size\ (tex), \qquad N\ = \frac{w \times k}{l} \tag{3.2}$$

where *l* is the length of yarn in meter and *k* is the constant which equals 1000 m/g for tex.

The density of the hemp fibres was determined by a Multipycnometer MVP D160E. Helium gas was used as a displacement medium. The helium was added to the fibres under vacuum conditions to ensure that all interior air cavities in the submerged fibres (e.g. the fibre lumen) were filled with helium. The data reported are the average and standard deviation of 3 measurements.

Fabrics were conditioned at 65% R.H. and 23°C for 24 hours prior to characterizing their moisture content. Moisture content of the fabric was determined by using a Sartorius Moisture Analyser MA100/MA50. This instrument will heat up the sample up to 105°C. The average value was calculated as follows:

$$Moisture\ content\ (\%), \qquad M = \left(\frac{m_1 - m_2}{m_2}\right) \times 100 \tag{3.3}$$

where m_1 is initial weight of fabric and m_2 is the weight of fabric after heating.

3.2.3 Thermogravimetric Analysis

Thermogravimetric analysis (TGA) and differential thermogravimetry (DTG) were carried out using a thermal gravimetric analyser (TGA-Model No. Q500) at the temperature range from 24 to 600°C with a heating rate of 10°C/min under a nitrogen environment purged at 20 ml/min.

3.2.4 Mechanical Properties

The tensile properties (ASTM D 5034) of hemp fabrics were characterized using a universal testing machine MTS Alliance RT/10. 75 mm wide test specimens were cut in the desired direction (warp or weft) and then equal numbers of yarns were removed from both sides until the specimen width was reduced to 50 mm. The same procedure was followed for test strips in both warp and weft directions. Tensile tests were performed using a gauge length of 75 mm and a crosshead speed 10 mm/min. The cross-sectional area used to convert load into stress was calculated from the test specimen width and the thickness of fabric obtained from the fabric characterization [26, 88].

Figure 3.3 shows a typical tensile test curve for the hemp fabric used in this work. According to Figure 3.3(a), the initial part of the curve was nonlinear but then increased its slope slowly until finally becoming linear. The hemp fabric's mechanical properties will be discussed further in the Section 3.3.7. Other mechanical properties of this material cannot be determined under the nonlinear curve. Hence, a linear trend line, as shown in Figure 3.3(b), was drawn to extend the linear part of the curve to the axis of strain. With this linear trend line extension for each stress-strain curve, the tensile modulus, tensile stress and strain at peak can be determined.

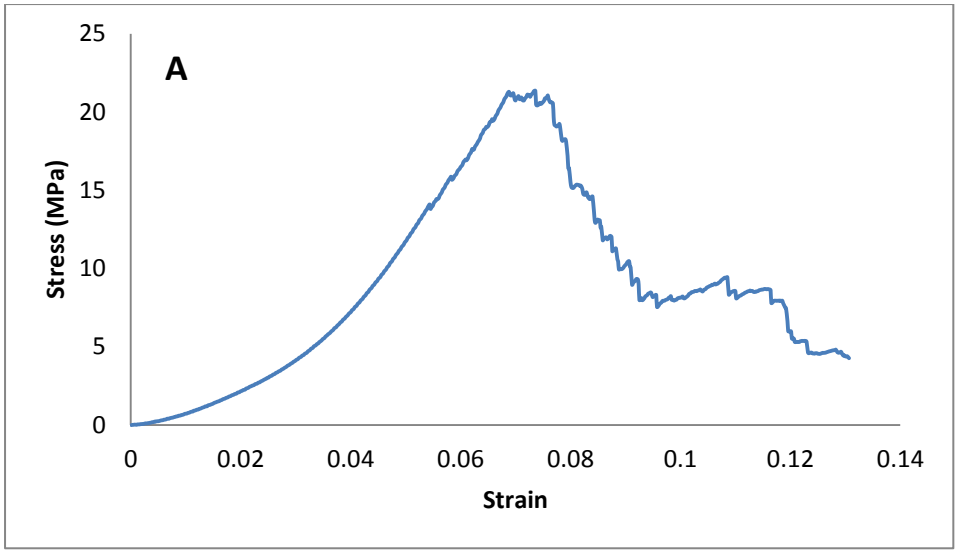

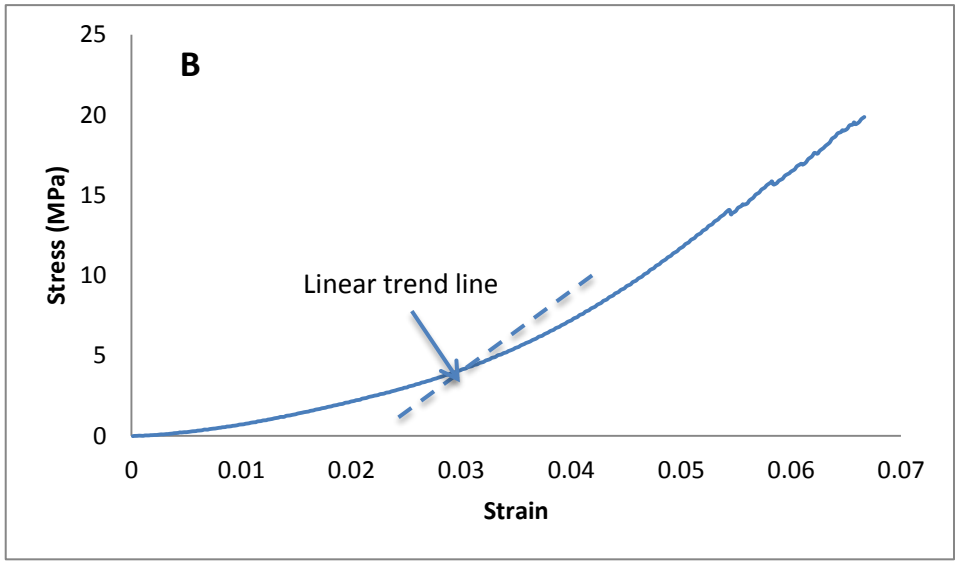

Figure 3.3 Typical curve of a stress–strain for hemp fabric: (a) is the whole complete curve and (b) is a detail of the initial non-linear part.

3.3 Results and Discussion

3.3.1 Physical Properties of WHF

The determined physical properties of hemp fabric are presented in Table 3.2. No difference was found in the weaving structure of either fabric. They were weaved in a perfect plain weave similar to Figure 3.1. When observing for fabric fault or defect,

no missing pick was found along the fabric length for at least 5 meters for both fabrics. A missing pick a defect in woven fabric which can be detected by missing or out-of sequence yarn. On the fabric, we can see an empty line throughout the width wise of fabric and this defect is usually repeated in sequence in fabrics. This is usually caused by the loom (weaving machine) due to poor insertion of the weft yarn. Fabric that has this defect will suffer in inconsistent mechanical properties and poor fabric handling especially in the weft direction. Both fabrics tested were free from this fault. Therefore, it can be concluded that all fabrics were manufactured in a good loom (probably shuttleless loom) and they were good-quality fabrics.

Table 3.2 Physical properties of WHF.

Fabric Types		Fabric A	Fabric B
Weave Structure		Plain	Plain
Fabric Density (per 2cm)	Warp	25	25
	Weft	23	23
Fabric Weight (Reading) (g/m^2)		231.410	228.520
Thickness (mm)		0.415	0.417
Yarn Size (Tex)	Warp	89.661	90.459
	Weft	92.896	92.970
Yarn Crimp (%)	Warp	5.4	6.0
	Weft	9.3	9.3

Fabric density indicates the number of warp and weft yarns in a certain length of fabric. Density of fabric can be used to indicate yarn spacing and this can relate to fabric compactness. The different in the property between the two fabrics relates to their different fibre density in fabric and weight. In this work the measurement was done in the metric system, which is centimetre (cm). Based on Table 3.2, both fabrics were determined to have a similar density that was 25 warps/2cm and 23 wefts/2cm (25 × 23 /2cm).

According to the specifications provided by the supplier, the weight of both fabrics was 271g/m^2. However, measurement revealed that both fabrics, Fabric A and Fabric B had different weights: 231.41 and 228.52g/m^2 respectively. The specification given by the supplier was at least 17% higher than the measurement determined. Therefore, further measurement on the fabric properties was needed to gain accurate results. The thickness of Fabric A was recorded at 0.4157 mm while for Fabric B was a bit higher at 0.4168 mm.

Yarn size or yarn linear density has a close relationship with fabric weight. Apart from measuring fabric weight, the density and compactness can also be determined from this property. For this reason, the warp and weft yarn sizes for both fabrics were determined. According to the supplier, the size of warp and weft yarns for the WHF is 100 tex. However, it was found that the determined yarn sizes in both fabrics were at least 7% less than what was mentioned by the supplier. From Table 3.2, Fabric A and Fabric B possess similar weft yarn size, which was 93 tex. Nevertheless, in the case of warp yarn, Fabric A possessed a bit smaller warp yarn size in comparison with Fabric B, which was 89.661 and 90.459 tex respectively. Fabric B should have been heavier as its weft yarn size was measured higher than Fabric A, yet based on the result, Fabric A was a bit higher than Fabric B. Again, further investigation on the fabric properties was needed to obtain accurate results.

Yarn crimp is the waviness of the yarn in the fabric due to the interlacing of warp and weft yarns. It is well known that yarn crimp in a woven fabric is an important property that affects most of its physical properties including the thickness and weight of fabric [89]. Based on the results in Table 3.2, both fabrics had a similar weft crimp percentage, which was 9.3%. In terms of warp yarn crimp, Fabric B had a slightly

higher crimp percentage than Fabric A with a percentage of 6.0 and 5.4% respectively. Through observation of the warp crimp percentage for both fabrics, Fabric B had a longer warp yarn running on the longitudinal direction of the fabric than Fabric A. However, the crimp percentage does not give the reason for the heavier weight of the Fabric A since its warp yarn crimp percentage was recorded as lower.

3.3.2 Measurement of Fabric Weight

Based on the fabric specification given by the supplier, both fabrics should had a similar aerial density or fabric weight of 271g/m^2. However, the determined data obtained from the measurement (Table 3.2) shows that Fabric A had a higher weight (231.41g/m^2) than Fabric B (228.52g/m^2). These figures are quite doubtful having said that Fabric B possessed a higher warp yarn crimp percentage and warp yarn size while the weft yarn crimp percentage and weft yarn size were identical.

Nevertheless, some other properties obtained from the measurement such as fabric density, yarn size and yarn crimp percentage can be used to measure and determine the fabric weight precisely [90] . The aerial density or fabric weight, W, can be measured using Equation (3.4):

$$Fabric\ weight\ (g/m^2), W\ = \frac{N_1(1+C_1)}{P_1} + \frac{N_2(1+C_2)}{P_2} \quad \textbf{(3.4)}$$

Where *N* is the yarn size calculated from Equation (3.2), *C* is the yarn crimp percentage calculated from Equation (3.1 while subscripts 1 and 2 refer to warp and weft yarn respectively). P is the yarn spacing in mm which can be calculated from Equation (3.5):

$$Yarn\ spacing\ (mm), \qquad P_n = \frac{t}{d} \tag{3.5}$$

Where subscript n = 1 or 2 which refer to warp or weft yarn, t is the constant value of length for certain fabric density which is equal to 20 mm and d is the respective fabric density.

Table 3.3 Results of fabric weight by calculation using Equation 3.4.

Fabric Types		FSA10 A	FSA10 B
Weight (g/m^2)	Total wt. of Warp	118.083	119.813
	Total wt. of Weft	116.712	116.859
Fabric Weight (g/m2)		234.796	236.672

Results of fabric weight using Equation (3.4 in Table 3.3 gave more reliable readings with Fabric B weighing more than Fabric A: 236.672 and 234.796g/m^2 respectively. The higher weight possessed by Fabric B is consistent with its higher yarn size and yarn crimp percentage. Therefore, the calculation on fabric weight using Equation (3.4) can be used to obtain reliable and accurate results.

ASTM D3776 is the standard method for measuring fabric weight and it is normally used by fabric manufacturers, in fabric merchandise and by buying officers. Nevertheless, error in fabric weight measurement is common and usually due to human factors. The most common error occurs when preparing the sample before the weight is taken. Without proper and suitable equipment, the testing officer can easily cut a little more or less fabric and this can lead to inaccurate results. It is believed that the uncertain results obtained when using this standard method was due to the cutting error on the fabric sample thus leading Fabric A possess a higher weight than the Fabric B. When this happens, an accurate calculation measurement is needed for the yarn size, yarn crimp percentage and yarn spacing for both warp and weft yarn.

It is advisable that, when a fabric is meant for use in an engineering application, (regardless of whether it is made of natural resources or man-made) measurement of the fabric weight should be done using the calculation as in Equation (3.4), which is reliable and accurate. This kind of measurement can eliminate the risk of results contaminated by human error, reduce the employment number of the standard method as well as save more fabric samples in the fabric characterisation analysis.

The results shown in Table 3.2 and the results from fabric measurement (Table 3.3) give an idea that both fabrics are designed as they should be physically and mechanically balanced in warp and weft direction. Even though it had a higher number of warp (25 yarns) than weft yarn (23 yarns), the weft yarn was coarser (93 tex) than the warp yarn (90 tex). However, even though it is designed to be mechanically equal in warp and weft direction, other factors such as total weight of warp or weft yarn, yarn crimp etc. will result in a slight difference in mechanical properties. The difference in their mechanical properties will be further discussed in Section 3.3.7.

3.3.3 Density of Fibre

The density of fibre for Fabrics A and B was determined by pycnometry and is presented in Table 3.4. Each series of measurements consisted of two specimens and three reading were taken for each fabric. The results show that, for each series of measurements, the fibre density was higher for Fabric A than Fabric B, with overall means of 1.512 and 1.473g/cm^3 respectively. The determined density of the hemp fabric fibres was within the typically reported densities of hemp fibres varying between 1.4 and 1.5g/cm^3 [10, 34]. The density of natural fibre is closely related to its cellulose content and for hemp fibre, this will be further discussed in Section 3.3.6.

Table 3.4 Density of fibre (g/cm^3) of the Fabrics A and B determined by 3 series of measurements.

	Series of measurement				
Fabric Types	I	II	III	Average	Stdev.
Fabric A	1.528	1.499	1.510	1.512	0.015
Fabric B	1.481	1.472	1.466	1.473	0.007

3.3.4 Fabric Appearance Structure

Figure 3.4 shows the appearance of the WHFs' structure. It was observed that the weave structure of both fabrics was a plain/taffeta weave structure. This is the most basic woven structure other than twill and satin. Most woven fabrics used for technical purposes are manufactured with a plain weave structure. Apart from being easy to produce, it reduces the cost of production as well as downtime of the loom, thus increasing productivity [82]. Other weave structures are more complex and the arrangement of yarns is more complicated leading to yarn breakage due to the friction between the yarns in the loom.

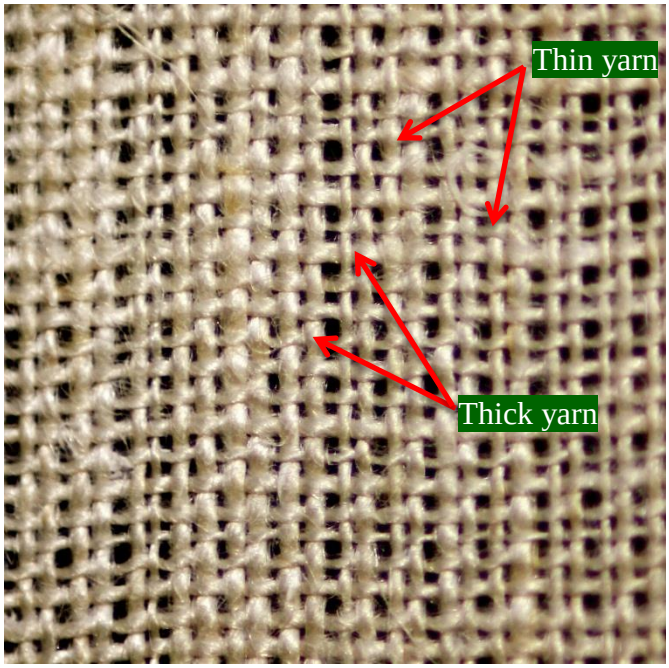

Figure 3.4 The structure of WHF.

When observing the structure of the hemp fabric, the yarns were not homogenous entities but varied in cross-sectional dimensions. Figure 3.4 shows that there were lots of thick and thin yarns running in the warp and weft directions. The yarn sizes determined for both fabrics were the average values (refer Table 3.2). Since the fabrics were made from natural fibres, these kinds of irregularities and inconsistencies within the yarn were expected. Yarn is produced in a long production line called 'spinning'. In the spinning process, drawing processes are purposely used to achieve the required yarn size. However, even with perfect drawing, the irregularities occur because natural fibres are usually short and it is difficult to control the total fibre along the yarn [34]. The yarns for both fabrics were observed to have twists with a right-handed angle to the yarn axis. This twist is also known as a Z-twist in contrast to a S-twist. According to the supplier, all the yarns for both fabrics either warp or weft had been spun with 430 twists per meter. Since the focus of this work is on the fabric rather than yarns, and the twist angles definitely will be varied slightly because of the nature of spun natural yarns, this twist value was accepted as specified by the supplier. More importantly, the properties related to the fabric appearance should be emphasized.

Then fabric cover factor indicates the extent to which the area is covered by one set of yarns. This is an important criterion for fabric applications. For instance it is a major concern to consider how is the level of shade for a fabric to be used as a shading material, or how good the resin penetration if certain textile fabric is used as a reinforcement. To determine the total fabric cover factor, a modified equation (Equation (3.6)) introduced by Chen and Leaf [90], was used and the K value was the ratio on how big the area is covered by the yarns:

$$Total\ fabric\ cover, K = C_1 + C_2 - C_1C_2$$

(3.6)

Where subscripts *1* and *2* refer to warp and weft yarn respectively and *C* is the fractional yarn cover which can be calculated from Equation (3.7):

$$Fractional\ yarns\ cover, C_n = s \times \sqrt{(N_n/f_d)} \times d_n \times 10^{-3}$$

(3.7)

Where subscript *n* = 1 or 2 refers to warp or weft yarn, *s* is the constant which is equal to 4.44, *N* is the yarn size calculated from Equation (3.2), f_d is the fibre density (refer Table 3.4) and *d* is the respective fabric density.

Table 3.5 Result of cover factor for both fabric used in this work.

Fabric Types	Fractional Yarn Cover		Total Fabric Cover
	Warp C_1	Weft C_2	K
Fabric A	0.435	0.406	0.664
Fabric B	0.433	0.405	0.663

The results of the cover factor are tabulated in the Table 3.5. The table shows no differences Fabric A and Fabric B. The results clearly show that, for both fabrics, 66% (0.66) of the fabric sheets were covered by yarn. The slight differences between them are most probably due to mechanical variations which occurred on the loom during their production. From the textile point of view, bot h fabrics share identical cover factor quality and can be used in a similar batch of textile product for a certain application. The effect of water penetration and air permeability should be also comparable for both fabrics. The yarns only covered 66% of the fabric sheet, meaning that the water and air will easily penetrate or pass through the fabric. In composite fabrication, the good penetration of resin into the whole fabric system is expected.

Nevertheless, in terms of technical applications, the physical, chemical and appearance properties of fabric are inadequate for a fabric used in technical applications. Therefore, assessment of their mechanical properties is more crucial to study how well they to external forces.

3.3.5 Thermal Analysis

Thermal analysis of WHF sample was determined using thermogravimetric analsyis (TGA) and derivatives thermogravimetric analysis (DTG) as shown in Figure 3.5. The thermal stability was studied in terms of weight loss as a function of temperature in nitrogen atmosphere. From the curves, the decomposition of both fabrics against increasing temperature was found a little different. Based on the both DTG curves, the highest mass loss rate for Fabric A was recorded higher than Fabric B at 1.51%/°C at 370°C and 1.38%/°C at 380°C respectively.

For Fabric A, the decomposition started from room temperature (25°C) up to about 120°C with a weight loss percentage of 4.75%. This was due to the evaporation of absorbed moisture in the fibres. Therefore, the sample weight dropped slightly in the initial process of heating [91].

Further decomposition happened with a 75.35% mass loss at the temperature between 220 and 400°C. This was due to the degradation of the hemicellulose and cellulose composition in the hemp fibres [91]. At first, as the temperature increases, hemicellulose is degraded due to the cellular breakdown and is then followed by cellulose at the higher temperature because it is highly crystalline [92].

The sample continued to decompose from 400 up to 458°C with the weight loss percentage of 3.52%. This is the phase of lignin degradation after hemicellulose and

cellulose. Lignin is the toughest component and responsible for the rigidity of the natural fibre. Thus, a higher temperature is needed for lignin to decompose. The Fabric A's curve stopped at 458°C and 15.64% mass remained. It was observed that the remaining component was nothing but the ash content. This ash contains inorganic material such as silica which can only degrade at a very high-temperature [91].

As for Fabric B, there was no difference in behaviour as compared to Fabric A. Initial reduction on the mass percentage was 4.26% which happened at the temperature of 25 to 120°C and was due to evaporation of moisture content. Then, the degradation of hemicellulose and cellulose occurred at 220 up to 400°C with the weight loss percentage lower than Fabric A which was 67.93%. Another weight loss percentage occurred in the phase of lignin degradation with the value recorded a bit higher than Fabric A which was 5.80% at the temperature of 400 to 458°C. Fabric B had a higher ash content with the amount recorded at 22%.

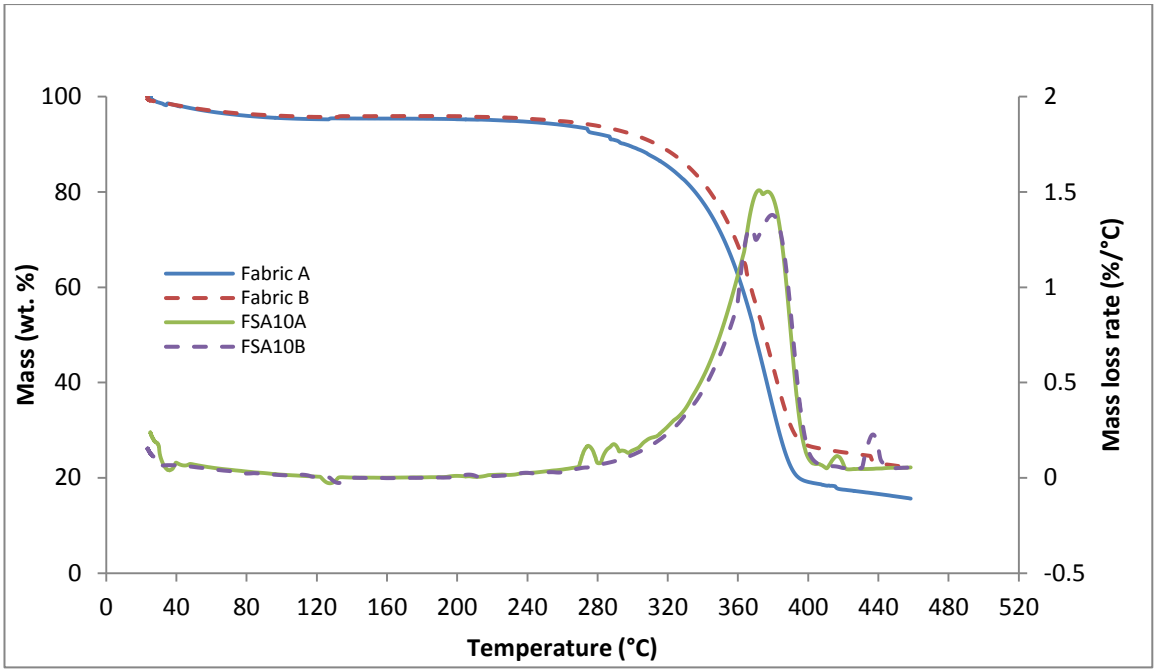

Figure 3.5 TGA and DTG curves of WHF.

3.3.6 Chemical Composition of Hemp Fabric

The chemical composition of WHFs was determined by using TGA analysis and estimation based on the pyrolysis study. Generally, there are four phases of thermal decomposition for natural or plant fibres. These phases are moisture evaporation, followed by hemicellulose decomposition, cellulose, lignin and lastly their ash [91]. Results obtained by Yang et al. [92] on the natural material pyrolysis can be used as a benchmark for estimating the chemical composition of WHF in this work.

The degradation of hemicellulose started at 220°C and finished at 315°C yet they produced 20% of solid residue. Hemicellulose consists of various saccharides appearing as a random amorphous structure and rich in branches which easily decomposes at lower temperatures. The cellulose decomposes at a higher temperature range (315 to 400°C) and produces fewer residues than hemicellulose, which is 6.5%. Cellulose does not start to decompose until the hemicellulose has completely

decomposed. The reason for this is that cellulose has a high crystalline chain in its structure than amorphous, thus making it relatively thermally stable. Lignin decomposes at a wide temperature range from 160 to 900°C. Lignin is a tough component that gives rigidity to the plant material and to the cell wall by becoming a binder to individual cells in the middle lamella region. This is the reason why the lignin is difficult to decompose at lower temperatures [92].

Based on the pyrolysis work above, the chemical composition of hemp fabric can be estimated using its TGA curves. Five compositions value can be obtained for moisture or water content, hemicellulose, cellulose, lignin and ash. Their content can be determined by measuring the weight loss percentage at the certain range of temperature from the pyrolysis work by Yang et al. [92]. Table 3.6 presents the determined chemical composition of WHF using the estimation method.

Table 3.6 Chemical compositions of WHFs.

Hemp Fabric Types		Fabric A	Fabric B
Composition (%)	Moisture	4.91	4.31
	Hemicellulose	8.46	5.95
	Cellulose	67.47	64.77
	Lignin	3.52	2.92
	Ash	15.64	22.05

Moisture content of WHF can be easily measured from the weight loss percentage from the TGA curves because it is the first phase of thermal decomposition of natural plants. In order to verify the results in Table 3.6, the content of moisture for both hemp fabrics were measured using a Sartorius Moisture Analyser MA100/MA50. This equipment measures the different weight of hemp fabric before and after heating. While, the result of moisture content measurement for Fabric A and B using this equipment were 4.75 and 4.42% respectively, the results measured from the TGA

curves for both fabrics were determined to be 4.91% for Fabric A and 4.31% for Fabric B. The results of the two methods are said comparable and the slight difference between them are most probably due to the effect of the different temperature and humidity when the tests were done.

Fabric A had a higher hemicellulose content in comparison with Fabric B, which was 8.46 and 5.95% respectively. These figures are comparable with the results obtained by several other works [93-95]. Since there is no information given by the supplier, the differences in value between two fabrics is most probably due to the chemical treatments given by the hemp fabric manufacturer. It is well known that sodium hydroxide (NaOH) is the common chemical used, not only in the yarn processing, but also in the weaving preparation process, and its usage can be as high as 30% w/w. Kabir et al. [94] found that the hemicellulose content reduced (5.40 to 4.51%) as the concentration of alkali treatment increased (0 – 10% w/w). Therefore, it can be said that the difference in hemicellulose content in Fabrics A and B is most probably due to the chemical treatment to both fabrics during their manufacturing.

The highest component is cellulose and it is the main constituent in any plant fibre. Cellulose content in Fabric A (67.47%) was recorded slightly higher than Fabric B (64.77%). The figures are comparable and within the results determined by other works [38, 94, 96-98]. The small difference in their density (refer Table 3.4) is due to the slightly higher cellulose content of Fabric A (refer Table 3.6). According to Madsen et al. [93], the density of hemp fibre can vary depending on how much the cellulose content in the fibres. When analysing the results obtained in as well as comparing with the results of other works, he concluded that the increase of cellulose content in the fibre, can lead to a higher density of the fibre. In his work, the

determined fibre density was much higher, in the range of 1.58 – 1.60g/cm^3 with the determined cellulose content in the range of 88 to 90% [93]. Therefore, the determined average density of hemp fibre in this work is relevant to the measured cellulose contents of both fabrics and the results' trend follows the trend obtained by Madsen et al. [93].

The lignin content in Fabric A and Fabric B were determined at the temperature of 400 to 458°C, where the burning was completed and the results were recorded as 3.52 and 2.92% respectively. Again, for a reason similar to hemicellulose, the lower content of lignin for both fabrics is most probably due to the chemical treatment used during their manufacturing. Sedan et al. [99] presented a hemicellulose and lignin content percentage of 10.9 and 6% respectively. The lignin composition in his work is high in comparison to the lignin composition in this work and their higher value is possible as they used hemp in fibre forms instead of woven fabric. Extracted hemp fibre is the raw material of hemp product before it is converted into other forms of material. Therefore, their hemp fibre did not go through chemical processes as compared to hemp fabric which has gone through many chemical processes such as in spinning (conversion of fibre into yarn) as well as in weaving (conversion of yarn into cloth).

The ash content for Fabric A and Fabric B were measured at 15.64 and 22.05% respectively. Ash is the component that contains inorganic material such as silica and can only be decomposed at a very high temperature [91]. Therefore, the higher ash content in the Fabric B is associated with the fabric containing a higher level of inorganic material than Fabric A. Nevertheless, this ash content does not affect the mechanical properties because the fibre is most affected by the contents of hemicellulose, cellulose and lignin [34, 49].

3.3.7 Mechanical Properties

A typical stress-strain curve of WHF is shown in Figure 3.3(A). Study on the behaviour of WHF in this work is clustered in three phases. The first phase is the initial region that demonstrates a curve with a low slope. Second phase is the linear region of the curve after fabric settlement which rises steeply until its summit is reached, and the third phase is the curve after it reached the peak.

In the initial phase, the curve rose with a low slope due to decrimping and crimp interchange. The decrimping and crimp interchange is internal interaction (crossover between warp and weft yarns) of a fabric that results in the initial curve. When a WHF is extended in either of the principal directions, a straightening of the crimped yarns occurs in the direction of force. In the direction of force, the yarns appear to become less flattened due to the consolidation into a more circular cross-section. As the pressure builds up for the yarn in the direction of force, the continuous interchange between the two yarns also occurred simultaneously, thus increasing the crimp in the yarn perpendicular to the force direction.

Yarns in the direction of force will become round and less flattened as the fabric is further extended. Here, yarn and fibre extensions will occur, but the yarn extension only accounts for a small portion as compared to the extension of the yarn in the first phase. The small extension of yarn here suggests that the interaction between the fibres due to the twist led to the yarn becoming tighter and stronger, creating a build in pressure for the yarn to resist tensioning force. The internal interaction still happened, but the contribution of the perpendicular yarns against the force direction was small. This behaviour is shown in the second phase in which the stress-strain curve increased sharply until it reached the peak and then broke.

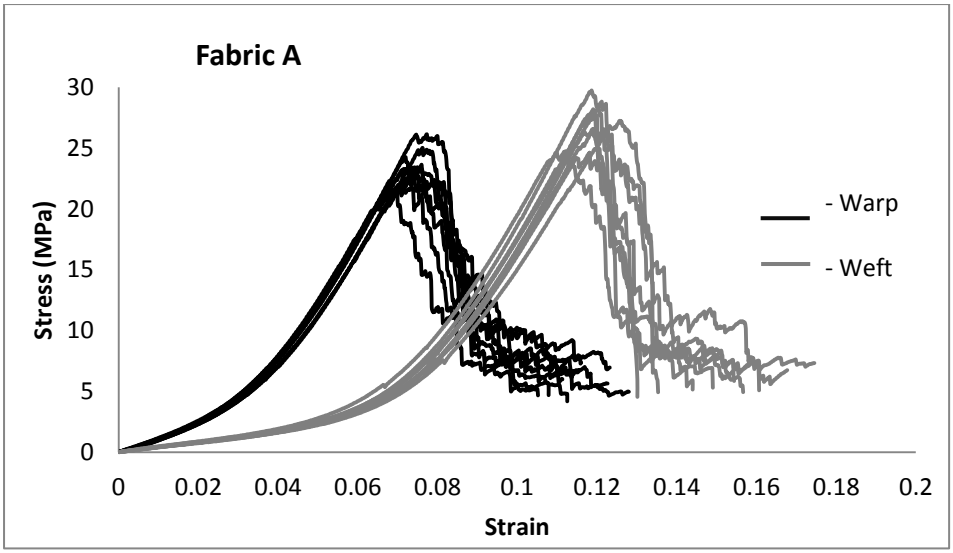

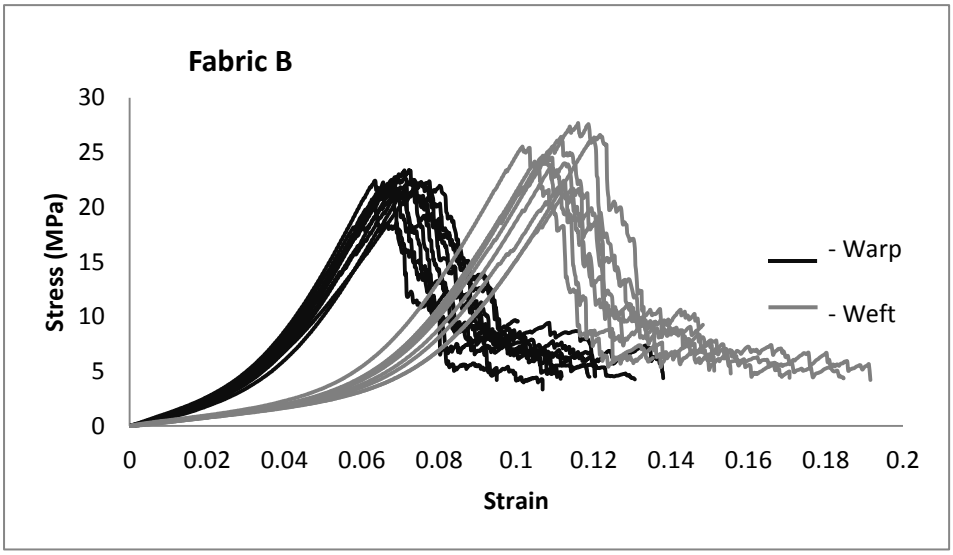

Figure 3.6 Tensile stress-strain response for Fabrics A and B.

Figure 3.6 shows the tensile stress-strain response for both Fabrics A and B. For each type of fabric, specimens were cut and tested in the warp and weft direction. Table 3.7 summarizes the average tensile properties for each WHF. The tensile properties reported are the average and standard deviation from all the specimens. The curves were cut off at the point of ultimate stress. For every type of fabric, the curves were clearly divided into two groups represented by the warp and weft yarns.

In the case of Fabric A (Figure 3.6), the initial curves rose with a low slope due to the decrimping and crimp interchange of fabric. This state was observed longer for the weft direction due to the higher crimp percentage that it possessed (9.3%) in comparison with the warp direction (5.4%). Therefore, it took more time for the weft yarn to be straightened, and most of the weft specimens had reached their settlement state at approximately 0.07 strains while warp specimens were recorded at about 0.03. After the decrimping and crimping state at initial stage, the curves for both fabrics rose steeply until their peaks were reached. The wefts' failures were observed mostly at higher stress than warps yarn. The higher yarn crimp percentage of wefts is the reason that it failed at higher stress than the warp on top of the higher yarn size it possessed (93 tex for weft and 90 tex for warp).

The curves rose consistently from the beginning, yet greater variation is noticeable near failures because failure initiates at thinner yarn places (Figure 3.7) which were scattered along the fabric specimens [35, 100]. Figure 3.7(a) shows an example of a specimen after being subjected to tensile force. From the figure, it is clearly shown that the yarn fractures are scattered along the fabric specimen and most likely to break at thin places. Figure 3.7(b) shows a magnified yarn fractures area on the fabrics. It was observed that the fractures occurred mainly at the area that had many thin yarns. Many pulled-out fibres were found at the fractured yarns suggesting that the fibres were resisting the tensile force acting on them.

There was not so much difference in the stress-strain behaviour for Fabric B (Figure 3.6) in comparison with Fabric A. Even its specimen curve started to reach the linear part at a similar strain. This is because the strength of warp and weft yarn for both fabrics was quite similar (refer Table 3.2). The slight difference between the

specimens' behaviour is due to fabric variations such as yarn irregularities and thick-thin places. Therefore, it can be said that both fabrics share similar behaviour in stress-strain.

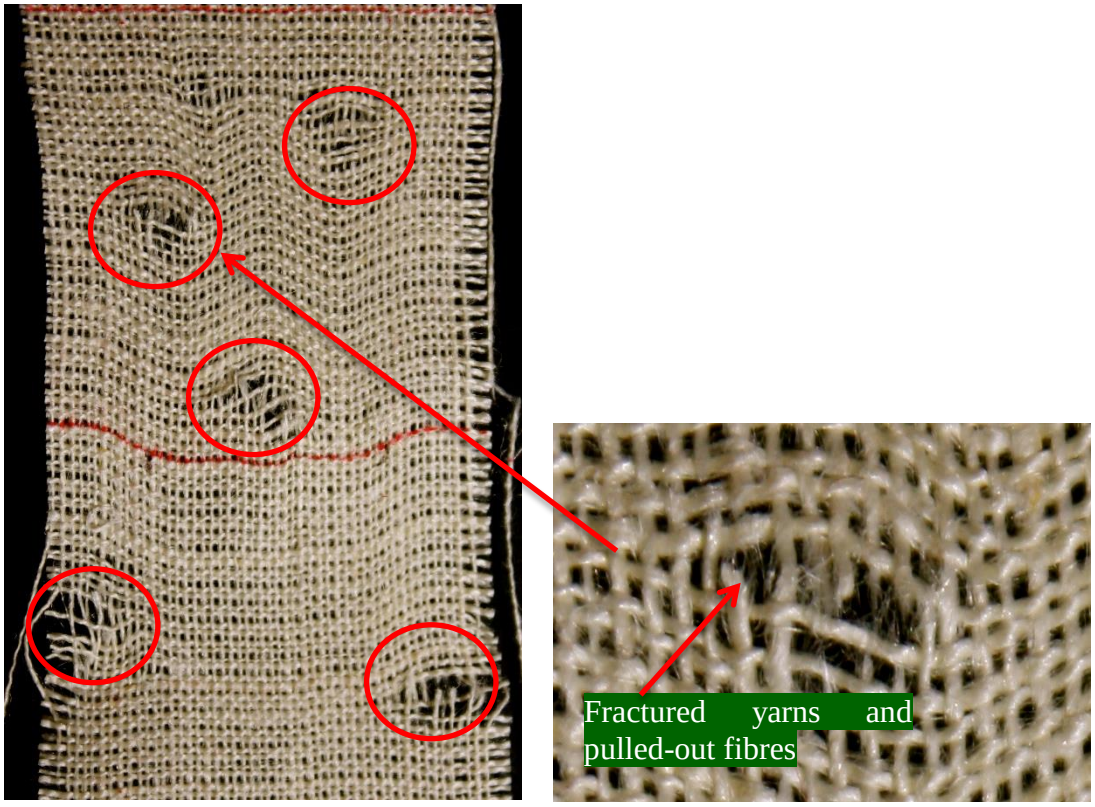

(a) (b)

Figure 3.7 Typical fabric fracture after subjected to tensile force, (a) whole specimen, (b) magnified fracture area.

The results of tensile properties for both WHF are shown in Table 3.7. The figures in the table are the average ± standard deviation for at least nine specimens. The summary for all tested specimen results can be found in Appendix A. Overall, it can be said that the tensile strength of Fabric A is higher than Fabric B. In terms of warp direction, the tensile strength of Fabric B was recorded at 6% less than Fabric A which was 24.883 and 26.304MPa respectively. A similar trend was found in the weft

direction specimens with the tensile strength of Fabric B determined to be 21.975MPa, 6.4% lower than Fabric A which was 23.392MPa.

When the fabric was fully stretched, that is after the decrimping process at internal interchange (refer to Figure 3.6), the yarns became straight and round. The tensile force acting on the fabric was divided and separated on the yarns in the force direction (either warp or weft) and against the build-up of pressure from each yarn. The build-up of pressure occurred due to the interaction of fibres in the yarns from the twist given to them which resisted the tensile force. How great the force yarns can resist depends on how much twist is given to the yarn because the twist is the reason that the fibres entangle with each other in a yarn [52]. In the normal practice, the higher the amount of twists given to them, the higher the build-up of pressure in the yarn can be produced (for both fabrics, warp and weft yarns were spun with 430 twists per meter). Other factors that contribute to the build-up of pressure in the yarns are fibre length, total fibres, fibre density and linear density (yarn size). All the factors are combined in a fabric and built-up pressure is accumulated against the tensile force.

Another factor that contributes to the strength of the fibres in the fabric is the cellulose content. Cellulose is the compound in the natural fibre that is responsible for giving strength. According to Azwa et al. [67], tensile strength and Young's modulus increase as the cellulose content increases. Based on Table 3.7, the tensile strength of warp and weft yarns for Fabric A were determined to be higher than Fabric B. This is consistent with a higher cellulose content in Fabric A than Fabric B with the overall content of 67.47 and 64.77% respectively (refer Table 3.6).

The tensile strain of Fabric B in warp direction was determined to be 20% higher than Fabric A; 0.093 and 0.074 respectively. As for weft direction, Fabric A was found to

be slightly higher (7%) than Fabric B with overall results of 0.121 and 0.112 respectively. The higher strain in weft direction for both fabrics was due to the higher crimp of weft yarn in the fabrics; that is 9.3%. The longer strain in warp direction for Fabric B was due to the higher crimp percentage, which was 6.0% compared to Fabric A which was 5.4% (refer Table 3.2).

A similar trend was observed for tensile modulus. For Fabric A, tensile modulus was recorded at 2% higher than Fabric B with average values of 0.54 and 0.53 respectively. In the weft direction, the tensile modulus of Fabric B was recorded at 0.493GPa, 3.7% lower than Fabric A (0.511GPa). Overall, it can be concluded that the tensile modulus for the warp was higher than the weft direction for both fabrics. Although the yarn size for the weft direction was measured higher the than warp direction, a higher density of yarn (fabric density) was found in the warp direction for both fabrics; 23 and 25 for weft and warp respectively (refer Table 3.2). This is the reason why the tensile modulus is slightly higher in warp direction. When comparing both fabrics, Fabric A can be said to have a slight higher tensile modulus than Fabric B due to the higher lignin content in its composition. Apart of cellulose contribution to the fibre stiffness (cellulose content of Fabric A is higher than B), lignin is the compound that is also responsible for the fibre stiffness. Lignin is a complex hydrocarbon that gives rigidity to a plant and it functions as a matrix for cellulose fibrils in fibres [67, 91, 92]. Therefore, the higher cellulose content and lignin are the reason for the slightly higher tensile stiffness for Fabric A compared with Fabric B (refer Table 3.6).

Table 3.7 Summary of average tensile properties for WHFs.

Fabric Types		Peak Load (N)	Tensile Strength (MPa)	Tensile Strain	Tensile Modulus (GPa)
Fabric A	Warp	442.1±29	23.392±1.52	0.074±0.004	0.540±0.023
	Weft	497.5±56	26.304±2.99	0.121±0.008	0.511±0.032

Fabric B	Warp	415.3±21	21.975±1.11	0.093±0.026	0.530±0.041
	Weft	469.3±38	24.833±1.99	0.112±0.006	0.493±0.044

Data in Table 3.7 cannot be used to accurately determine the significant difference between the average values because of the variation of raw data to their mean/average. Therefore, an inferential statistic should be applied to test significant difference between the mean values. The results come from inferential statistic are more valuable especially for the manufacturers to decide the suitable material to be used. An analysis of variance (ANOVA) was conducted using IBM® SPSS® Statistics version 21 to test the significant difference between all samples in this work. ANOVA uses F distribution that compares three or more population means to determine whether all the populations or samples are equal. Taking tensile strength in Table 3.8 as an example; in this case, 'sum of squares' is the sum of the squared deviation of tensile strength. The 'df' is the degree of freedom, which is used to obtain the observed of significance level. 'Mean square' is the sum of square divided by degree of freedom. 'F' is the ratio of two means square, which is used to test the null hypothesis that can be rejected if the significance is small at the P-level (P-level is also similar to Sig. in the Duncan test) of 0.05 or 0.01. Table 3.8 was originally provided and automatically calculated by SPSS. The concern here however, is the focus on the column 'Sig. = 0.000' which means that there is a significant difference between the materials, and if the value is more than 0.05, that means the different is 'insignificant' or 'not significant'.

The results of ANOVA in the Table 3.8 show that, for tensile strength and tensile strain, there is a significant difference among the warp and weft yarn directions considering the significant value (Sig.) were all 0.000. In the case of tensile modulus,

the significant value was recorded 0.034, which is also lower than 0.05 indicating that there is a significant difference among the groups. In order to extend the analysis in Table 3.8, ANOVA post hoc multiple comparison tests employing Duncan were used to look for more detail in significant differences of each composite sample within each category.

Table 3.8 ANOVA results for hemp fabric mechanical properties.

ANOVA						
		Sum of Squares	df	Mean Square	F	Sig.
Tensile Strength	Between Groups	108.032	3	36.011	8.931	0.000
	Within Groups	145.161	36	4.032		
	Total	253.193	39			
Tensile Strain	Between Groups	0.013	3	0.004	19.613	0.000
	Within Groups	0.008	36	0.000		
	Total	0.021	39			
Tensile Modulus	Between Groups	0.013	3	0.004	3.223	0.034
	Within Groups	0.047	36	0.001		
	Total	0.059	39			

Table 3.9 shows Duncan multiple comparison tests for warp and weft directions of the WHF for all categories of mechanical properties. While the comparison involved all warp and weft yarns in both fabrics, attention should be focused on the comparison between both fabrics' warp as well weft yarn directions. In terms of tensile strength (Table 3.9(a)), both warps and wefts were clustered under Group 1 and 3 respectively and this means that the differences between warp and weft yarn tensile strength is significant. The significant value (Sig.) for warp and weft are 0.124 and 0.111 respectively. This value is far higher (than 0.05) to deny the differences between their means. Therefore, it can be concluded that even though the warp and weft yarn is dissimilar, the tensile strength between the warp and weft yarns for both fabric are

similar. It does not refute the truth that the differences of cellulose content in both fabric contribute to different tensile strengths, but the differences of cellulose content between Fabric A and B is too small (67.47 and 64.77% respectively) to contribute a bigger gap in tensile strength.

In terms of tensile strain, Table 3.9(b) shows that the differences between warp yarn strain for Fabric A and Fabric B is significant with the p-value of 1.00. However, for weft yarns of both fabrics, they were clustered under Group 3 which means that their difference is insignificant, with a significant value of 0.207. Therefore, it is true that the different yarn crimp percentage in warp yarns could affect the tensile strain while the weft crimps for both fabrics are recorded as similar (refer Table 3.2).

Similar statistical results were found for tensile modulus (Table 3.9(c)). The tensile modulus of weft yarns for both fabrics was clustered into Group 1 with the significant value of 0.292 which means that their tensile moduli are insignificantly different. A similar result with warp yarns for both fabrics was found with the significant value of 0.091 which denied the differences between their tensile moduli. Again, similar to tensile strength, the influence of cellulose and lignin content in the warp and weft fibre is too small to give a bigger gap in tensile modulus for both fabrics.

With the proof of statistical method, there are no difference between Fabric A and B in terms of tensile strengths and tensile moduli. Both fabrics presumably could perform similar mechanical effects and behaviours in warp and weft directions. Therefore, it can be suggested that both fabrics, which come from different batches, can be used in a same batch composite production.

Table 3.9 Duncan multiple comparison test result for WHFs; (a) tensile strength, (b) strain, and (c) tensile modulus.

Tensile Strength (MPa)				
Fabric	N	Subset for alpha = 0.05		
		1	2	3
Fabric B – Warp	11	21.975		
Fabric A – Warp	10	23.392	23.392	
Fabric B - Weft	9		24.833	24.833
Fabric A - Weft	10			26.304
Sig.		0.124	0.118	0.111

(a)

Tensile Strain				
Fabric	N	Subset for alpha = 0.05		
		1	2	3
Fabric A – Warp	10	0.074		
Fabric B – Warp	11		0.093	
Fabric B - Weft	9			0.112
Fabric A - Weft	10			0.121
Sig.		1.000	1.000	0.207

(b)

Tensile Modulus (GPa)			
Fabric	N	Subset for alpha = 0.05	
		1	2
Fabric B - Weft	9	0.493	
Fabric A - Weft	10	0.511	0.511
Fabric B – Warp	11		0.530
Fabric A – Warp	10		0.540
Sig.		0.292	0.091

(c)

3.4 Conclusions

This work has shown some important points regarding the utilisation of natural woven fabric especially WHF. In order to incorporate this material for engineering or technical purposes, one cannot rely on the fabric specification given by the supplier.

Independent analysis and measurement of the material should be undertaken. The measurements analyses, as shown in Sections 3.2.1, 3.3.2 and 3.3.6, are very useful to understand the behaviour of WHF, thus prediction or anticipation can be made before it is used in any technical application.

The presented detailed characterisation of textile WHFs shows a number of findings, some of which are important in the prediction and interpretation of the properties of hemp fabric reinforced composites:

- Both fabrics possess similar fabric density which is 25 × 23 (warp × weft) and similar fabric thicknesses 0.41 mm
- The average warp and weft yarn size for both fabrics are 90tex and 93tex respectively
- Yarn crimps' percentage in weft direction for both fabrics is 9.3%, but in warp yarn is different for Fabrics A and B which are 5.4 and 6.0% respectively
- The measured weight using the calculation for Fabrics A and B is 234.80 and 236.67g/m^2 respectively
- In the thermogravimetric analysis, the highest mass loss rate for Fabric A was recorded higher than Fabric B which was 1.51%/°C at 37°C and 1.38%/°C at 380°C respectively
- The cellulose contents for Fabric A and Fabric B were determined as 67.47 and 64.77% respectively, while for lignin content were 3.52 and 2.92% respectively.
- The density of fibre for Fabric A is slightly higher than Fabric B which is 1.512 and 1.473g/cm^3. The relatively high density of Fabric A fibres correlates well with their higher cellulose content than Fabric B

- The total cover factor for both fabrics is similar, with a K-value of 0.66 which means that 66% of the fabric sheets are covered by yarn and it is presumed that the resin could penetrate the whole fabric systems and wet all the fabric thus producing a good composite material
- The mechanical properties for both fabrics reflect according to their physical properties, cellulose content as well as lignin content that they possessed. However, the inferential statistic has proven that the differences in their tensile strengths and tensile moduli are insignificant. This is because of the difference in their cellulose and lignin contents are too small to affect their mechanical properties. Therefore, both fabrics can be used or combined in the composite fabrication.

It also can be concluded that the properties of the two batches of similar nominal quality WHF obtained within a time interval of three months, are most likely not only identical from a textile point of view; such as they share almost the same fabric density, yarn size and fabric weight, but are also similar from an engineering point of view. Therefore, utilisation of both fabrics can be presumed to give a similar effect and behaviour.

Chapter 4 Characterisation of WHF Reinforced Vinyl Ester Composite

4.1 Introduction

In the previous chapter, the quality of fabrics was measured thoroughly to precisely identify their properties. This is important because fabric properties affect the behaviour of composite materials. Information about WHF properties enable the stakeholder to utilise it in many fields. As mentioned in Chapter 2, less work has been done on the WHF composites; especially on the different fabric stacking sequences in relation to fabric properties.

Therefore, in this work, WHF was used to fabricate bio-based composites employing the hand lay-up method. The composites were fabricated in different fabric layer orientations in order to investigate the stacking sequence effect on the mechanical properties. The fabric properties determined and measured in the previous chapter were used to study how these properties affect the physical properties and mechanical behaviour of composites. Some comparisons to wood and engineered wood products were also made to identify the potentiality, suitability and readiness of WHF reinforced vinyl ester (HVE) to be used in the building industry. In the end, the best fabricated composite with a certain fabric layer will be used for the next chapters.

4.2 Materials and Methods

4.2.1 Materials

A commercial WHF, with the product code, FSA10 was supplied by Hemp Wholesale Australia. Table 4.1 shows the physical and mechanical properties of the WHF adaptation from previous chapter. Once more, it is worth mentioning that according to

the specifications given by the supplier, the fabrics were produced by 100% yarn hemp in both warp and weft. The yarns were converted from cleaned hemp fibre through spinning processes and the twist given was 430 twists per meter. These yarns were then converted into fabric via weaving processes and the fabrics were woven by employing a loose plain weave (taffeta) structure. All fabric characterisations have been determined by employing several textile materials' standard methods. These standard methods (refer Table 4.1) are commonly used in the textile industry for characterisation as well as product quality determination purposes. The fabric characterisations have also been discussed in details in Chapter 3. Vinyl ester resin, SPV 1356 PROM THIX and the catalyst methyl ethyl ketone peroxide (MEKP), NOROX 925H were supplied by Nuplex® Composite Industry (Australia). Table 4.2 shows the properties of vinyl ester resin used for this work.

Table 4.1 Physical properties of WHF

Fabric Types			Standard Methods
Physical Properties			
Weave Structure		Plain/Taffeta	
Fabric Density (per 2cm)	Warp	25	ASTM D3775 [83]
	Weft	23	
Total yarn weight (measured) (g/m^2)	Warp	119.813	
	Weft	116.859	
Thickness (mm)		0.417	ASTM D1777 [85]
Yarn Size (Tex)	Warp	90.459	ASTM D1907 [86]
	Weft	92.970	
Yarn Crimp (%)	Warp	6.0	ASTM D3883 [87]
	Weft	9.3	
Density of Fibre (g/cm^3)		1.473	
Total Fabric Cover, K		0.663	
Mechanical Properties			
Tensile Strength (MPa)	Warp	21.975	
	Weft	21.833	
Tensile Strain (%)	Warp	9.3	
	Weft	11.2	
Tensile Modulus (GPa)	Warp	0.530	
	Weft	0.493	

Table 4.2 Properties of vinyl ester resin

Tensile Strength (MPa)	Tensile Modulus (MPa)	Tensile Strain (%)	Flexural Strength (MPa)	Flexural Modulus (MPa)	Density (g/cm^3)
86	3200	5-6%	150	3400	1.14

4.2.2 HVE Fabrication Method

Resin was prepared by adding MEKP to vinyl ester with the ratio of 1:44 by weight. This prepared resin was then applied to 10 fabric layers (30 × 30 cm for each layer) by employing the hand lay-up technique. Trapped air was gently squeezed out using a roller after pouring the resin on the fabric. This mixture (wet fabrics) was then laid in between of thick glass plates (40 × 40 × 10 cm in dimension) which were coated with a polymer mould release agent. The assembly was compressed with a weight placed on top to stabilize and remove the access resin, and the calculated pressure given to this assembly was 4.360 kPa. The mixture was then left to cure at room temperature for 24 hours. Then it was post cured in an oven for four hours at 80°C. This curing schedule (left 24 hours in room temperature and post cure temperature) is recommended by the supplier or manufacturer. Four types of composites which differ in their layer orientations were fabricated as shown in Table 4.3. Since the layer orientations is the main focus of this work, it should be noted that 0° direction is based on the warp direction of the WHF.

Table 4.3. List of HVE samples and their abbreviations

Sample Abbreviation	Layer Orientation
HVE[0]	$[0]_{10}$
HVE[90]	$[90]_{10}$
HVE[0,90]	$[0,90]_{5}$
HVE[S]	$[0/45/90/-45/0]_{S}$

*HVE stands for WHF reinforced vinyl ester

4.2.3 Physical Properties Testing of the Composites

The density of the HVEs was determined by a Multipycnometer MVP D160E in accordance to ASTM D792 [101]. Helium gas was used as a displacement medium. The helium was added to the fibres under vacuum conditions to ensure that all interior

air cavities in the submerged fibres (e.g. the fibre lumen) were filled with helium. The data reported are the average and standard deviation of three measurements.

The constituent contents of the HVEs (weight percentage and volume fraction) were determined according to the ASTM D3171 [102] test method II. This test method II was employed because the distribution of fibres in the fabric form (in this case hemp) was acceptably consistent [34]. As the densities and weights of the WHF, vinyl ester and their fabricated composites were known; the reinforcement and matrix contents were calculated. The void content of composite was calculated using Eq. (4.1) in accordance to ASTM D2734 as follows:

$$V_V = 100 - \rho_c \left(\frac{w_f}{\rho_f} + \frac{w_m}{\rho_m} \right) \quad \textbf{(4.1)}$$

Where V_v is the volume fraction of voids, ρ_c the density of composite, w_f the weight percent of fibre (%), w_m the weight percent of matrix (%), ρ_f the density of fibre g/cm^3 and ρ_m is the density of matrix g/cm^3.

4.2.4 Mechanical Testing Methods

Tensile and flexural tests were performed on a universal testing machine MTS Alliance RT/10 with the capacity of 10kN. Tensile properties were characterised in accordance to ASTM D638 [103] with a span length of 150 mm. Specimens with the dimension of 250 × 25 × 5 mm^3 were cut from the fabricated samples. Ten composite specimens from each sample were tested. The tensile load was applied at a constant displacement rate of 2 mm/min. A laser extensometer was used to measure the axial strain. Testing stopped immediately after the failure of the specimen. The ultimate

tensile stress was calculated as the maximum load measured divided by the area. The tensile modulus (modulus of elasticity) was measured from the initial slope. Figure 4.1 shows the test setup and its specimens.

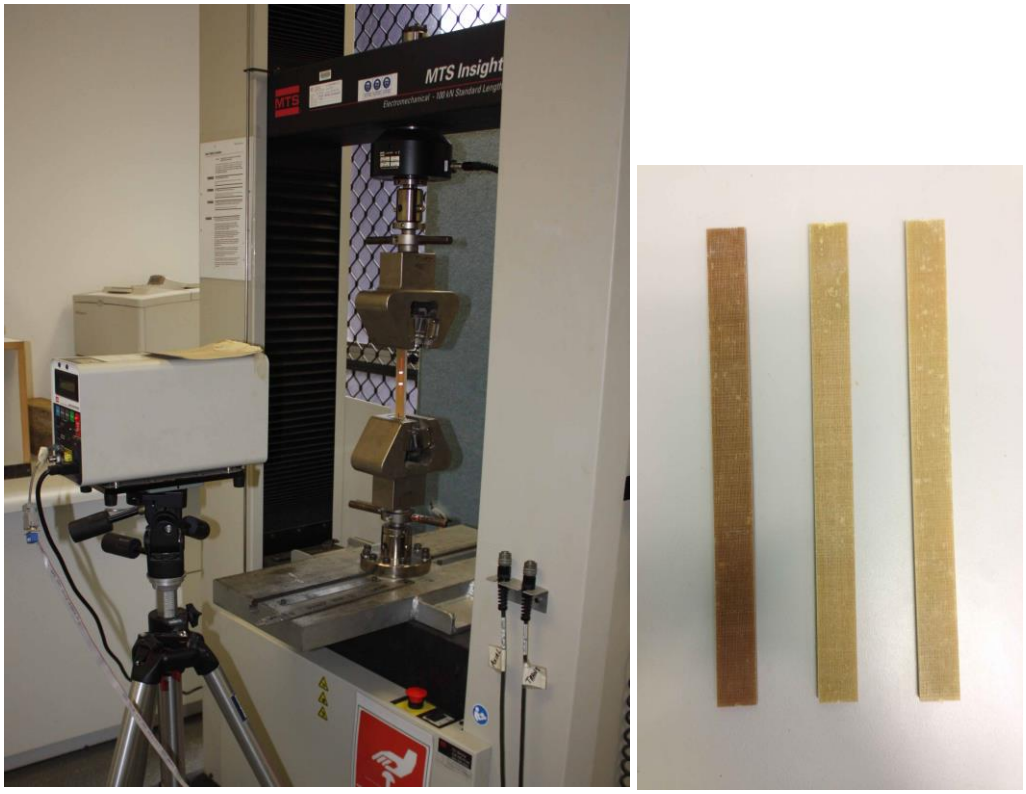

Figure 4.1 Tensile test setup with laser extensometer and tensile specimen.

A flexural test was conducted, according to ASTM D790 [104] (three-point bending), to determine the flexural properties of the composites as shown in Figure 4.2. A three-point bending fixture with cylindrical support with 5 mm radius was mounted on the table-top tester. The span length, according to the standard should be 15 times of the specimen's thickness (in this study was measured as 80 mm). The specimen dimension used for this test was 100 × 12 × 5 mm^3. The load was applied at a constant crosshead speed of 2 mm/min. Similar to tensile test, 10 specimens were tested for each sample. The load was applied at a constant crosshead speed of 2 mm/min. Specimens were monitored until fibre rupture occurred and at this point, the load was taken to calculate

the flexural stress. Flexural modulus was calculated as the slope in the linear range of the stress vs. deflection between a point at a deflection just above zero. It is noted that neither nonlinear behaviour nor differences in compressive and tensile behaviour are accounted for in this method. However, it is assumed to be a reasonable estimation of material properties for comparison with other reported material properties.

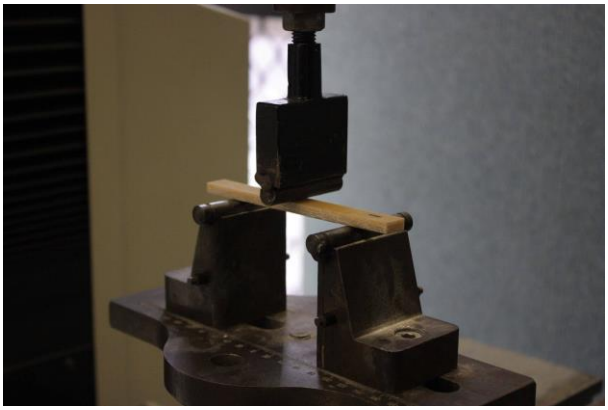

Figure 4.2 Flexural test setup with MTS Alliance RT/10 machine.

Impact testing was conducted in accordance with ASTM D256 [105] by using an INSTRON Dynatup model 8200 instrument (Figure 4.3). The weight used was 2.84 kg released from 1 m height at 2.9 m/s velocity. The specimens were cut in a dimension of 5 × 20 × 140 mm^3 and the impact strength was tested for at least five composite specimens. The information on the materials tested including total impact energy, load-time-energy characteristics and deflection at peak load were automatically measured and recorded from the Dynatup machine [106]. Impact energy in kJ/m^2 was calculated by dividing the net value of absorbed energy with the cross-sectional area of the specimen.

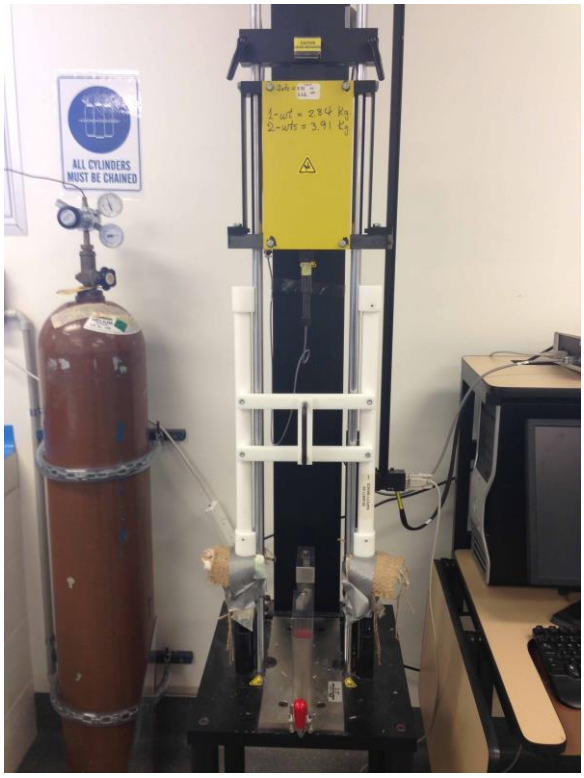

Figure 4.3 INSTRON Dynatup model 8200 instrument.

In the preliminary study, an in-plane shear test by tension loading based on ASTM D3518 was also conducted on selected sample composites for the purpose of comparison to wood using similar machine to test tensile and flexural strength. Specimens with dimensions of 250 × 25 × 5 mm3 were cut in ±45° angle from each sample. For tensile and flexural tests, 10 specimens were run in displacement-controlled mode with a displacement rate of 2 mm/min on a similar machine.

4.3 Results and Discussion

4.3.1 Physical Properties of HVEs

Table 4.4 shows the physical and mechanical property result of the WHF used in this study and will be used to analyse the properties of fabricated composites (HVEs). The density results of HVEs shown in the table do not reveal any significant difference

between samples, with the average value of 1.1g/cm^3. The fibre volume fractions for all samples were also similar while the void contents of all samples ranged from 7.13 to 7.36%. The increase in the fibre volume fraction also increased the void content in composite [38]. Dhakal et al. [38] fabricated a composite using non-woven hemp fabric to reinforced unsaturated polyester, employing hand lay-up method. With the different layers of fabric, the void content increased with ranges from 12.56 to 18.64%. These void content figures are more than double of the composites fabricated in this work. Non-woven fabric is made by entangling the fibre by means of needle punch, hydro-entangling, plastic fuse etc. The transformation of fibres into fabric in one stage could lead to the uneven fibre distribution especially when using natural fibre. The direction of fibres in non-woven fabric is scattered and it is very common for the non-woven to have many holes as a result of the entangling mechanism. This can create a kind of cavity on the fabric and thus create a void in the composite. Unlike non-woven, hemp fibre goes through several processes before it becomes fabric. These processes ensure the uniformity of fibres distribution thus giving consistency in density in fabric. In the case of a small difference between void contents among woven hemp composites, it is believed that the hand lay-up technique might contribute to the creation of voids [38]. However, since the volume fraction of fabric for all composite, as well as density of composites are similar, similar voids were expected for woven hemp composite samples and this would affect the mechanical properties directly.

The consistent density of all samples is attributed to the woven fabric properties which was determined before the fabric was woven [32, 34]. The WHF used in this study was designed to be balanced so that it had a similar weight on warp and weft yarns reflecting fibre distribution in both directions. The fibre distribution can be determined based on: (1) fabric density, (2) yarn size and, (3) yarn crimp percentage. Fabric count

or density is always used to explain the fibre distribution in WHF composites [33, 35, 45, 95]. However, even though a fabric has similar fabric count, the fibre distribution in warp and weft direction is not necessarily equal because it depends on the warp and weft yarn size and the crimp percentage. Therefore, by taking into consideration the three woven fabric properties mentioned above, the weight of yarn in warp and weft directions can be measured, thus enabling fibre distribution to be determined.

Based on Table 4.1, although the total warp number is higher (25 yarns/2 cm) than weft yarn (23 yarns/2 cm), the size and crimp percentage of weft yarn are higher than warp. The result of the measured warp weight was slightly higher than weft. The slight difference between the warp and weft yarn in WHF is due irregularities (Figure 4.4) that are known to exist in natural textile materials. Figure 4.4 clearly shows that the rough surface and uneven fibres causing yarn irregularities. Therefore, the differences between the weights can be said to be insignificant and this can been proven statistically [107].

The good fibre distribution in warp and weft direction leads to consistent fibre volume fraction in all HVEs (Table 4.4). Whether the fibres are man-made or natural, only in fabric form can good fibre distribution be achieved, thus producing consistent fibre fraction [32-34, 108]. This is because the fibre in woven fabric has been arranged twice before it becomes a woven fabric. Usually, depends on the fabric design and the manufacturing machines, the amount of fibre per area should be consistent [31, 32, 34]. That is why, for a woven fabric and similar number of layers used in composite fabrication, the fibre volume fraction is normally consistent throughout the plate. Christian and Billington [35] used WHF to reinforce cellulose acetate and

poly(hydroxybutyrate) matrices and the fibre volume fraction of their composite is consistent.

It is not easy to control the distribution of fibre per area in the plate when using short fibres, and this results in an inconsistency in density and fibre volume fraction. The density and volume fraction of hemp short fibre composite made by Hu and Lim [20] varied most probably due to inconsistent fibre distribution since the fibre was randomly laid. The density and fibre volume fraction of hemp yarn composite made by Madsen et al. [109] was more consistent and this was because of the arrangement of fibre in yarn form and the filament winding technique that they employed for their composite. Therefore, employing woven fabric can produce composite materials with consistent density and fibre volume fraction.

Fabric density, yarn size and yarn crimp percentage determine the mechanical properties of fabric [107]. These properties affect the tensile strength, modulus and strain of the fabric (refer Table 4.1). Another property that relates to a fabric's mechanical properties is its woven structure [33]. However, since the structure of the hemp fabric utilised in this study was similar (plain/taffeta weave), the comparison of mechanical properties of WHF is free from the woven structure influence. The mechanical properties of WHF are closely related to the mechanical performance of the HVE and this topic will be discussed in further detail in the next section.

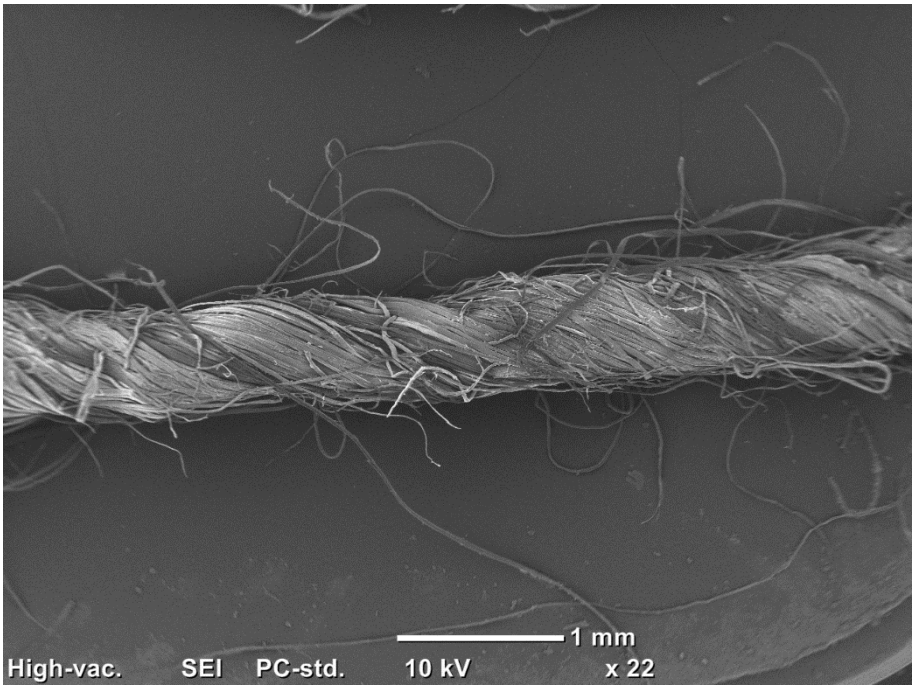

Figure 4.4 Scanning electron image of hemp yarn in WHF.

Table 4.4. Constituent content results of HVEs.

Sample	Thickness (mm)	Density (g/cc)	Reinforcement content (wt.%)	Reinforcement content (vol.%)	Matrix content (wt.%)	Matrix content (vol.%)
HVE[0]	4.794	1.10	44.638	33.335	55.362	59.297
HVE[90]	4.800	1.12	44.638	33.335	55.362	59.297
HVE[0,90]	4.929	1.10	44.271	33.060	55.729	59.690
HVE[S]	4.918	1.08	43.909	32.790	56.091	60.078

4.3.2 Tensile Properties of HVEs

Table 4.5 summarizes the average tensile properties for each type of HVE. For each sample, it was observed that the stress-strain behaviour of all specimens cut from the plate were consistent. The typical tensile stress-strain response for each sample is shown in Figure 4.5. As will be discussed further, typical behaviour shows a linear trend in the earlier stage (strain < 0.5%), then becoming non-linear as the acting tensile force gets higher which is attributed by woven hemp fabric behaviour. Since, the fibre volume fraction for all the samples was found to be similar (refer to Table 4.4), the difference for all the samples is strongly attributed to fabric properties and the layering

orientation of the fabric rather than the volume fraction or matrix behaviour. Christian and Billington [35] found that their woven hemp composite behaviours were bi-linear for warp and tri-linear for weft and that these were attributed to the non-linear polymer matrices and higher weft yarn crimp respectively. The tensile strains of their composites were found to be relatively high, ranging from 4 to 10% because the biodegradable resins they used were thermoplastic. Vinyl ester is a thermoset type resin which is well known to be more rigid and brittle. Therefore, the tensile strain of composite fabricated in this work is less than 3%.

When subjected to tension, all specimens, faded and lightened in colour (from light brown to whitish brown) within the gauge length. This colour fading is due to the crazing of the matrix, yet no cracking was visually observed. No significant cracking was observed between any of the samples. The failure occurred from resin failure, followed by reinforcement failure [33, 110]. Therefore, the crazing that happened during the tensile loading showed a failure initiation on the vinyl ester resin before the WHF. Since the tensile strength and modulus of the fabric in warp direction were recorded slightly higher than its weft direction, the stress concentrations and high localized straining in the matrix existed at the weft yarn fibre surface within the cross-section of the transverse fibres (refer to Table 4.1). Thus, the matrix was more likely to fail (crack) here, leading to ultimate composite failure at the cracked cross-section.

The failure of all the specimens was perpendicular to the longitudinal sample direction. Figure 4.6 shows the scanning electron microscope image taken from the fracture surface of the HVE. From the figure, it can be seen that there are short ruptured protruding yarns as well as the yarns pulled-out from the surface. This figure confirms

the failure mode that, while the fibres within the yarn ruptured, the yarn is pulled-out from the matrix near the failure surface.

The composite tested in the warp direction, HVE[0] possessed the highest strength and stiffness of all samples. This was expected because the tensile strength and tensile modulus of the fabric in warp direction were slightly higher than weft direction (refer Table 4.1). Additionally, the lower tensile strain was due to a lower crimp percentage of warp than weft direction, leading to higher stiffness for sample the HVE[0]. As for the sample HVE[90], its tensile properties were recorded as the lowest in comparison with other samples. As expected from the fabric properties, this was due to the slightly lower tensile properties of the weft direction as compared to the warp direction.

The tensile properties of sample HVE[0,90] possessed higher results than sample HVE[90] due to the changing half of the total fabrics (in warp direction) which were layered in 90° orientations. The higher tensile modulus than sample HVE[90] is attributed to the layering in 0° orientations in the fabricated composite which effectively reduced the crimping in the weft direction. Sample HVE[S] possessed a lower tensile property than sample HVE[0,90]. With 4 layers layered in the 45° direction and two layers layered in 90° direction out of the total of 10 layers of WHF, the sample was subjected to the tensile force in 0° direction. The tensile strain was reduced to 2.27% in comparison with sample HVE[90] and thus increased the tensile modulus. The tensile properties of the composite fabricated in this work are comparable with the composite made by Christian and Billington [35] and Song et al. [33].

Table 4.5. Tensile properties results of HVEs.

Composite Types	Tensile Strength (MPa)	Tensile Strain (%)	Tensile Modulus (GPa)

HVE[0]	68.89(±5.51)	2.05(±0.12)	6.91(±0.60)
HVE[90]	64.05(±2.00)	2.42(±0.20)	6.22(±0.50)
HVE[0,90]	67.41(±1.08)	2.10(±0.07)	6.44(±0.26)
HVE [S]	64.48(±0.97)	2.27(±0.14)	6.31(±0.61)

*Figures in bracket indicate standard deviation.

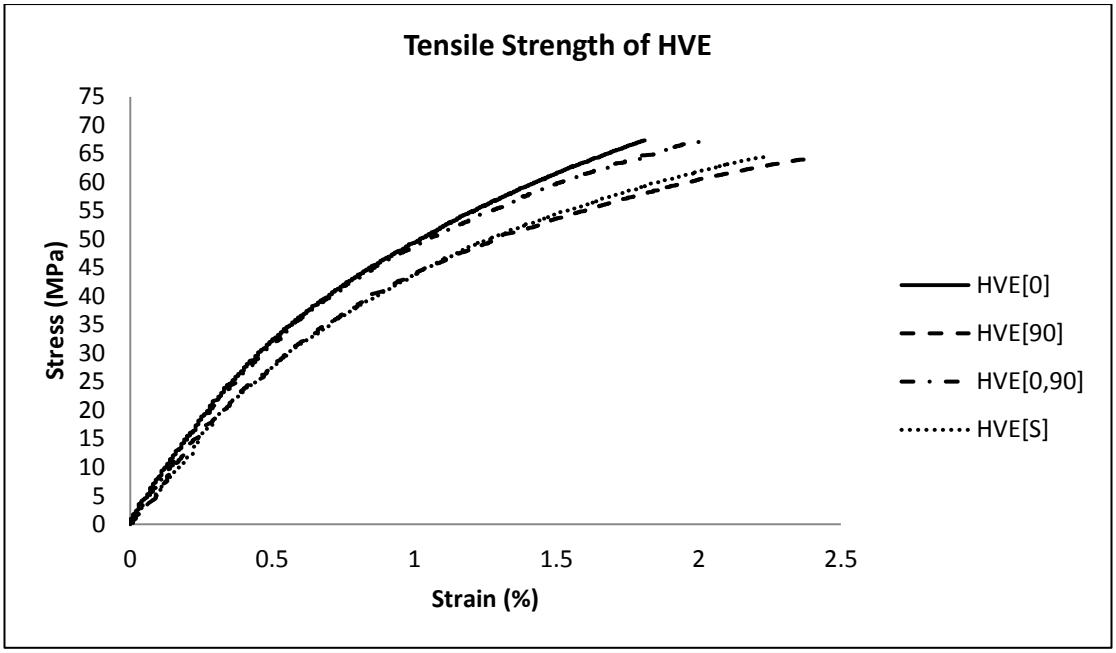

Figure 4.5 Tensile stress-strain response for HVEs.

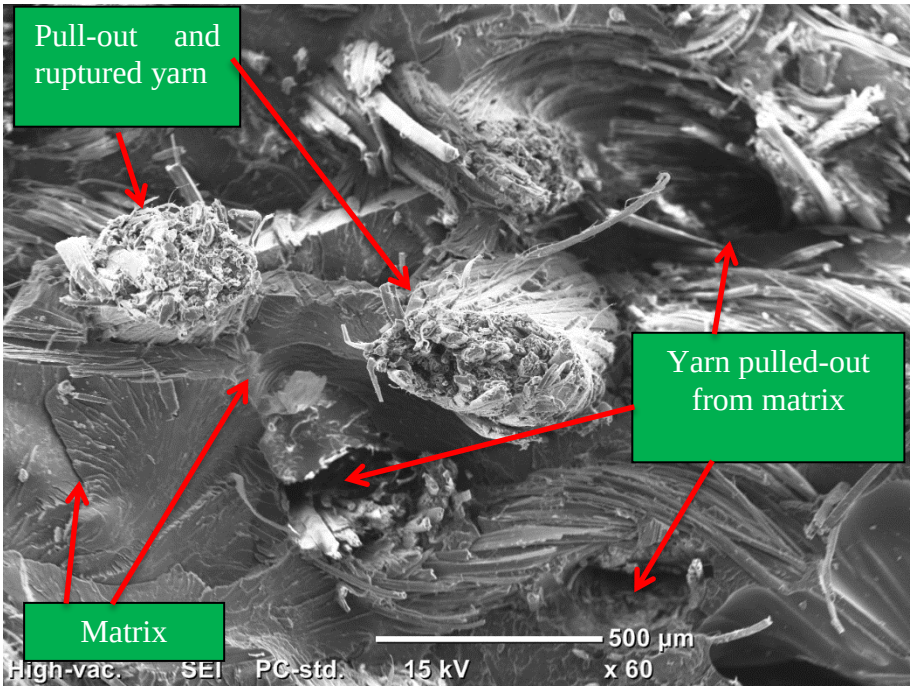

Figure 4.6 Scanning electron image of HVE failure surface.

Some other works utilised different types of fibre and reinforcement to reinforce vinyl ester resin. Tensile strength and tensile strain of banana fibre (untreated, treated with 5% NaOH and hybrid of banana and coconut shell fibre) reinforced with vinyl ester

made by Santhosh et al. [111] ranged from 11.41 to 19.61MPa and 4 to 7% respectively. Kim and Seo [112] worked with woven sisal fabric reinforced with vinyl ester and the tensile strength and strain were recorded at 36MPa and 1.9% respectively. Non-woven kenaf fibre reinforced vinyl ester made by Rassmann et al. [113] differed in fibre volume fraction loading which were 15, 22.5 and 30%. These composite tensile strength and tensile modulus were recorded ranging from 44 to 55MPa and 4.5 to 5.6GPa respectively. These composites tensile properties were found to be lower in comparison to composites fabricated in this work due to the utilisation of different fibres (banana, sisal and kenaf), different fibre reinforcement types (fibre, woven fabric and non-woven) as well as different fibre volume fractions [34].

Nevertheless, none of the tensile strengths measured in this work as well as elsewhere [113] exceed the strengths of the typical unreinforced vinyl ester resins. Typical tensile strength, modulus and strain of vinyl ester was 86MPa, 3.2GPa and 5-6% respectively [113]. He emphasised that the reduction in strength was due to the inclusion of defects such as voids and poor adhesion during manufacturing of the reinforced laminates. As far as voids in a composite sample are concerned, the void content in this work were measured ranging from 7.13 to 7.36% (refer to Section 4.3.1). It is believed that this is the main reason that the HVE of this work did not exceed typical vinyl ester tensile strength. Even though there is a negative point in tensile strength, a positive side can be sighted from the tensile modulus. The incorporation of WHF can enhance tensile modulus or stiffness of vinyl ester from 3.2GPa to at least 6.22GPa and this is almost a 50% increment. As a result of the tensile modulus increment, there was reduction in the tensile strain ranging from 2.05 to 2.42%, less than half the typical vinyl ester resin strain.

4.3.3 Flexural Properties of HVEs

The flexural properties determined from the load-displacement results are summarised in Table 4.6. The typical stress-strain response for each sample of the HVE tested by flexural test is shown in Figure 4.7. The difference between the samples' responses is attributed to the different fabric layering orientations since the matrix used for all samples was similar. The curves were non-linear as the flexural loading increase and all specimens failed at a single (crack) located at mid-span, where the loading was applied.

The flexural strength and modulus of sample HVE[0] was slightly higher than the other samples fabricated in this work. This was due to the lower warp yarn crimp percentage than weft yarn crimp percentage. Thus, the lower flexural strength and modulus of sample HVE[90] than the sample HVE[0] was also due to the higher crimp percentage of the weft direction of the WHF (refer Table 4.1). The flexural strains here contradict the tensile strain trend. It must be remembered that the flexural strain here actually represents the deflection of the specimen when subjected to the flexure load, not the differences of elongation of sample as in tensile strain. Thus flexural strains and yarn crimp percentages are unrelated.

In the case of sample HVE[0,90], the flexural strength and modulus were recorded higher than the sample HVE[90]. Therefore, changing half of the total fabrics layer in 0° orientation increased the flexural properties of sample HVE[90]. Changing half of the total fabrics layer in 0° orientation reduced the yarn crimping percentage in the weft direction thus reducing the flexural strain. This reduction on the flexural strain led to increase the sample stiffness and increased the flexural modulus.

The flexural properties of sample HVE[S] were found to be the lowest in comparison with all other samples. The reason for this is the total of four layers of 45° fabric orientation layered in HVE[S] sample, which had lessened the fibre concentration in the 0° and 90°. Since the sample was cut and tested in 0° orientation of the samples, the existence of 45° fabric orientation made the flexural force distribution throughout specimens almost ineffective. The flexural force acted along the width and perpendicular to the length of the samples by loading nose. Therefore, the higher concentration of fibre loading on the width and length directions of the sample (like other samples) enhanced the resistant of acting flexural force more effectively. That is the reason for the lowest flexural properties of the sample HVE[S]. Flexural properties of the composites made by Muralidhar et al. [114] were lower in 0° orientation in comparison with their 90° orientation samples. Most of their results were contradicted by the results in this study. The only reason is that, with the similar size of yarn in their fabric, the fabric density in warp direction (0°) was lower than in the weft direction. However, without taking into consideration the orientation, their composite flexural properties are relatively comparable with the material fabricated in this study.

Table 4.6. Flexural properties results of fabricated HVEs.

Composite Types	Flexural Strength (MPa)	Flexural Strain (%)	Flexural Modulus (GPa)
HVE[0]	109.35(±1.96)	3.00(±0.10)	6.31(±0.06)
HVE[90]	102.45(±1.98)	3.23(±0.10)	5.51(±0.12)
HVE[0,90]	104.26(±4.21)	2.91(±0.21)	5.91(±0.11)
HVE [S]	96.72(±2.30)	2.91(±0.15)	5.29(±0.08)

*Figures in bracket indicate standard deviation.

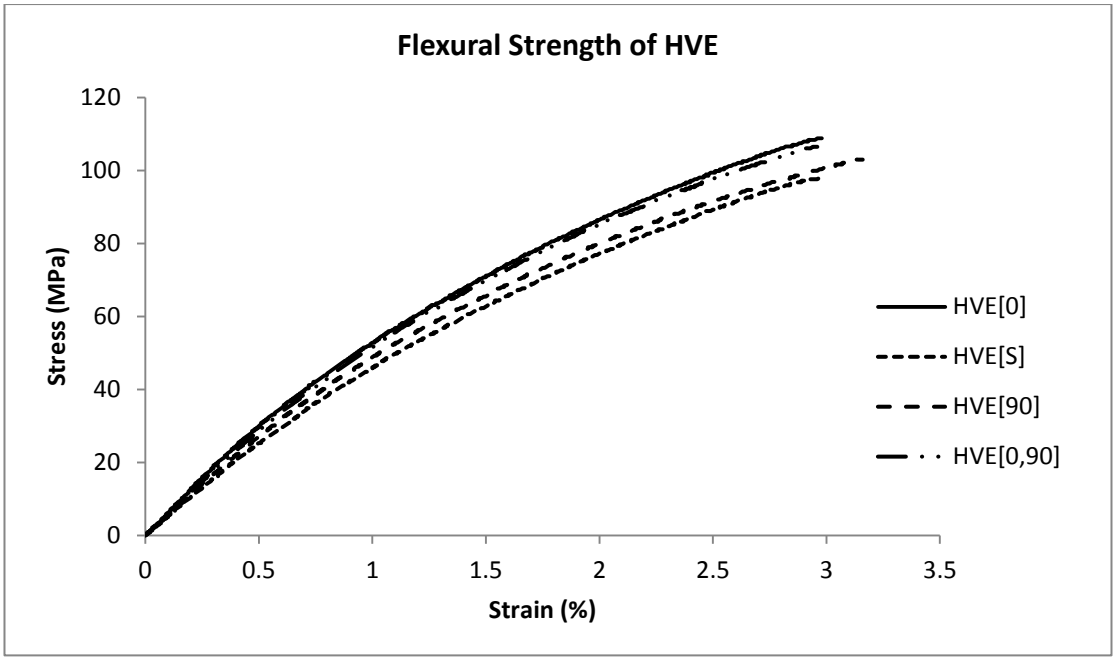

Figure 4.7 Flexural stress-strain responses of HVEs.

Flexural properties of banana fibre/vinyl ester composite made by Santhosh et al. [111] were recorded in the range from 33.84 to 48.21MPa for flexural strength and from 1.7 to 2.8% for flexural strain. Reinforcing vinyl ester with non-woven kenaf fabric seemed to enhance flexural properties better than banana fibre. The flexural strength and modulus of non-woven kenaf/vinyl ester fabricated by Rassmann et al. [113] were recorded ranging from 70 to 85MPa and from 2.8 to 3.8GPa respectively. This is almost a 50% enhancement by non-woven kenaf fabric as compared to banana fibre. The addition of jute fabric could enhance the composite even better than kenaf and banana. Rodriguez et al. [115] fabricated bi-directional jute fabric/vinyl ester and the flexural strength and modulus were recorded ranging from 83 to 103MPa and from 5.5 to 6.6GPa respectively. Although the flexural properties of composites fabricated in this work were recorded higher than other types of fibre, the variation of results are influenced by type of fibre (banana, kenaf and jute), fibre reinforcement (fibre, woven fabric and non-woven) as well as fibre volume fractions.

4.3.4 Impact Properties of HVEs

The overall impact toughness of the all manufactured samples in this study is attributed to the higher volume fraction of vinyl ester matrix in the composite. Since the volume fractions of WHF in all the HVEs are similar (refer Table 4.4), the impact properties were not influenced by this factor but by fabric layering orientation [33, 114]. Typical impact responses in Figure 4.8 show a similar trend for all samples fabricated in this study and the differences between them were only in the intensity of the peaks which indicate the level of energy absorption.

Based on the Table 4.7, sample HVE[0] clearly possesses the highest impact strength (17.97 kJ/m^2) compared to sample HVE[90] and all the other samples. Unlike flexural properties, the impact strength of the sample HVE[0,90] was found to be lower than the sample HVE[90]. This shows that the combination of 0° and 90° orientation could not tolerate the immediate load applied to them. A similar thing happened to sample HVE[S] which was found to have an impact strength result lower than HVE[0,90]. Apparently, the existence of woven fabrics in 45° layer orientation does not help to enhance the impact strength of the samples.

The crimp percentage of warp (0° direction) of WHF was recorded as lower than weft (90° direction) in the fabrics thus the energy dissipation should be better for weft since it could be elongated more than the warp yarns [11, 116]. This means that the impact resistance of HVE[90] is expected to be better than the sample HVE[0]. Nevertheless, the impact properties results for both samples respond as expected and were contradicted.

SEM images of the fracture surface of the impact specimen in Figure 4.9(a) confirms its fracture mode. Pulled out yarns and consistent holes are observable in the impact

specimen, and the surfaces of the pulled out fibres are quite clean (Figure 4.9(b)). The protruded yarns and holes indicated poor adhesion between the fibre (in this case, yarn) and matrix [117]. This can be seen from Figure 4.9(b) where there are the gap between the fibre (surface of yarn) and vinyl ester could be due to debonding during impact testing or the incompatibility fibre and resin. The WHF used in this study possessed a total fabric cover of 0.663 (refer Table 4.1). This means that 66.3% of the WHF sheets were covered by yarns and a good penetration of resin to the whole fabric system could be expected [107]. The yarns in the fabric did not completely fill the gap due to the normal irregularities of natural yarns (refer Figure 3.5 in Section 3.3.6). Hence, with these gap spaces in the fabric structure, the WHF in this study can be considered fully wet with vinyl ester resin at least on the surface of the yarns. This can be observed from Figure 4.10(a) where the ruptured yarn is fully surrounded by vinyl ester and proving that the fabric was fully wet by vinyl ester during its fabrication. Under tensile and flexural load, the degradation of the specimen occurred in two phases, beginning with the cracking of resin and followed by the fibre rupture. When the resin cracked, the force transferred to the fabric and from there, the crimp from the yarn straightened thus affecting specimen performance of either strength or stiffness. This happened because the test was executed under a low speed (says 2-5 mm/min) and steadily increasing load [33, 110]. However, under impact load, the fabricated specimen failed catastrophically and in an instant. Since the resin penetrated the fabric well, the resin restricted the movement of yarns and the impact of energy from the hammer was not well absorbed by the fabrics. Therefore, the ability of the crimp percentage to dissipate immediate impact force (high velocity) can be said to be insignificant.

Returning the impact property results of all samples in this study; the impact strength is influenced by the concentration of fibres. The highest impact energy was possessed by sample HVE[0] and this is due to the highest concentration of fibre in 0° orientation which perpendicular to the impact direction acted on the specimens. The higher concentration of fibre in 0° (warp) than 90° (weft) can be translated by slight differences in weight as recorded in Table 4.1. Regardless of the adhesion of fibre and matrix, it is true that with the yarns' total cover factor of 0.663, the resin can easily wet all the fibres. Nonetheless, with the higher density of fibres (in this case 0° orientation for HVE[0]) and the pressure given during the fabrication processing, the resin is only wet at the surface of yarn and penetrated into the whole fibres in the yarns much less. As a result, there was a corresponding decreased of bridging matrix among the fibres. The less penetrated matrix to the fibres in yarn is obvious in Figure 4.10(b) as an evidence.

This makes the samples less rigid internally, creating a cushioning effect when the hammer hit the specimen, thus the impact forces were not only absorbed by the matrix, but also by the fibres [118]. Therefore, sample HVE[0] could withstand an impact energy higher than all other samples. Muralidhar et al. [114], in their work, implied that there is no obvious effect of lay-up angle on the impact properties of woven preform reinforced composite laminates. However, even though the difference between the samples was quite insignificant in this work, the trend was obviously related to the fabric layer orientation and this matter is worth discussion to justify the slight differences in their impact properties. The impact strength of banana fibre (untreated, treated with5% NaOH and hybrid banana and coconut shell powder) reinforced vinyl ester made by Santhosh et al. [111] was recorded ranging from 2.56

to 3.63kJ/m^2. This is too low in comparison with woven hemp composite due to the low fibre volume fraction (30%) or the mechanical properties of banana itself.

Table 4.7. Impact property results of HVEs.

Composite Types	Energy to failure-1 (J)	Total time-1 (ms)	Total energy-1 (J)	Impact Strength (kJ/m^2)
HVE[0]	1.73(±0.11)	1.68(±0.06)	1.73(±0.11)	17.97(±1.18)
HVE[90]	1.48(±0.10)	1.75(±0.14)	1.55(±0.12)	16.23(±1.2)
HVE[0,90]	1.40(±0.13)	1.66(±0.11)	1.45(±0.11)	14.97(±1.16)
HVE[S]	1.26(±0.22)	1.31(±0.09)	1.24(±0.10)	12.67(±1.04)

*Figures in bracket indicate standard deviation.

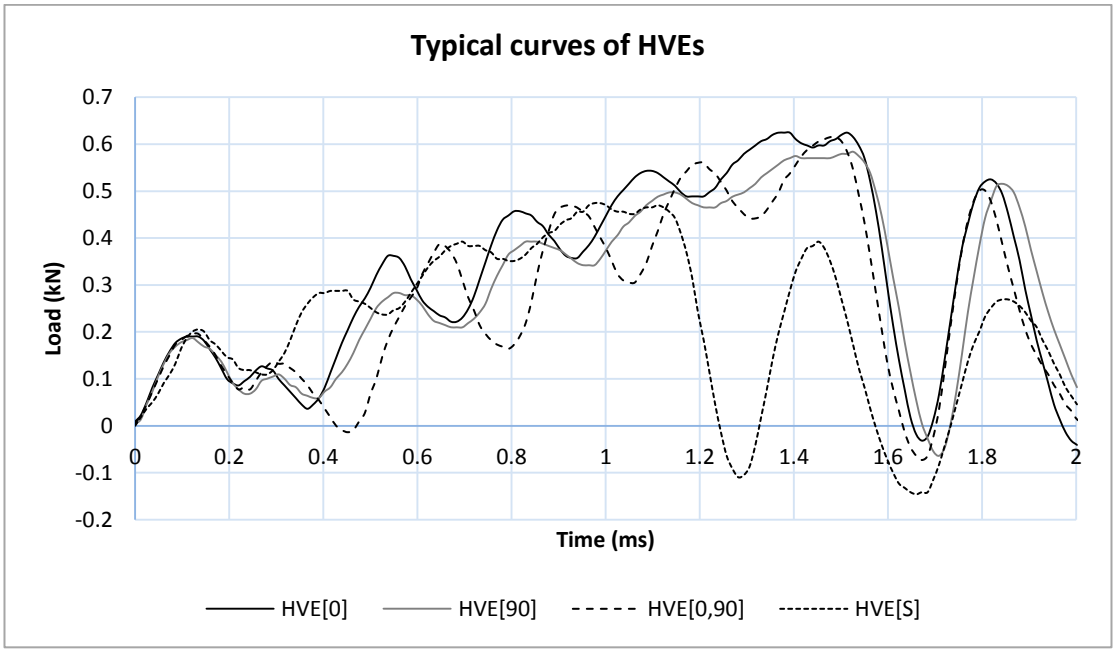

Figure 4.8 Typical impact responses of HVEs.

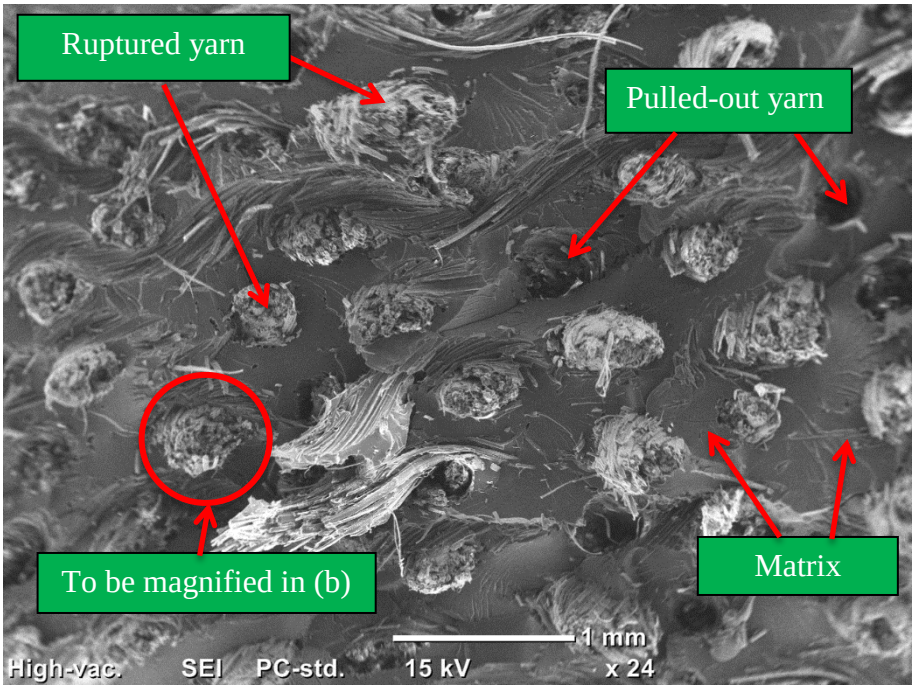

(a)

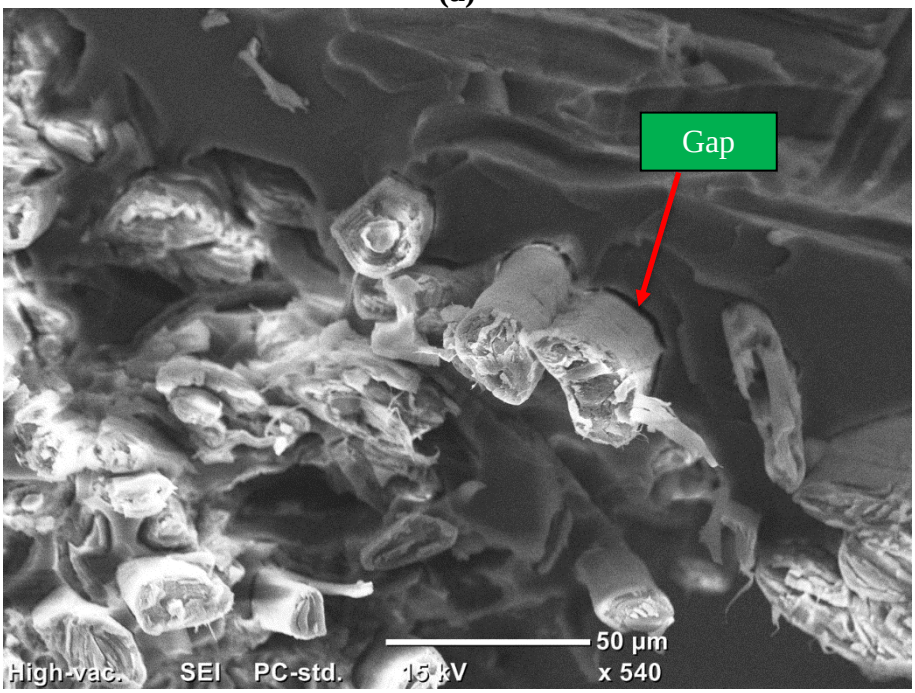

(b)

Figure 4.9 Scanning electron image of an impact failure surface; (a) overview of the fracture surface of specimen, (b) magnified images from the indicated surface from image (a).

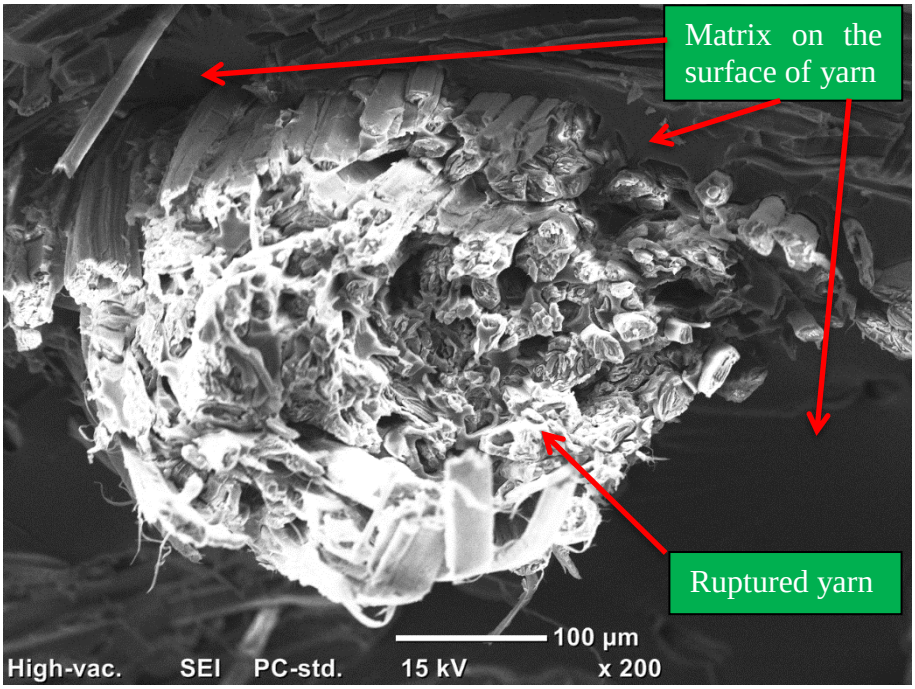

(a)

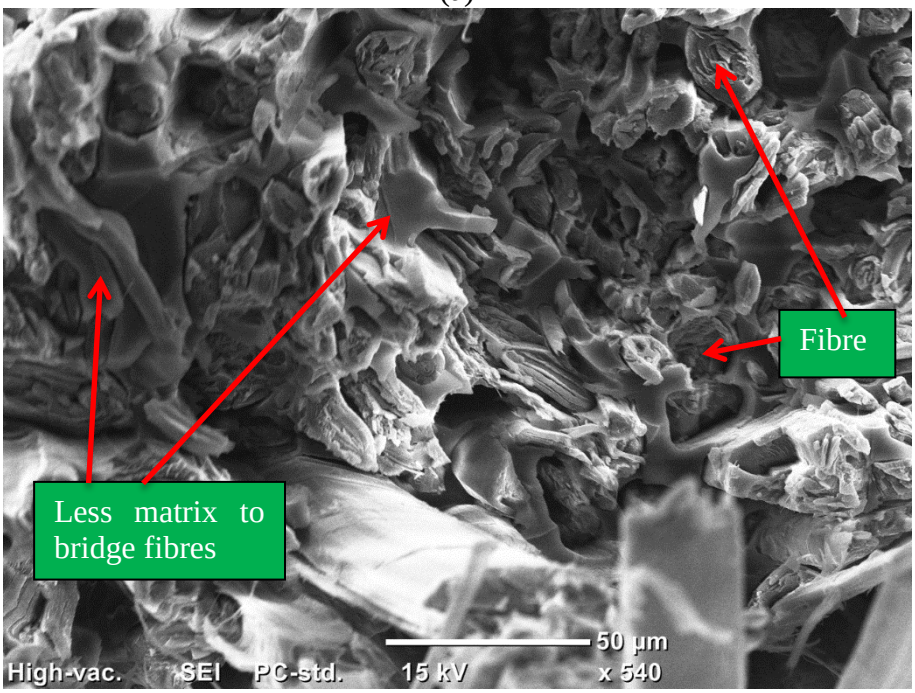

(b)

Figure 4.10 Scanning electron image of an impact specimen; (a) ruptured yarn is fully enclosed by vinyl ester, and (b) magnified image from image (a) indicates the penetration by vinyl ester resin into the yarn

4.3.5 Statistical Analysis

The results of ANOVA for all mechanical properties of the fabricated samples in Table 4.8 shows that there are significant differences among all samples considering that the significant values (Sig.) were all lower than 0.05 (mostly their 'sig.' are 0.000) except for the tensile modulus which was recorded at 0.069. To extend the analysis in Table 4.8, ANOVA post hoc multiple comparison tests were employed using Duncan to look for more detail in the significant differences of each composite sample within each category.

Table 4.8. Result of ANOVA for the HVEs mechanical properties.

ANOVA						
		Sum of Squares	df	Mean Square	F	Sig.
Tensile Strength (MPa)	Between Groups	115.173	3	38.391	5.382	0.005
	Within Groups	192.602	27	7.133		
	Total	307.775	30			
Tensile Strain (%)	Between Groups	0.661	3	0.220	11.291	0.000
	Within Groups	0.527	27	0.020		
	Total	1.188	30			
Tensile Modulus (GPa)	Between Groups	2.016	3	0.672	2.643	0.069
	Within Groups	7.120	28	0.254		
	Total	9.136	31			
Flexural Strength (MPa)	Between Groups	695.978	3	231.993	26.066	0.000
	Within Groups	284.806	32	8.900		
	Total	980.784	35			
Flexural Strain (%)	Between Groups	0.635	3	0.212	9.103	0.000
	Within Groups	0.745	32	0.023		
	Total	1.380	35			
Flexural Modulus (GPa)	Between Groups	5.173	3	1.724	189.997	0.000
	Within Groups	0.290	32	0.009		
	Total	5.464	35			
Impact Strength (kJ/m^2)	Between Groups	116.660	3	38.887	34.914	0.000
	Within Groups	37.869	34	1.114		
	Total	154.529	37			

Table 4.9 shows the Duncan multiple comparison tests for all HVE samples for all categories of tensile properties. In terms of tensile strength (Table 4.9 (a)), samples were divided into two groups, in which samples HVE[0] and HVE[0,90] were in Group 2 ('Sig.'=0.294), while samples HVE[90] and HVE[S] were in Group 1

('Sig.'=0.755). This means that there are no significant difference among members in the similar group. In Group 2, the insignificant difference in mean was due to layer orientation. With the 50% of the fabrics layered in 90° directions for HVE[0,90] the total fibre concentration (weight) in warp is slightly higher than weft direction (refer Table 4.1). While in the Group 1, the differences became more obvious because all the WHFs were layered at 90°, and the existence of fabric at the 45° direction did not enhance the tensile strength thus makes both of them clustered under the same group. Therefore, the results shown in Table 4.9(a) confirm that the reduction of WHF in the 0° direction results in lower tensile strength.

In terms of tensile strain, Table 4.9 (b) shows a similar trend to Table 4.9(a). The results show that the higher tensile strength, the lower the tensile strain will be. This reflects the tensile strain of the WHF which is attributed to the crimp percentages of warp and weft yarns. The crimp percentages and tensile strains of the warp were recorded to be lower than the weft yarn (refer Table 4.1) and this makes the tensile strain of sample HVE[0] and HVE[0,90] lower. Again, because of the slight difference in the fibre concentration in the 0° direction in sample HVE[0,90], tensile strain was found to be insignificant with sample HVE[0]. For the case of sample HVE[90] and HVE[S], due to the lowest fibre concentration in warp direction, the influence of a longer crimp percentage of weft yarn was significant and this can be proven by the information in Table 4.9(b).

The results of the Duncan multiple comparison tests in Table 4.9(c) show that the highest tensile modulus of sample HVE[0] is confirmed since the sample HVE[0,90]'s tensile modulus became the subset to Groups 1 and 2. There are no significant differences between samples HVE[90] and HVE[S]. The lesser significance of the

tensile modulus for all fabricated samples is due to the higher volume fraction of vinyl ester resin that lessen the influence of WHF. Thus, the results shown in the Table 4.9(c) confirm that tensile modulus is not affected by fabric layering orientations.

Table 4.9. Duncan multiple comparison test results for HVEs; (a) tensile strength, (b) strain, and (c) tensile modulus.

Tensile Strength (MPa)			
		Subset for alpha = 0.05	
Composite Types	N	1	2
HVE[90]	7	64.04808	
HVE[S]	9	64.48154	
HVE[0,90]	9		67.41315
HVE[0]	6		68.88722
Sig.		0.755	0.294

(a)

Tensile Strain (%)			
		Subset for alpha = 0.05	
Composite Types	N	1	2
HVE[0]	6	2.0150	
HVE[0,90]	9	2.1011	
HVE[S]	9		2.2689
HVE[90]	7		2.4157
Sig.		0.242	0.051

(b)

Tensile Modulus (GPa)			
		Subset for alpha = 0.05	
Composite Types	N	1	2
HVE[90]	7	6.22200	
HVE[S]	9	6.31144	
HVE[0,90]	9	6.44256	6.44256
HVE[0]	7		6.91014
Sig.		0.421	0.076

(c)

Table 4.10 shows the Duncan multiple comparison tests of flexural properties for all HVE samples. In terms of flexural strength (Table 4.10(a)), sample HVE[0] is confirmed to possess the highest flexural strength in comparison with the other samples whilst sample HVE[S] possessed the lowest,s with each of their p-values of 1.00 and both of them clustered under Groups 3 and 1 respectively. Samples HVE[0,90] and HVE[90] were in Group 2 with the ‘Sig.’ value of 0.207 which is far

higher than 0.05 indicating that the different mean values between the samples are insignificant. With all samples divided into three groups, the flexural strength of all HVEs is confirms to be affected by fabric layering orientations.

In terms of flexural strain/deflection, the results in Table 4.10(b) show that there are no significant differences between the samples HVE[0], HVE[0,90] and HVE[S] with the significant value of 0.22. However, for some reason, sample HVE[90] is clustered in a group with the significant value of 1.000. Overall, based on the results shown in this table, the layering orientation does not give significant impact to the flexural strain.

Even though the layering orientations do not significantly affect the flexural strain, it does affect the flexural modulus of all the fabricated samples. Table 4.10(c) shows that the differences among all sample means are significant, with a significance value for each sample of 1.00. These results confirm that fabric layering orientations do affect the flexural modulus of HVEs.

Table 4.11 shows the results of the Duncan multiple comparison tests of impact strength for all fabricated samples in this study. Each sample mean is clustered under a different group with a significant value of 1.00. This shows that the differences between all sample means are significant. Again, as with flexural modulus, this Duncan results in Table 4.10 confirm that the impact strength of HVEs are influenced by the fabric layering orientation.

Table 4.10. Duncan multiple comparison test results for HVEs; (a) flexural strength, (b) flexural strain, and (c) flexural modulus.

Flexural Strength (MPa)				
		Subset for alpha = 0.05		
Composite Types	N	1	2	3
HVE[S]	9	96.71730		
HVE[90]	9		102.44772	
HVE[0,90]	10		104.26277	
HVE[0]	8			109.34561
Sig.		1.000	0.207	1.000

(a)

Flexural Strain (%)			
		Subset for alpha = 0.05	
Composite Types	N	1	2
HVE[S]	9	2.90556	
HVE[0,90]	10	2.91400	
HVE[0]	8	3.00125	
HVE[90]	9		3.23222
Sig.		0.220	1.000

(b)

Flexural Modulus (GPa)					
		Subset for alpha = 0.05			
Composite Types	N	1	2	3	4
HVE[S]	9	5.28611			
HVE[90]	9		5.51122		
HVE[0,90]	10			5.90620	
HVE[0]	8				6.30700
Sig.		1.000	1.000	1.000	1.000

(c)

Table 4.11. Result of Duncan multiple comparison test for impact properties of HVEs.

Impact Strength (kJ/m^2)					
		Subset for alpha = 0.05			
Composite Types	N	1	2	3	4
HVE[S]	10	12.67142			
HVE[0,90]	10		14.96903		
HVE[90]	10			16.23209	
HVE[0]	8				17.47929
Sig.		1.000	1.000	1.000	1.000

With the proof of statistical method, several conclusions can be drawn from the results' analysis. Fabric layering orientations affect the tensile properties of all fabricated samples. However, since the weight of warp yarn is just slightly higher than weft yarn, the differences in layering orientations were only significant for several samples for

tensile strength. Similarly, for tensile strength, tensile strain is affected by layering orientation reflecting crimp percentage or tensile strain of the warp and weft yarns. Fabric layering orientations did not affect the tensile modulus of all samples due to the higher volume fraction of the vinyl ester compared to the WHF. In terms of flexural properties, it is confirmed that different fabric layering orientations affect their flexural strength and tensile modulus, but not flexural strain or deflections. Nevertheless, in terms of impact properties, it is proven that fabric layering orientations can influence the impact strength of the HVEs. From the statistical analysis which was discussed above, even with the different layering orientations, some results do not show any significant differences in their mean. Therefore, analysis of the results should not only be restricted to the effect of the layering orientation, but needs to be widened to the physical and mechanical properties of the WHF. This shows the importance of fabric properties when analysing the mechanical properties of HVEs.

The important fact coming from this statistical analysis is that the influence of fabric layering orientations in the HVEs for this study can be said to be small. The difference among all the mechanical properties for the composites in this study were found to be less than 10%. Based on the properties of the WHF in Table 4.1, the woven fabric is designed to have similar properties either in warp or weft directions. The details of the fabric analysis can be found elsewhere in [107]. This is the reason that the mechanical properties of HVE fabricated in different fabric layering orientations did not give any large differences. Since the effect of layering orientations does not give any big enhancement on the mechanical properties (less than 10%), regardless of how many layers of fabric used in the fabrication, the fabric can be used in any layering orientation.

4.3.6 Comparison with Wood and Engineered Wood Products

Natural-based composite materials have properties mostly similar to wood and engineered wood products [35]. A comparison of these is briefly presented here, focusing on properties of several woods commonly used in construction; namely Douglas Fir (coastal), Western Hemlock and Ponderosa Pine, and engineered wood products plywood, oriented strand board (OSB) and glue laminated timber (glulam). Table 4.12 shows a comparison between HVE's mechanical properties tested here and wood used in construction. The values shown by woods and engineered wood products in this table were the values of samples tested/loaded parallel to grain.

When compared with woods, HVE demonstrated a shear strength at least three times higher than the woods. The flexural strength of the HVE is comparable and even higher than the woods loaded parallel to the grain. In terms of flexural modulus, the HVE is roughly half than that of wood parallel to grain. Nevertheless, Hurd [119] reported that the flexural modulus of wood perpendicular to the grain is about 11 to 35 times less than parallel to grain. Therefore, while the HVE has a more balanced bidirectional strength and stiffness as expected, the example of woods given in Table 4.12 suffer in lower flexural strength and modulus in perpendicular to grain direction.

For design purposes, the wood properties must be adjusted to consider for their defects, variation in density, moisture content and the grain slope typical in structure lumber. This adjustment is needed because wood's mechanical properties exhibit a large coefficient of variations thus making the design values established near minimum strength and stiffness for the population of lumber. Table 4.13 shows the allowable mechanical properties used for design with the woods considered here in comparison with biocomposites made by Christian and Billington [35] as per ASTM D245 [120].

They expected that their biocomposites possessed higher mechanical properties than the allowable wood design except for the biocomposites' modulus of elasticity. A similar expectation can be used for the case of HVEs fabricated in this study as its mechanical properties were recorded higher (refer Table 4.12) than the biocomposites in Table 4.13.

The HVE fabricated in this study has the mechanical properties comparable to, or even higher than, the properties measured for the engineered wood products, except for the flexural modulus of glulam. The flexural modulus of plywood stated in Table 4.12 is for a ply parallel to grain. However, in practice, the plies are always in a combination of parallel and perpendicular to grain thus making the modulus 35 times smaller than parallel to grain. Therefore, the modulus of HVEs can be considered higher than that of plywood. With the comparison shown in Table 4.12, the composite fabricated in this study can directly replace engineered wood products and woods considering some other advantages it possesses such as ease of tailoring properties and ability to mould into structural shapes (including hollow sections).

The only significant problem with the HVE is its greater densities (1000-1100 kg/m^3) as compared to the woods and engineered wood products (320-810 kg/m^3). In order to replace wood products, a composite should be engineered to possess a lighter weight. Nevertheless, at least the densities of the fabricated composite in this study are lower than the biocomposites fabricated by others [20, 35, 44].

Table 4.12. Mechanical properties of HVEs, wood and engineered wood products.

Material	Tensile Strength (MPa)	Tensile Modulus (GPa)	Shear Strength (MPa)	Flexural Strength (MPa)	Flexural Modulus (GPa)	Density (kg/m^3)
HVE	69	7.0	*27.4-28.2	109	6.3	1000-1100
Douglas-Fir (Coast) [121]	-	-	7.8	85	13.4	480
Western Hemplock [121]	-	-	8.6	78	11.3	450
Ponderosa Pine [121]	-	-	7.8	65	8.9	400
Plywood (B-B Class 1) [35, 119]	27	10.3	1	27	10.3a	400-810
Oriented Strand Board [122]			1.2	21.2	5.25	490-810
Glulam [121, 123]	-	-	-	26-72	10.6	320-720

*Shear strength of sample HVE[0] and HVE[0,90] from preliminary testing.
[a] Modulus for ply parallel to grain.

Table 4.13. Allowable design properties of several woods used in construction [35]

	Material	Flexural modulus of rupture (MPa)	Flexural modulus of elasticity (MPa)	Shear strength (MPa)
Clear green properties	Douglas-Fir (Coast)	53	10,800	6.2
	Western Hemplock	46	9000	5.9
	Ponderosa Pine	35	6900	4.8
Strength ratio/quality factor		4%-98%	80%-100%	-
Adjustment factor		2.1	0.94	2.1
Properties adjusted for defects	Douglas-Fir (Coast)	2.1-51.9	8640-10,800	6.3
	Western Hemplock	1.9-41.2	7200-9000	5.9
	Ponderosa Pine	1.5-34.2	5520-6900	4.8
Allowable properties	Douglas-Fir (Coast)	1.0-24.7	9190-11,490	3.0
	Western Hemplock	0.9-21.5	7660-9575	2.8
	Ponderosa Pine	0.7-16.3	5870-7340	2.3
Biocomposite properties	Hemp/CA	95	6560	12.3
	Hemp/PHB	65	5050	9.9

4.4 Conclusions

The results of this work have positively shown that the properties of fabric can affect the mechanical properties of composite materials. The characterisation established in this work shows a number of findings which relate to the physical properties and mechanical behaviours of the HVEs attributed to fabric properties and layering orientations:

- Density and fibre volume fraction (1.1g/cm^3 and 33% respectively) was consistent for all samples due to the good fibre distribution in the fabric which can be determined by the weight of the warp and weft yarns
- A composite which has all fabric layered in warp direction will have higher tensile properties and the reduction of layer fabric in warp direction will lead to reduce tensile strength due to slightly higher fabric strength in warp rather than weft direction. The flexural strength and modulus for composites also show similar trends with tensile properties
- Impact energy is mostly dissipated by vinyl ester since its volume fraction (60%) is higher than the WHF in the composites. The impact strength of Hs is influenced by loose fibres rather than yarn crimps. The slight difference in weight made the warp to have higher loose fibre than weft direction thus energy can be dissipated more effectively in 0° than 90° directions
- Statistical analyses confirm that the fabric layering orientations affects the tensile, flexural and impact properties. However, the influence of the fabric layering orientation in composites is small and the differences among all the mechanical properties are less than 10% due to the hemp fabric which is presumably designed to have similar properties in warp and weft. Since the

differences are lower than 10%, in normal practice, the fabric can be used in any layering orientations

- Based on the comparison to some of the woods, shear strength and flexural strength of the composite is higher than that woods and its balanced properties made the composite even better, much more consistent and stable. When comparing to the engineered wood products, the composite flexural modulus can be considered higher than that of plywood and this confirms that it can directly replace the engineered wood product
- The main problem for this composite is its density which relatively higher than those woods and engineered wood products listed. However, the composite densities in this work are lower than hemp composite explored in other works

Altogether, the study shows the influence of fabric properties on the physical and mechanical properties of hemp fabric composites. Hence, fabric properties are worthy of analysis, not only to determine fibre distribution and to comprehend the mechanical properties of the composite, but also for the consistency of material production. Hemp fabric composites also demonstrate good performances which potentially become an alternative material for woods and engineered wood products. Even though the difference in mechanical properties for all samples was only 10%, overall composite fabricated by $[0, 90]_5$ layer orientation exhibited better results than the others. Therefore, the next composite material will be fabricated using this layer orientation (Chapter 6 and Chapter 7).

Chapter 5 Fire Retardant Treatments on the WHF

5.1 Introduction

The work in Chapter 3 focused on and emphasized on the characterisation methods in measuring, analysing and evaluating woven hemp fabric (WHF) for technical applications. The characterisation methods are important for gathering as much data about the fabric material as we can in order to confirm the data from the supplier, to justify and rectify the suitability of the fabric for the application, and latter to predict and presumption fabric's influences on the application's behaviour.

Since this composite material is purposely used and designed for infrastructure application, safety issues should be considered, and one criterion that should establised is the material's ability to inhibit flame. As mentioned in Section 2.6.2, most of research highlights a concern about the flammable nature of natural fibres (more than the resin). However, as far as WHF is concerned, there are fewer works applying fire retardant agent to the reinforcement directly and assessing the effect of this treated reinforcement in the composite material.

As for fire retardant treatments, manufacturers are very particular and concerned about how finishes are applied to material, especially to natural fibres. This is because applying complicated finishing to natural fibre will increase cost. Putting aside cost, applying commercial fire retardant chemicals which are available in the market is a good alternative to pre-treating. Fire retardant chemical is easy to apply and is usually formulated without specificity to a certain fibre but for a generic group of fibres. Several researchers introduced sodium hydroxide treatment to improve fire retardant performance of textile fabrics [124-126]. This treatment seems cheap and it is

recognised as a fire retardant for natural textile fabric, thus it is worth trying on the hemp fabric.

The purpose of this work is to assess fire retardant properties of WHF treated with fire retardant substances. One of the reasons for this exploration, is to reduce the cost of chemical treatment on the WHF for composite reinforcement. In this work, three types of treatment were applied to WHF: sodium hydroxide (NaOH), flame retardant (FR) solution and combination of NaOH and FR chemicals. The fire retardant properties were evaluated by means of a burning test, thermogravimetric analysis as well as the limiting oxygen index. Last, the treated WHF will be used in the composite fabrication in the next chapter (Chapter 6).

5.2 Materials and Methods

5.2.1 Materials

WHF was supplied by Hemp Wholesale Australia. The physical properties of the WHF (untreated) used were determined in preliminary work shown in Table 5.2.. According to the specifications given by the supplier, the fabrics were produced with 100% yarn hemp in both warp and weft. It is worth mentioning that the yarns were converted from cleaned hemp fibre into yarn through spinning processes and the twist given was 430 twists per meter. These yarns were then converted into fabric via weaving processes and the fabrics were woven by employing a loose plain weave (taffeta) structure. Commercial grade NaOH was supplied by Science Essential Australia and the commercial flame retardant (FR) chemical was supplied by Cyndan Chemicals, Australia. According to the supplier, the main active ingredient in this flame retardant is ammonium polyphosphate. Information from the technical and

material datasheet says that this chemical is water-based, not classified as hazardous and environmental friendly.

5.2.2 Fire Retardant Treatments of WHF

The WHF was treated with (NaOH), (FR) and a combination of both chemicals (NaOH + FR). For the first treatment, fabrics were soaked in a NaOH solution (10% concentrations) for three hours at room temperature. The fabrics were then washed with distilled water several times to remove excess alkali from the fabric. The washed fabrics were dried at room temperature for eight hours, and then oven dried at 100°C for another six hours. The subsequent neutralisation treatment was abandoned to retain the alkali cellulose formed on the fabric surface [125]. The dried fabrics were stored in a sealed plastic bag to avoid atmospheric moisture contamination prior to chemical and thermal analyses.

For the FR treatment, according to the supplier, the FR can be used as it is by spraying or dipping and that drying is not necessary. However, in this work, the dips and nips method was employed to treat the fabrics. The nipping process was set carefully so that the chemical uptake was consistent and maintained within the range of 100-105%. The treated fabrics were then left to dry at room temperature for eight hours.

For the combination of NaOH + FR, the fabric was firstly treated with NaOH followed by the FR using the procedures mentioned above. The abbreviation for WHF; untreated, treated with sodium hydroxide, treated with FR chemical and treated with sodium hydroxide combined with FR are WHF-UT, WHF-NaOH, WHF-FR and WHF-NaOH+FR, respectively.

5.2.3 Characterisation of Treated WHF

It was observed that woven fabrics were physically changed after treatment. Therefore, the characterisation of their physical properties should be undertaken in order to investigate the composites' properties latter. The chemical uptake or pick-up for all treated WHF was calculated using Equation (5.1)[127, 128]:

$$Chemical\ pick-up\ (\%), A = \frac{W_2 - W_1}{W_1} \times 100 \quad (5.1)$$

Where, W_2 is the weight of fabric after treatment and W_1 is the weight of fabric before treatment and both should be in a dry condition.

The fabric shrinkages after the treatments were measured using Equation (5.2) as follows:

$$Fabric\ Shrinkage\ (\%), B = \frac{L_2 - L_1}{L_1} \times 100 \quad (5.2)$$

Where, L2 is the length of fabric after treatment, and L1 is the length of fabric before treatment.

The density of the treated fabrics was measured to determine the changes before and after treatment using a Multipycnometer MVP D160E. Helium gas was used as the displacement medium. The helium was added to the fibres under a vacuum condition to ensure that all interior air cavities in the submerged fibres (e.g. the fibre lumen) were filled with helium. The data reported are the average and standard deviation of three measurements.

WHF properties were characterised for their thickness and fabric density/fabric count, while their yarn was characterised for its yarn size (linear density) and crimp (for warp

and weft). All tests were performed employing several textile material standard methods as stated in Table 5.1. These standard methods are commonly used in the textile industry for characterisation as well as product quality determination purposes. Detailed measurements on these can be found in the Chapter 3.

Table 5.1 Standard method used to determine fabric properties.

Properties	Testing	Standard Method
Fabric Density	Warp (end) and filling (pick) count of woven fabrics	ASTM D3775
Fabric Thickness	Thickness of textile materials	ASTM D1777
Yarn Size	Yarn number (linear density)	ASTM D1907
Yarn Crimp	Yarn crimp and yarn take-up in woven fabrics	ASTM D3883

The weight of each fabric (untreated and treated) was calculated by total weight of warp and weft yarn. The weight can be measured using Equation (3.4) in the Section 3.3.2.

The total fabric cover factor was measured using a modified equation (Equation (3.6)) introduced by Chen and Leaf [90] and the K value indicates amount of yarns on an area of fabric (refer Section 3.3.4).

5.2.4 Burning Test

Ignition time and burning behaviour, as well as flame spread properties were carried out to determine the flammability properties of treated hemp fabrics. The ignition time and burning behaviour of the samples were measured using a James Heal and Halifax Flammability Tester in accordance with BS 5438 at 24°C and 65% relative humidity room conditions. In this test, a sample with the dimension of 220 × 170 mm was mounted in a steel frame, as shown in Figure 5.1 (a) after being conditioned for 24

hours also at 24°C and 65% relative humidity. A standardized flame source was applied to the surface from the bottom, and the ignition time was set at 12 seconds (refer Figure 5.1(c)). Three specimens from warp and weft samples for each textile fabric were processed and average was taken for interpretation. The ignition time, flame and smouldering time (after glows) and burning characteristics were recorded [128].

A spreading of flame test was conducted in accordance to ISO 6941 by mounting the fabric sample on a steel frame as shown in Figure 5.1. The specimen was exposed from below to the flame source for 12 seconds. At four different places, a standardized marker thread was placed to determine the spreading rate of flame. Two threads were placed horizontally at two different heights across the sample surface: at 300 mm and 600 mm horizontally to measure the vertical spreading flame refer Figure 5.1(d)). The other two threads were placed vertically on the both left and right sides of the fabric specimens to measure the horizontal flame spreading rate [129-132]. When the flame spread and reached any mark, the thread was burnt and the respective marker timer stopped. Three specimens (600 ×170 mm) of warp and weft for each treated fabric type were conditioned and the time of flame spreading for both vertical and horizontal were recorded and their average was calculated.

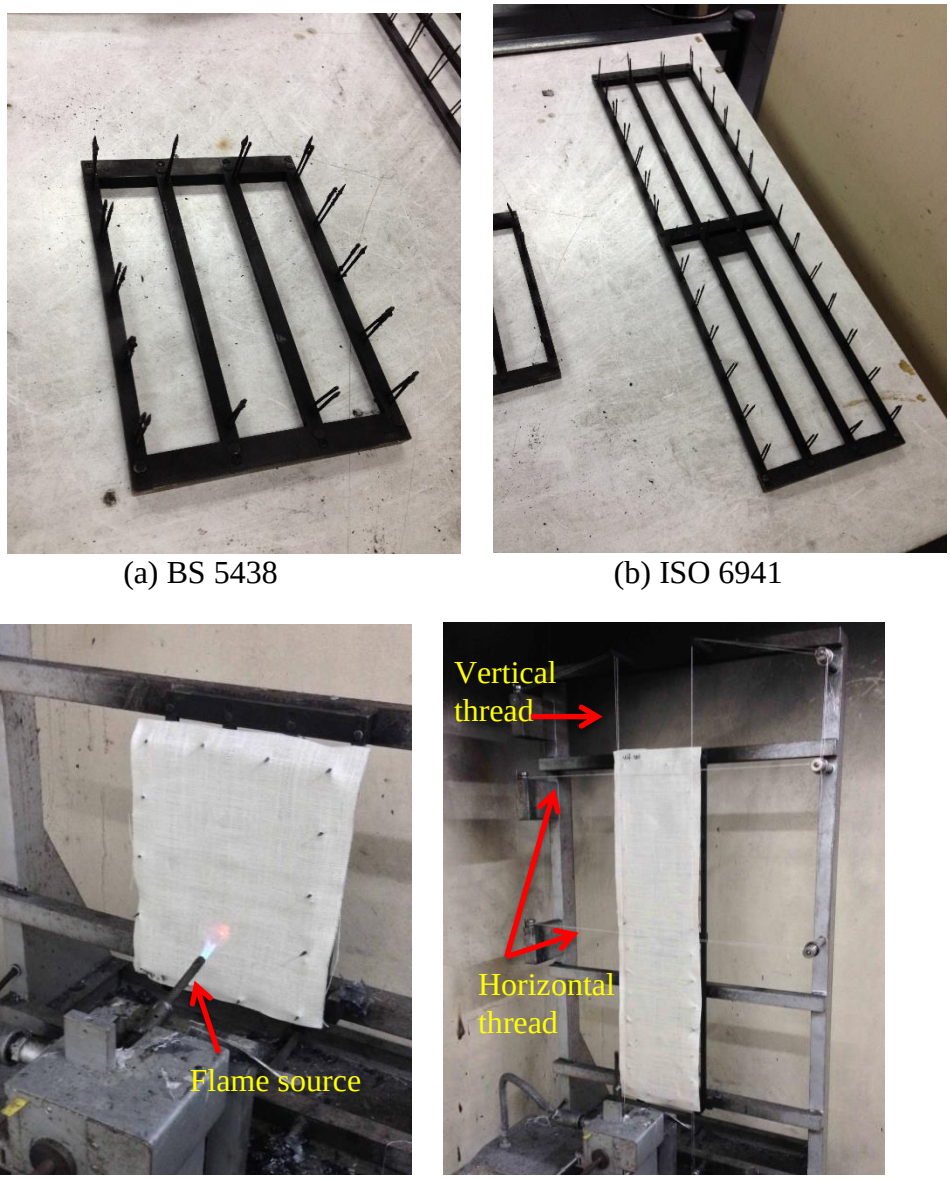

(a) BS 5438 (b) ISO 6941

(c) BS 5438 test set up (d) ISO 6491 test set up

Figure 5.1 Steel frame used to mount fabric sample for (a) BS 5438 and (b) IS) 6941 and their test setup

5.2.5 Thermogravimetric Analysis

Thermogravimetric analyses (TGA) were carried out on a TA Instruments Model TGA Q500 operating under nitrogen and air atmosphere using a platinum pan. The runs were performed over a temperature range between 30 and 600°C at 10°C/min heating rate and 20 ml/min flow.

5.2.6 Limiting Oxygen Index

The Limiting Oxygen Index (LOI) is a method used to determine the minimum oxygen concentration in an oxygen/nitrogen mixture that will sustain a flame. It is a convenient, reproducible, and inexpensive way to determine the tendency of a material to sustain flame. The LOI test was carried out using an LOI instrument model number M606 in accordance with ASTM D2863. A test sample of 150 × 50mm was placed in a transparent test chamber and ignited at the top. The oxygen concentration in the mixture of oxygen and nitrogen was increased slowly until the sample sustained burning. The volume fraction of the oxygen in the gas mixture was reported as the LOI.

5.2.7 Tensile Test

The tensile properties (ASTM D5034) of hemp fabrics were characterized using a universal testing machine, MTS Alliance RT/10. A 75 mm wide test specimen was cut in the desired direction (warp or weft) and then equal numbers of yarns were removed from both sides until the specimen width was reduced to 50 mm. The same procedure was followed for test strips in both warp and weft directions. The tensile tests were performed using a gauge length of 75 mm and a crosshead speed of 10 mm/min. The cross-sectional area used to convert load into stress was calculated from the test specimen width and the thickness of fabric obtained from the fabric characterization [26, 88].

Typically, the tensile curve (in stress-strain curve) for most of textile fabrics started in nonlinear and then the slope increased slowly until finally becoming linear. The mechanical properties of textile fabrics cannot be determined under the nonlinear curve. Therefore, a linear trend line was drawn to extend the linear part of the curve

to the axis of strain in order to determine the tensile stress and tensile modulus as well as strain at peak of the hemp fabric [107, 133].

5.3 Results and Discussion

5.3.1 Effects of Fire Retardant Treatments on the Physical Properties of WHFs

Changes in the physical properties of WHFs before and after chemical treatment are shown in Table 5.2. The chemical pick-up on WHF was measured based on the changes in weight before and after treatment with the assumption that there was no yarn lost when the treatment was carried out. Some 18.18% of weight was added to WHF treated with NaOH whilst the fabric treated with FR was recorded higher at 24.94%. WHF treated with NaOH and FR was recorded even higher due to the deposition of both treatments, which was 30.10%. The density of treated WHF increased drastically as compared to the untreated WHF due to the effect of the treatment applied to them.

The changes in fabric dimension were also observed where all the treated samples experienced shrinkage for both warp and weft directions. Shrinkage from the sample treated with NaOH (WHF-NaOH) was the highest among all the samples. The combination of NaOH and FR treatment shrunk the sample (WHF-NaOH+FR) a bit less than the NaOH treatment, and the least change was shown by the sample treated with only FR (WHF-FR). Observing the differences in shrinkage percentages of all the samples, it seems that NaOH treatment was responsible for the highest shrinkage. It can be observed that FR showed the lowest of all the samples. In the combination treatment, WHF was firstly treated with NaOH and this process made the fabric shrink but the shrinkage was a bit lower than WHF-NaOH due to the FR treatment.

During the alkali treatment, NaOH removed the organic component in the WHF. In the textile industry, this treatment is similar to ‘mercerisation’ where concentrated alkaline is applied to cotton fabric. This process is meant to increase lustre, hygroscopicity, and strength as well as the dye affinity of the cotton fabric [125, 134]. By generic, cotton is like hemp, which is categorised under natural textile fibres; thus a similar effect is expected to occur with the WHF. Under the action of this treatment, physicochemical and structural modifications of the cellulose take place. Apart of the hemicellulose and lignin removal in structural modification by alkali treatment, the structure of the fibre inter-converts from alpha-cellulose and beta-cellulose mixture into a thermodynamically favourable cellulose II polymorph [134]. This chemical reactions lead to formation of alkali cellulose, to intensive swelling of fibres and structural reactions and, to a change in the arrangement of units in the cellulose macromolecule. When the fibre swells, its volume undergoes considerable changes; increases in water absorption due to the increase of pore size which then leads to an increase in the cross-section of fibre by 40 to 50% [125, 134].

The scanning electron image in Figure 5.2(a) shows a WHF-UT sample which has not gone through any treatment. The cross-section image shows that the fibres have thin and lenticular shape and its surface is rough due to hemicellulose and lignin. Contrasting with the WHF-UT, from Figure 5.2(b), the WHF-NaOH sample shows that the fibre's cross-section changed from elliptical to become rounder suggesting that the fibres were swollen and the diameter was increased. The surface of fibres became clean due to the removal of hemicellulose, lignin and fat [125, 134].

In the case of FR treatment, there were FR particles (marked in red circles) ranging from several micro to nanometres in size deposited on the fibre surface (Figure 5.2

(c)). The fibres cross-sections also changed from lenticular to become rounder, and the surface was observed to be quite clean from hemicellulose and lignin as compared to Figure 5.2(a). Since the main chemical in FR is ammonium polyphosphate, the presence of phosphorus (or sulphur) derivatives is able to generate acid or acid-forming agents [135]. This acid could also could remove some hemicellulose and lignin thus increasing the fibre density beside the chemical deposition on the fibres (24.94%) during the treatment. However, the acid is not strong enough to roughen the fibres as happened to the cotton fibre treated with fire retardant in Lam et al. [136] work.

The hemp fibre also swelled when treated with combination of NaOH and FR (NaOH+FR) and this can be seen from the Figure 5.2(d). This sample exhibited the highest chemical pick-up (30.10%) as a result of the combination treatment with NaOH and FR. The sputtering on fibre surfaces shown in Figure 5.2(d) was due to the reaction between the two chemicals. When the fabric was treated with NaOH, no neutralisation was done to optimise the effect of fire retardant on the fibre, thus the content of the alkali remaining in the fibre can be said to be higher (refer Section 5.2.2). As mentioned above, the FR chemical was slightly acidic suggesting that a reaction between the chemicals was happened. Therefore, the sputter as shown in WHF-NaOH+FR surface is salt, products of the reaction between a generated acid and pure alkali from FR and NaOH respectively. It is worth mentioning that, in addition to the consequences of the treatment, are the elimination of hemicellulose and lignin on top of the addition of salt to the fibre surface which latter caused the increment of the fibre density of this sample.

In referring to Table 5.2, as a consequence of the swollen fibres, all the treated hemp fabrics experienced an increment on their yarn crimps because the yarn was releasing the tension which developed during yarn spinning, fabric weaving and fabric finishing [136]. This also lead to an increased thickness and density of fabric because, when crimping yarn, the whole fabric shrinks due to strictly yarn interlacement making the fabric thicker and contract more yarns per area. The total fabric cover is also increased due to the fabric shrinking and yarn contraction. The increment in fabric weight is not only due to the yarn crimping which make it shrink and become thicker, but also to the deposition of chemical treatment on the yarns and fibres.

Table 5.2 Physical properties of all WHFs.

Physical Properties		Untreated	NaOH	FR	NaOH + FR
Chemical pick-up (%)		N/A	18.19	24.94	30.10
Fabric Shrinkage (%)	Warp	N/A	5	1.67	4.33
	Weft	N/A	3	0.67	1.67
Fibre density (g/cm^3)		1.47	1.51	1.54	1.53
Fabric density (per 2cm)	Warp	25	26	26	26
	Weft	23	25	23	25
Total yarn weight (g/m^2)	Warp	119.81	139.48	148.48	155.56
	Weft	116.86	140.24	147.23	152.34
Fabric weight (g/m^2)		236.67	279.72	295.71	307.90
Thickness (mm)		0.42	0.46	0.43	0.45
Yarn Size (Tex)	Warp	90	96	105	108
	Weft	93	100	116	110
Yarn Crimp (%)	Warp	6.0	11.4	8.66	10.40
	Weft	9.3	12.2	10.53	10.86
Total Fabric Cover, K		0.66	0.71	0.72	0.74

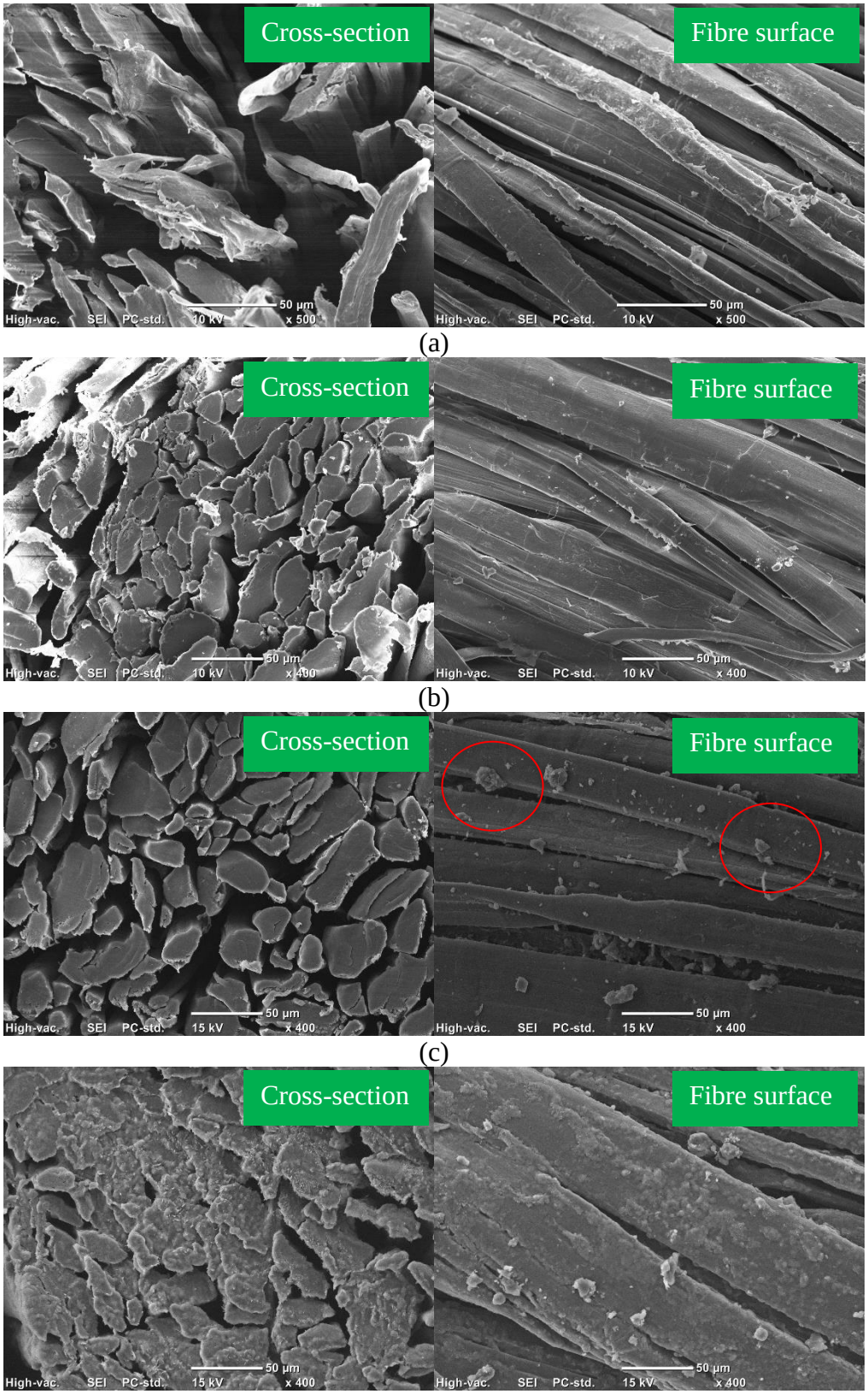

Figure 5.2 Scanning electron images of all WHF samples fibres in cross-section and fibre surface views; (a) untreated, (b) NaOH, (c) FR, and (d) NaOH + FR

5.3.2 Effect of Fire Retardant Treatment on Ignition Time and Burning Behaviour of WHFs

The differences in the burning behaviour of the untreated and fire retardant treated WHF can be observed from the ignition time and burning behaviour tests. In this test, the time exposure to small flame was set for 12 s. The fabric was exposed to flame in both warp and weft directions and the results for each sample was the average of the three specimens. Table 5.3 shows the results of ignition time for all fabric samples in this work.

Among the samples, only the untreated sample was completely burnt. There are no notable differences between the times taken in between warp and weft specimens. The ignition time for WHF was about 3 to 3.5 s and, after the flame source was removed, the fabric burnt rapidly. The time taken for the whole specimen to burn was between 247 to 249 s. When the flame was extinguished, the fabric continued to smoulder for another 27 s leaving a very poor residue behind. Figure 5.3(a) shows the image of the burning test, which was taken when the fabric was still burning, while Figure 5.3(b) is after the flame was extinguished. It was also observed that the fabric was burnt with yellow flames, released white smoke and smelt like burnt paper, which is common for natural fibres.

In the case of the WHF-NaOH sample, the time taken for the fabric to ignite was longer than the WHT-UT sample at about 7 to 8 s. Moreover, the flame typically only continued for about 3 to 5 s after the fabric was exposed to flame for 12 s. Figure 5.3(c) shows the burning test for the WHF-NaOH right after the flame self-extinguished and it was observed that the fabric continued to smoulder for another 42 to 46 s before the fire was totally extinguished. The fabric that was exposed to the flame source was

burnt (including burning during smouldering) to ash as can be seen in Figure 5.3(d). The total burning process for sample WHF-NaOH from flame exposure until it was extinguished were 57 s and 63 s for both warp and weft directions respectively. Other characteristics observed during the burning were: the flame was yellow in colour, released white smoke and produced an intense smell due to the burning of the alkali content in the fabric. In terms of total burning times, the fire retardant property for the WHF was improved with the NaOH treatment in comparison with the untreated sample (WHT-UT).

From Table 5.3, sample WHF-FR shows good properties against fire. It was observed that neither ignition nor flame sparked on the fabric sample when exposed to the flame. Only the charring process occurred at the contacted point of the flame source, and the carbonaceous char spread a bit to the upper part of the fabric during exposure to the flame source. Figure 5.3(e) shows the WHF-FR sample after flame source exposure and its char formation size was small in comparison with the WHF-NaOH sample. It was also observed that the exposure of WHF-FR to the flame produced white smoke and an intense smell similar to the WHF-NaOH sample. From Figure 5.3(f), the WHF sample treated with NaOH and FR chemicals (WHF-NaOH+FR) exhibited effects comparable with WHF-FR. Neither ignition nor smoulder was observed during the flame test and it also produced white smoke and an intense smell.

In the case of WHF-FR and WHF-NaOH+FR, char formed and successfully extinguished the fire. This char is undoubtedly attributed to ammonium polyphosphate and NaOH contents in the FR chemical [135]. Char formation can make the carbon and hydrogen remain in the condensed phase thus reducing the mass of volatile combustible degradation fragment evolved. Char also acts as thermal insulation by

remaining on the virgin polymer substrate, absorbing some of the heat input thereby reducing the heat flux reaching the virgin polymer [137, 138]. As the char surface temperature increased, re-radiation loss increased significantly helping to prevent thermal degradation. Char formed at substrate surfaces also acted as a physical barrier to obstruct the flow of combustible gases generated from the degradation of the underlying unburnt material hindering the access of oxygen to the surface of the polymer [138] In the case of WHF-NaOH, it can be said that the extinguishing of the fire was not only due to the char formation because there was smouldering after the fire was extinguished (Figure 5.3(c)). This was due to some combustible gas leakages that reacted with oxygen and continued to burn the residual virgin polymer of hemp fabric (charred parts) [137, 138].

Table 5.3 Results of burning behavior and ignition time.

Sample	Ignition time (s)		Total burning time (s)		Duration of afterglow (s)	
BS 5438:1976	Warp	Weft	Warp	Weft	Warp	Weft
WHT-UT	3.5(0.3)	3.4(0.1)	247.3(2.61)	249(5.29)	274(7.94)	276(6.24)
WHT-NaOH	8 (0.9)	7 (0.91)	15(1.53)	17 (2.01)	57.7(7.51)	63 (13.96)
WHT- FR	X	X	X	X	X	X
WHF-FR+NaOH	X	X	X	X	X	X

X – Indicates the expected event had not happened.

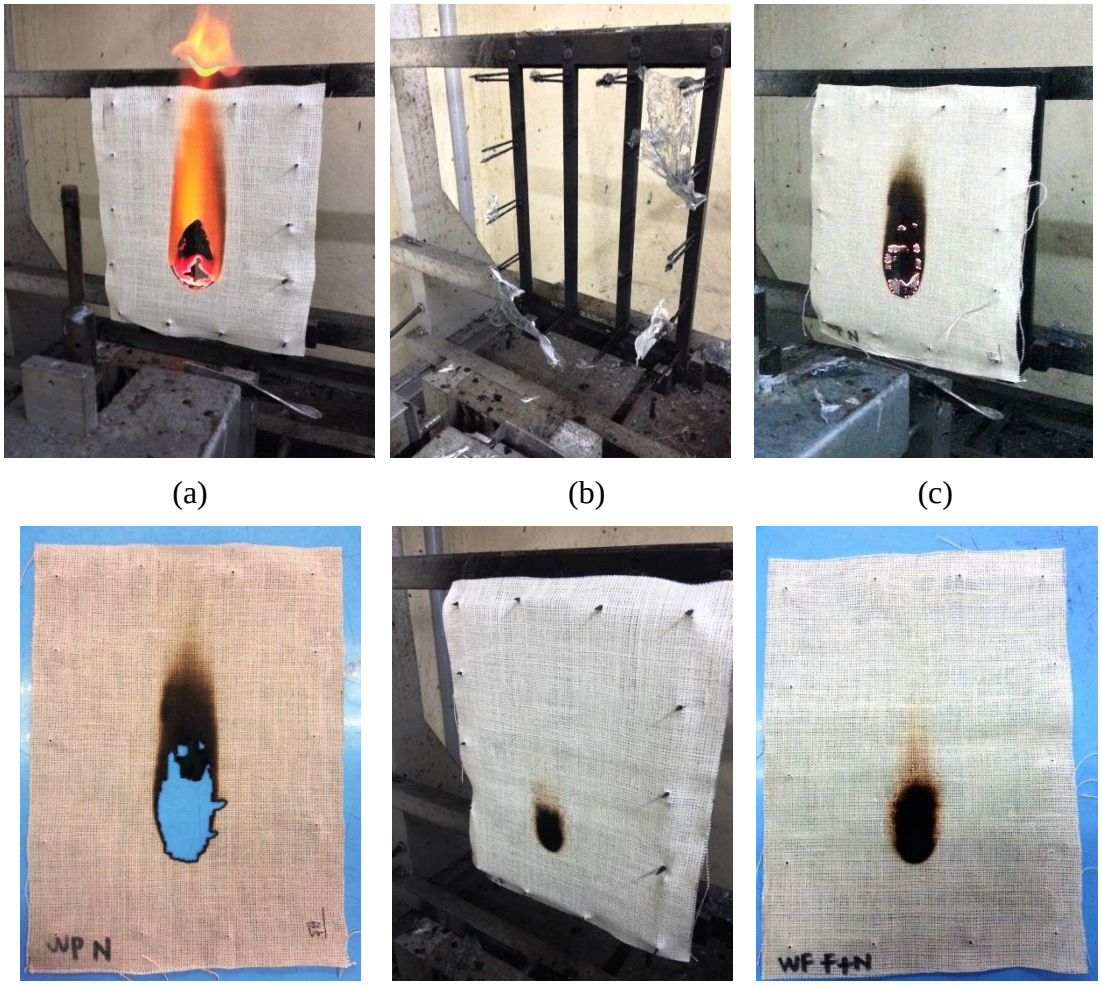

Figure 5.3 Burning characteristic of WHF sample; (a) WHF-UT sample during the test, (b) WHF-UT sample after burning and, (c) WHF-NaOH sample smouldering (after glow). (d) WHF-NaOH, (e) WHF-FR and, (f) WHF-NaOH+FR after burning characteristic test.

5.3.3 Spreading of Flame

The spreading of flame was tested for the untreated and all treated WHF samples. The time taken (in seconds (s)) for flame travel along the fabric was recorded at three different marks (yarn tread) which were at the height of 300 mm, 600 mm and to the horizontal direction either left or right. The burning rates were calculated by means of dividing the length of fabric vertically (600 mm) by their burning times in seconds (s) [125]. The flame spreading results for all WHF samples is shown in Table 5.4 and it was found that only the untreated sample (WHF-UT) was completely burnt. It took

only 22 and 23s after exposed to the flame source for the flame to reach the first mark and the total times to reach the second mark were recorded 46 and 50s for both warp and weft, correspondingly. The movement of flame to the horizontal part was slower and recorded at 77 and 74s in total of time for both warp and weft specimen respectively. The burning of this WHF-UT sample can be depicted in Figure 5.4(a), when it was exposed to the flame source and, in Figure 5.4(b), when it reached all three marks. The burning rate of this sample was measured in the range of 1.2 to 1.3 cm s-1 for both warp and weft directions.

Contrasting with the untreated WHF-UT sample, all the treated WHF samples did not reach all three marks because they did not burn when they were exposed to the flame source. Therefore, the burning time cannot be measured for all the treated WHF. These flame spreading test results were expected. The short flame source exposure in 12s did not affect all the treated WHF samples.

Table 5.4 Flame spreading results of all WHFs.

	1st mark (300 mm) (s)		2nd mark (600 mm) (s)		Horizontal (s)		Burning Rate (cm s^{-1})
ISO 6491	warp	weft	warp	weft	warp	weft	Vertical
WHF-UT	22.33 (1.53)	22.25 (1.09)	46.17 (1.04)	50.43 (1.50)	77.08 (1.01)	73.17 (1.04)	1.2-1.3
NaOH	X	X	X	X	X	X	X
FR	X	X	X	X	X	X	X
NaOH + FR	X	X	X	X	X	X	X

X – Indicates the expected event did not occur.

Therefore, in order to investigate the WHF flammability properties further, especially the burning rate or char burning rate, it was suggested that flame exposure be extended from 12 s to 2 minutes. In this way, particularly for the FR treated fabrics, the burning rate or char formation rate can be measured under the exaggeration of flame. This also imitates a real fire situation in which the hemp fabric might be exposed to continuous

fire from other sources such as burning woods, papers etc. Table 5.5 shows the results of the spreading flame test for all treated WHF samples subjected to 2 minutes flame exposure. Even with the longer exposure to flame, all types of treated samples did not reached first mark. The WHF-NaOH sample did burn, but as soon as the flame source was removed, the flame continued for several seconds before extinguishing with some smouldering for another 20 to 50 s. However, the flame and smoulder had burned the char into ash and this was similar to what was been discussed in Section 5.3.2.

Table 5.5 Flame spreading results for all treated WHF samples when subjected to 2 minutes flame exposure.

	1st mark (300 mm) (s)		2nd mark (600 mm) (s)		Horizontal	
ISO 6491	warp	weft	warp	weft	warp	weft
WHF-NaOH	X	X	X	X	X	X
WHF-FR	X	X	X	X	X	X
WHF-NaOH + FR	X	X	X	X	X	X

X – Indicates the expected event did not occur.

In the case of another two treated samples, it was observed that during the flame source exposure, char formed on both the WHF-FR and WHF-NaOH+FR samples and grew towards the end of exposure. The width and height of the burnt area or char formation on the treated WHF as well as the char formation rate were measured to analyse the different effects of flame exposure duration (results are shown in Table 5.6). The recorded figures was an average of three readings for the respective treated WHF sample.

Comparing all the samples in Table 5.6, the WHF-NaOH sample's burnt area was bigger than those of the other samples when exposed to flame. This can be seen from

Figure 5.4(c), (d) and (e). The WHF-NaOH sample burn width increased 75%, from 42 to 71mm when exposed to flame for 2 minutes, while the height increased 124.5%, from 98 to 220mm. For the WHF-FR and WHF-NaOH+FR samples, the width and height of the char formation area were about 50% less than the WHF-NaOH sample for both flame exposure times. Nevertheless, it was observed that the char formation from the WHF-NaOH+FR sample was a little lower than the WHF-FR sample indicating that the combined treatment can give a better effect on fire retardant properties.

Since all the treated WHF samples were exposed longer to the flame source, the char formations on the fabrics were bigger. Therefore, the char formation rates of all treated WHF samples were able to be measured. The char formation rate of the WHF-NaOH sample was the highest of all the samples, but this rate was far lower than the burning rate of WHF-UT (refer Table 5.4). The char formation rates of WHF dropped about 55% with the incorporation of the FR chemical in comparison with WHF-NaOH, and the lowest was possessed by theWHF-NaOH+FR sample. With this char formation rate, in spite of the under exaggeration of longer flame time, there is no way that all treated WHF could reach even the first mark (300mm) on the test. Nevertheless, it was shown that all the treatments on the WHF samples enhanced the flame retardant properties with the best result from the combination of NaOH+FR, followed by FR, and then NaOH.

Table 5.6 Spreading of burnt or char formation for all treated WHF samples

ISO 6491	Burnt/Char formation (mm)	

	12 s		120 s		Char Formation Rate for 120 s (cm s^{-1})
	Width	Height	Width	Height	
WHF-NaOH	43 (2.52)	100 (2.08)	71 (2.08)	220 (2.00)	0.183
WHF- FR	23 (1.00)	31 (1.53)	38 (1.52)	98 (0.91)	0.082
WHF-NaOH+ FR	20 (0.99)	30 (0.95)	36 (0.97)	87 (1.53)	0.073

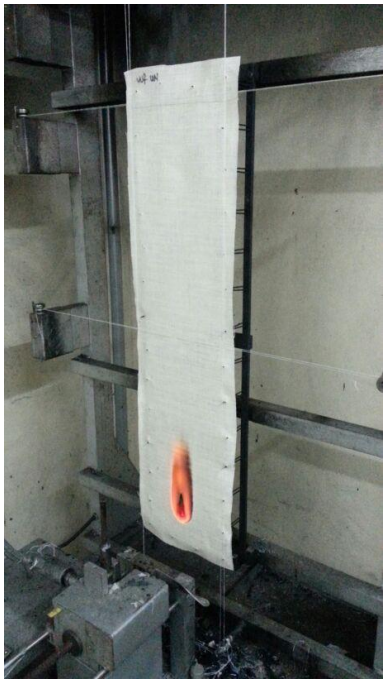

(a) (b)

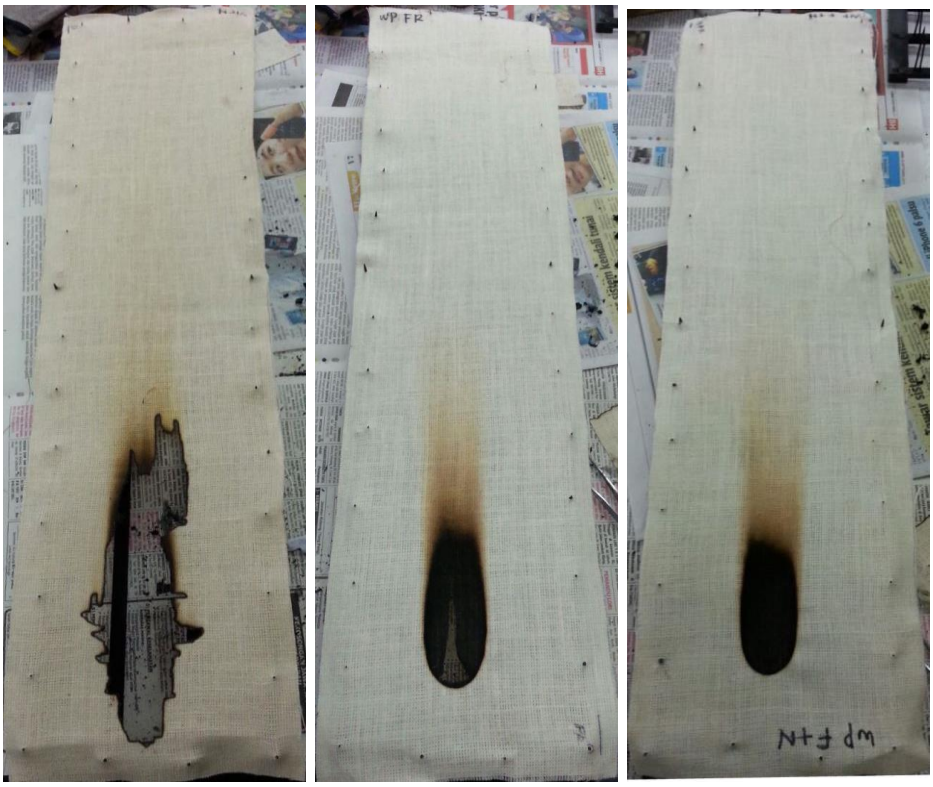

(c) (d) (e)

Figure 5.4 Flame spreading test photos, a) and b) are WHF-UT specimen under flame spreading test, and samples, c) WHT-NaOH, d) WHF-FR and e) WHF-NaOH+FR after the test.

5.3.4 Thermal Properties/Behaviour of Untreated/Treated WHF

Studies of the thermal decomposition of the treated fabrics were carried out by thermogravimetric (TG) and derivatives themogravimetric (DTG) analyses. Figure 5.5(a) and (b) show the TG and DTG curves, respectively, for all the samples while Table 5.7 shows the temperature at maximum mass loss rate, mass loss rate and char yield. The TG analysis of the untreated WHF (WHF-UT) sample shows that the main pyrolysis started from the onset temperature of degradation at about 220 until 400°C and the temperature of the maximum mass loss rate was at 379°C (refer Table 5.7). At the end of the main pyrolysis, the mass loss due to completed cellulose dehydration

accounted for 80% at 400°C. The mass loss during this stage was very fast due to the degradation of hemicellulose and cellulose composition in hemp fibres. As the temperature increased, hemicellulose was firstly degraded due to the cellular breakdown and then followed by cellulose degradation at a higher temperature because cellulose is highly crystalline [91, 92]. Most of the pyrolysis by-products of cellulosic are produced in this stage, including L-Glucose as the major product, and combustible gases [128]. The main pyrolysis behaviour of hemp on the TG curves is similar to cotton, but its main degradation starts at a higher temperature which is at 300°C and ends at lower than hemp which is 380°C [127]. This is because cotton has a lower cellulose content (about 45%) than hemp (about 75%) fibre [67].

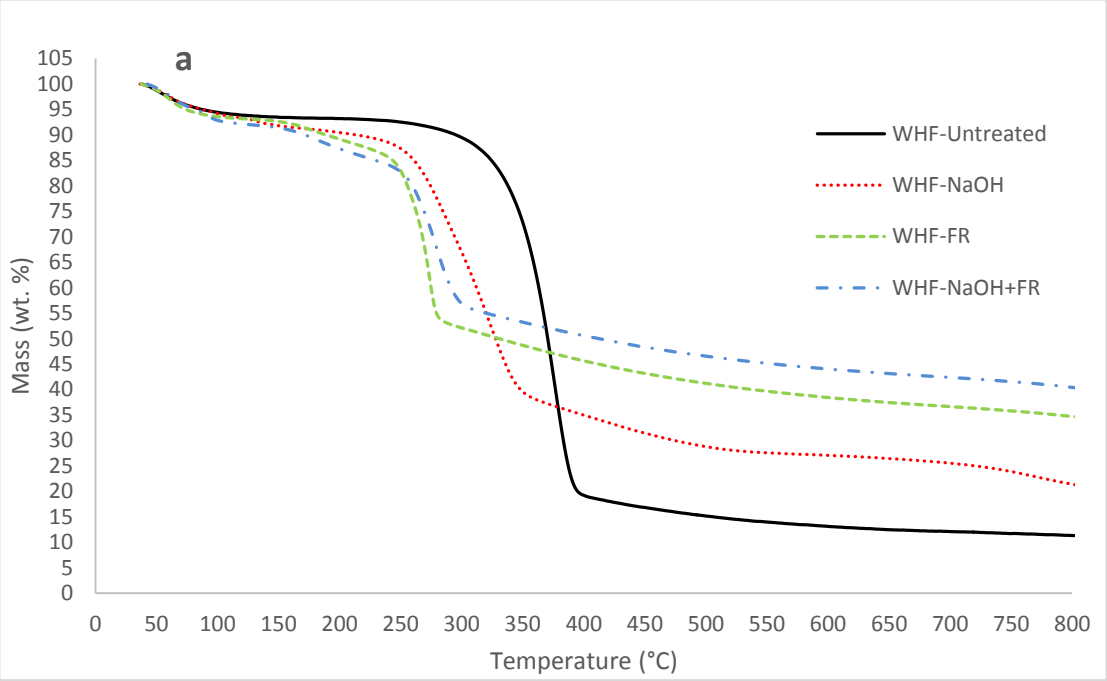

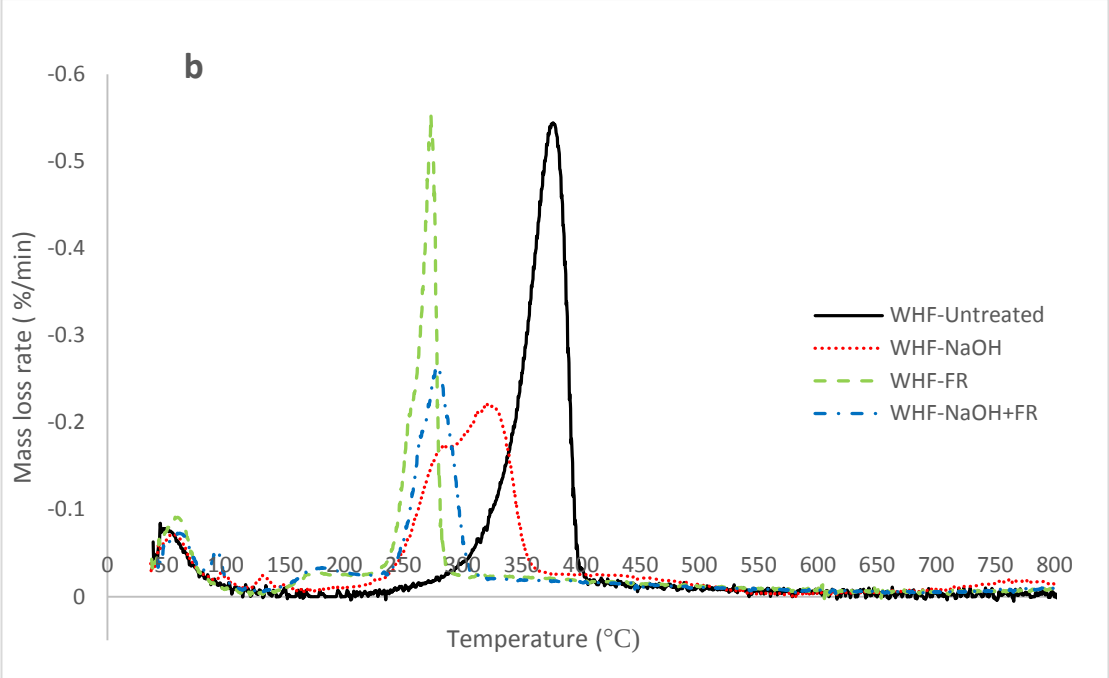

Figure 5.5 TG (a) and DTG (b) curves of untreated and treated WHF samples.

Table 5.7 Temperature at maximum mass loss rate and char yield at 800°C of all WHF samples

Sample	Max. temperature of mass loss rate (°C)	Mass loss rate (%/min)	Onset temperature of charring reaction (°C)	Char Yield (%)	
				Charring reaction onset temp.	800°C
WHF-UT	378.667	0.54	400	19	11
WHF-NaOH	320.528	0.22	360	38	21
WHF-FR	273.219	0.55	285	53	35
WHF-NaOH+FR	278.218	0.26	310	56	40

The charring reaction or char pyrolysis of WHF-UT tends to end above 400°C. During this process, dewatering and charring reactions are more dominant than L-glucose

production. As the dewatering and decarboxylization continue, water and carbon dioxide are released, thus producing double bonds, carboxyl and carbonyl products. The carbon content becomes higher as the decomposition continues thus forming charred residues. This phenomenon is common during the pyrolysis process of cellulosic fibres [127].

As presented in Figure 5.5, the TG curves for all treated WHF samples indicated that the mass loss began at a lower temperature (shift of about 20 – 80°C) in comparison with the untreated WHF. This is common behaviour for those natural fibres treated with chemicals mean to enhance its flame retardancy which related to either condensed phase and/or vapour phase mechanisms. Most of fire retardant treated natural fibres are experienced a decrement in their onset decomposition temperature due to the dehydration of cellulose which promoting water vapour and char on the fibre surfaces and later dissipates heat from the flame and/or reducing volatile gas (being the fuel to the combustion). However, after the decrement on the onset decomposition temperature the pyrolysis of hemp fibre become slower than the untreated specimen [78, 125, 140, 141]. In the case of the WHF-NaOH sample, the mass loss started at 200°C, reached the maximum mass loss rate at the temperature of 360°C, and completed dehydration of cellulose accounts 63% at 360°C. The loss of mass which was 20°C lower than the onset temperature of the WHF-UT sample is due to the removal of absorbed water plus carbon dioxide gained over the time [125].

According to Mostashari et al. [125], NaOH plays the role of dust or wall which causes heat absorption and dissipation at the combustion's zone, and consequently if the concentration of NaOH is high enough, no flame can propagate. This is because NaOH is highly stable at elevated temperatures and does not decompose on heating [139].

Hence, for the case of WHF-NaOH sample, NaOH which remains intact in hemp fibres absorbs and dissipates the heat thus lowering the temperature and extinguishing the flame.

Another aspect that should be taken into account is that several flame retardants generate inert gasses such as CO_2, SO_2, H20 and NH_3 during thermal decomposition. The environment in the area of inflamed substrate could be diluted by the inert gasses and this situation complicates fuel gas such as oxygen access into the flammable volatiles of combustion's product [140]. This situation creates flame retardancy and this mechanism is also known as 'gas dilution theory' [141]. With respect to WHF-NaOH, the incorporation of NaOH into hemp fibre allows it to expel water vapour (at similar function to inert gas) under burning condition. Therefore, forming of water vapour can absorb a lot of heat in combustion and this treatment could act as a dehydrating flame retardant agent.

The TGA curves for the WHF-FR and WHF-NaOH+FR samples indicate weight loss starting at almost 140°C and this is much earlier which about 80 and 60°C than WHF-UT and WHF-NaOH, respectively. The maximum mass loss temperatures for both samples are given in Table 5.7 at the temperatures of 273°C and 278°C respectively. The process finished at about 285 to 310°C for WHF-FR and WHF-NaOH+FR correspondingly. It shows that, the main pyrolysis stage for WHF-FR and WHF-NaOH+FR began and ended earlier than the other two samples. This is due to the presence of ammonium polyphosphate which promotes dephosphorylation and acid-catalyzed dehydration of samples catalysed by the nitrogen [78, 142]. This is further supported by the accompanying higher weight loss (~10%) compared with untreated WHF (~6%) for temperatures up to 140°C the TG curves. Thus, the incorporation of

fire retardant chemical (ammonium polyphosphate) and combination of NaOH and fire retardant chemical promotes cellulose dehydration at a higher degree than the sample treated with NaOH alone. The char reaction phase for both WHF-FR and WHF-NaOH+FR samples also occurred earlier than the other two samples, which began at about 285 and 310°C respectively, and their mass loss was also became slower. This is because the phosphorus in a sample affected the composition of the intermediate chars in the second stage during thermal degradation, slowing down the reaction of the already decomposed residue [78].

The char yield percentages for all the samples were also extracted from the thermogravimetric curves as shown in Table 5.7 at the char reaction onset temperature and 800°C. The char yield percentages at the char reaction onset temperature in high-to-low order were WHF-NaOH+FR, WHF-FR, WHF-NaOH and WHF-UT with the value of 56, 53, 38 and 19% correspondingly. Whilst, at the end of the themogravimetry tests (800°C), a similar trend of char yield for all samples in high-to-low order was found with the value of 40, 35, 21 and 11%, respectively. The highest char yield possessed by the WHF-NaOH+FR sample is due to the addition of NaOH. Xu et al. [78] suggested that the fire retardant properties increase with the increases of char yield. Thus, at this point, in terms of thermogravimetry analyses, the treatment with the combination of NaOH and the fire retardant chemical could performed the best thermal properties to WHF as well as a char yield suggesting the best fire retardant properties in comparison to all other samples. This is followed by the WHF-FR, and lastly the WHF-NaOH sample.

5.3.5 Limiting Oxygen Index Results

The LOI measurement test is widely used to evaluate the flammability of materials. It shows the minimum amount of oxygen in an oxygen–nitrogen mixture required to support complete combustion of a vertically held sample that burns downward from the top of the sample. The higher the LOI value, the more effective the flame-retardant treatment [77, 78]. The ASTM D2683 gives no fire retardant base level with LOI value. However, according to Kamath et al. [79] a LOI value more than 28 is generally classified as fire retardant. In accordance to the GB50222-1995 standard method, 1) value of < 21 indicates the material is flammable; 2) value of ≥ 24 and < 27 indicates the material is combustible, and; 3) value of ≥ 28 indicates the material is fire retardant.

The results of LOI as shown in Table 5.8 explains the fire retardant phenomenon discussed in Section 5.3.3. The highest LOI value was shown by the WHF-FR sample followed by WHF-NaOH+FR. Their values are about double that of the LOI value of the sample treated with NaOH only. The untreated sample possessed the lowest value of all the samples.

The LOI value for WHF-UT is comparable with the untreated hemp fabric tested by Xu et al. [78]. Since the value is lower than 21, thus the hemp fabric is classified as a flammable material. That is why the untreated hemp was completely burnt and left very minimal residue in the burning test. Treatment with NaOH on the hemp fabric increased the LOI value to 24 and this is clustered under combustible material. When the WHF-NaOH sample is subjected to the burning test, the ignition of fire produced a yellow flame. Even though the flame could be self-extinguished, smoulder was produced and kept burning char residue (refer Section 5.3.3) and this fabric could still burn by the exaggeration of other fire sources.

The LOI value for the WHF-FR sample was more than 28, thus this sample is clustered as fire retardant. During the burning test, there was no ignition or smoulder produced, but the rapid formation of char was noticed. In Xu et al. [78] work, hemp fabric treated with phosphorus only compound possessed LOI value of 27 and this value is just enough to contribute as fire retardant. However, with the addition of a phosphorus percentage and other compounds such as nitrogen, halogen and boron in the formulation, they managed to increase the LOI value of treated hemp fabric to 41. Therefore, it can be assumed that either the ammonium polyphosphate content is high or another chemical compound exist in the fire retardant chemical to which the highest LOI value to the WHF in this work is attributed. In the case of WHF-NaOH+FR, there is a high probability that the NaOH content leads to the decrement of the LOI value. However, under the burning test, the burning characteristics were physically similar to the WHF-FR sample.

Table 5.8 LOI results of all WHF samples.

Samples	LOI
WHF-UT	18.6
WHF-NaOH	24.2
WHF-FR	51.0
WHF-NaOH+FR	49.4

5.3.6 Effect of Chemical Treatment on the Mechanical Properties

The study on the behaviour of WHF can be clustered into three phases. The first phase is the initial region, demonstrated by a curve with a low slope. The second phase is the linear region of the curve, which rises steeply until its summit is reached and the third phase is the curve after it reaches the peak [107, 133].

Figure 5.6 shows the typical tensile stress–strain response for all the WHF samples. Each sample was cut and tested in the warp and weft directions. Table 5.9 summarizes the average tensile properties for each WHF sample. The tensile properties reported are the average and standard deviation from all the specimens.

For the warp direction (Figure 5.6(a)), every WHF sample possessed different curves due to the variation in the strain percentage. The strain percentages were varied due to the chemical treatments applied to each WHF sample which affected their yarn crimp (originally 6% as shown in Table 5.2) and was disclosed as the fabric shrinkage percentage. When the treatments were applied on the WHF samples, the fibres were swollen and, as a consequence, the whole fabric system experienced shrinkages as discussed in detail in Section 5.3.1. Based on Table 5.2, in the warp direction, the WHF-NaOH sample exhibited the highest fabric shrinkage, followed by WHF-NaOH+FR and the lowest was possessed by WHF-FR. For the sample which had the higher fabric shrinkage, it took more time for the yarn to be straightened, thus affecting the overall strain percentage (Table 5.9) of each sample.

In terms of tensile strength, the highest was possessed by the WHF-UT sample and then decreased by the chemical treatment applied to them. In the case of WHF-NaOH, NaOH removes hemicellulose and lignin partially from the fibres resulting in easy deformations of cellulose microfibrils during tensile loading. The presence of hemicellulose and lignin held the mircrofibrils in position and resisted slippage when subjected to tensile loading. Thus the losses of some hemicellulose and lignin in fibre weakened the bonding of the microfibrils thus resulting in lower tensile properties as compared to untreated fibres [94, 109]. For the WHF-FR sample, there is a high possibility that some amount of cellulose in the hemp fibre is hydrolysed during the

fire retardant treatment causing minor degradation then resulting in a decrease in strength [136, 143, 144]. This is because the ammonium polyphosphate compound in fire retardant is an inorganic salt of polyphosphoric acid and it is dissolved or hydrolysed in acid solution [53, 145]. In the case of WHF-NaOH+FR, since the fabric was firstly treated with NaOH, the strength was reduced due to the reason discussed above. It was then further decreased due to the FR treatment but, since the fibres were already deposited by NaOH, the FR (ammonium polyphosphate) reacted with NaOH to produce salt. Therefore, the tensile strength of WHF-NaOH+FR was a little higher than WHF-FR.

In terms of tensile modulus for the warp direction, from Table 5.9, it can be seen that all treatments reduced the tensile modulus of WHF. Apart from the increment of yarn crimp percentage which latter increased the fabric shrink, thus decreasing the stiffness of fibres, there are other suggestions on this. According to Christian and Billington [35] a higher tensile modulus is also attributed to the higher fibre density in fabric. Nevertheless, the mechanical properties of WHF in this work, especially in tensile modulus, did not entirely fulfil the statement made by Christian and Billington [35] because they did not perform any treatment on their hemp fabric. In this work, even though the densities of all treated WHF were higher than the untreated sample, the treated WHFs exhibited a lower tensile modulus. This is because all the treatments employed in this work eliminated some hemicellulose and lignin and hence reduced the stiffness of the WHF because, other than tensile strength, the stiffness of the hemp fibre is depended on these two compounds [67].

It was worse when the WHF was treated with the FR chemical (WHF-FR) due to the hydrolisation of some of the cellulose compound. In the case of WHF-NaOH+FR,

higher tensile strength was achieved but it possessed lower tensile modulus than WHF-FR. Since the WHF was firstly treated with NaOH and consecutively with the FR chemical, the FR chemical was responsible for the further elimination of hemicellulose and lignin thus decreasing the tensile modulus of WHF-NaOH+FR sample.

In terms of the weft direction, all mechanical properties shown in Table 5.9 followed a similar trend to the warp direction except for the tensile strain. The original yarn crimp for weft yarn (9.3%) was longer than warp (6%) (refer to Table 5.2). It is normal for weft yarn to have a higher yarn crimp than warp yarn due to the tension arrangement during the process of weaving [53, 107, 133]. After the treatments, all treated samples in the weft direction WHF had shrunk but the shrinkage percentages were lower than the warp direction. This is due to the higher density of fabric in the warp direction which prevents the weft yarn to shrink further. As a consequence, the built- up pressure in the weft is gets higher and this is the reason why the tensile strength and modulus of weft yarn were higher than warp yarn tension. Thus, a higher load is needed to overcome the weft yarns ' built- up pressure apart from its higher yarn size (refer to Table 5.2). Sample WHF-NaOH exhibited the highest tensile strain as a result of its highest fabric shrinkage (refer to Table 5.2) from the swollen fibres. From Table 2, it can be seen that WHF-FR possessed lower fabric shrinkage than WHF-NaOH+FR, and as a result, a similar trend was shown in their tensile strain. However, their tensile strains were less than the untreated sample (WHF-UT). This was due to the effect of FR chemical which disturbs the decrimping process when treated WHF is subjected to tension loading. Although all the chemical treatments did increase the fire retardant properties of WHF, the WHF suffered from a decrement in mechanical properties.

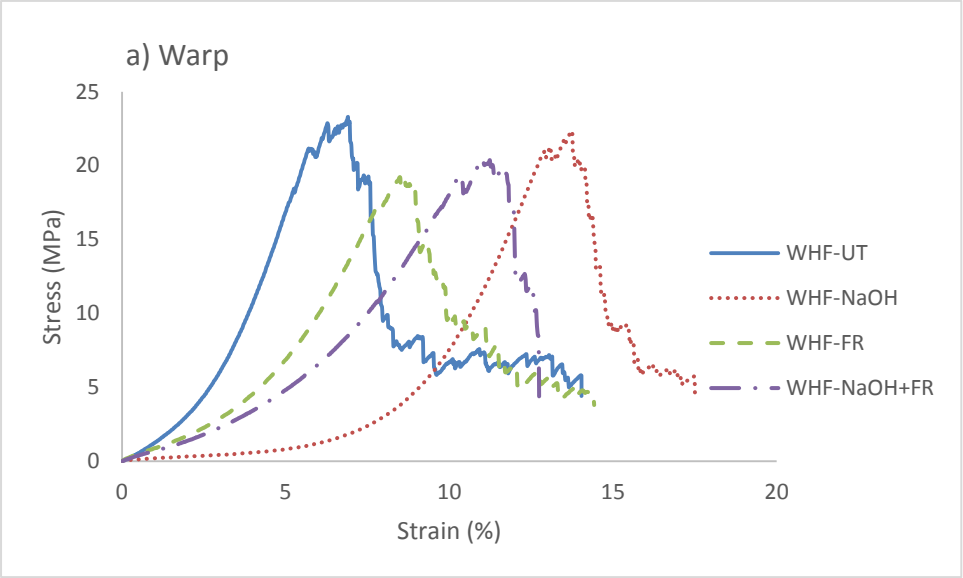

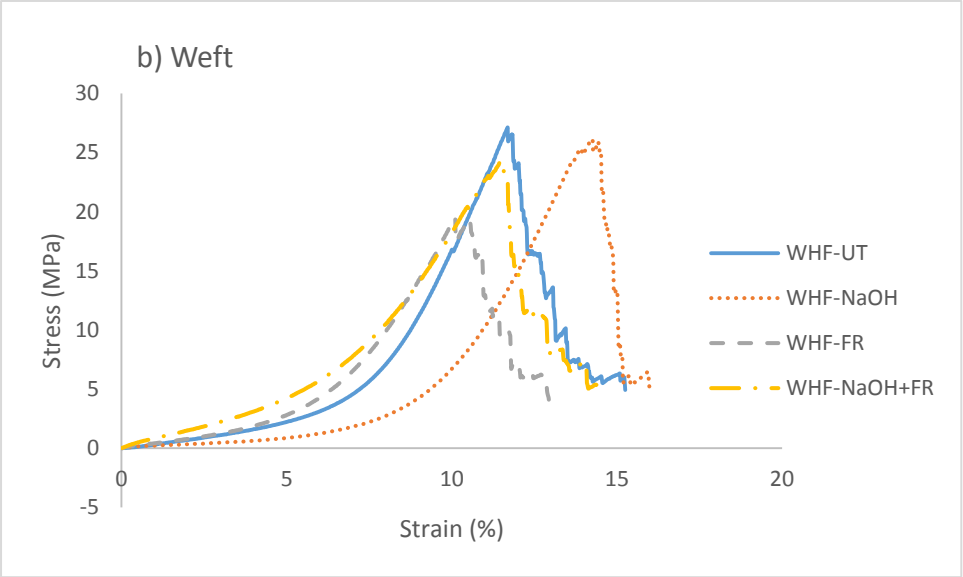

Figure 5.6 Typical tensile stress-strain response for, (a) warp and (b) weft of all WHF samples

Table 5.9 Summary of tensile properties for all WHF samples

Sample		Peak Load (N)	Tensile Strength (MPa)	Tensile Strain at Peak (%)	Tensile Modulus (GPa)
WHF-UT	Warp	444.440 (13.65)	23.515 (0.72)	6.459 (0.389)	0.590 (0.0098)
	Weft	510.88 (8.396)	27.031 (0.448)	11.187 (0.37)	0.621 (0.026)
WHF-NaOH	Warp	427.420 (30.74)	22.615 (1.63)	13.992 (0.508)	0.442 (0.0103)

	Weft	493.18 (24.73)	26.094 (1.308)	14.893 (0.787)	0.445 (0.008)
WHF-FR	Warp	365.740 (6.395)	19.351 (0.338)	8.323 (0.417)	0.398 (0.026)
	Weft	394.26 (33.61)	20.860 (1.778)	11.048 (0.647)	0.41263 (0.0100)
WHF-NaOH+FR	Warp	380.080 (24.66)	20.110 (1.302)	11.096 (0.0044)	0.338 (0.028)
	Weft	462.64 (10.779)	24.478 (0.571)	11.650 (0.362)	0.360 (0.0391)

*Figures in bracket indicate standard deviation

5.4 Conclusions

Impregnation of NaOH, FR chemicals and a combination of both demonstrated an improvement in flame retardant properties of WHF. The detailed analyses on the treated WHFs showed several findings which are important for this material if it is to be used, not only in textile and apparel, but also in technical and engineering fields. The treatments really affect the physical properties of the WHF. The densities increased from 1.47 to 1.53g/cm^3 depending on the treatments. The fabric also shrank within the range of 1.67 to 5% and 0.67 to 3% for warp and weft, respectively. The changes are attributed to the changing of the physical properties of woven hemp fibre. The fibre cross-section changed from elliptical to a rounder and cleaner surface by NaOH, deposition of particle by FR on the fibre surfaces and salt deposition by the combination of the NaOH and FR treatments. Under the burning test, the treated WHF showed good results against the fire. Nevertheless, WHF treated with FR and combination between NaOH and FR were found to be better than the NaOH treatment.

In terms of thermogravimetric analyses, impregnation of treatments improved the onset of WHF main pyrolysis from 220°C to much earlier which at 140°C. The earlier pyrolysis indicated faster cellulose dehydration and promoted char formation. The char yield at 800°C showed that the treatment with the combination of NaOH and FR

chemical could produce a good char residue which was 40%. In terms of LOI, the sample treated with the FR chemical showed the highest value of all other samples (51) suggesting that this is fire retardant material and is followed by the sample treated with combination of NaOH and FR (49.4). The sample treated with only NaOH is clustered under combustible because its LOI was lower than 27. In terms of tensile properties, the treatment reduces the strength of WHF for all tensile parameters ranging from 18 to 32% and 23 to 39% for warp and weft respectively. All the treatments really improved the fire retardant properties of the WHF however the mechanical properties were reduced. The next module of work is to investigate whether a composite fire retardant properties can be improved by utilising all treated WHFs.

Chapter 6 Fire Retardant Treatments on HVE Composites

6.1 Introduction

As mentioned in Chapter 2; Section 2.6.2, there are few works on applying a fire retardant agents to reinforcement directly (especially to hemp fabric) and studying the effect of this treated reinforcement in composite materials. Therefore, in the Chapter 5, the fire retardant properties of WHFs treated with several fire retardant treatments were analysed. In general, it is proven by burning, thermogravimetry and limiting oxygen index tests that, all treatments enhanced the fire retardancy of WHF. It is expected that these treated fabrics could give better fire retardancy to composite materials when they are utilised as reinforcement for a resin.

Therefore, in this chapter, all treated fabrics from Chapter 5 are converted to a composite material (HVE) using the best layer orientation mentioned in Chapter 4. Untreated fabric reinforced vinyl ester was fabricated as a comparison to all the treated fabric composites. The aim of this work was to investigate the fire retardant properties of the HVEs which were reinforced with treated WHFs. The WHFs were treated with sodium hydroxide (NaOH), commercial fire retardant chemical (FR) and the combination of both NaOH and FR (NaOH+FR). Investigation of fire retardant properties was done by means of burning test, thermogravimetry analysis and limiting oxygen index test. The characterisation of the treated WHF and the fabricated composites' mechanical properties was also done to analyse the effect of the fire retardant treatments. The assessment on their mechanical properties was again done in order to analyse the feasibility and readiness of the composites as a building construction material. The best treated sample will be chosen for further analysed in the next chapter.

6.2 Materials and Methods

6.2.1 Materials

All WHFs (untreated and treated) used to fabricate the HVE samples in this chapter are similar fabrics to those discussed in Chapter 5. The treatments applied to the fabric were as discussed in Chapter 5; Section 5.2.2. The physical characterisation of WHF are as follows;

- The chemical uptake or pick-up as well as fabric shrinkage for all treated WHF were measured using Equation (5.1) and (5.2) respectively and the detailed procedures of both measurement can be seen in the previous chapter, Section 5.2.3.

- The density of the treated fabrics were measured as explained in Chapter 5; Section 5.2.3
- The tests for measuring WHF thickness, fabric density/fabric count, yarn size (linear density) and yarn crimp percentage (for warp and weft) followed the particular standard methods. The standard methods for all the tests undertaken can be seen in Table 3.1 in Chapter 3; Section 3.2.1. The detailed measurements can also be found in the same chapter and section or in the [107].
- The weight of each fabric (untreated and treated) and total fabric cover factor (K-value) were also measured, and the detailed measurement processes can be seen also in Chapter 3; using Equation (3.4) in the Section 3.3.2 and Equation (3.6) in the Section 3.3.4 respectively.
- The mechanical properties were identified as discussed in Chapter 3; Section 3.2.4.

The abbreviations for WHF; untreated, treated with sodium hydroxide, treated with FR chemical and treated with sodium hydroxide combined with FR are UT, NaOH, FR and NaOH+FR, respectively. Table 6.1 and Table 6.2 show the physical and mechanical properties of untreated and treated WHFs adapted from Tables 5.2 and 5.9 respectively. The vinyl ester resin product code of SPV 1356 PROM THIX and the catalyst methyl ethyl ketone peroxide (MEKP), product code of NOROX 925H were supplied by Nuplex® Composite Industry (Australia). A commercial flame retardant (FR) chemical was supplied by Cyndan Chemicals, Australia.

Table 6.1 Physical properties of all WHFs (untreated and treated) adaptation from Table 5.2.

Physical Properties		UT	NaOH	FR	NaOH + FR
Chemical pick-up (%)		N/A	18.19	24.94	30.10
Fabric Shrinkage (%)	Warp	N/A	5	1.67	4.33

	Weft	N/A	3	0.67	1.67
Fibre density (g/cm^3)		1.47	1.51	1.54	1.53
Fabric density (per 2cm)	Warp	25	26	26	26
	Weft	23	25	23	25
Total yarn weight (g/m^2)	Warp	119.81	139.48	148.48	155.56
	Weft	116.86	140.24	147.23	152.34
Fabric weight (g/m^2)		236.67	279.72	295.71	307.90
Thickness (mm)		0.42	0.46	0.43	0.45
Yarn Size (Tex)	Warp	90	96	105	108
	Weft	93	100	116	110
Yarn Crimp (%)	Warp	6.0	11.4	8.66	10.40
	Weft	9.3	12.2	10.53	10.86
Total Fabric Cover, K		0.66	0.71	0.72	0.74

Table 6.2 Mechanical properties of all WHFs (treated and untreated) extracted from Table 5.9.

Treated Sample		UT	NaOH	FR	NaOH+FR
Tensile Strength (MPa)	Warp	23.52	22.62	19.35	21.83
	Weft	27.03	26.09	20.86	24.48
Tensile Strain (%)	Warp	6.5	14	8.3	9.6
	Weft	11.2	14.9	11.0	11.7
Tensile Modulus (GPa)	Warp	0.59	0.44	0.40	0.34
	Weft	0.62	0.45	0.41	0.36

6.2.2 HVE Fabrication Method

The resin was prepared by adding MEKP into the vinyl ester at the ratio of 1:44 by weight. This prepared resin was then applied to 10 fabric layers (300 × 300 mm for each layer) by employing the hand lay-up technique. The fabrics were layered in warp and weft alternately ($[0,90]_5$). Trapped air was gently squeezed out using a roller after pouring the resin onto the fabric. The mixture (wet fabrics) was then laid between

thick glass plates (400 × 400 × 100 mm in dimension) which were coated with a polymer mould release agent. This assembly was compressed with a weight placed on top of the mixture to remove the excess resin and the calculated pressure given to this assembly was 4.360 kPa. It was then left to cure at room temperature for 24 hours. After the 24 hours, post cured in an oven for four hours at 80°C. Four types of HVEs were fabricated as shown in Table 6.3.

Table 6.3 List of HVEs and their abbreviations.

Sample Abbreviation	Treatment
HVE-UT	Untreated
HVE-NaOH	Sodium Hydroxide (10%)
HVE-FR	Commercial Fire Retardant chemical
HVE-NaOH+FR	Combination of NaOH and FR

6.2.3 Physical Properties of HVE

The density of the HVEs was determined using similar a method and apparatus as discussed in Section 4.2.3, whilst the constituent contents of the HVEs (weight percentage and volume fraction) were determined according to ASTM D3171 test method II. Test method II can be employed as the distribution of fibres in the fabric form (in this case hemp) is acceptably consistent. By the densities and weights of WHF, vinyl ester and their fabricated composites are known; the reinforcement and matrix contents were calculated.

6.2.4 Burning Test

The fire retardant test was carried out according to ASTM D635. This fire-test response test method was used to compare the relative linear rate of burning of the HVEs in the form of a rectangular specimen in the horizontal position. Figure 6.1 shows a schematic illustration of the flame retardant test fixture. The gas was supplied

with a technical grade methane gas and the measured data was the rate of burning for the material. The burning rate was calculated according to the formula:

$$V = 60L/t \qquad \textbf{(6.1)}$$

Where V is the burning rate (in mm/min); L is the burning length (mm); and t is the time (s) for the flame to travel L (mm). The burning rate data reported were the average of five replicated experiments.

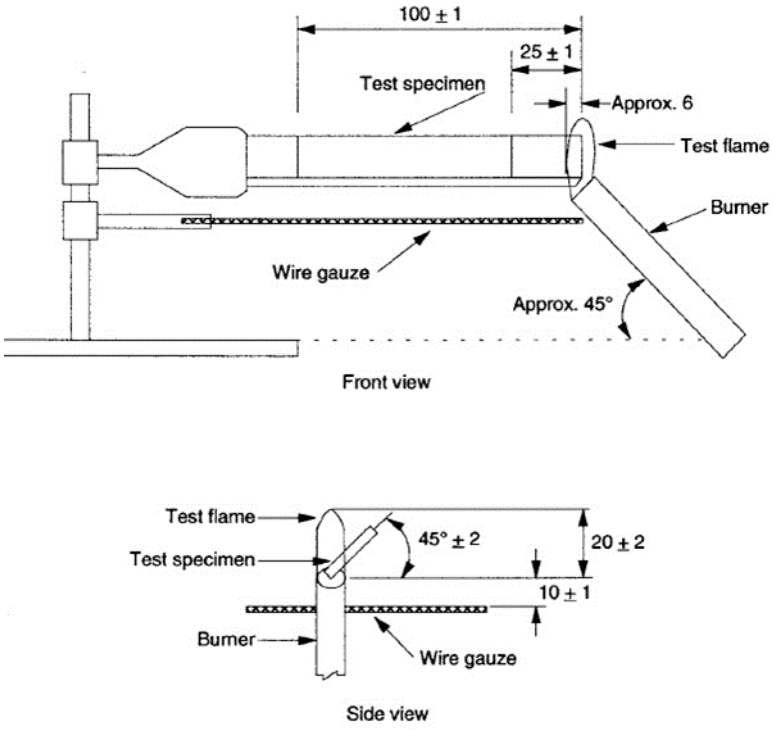

Figure 6.1 Test fixture for burning test in accordance to ASTM D635.

Thermogravimetric analyses (TGA) were carried out on a TA Instruments Model TGA Q500, operating under nitrogen and air atmosphere using a platinum pan. The runs

were performed over a temperature range between 30 and 600°C at 10°C/min heating rate and 20 ml/min flow.

Limiting oxygen index (LOI) is a method used to determine the minimum oxygen concentration in an oxygen/nitrogen mixture that will sustain a flame. It is a convenient, reproducible, and inexpensive way of determining the tendency of a material to sustain flame. The LOI testing was carried out using an LOI instrument model number of M606 in accordance to ASTM D2863. A test sample of 150 × 50mm was placed in a transparent test chamber and ignited at the top. The oxygen concentration in the mixture of oxygen and nitrogen was increased slowly until the sample sustain burning. The volume fraction of the oxygen in the gas mixture was reported as the LOI.

6.2.5 Mechanical Test

Tensile and flexural tests were performed on a universal testing machine MTS Alliance RT/10. The tensile properties were characterised in accordance to ASTM D638. Specimens with the dimension of 250 × 25 × 5 mm3 were cut from the fabricated samples. The tensile load was applied at a constant displacement rate of 2 mm/min. A laser extensometer was used to measure the axial strain. Ten specimens were tested from each sample and tensile modulus (modulus of elasticity) was measured from the initial slope for each specimen.

A flexural test was conducted according to ASTM D790 (three-point bending) in order to determine the flexural properties of the HVEs. A three-point bending fixture with cylindrical support with 5 mm radius was mounted on the table-top tester. The span length, according to the standard should be 15 times of the specimen's thickness (in this study was measured as 80 mm). The specimen dimension used for this test was

100 × 12 × 5 mm3. The load was applied at a constant crosshead speed of 2 mm/min. As with tensile testing, ten specimens were tested for each sample. The specimens were monitored until fibre rupture occurred and, at this point, the load was taken to calculate the flexural stress. The flexural modulus was calculated as the slope in the linear range of the stress vs. strain between points at a deflection just above zero.

6.3 Results and Discussion

6.3.1 Effects of Fire Retardant Treatments on the Physical Properties of WHFs

The effects of fire retardant treatment on the physical and mechanical properties of the WHF has been discussed in depth in Chapter 5; Section 5.3.1 and 5.3.6. Thus, this section will briefly discussed the effect of the fire retardant treatments on the WHFs. In general, the incorporation of chemical treatment increased the weight of fabric due to the chemical pick-up on the hemp fibres and the weight imparted to the WHFs were 18.18 to 30.10% (refer Table 6.1). The density of all treated WHFs increased drastically as compared to the untreated fabric due to the effect of treatment applied to them. The differences in density among treated fabric were small and can be said to be insignificant.

The intensive swelling occurred when the hemp fibre was treated with NaOH duet to the hemicellulose and lignin removal as well as structural modification by alkali treatment [94, 134]. The reduction of hemicellulose and lignin is the reason that the fibre density increased to 1.51g/cm^3 because when the two compound decreased, the content of cellulose becomes higher, thus increasing the density of fibre [93].

Ammonium polyphosphate in FR chemical has provided the phosphorus derivatives which is able to generate acid or acid forming agents [135]. This acid could also

remove some hemicellulose and lignin thus made the hemp fabric increased in its fibre density besides the chemical deposition on the fibres (25.01%) during the treatment. This treatment also in swollen fibres which increased the fibre diameter.

Sputters were detected on the swollen hemp fibres when the fabric was treated with NaOH+FR treatment. This sample exhibited the highest chemical pick-up (30.30%) as a result of the combination treatment of NaOH and FR chemicals. The fibres' surfaces were sputtered with salt due to the reaction between the generated acid and pure alkali from the FR and NaOH respectively. The elimination of hemicellulose and lignin in addition to the salt on the fibre surface also occurred due to the generated acid and alkali which latter caused an increment of the fibre density of this sample.

As a consequence of the swollen fibres, all the treated hemp fabrics experienced some increment on their yarn crimps thus leading to the increased of thickness and density of the fabric. The total fabric cover also increased due to the fabric shrinking and yarn contracting.

Table 6.2 summarizes the average tensile properties for each WHF. The strain percentages were varied due to the different yarn crimp percentages as shown in Table 6.1. For the sample with the higher yarn crimp percentage, it took more time for the yarn to be straightened, thus affecting the overall strain percentage (Table 6.2) of each sample.

In terms of tensile strength, all treatments reduced the strength of the WHFs. The NaOH treatment partially removed hemicellulose and lignin from the fibres resulting in easy deformation of the cellulose microfibrils during tensile [94, 109] while in the FR treatment, some cellulose in the hemp fibre was hydrolysed during the fire

retardant treatment which caused minor degradation resulting in a decrease in its strength [136, 143, 144].

In terms of tensile modulus, from Table 6.2, either in warp or weft direction, it shows that all treatments reduced the tensile modulus of the WHF. Apart from the increment of yarn crimp percentage which later decreased the stiffness of fibres, there is another suggestion on this. All the treatments employed in this work eliminated some hemicellulose and lignin and hence reduce stiffness of WHF because the stiffness of the hemp fibre is also depends on these two compounds [67]. It is normal for weft yarn to have a higher yarn crimp than warp yarn due to the tension arrangement during the process of weaving [53, 107, 133].

6.3.2 Physical Properties of HVEs

Table 6.4 shows the results of constituent content of all fire retardant treated HVEs fabricated in this study. The differences in the samples' density were due to the higher densities of all treated WHFs than the untreated fabric sample (refer Table 6.1) while the density of vinyl ester resin remained the same at 1.027g/cm^3. The differences in treated woven fabrics' density, as mentioned above, were due to the swollen fibre as well as the deposition of chemical particles on the fibre and this affected the density and the composition of the HVEs (Table 6.4).

Table 6.4 Constituent content results of all treated HVEs.

Sample	Sample Thickness (mm)	Density (g/cm^3)	Reinforcement content (wt.%)	Matrix content (wt.%)	Reinforcement content (vol.%)	Matrix content (vol. %)
HVE - Untreated	4.93	1.10	43.6461	56.36	32.65	60.36
HVE - NaOH	5.5	1.14	44.80	56.23	33.68	61.01
HVE - FR	5.29	1.21	46.02	53.98	36.3	63.83
HVE - NaOH + FR	5.42	1.16	49.08	50.92	37.12	57.39

6.3.3 Mechanical Properties of HVEs

Table 6.5 shows the average tensile properties for all HVEs. It is worth mentioning that, it was observed from each sample that the stress-strain behaviour of all specimens cut from a plate were consistent. The typical tensile stress-strain response for each sample is shown in Figure 6.2. As will be discussed further, the typical behaviour shows the linear trend in the earlier stage (strain < 0.5%) then becoming non-linear as the acting tensile force rises, and this is attributed to the nonlinear behaviour of the woven hemp fabric. Unlike thermoplastic, vinyl ester is the thermoset type resin which is well known to be more rigid and brittle. Therefore, the tensile strain of HVEs fabricated in this work is less than 3%.

It was observed that, when the all specimens were subjected to tensile loading, the specimens faded and lightened in colour (for instance, from light brown to whitish brown) within the gauge length. This was due to the crazing of the matrix, though cracking was visually observed. No significant cracking was observed of all the samples. Since the fibres were covered by resin, the failure normally began when the resin failed and then followed by reinforcement failure [33, 110]. The crazing that happened during the tensile loading showed a failure initiation on the vinyl ester resin before the WHF.

The failure of all the specimens was perpendicular to the longitudinal sample direction. Figure 6.3 shows the scanning electron microscope image taken from the fracture surface of the HVE. From the figure, it can be observed that there were short ruptured protruding yarns as well as yarn pulled-out from the surface. This figure confirms the failure mode that, while the fibres within the yarn ruptured, the yarn was pulled-out from the matrix at the failure surface.

Table 6.5 Results of tensile properties results of all HVEs.

Composite Types	Tensile Strength (MPa)	Tensile Strain (%)	Tensile Modulus (GPa)
HVE-UT	61.68 (±1.00)	1.82 (±0.06)	6.20 (±0.23)
HVE-NaOH	56.30 (±1.36)	1.78 (±0.117)	6.19 (±0.82)
HVE-FR	51.51 (±0.75)	1.59 (±0.07)	5.96 (±0.34)
HVE-NaOH+FR	46.61 (±2.04)	1.79 (±0.17)	5.81 (±0.39)

*Figures in bracket indicate standard deviation.

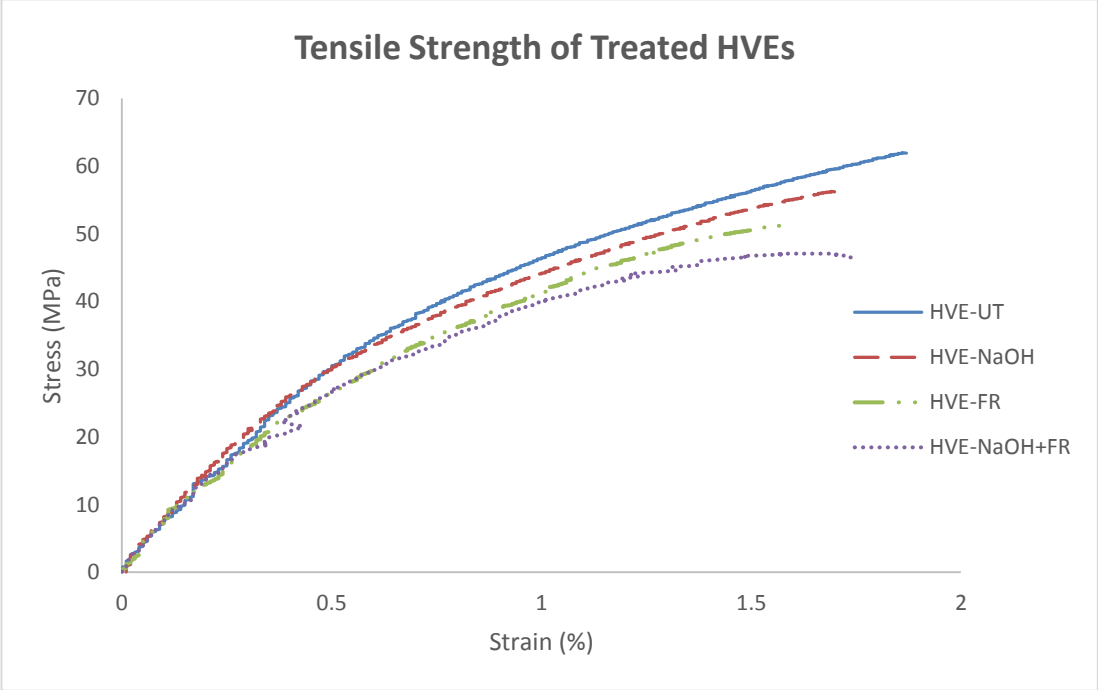

Figure 6.2 Typical tensile stress-strain response for all HVE samples.

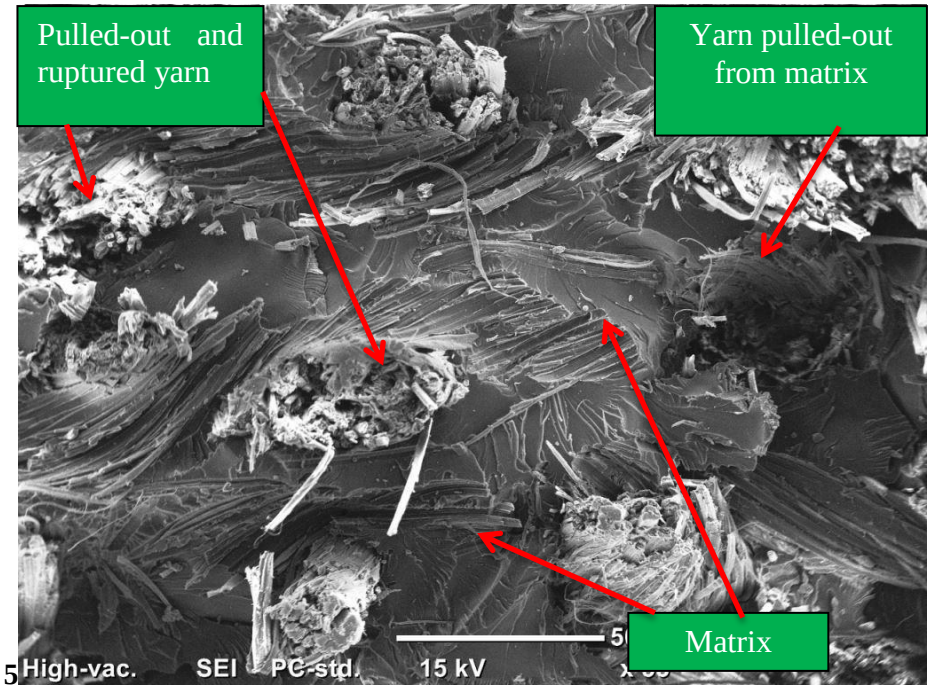

Figure 6.3 Scanning electron image of HVE's failure surface.

Table 6.5 shows that the tensile strength of the HVE fabricated with treated WHFs were lower than sample HVE-UT. Besides the lower tensile strength exhibited by all treated WHFs (Table 6.2), it is believed that the decrement in treated HVEs' strength is attributed to the poor compatibility between the added treatment and vinyl ester resin. Not only that, the tensile modulus of HVE made of treated hemp fabric also exhibited lower than the sample HVE made of untreated hemp fabric.

In the case of HVE-NaOH sample, the tensile properties reduced because the hemp fabric was treated with a high concentration of alkali (10%). According to Mwaikambo and Ansell [146], a very high concentration of NaOH would certainly damage the fibre and consequently reduce the strength of the fibre. Kenaf composite made by Shukor et al. [77] experienced a similar behaviour as the HVEs in this work when strength was reduced by the treatment of 9% alkali. They claimed that the reduction was due to cell wall thickening, which led to poor adhesion with the matrix. As for the HVE sample made of hemp fabric treated with FR chemical and NaOH+FR, the decrease in

its tensile properties was also due to poor compatibility between the fibres which deposited with ammonium polyphosphate and vinyl ester resin (refer Figure 6.4 (c) and (d)) [77]. Shumao et al. [147] found that the loading of ammonium polyphosphate on the polylactic acid and ramie fibres resulted to the incompatibility of the fibre and polymer matrix. Figure 6.5 shows the tensile fracture surfaces of all fabricated samples in this work, indicating the poor compatibility between reinforcement and matrix (indicated with arrow) for all samples fabricated with treated fabrics. Therefore, based on these results shown in Table 6.5 and Figure 6.4, the chemical treatments applied on the WHF degraded the tensile properties of all HVEs.

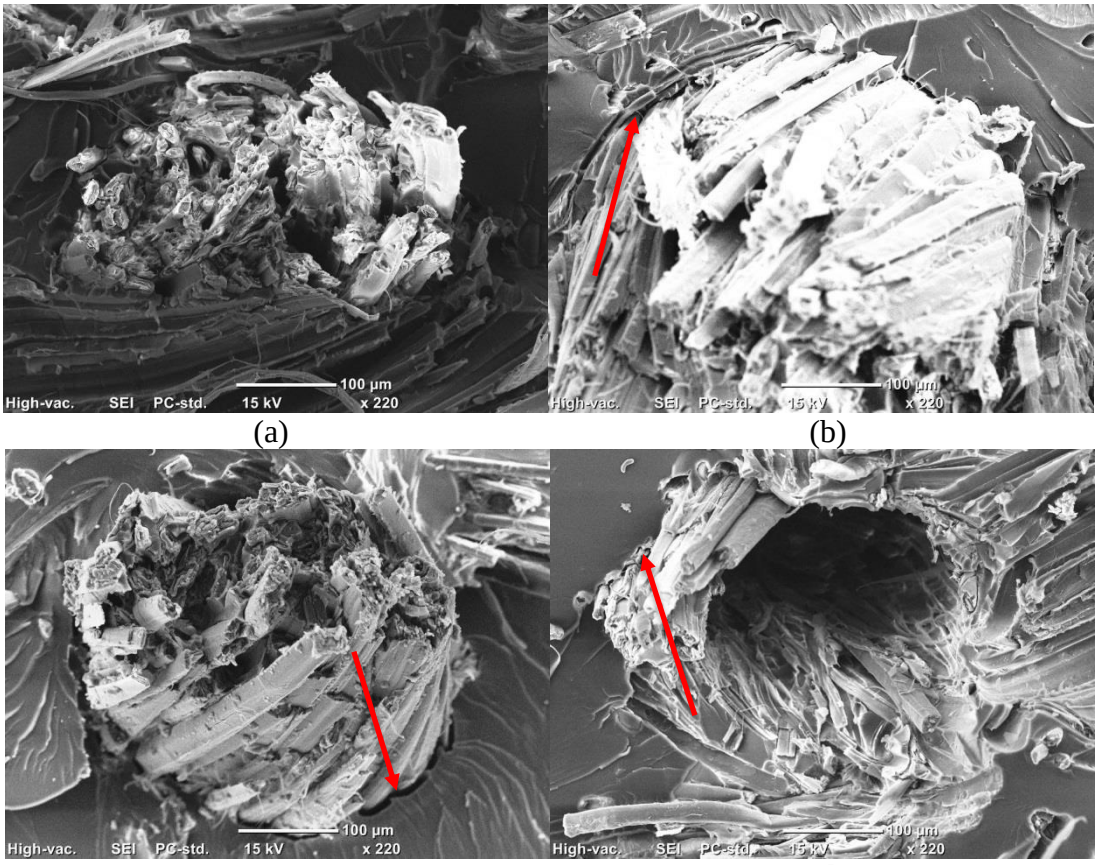

Figure 6.4 SEM micrographs of tensile fracture surface; (a)HVE-UT, (b) HVE-NaOH, (c) HVE-FR and (d) HVE-NaOH+FR

The flexural properties determined from the load-displacement results are summarised in Table 6.6. The typical stress-strain response for each sample of the WHF reinforced vinyl ester tested in flexural test is shown in Figure 6.5. The difference between the samples' responses was attributed to the different treatments applied to the WHFs. The response was similar to the tensile curve with the linear parts of the typical behaviour less than 0.6%, and then becoming non-linear as the flexural loading increased which is attributed to the non-linear behaviour of the woven hemp fabric. All specimens failed in a single crack located at mid-span where the loading was applied.

The flexural properties in Table 6.6 show the decrement in strength with the HVEs made of the treated hemp fabric in comparison with sample HVE-UT and this scenario was similar with tensile strength. Again, similar to tensile properties, this was attributed to the poor adhesion between the reinforcement with matrix and this incompatibility was due to the treatments applied to the fibres. However, the decrement in flexural properties was about 3.3 to 17.64% as compared to the reduction in tensile properties which was about 8.7 to 24.43%.

Table 6.6 Flexural property results of all HVEs.

Composite Types	Flexural Strength (MPa)	Flexural Strain (%)	Flexural Modulus (GPa)
HVE-UT	93.65 (±2.62)	3.00 (±0.20)	5.62 (±0.18)
HVE-NaOH	90.54 (±1.70)	3.04 (±0.19)	4.88 (±0.12)
HVE-FR	85.20 (±2.14)	3.16 (±0.26)	5.07 (±0.18)
HVE-NaOH+FR	77.13 (±2.11)	3.75 (±0.18)	4.28 (±0.11)

*Figures in bracket indicate standard deviation.

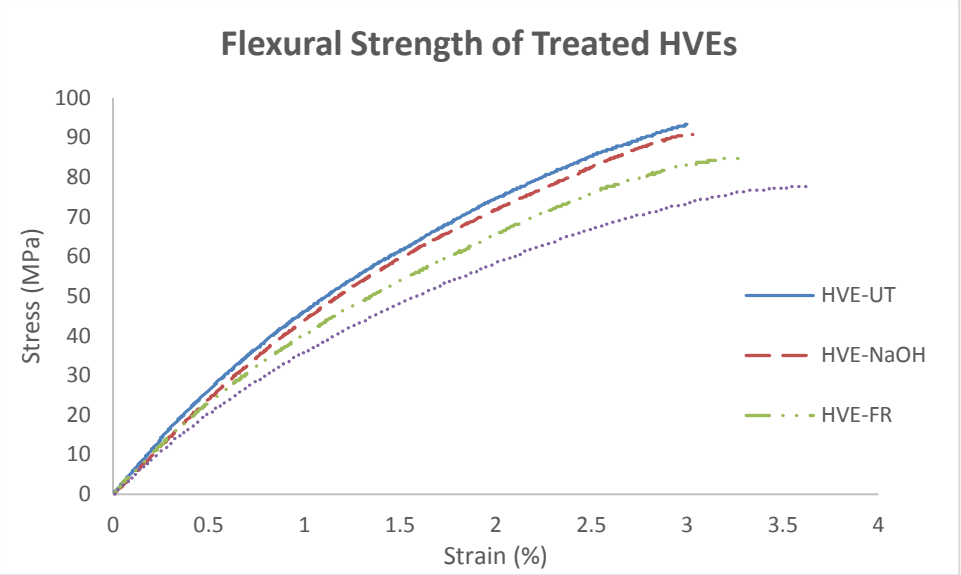

Figure 6.5Flexural stress-strain response of all HVEs.

6.3.4 Burning Test Results of HVEs

The results of burning test in accordance to ASTM D635 are shown in Table 6.7. In this test, each sample was exposed to the flame source for 30s. Only the untreated sample was burnt and the flame spread until it reached the secownd mark. The total burning time for this sample was recorded as 983.66 s including the smoulder burning time which was observed for another 354.33 s after the flame was extinguished. Also observed was that the sample was burned with a yellow flame and released black smoke and the smell was like the mix of light burnt paper and stronger burnt plastic due to the hemp fabric and vinyl ester resin correspondingly. The burning rate of this sample was recorded the highest among all samples which was 9.53 mm/min. As an example of the test, Figure 6.6 shows time-elapsed photos of the untreated HVE sample (HVE-UT) during the burning test. The sample was ignited when it was exposed to the flame source and burned from the very beginning until the second marker (100 mm).

As for sample HVE-NaOH, it was observed that the samples were burning with a yellow flame which kept burning for 10 seconds after the flame source was removed. After the fire was extinguished, the sample kept burning by the smoulder for 283 s (refer Table 6.7). Nevertheless, the sample did not burn even to the first marker (25 mm). The sample was burned at 4.25 mm/min and this burning rate was about 50% lower than the sample HVE-UT, plus under the exaggeration of flame and smoulder. In addition to its burning characteristics, this sample was observed to produce smoke and an odour similar to sample HVE-UT. The image of HVE-NaOH subjected to burning test can be seen in Figure 6.7(b). From this image, we can see that there was just a small area affected by the flame and some part this was burned by the smoulder and became ash. Based on the discussion above and comparative observation between the images in Figure 6.7(a) and (b), it is suggested that the NaOH treatment of the WHF increased the fire retardant of the HVEs.

In terms of sample HVE-FR, it shows good properties against the fibre and this can be proved by the results from Table 6.7. It was observed that neither ignition nor flame was sparked on the sample after the flame source was removed. However, during the flame exposure, charring happened to area reached by the flame. Since the burning was stopped as soon as the flame source was removed, the burning did not reach to the first mark and the burning rate could not be measured. Figure 6.7(c) shows the images of sample HVE-NaOH after being subjected to the burning test. It shows a small burnt part of the sample. Similar condition happened to the sample HVE-NaOH+FR when the flame was extinguished as soon as the flame source was removed and the carbonaceous char did not reach the first mark. It was also witnessed that, during the test, both samples released black smoke, an intense smell of burnt plastic, burning of a yellow flame, and residue that was hard. Sisal fibres reinforced

polypropylene composites mixed with ammonium polyphosphate fabricated by Jeencham et al. [148] did not burn during the burning test (ASTM D635) as compared to the untreated sample and they suggested that the fire retardant of this sample was improved. Duquesne et al. [149] fabricated a composite using woven flax fabric and bio-based matrix and they found that, with the addition of ammonium polyphosphate, their composite did not burn during the burning test. Therefore, based on the results of Table 6.7 and the images shows in Figure 6.7(c) and (d), HVE-FR and HVE-NaOH+FR showed good resistance and retardant against the fire due to the treatments of the WHF.

Table 6.7 Results of burning test of all HVEs.

Sample Types	1st mark (25 cm) (s)	2nd mark (100 cm) (s)	Smoulder (s)	Total burning (s)	Burning rate (mm/min)
HVE-UT	38.00	591.33	354.33	983.66	9.53
HVE-NaOH	x	x	283.00	283.00	4.25
HVE-FR	x	x	x	x	x
HVE-NaOH+FR	x	x	x	x	x

X – Indicates the expected event had not happened.

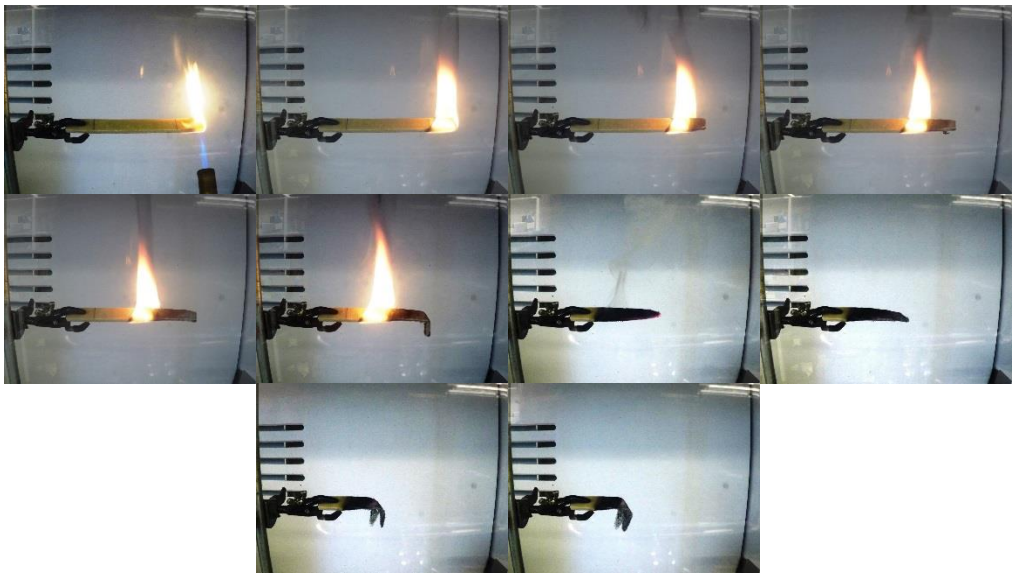

Figure 6.6 Time-elapsed photos of burning test on the untreated sample.

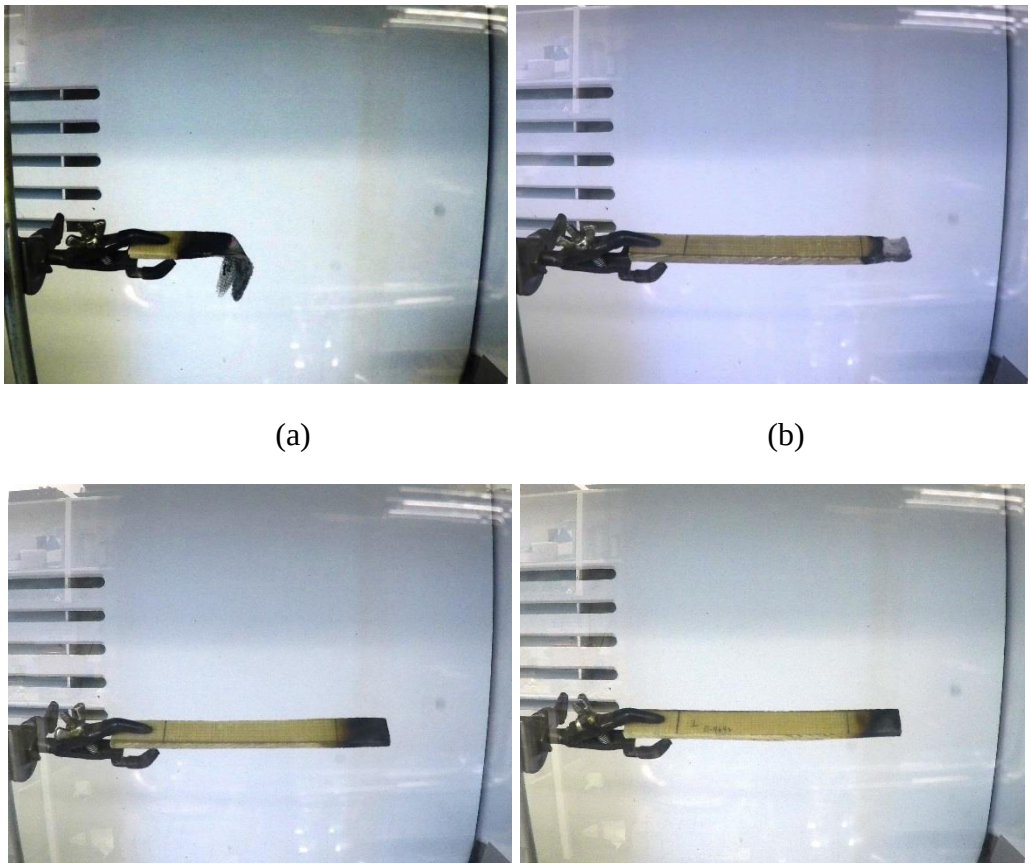

(a) (b)

(c) (d)

Figure 6.7 Images of all types of fabricated samples after burning test; (a) HVE-UT, (b) HVE-NaOH, (c) HVE-FR and (d) HVE-NaOH+FR

6.3.5 Thermal Properties of HVEs

Analysis of the thermal decomposition of all HVEs was carried out by thermogravimetric (TG) and derivatives themogravimetric (DTG) analyses, and the curves are shown in Figure 6.8. While Table 6.8 shows all thermal analysis data extracted from the TG and DTG curves which show the exact temperature ranges for the first and second stages, their maximum temperature of mass loss rate in each stage and char yield percentages for the present samples were extracted. Overall, the decomposition of all HVE samples was divided into two stages. The first stage is attributed to the pyrolysis of natural fibre[76, 77, 150]. According to Yang et al. [92]

the decomposition of hemicellulose and cellulose happens at a temperature ranging from 215 - 400°C. In the specific case of hemp fibre, the decomposition of hemicellulose and cellulose is recorded ranging from 220 to 400°C [107](refer to Section 5.3.4). Thus, the first stage of degradation is mainly due to the decomposition of hemp fibres. The second stage, according to Zhang et al. [150], is due to the decomposition of the matrix. The onset degradation temperature of vinyl ester was recorded at 370°C in Ehsani et al. [151] and Alhuthali et al. [152]. Therefore, it can be said that the degradation of the second stage is attributed mainly to the vinyl ester resin. The decomposition after second stage is due to the char pyrolysis which primarily happens above 400°C. These two stages of decomposition were also witnessed by [77, 147, 148, 150]

As regards to the HVE-UT, the first stage happened from 255 to 395°C with the maximum mass loss rate at 376.91°C (refer Table 6.8). The total mass loss during this stage was 35%. This mass loss, as discussed above, is attributed to the degradation of hemicellulose and cellulose in the sample [76, 77, 91, 92, 150]. Most of the pyrolysis by-products of cellulosic are produced in this stage and include L-Glucose as a major product and combustible gases [128]. The second stage occurred from 395 to 470°C with the temperature of maximum mass loss rate at 440.17°C. It was also observed that the sample experienced rapid and higher total mass loss (55.2%) in second stage as compared to the first stage. The behaviour of vinyl ester decomposition in the second stage for HVE-UT is consistent with the vinyl ester resin tested by Ehsani et al. [151] and Alhuthali et al. [152]. The char pyrolysis for HVE-UT began at 470°C. Normally, during this process, dewatering and charring reactions are more dominant than the dehydration of cellulose and the decomposition of resin.

In the matter of sample HVE-NaOH, the first stage of decomposition was commenced 70°C earlier than the sample HVE-UT which was recorded from 182 to 356°C. The maximum mass loss rate for this stage was at a temperature of 338.17°C with a total mass loss of 28%. The second stage occurred at the range of 356 to 474°C with the temperature at the maximum mass loss rate being 437.61°C and the mass loss was 59%. In both stages, the decomposition of HVE-NaOH slowed by reason of the NaOH treatment on the WHF. According to Mostashari et al. [125], in the matter of sample HVE-NaOH, the first stage of decomposition commenced 70°C earlier than the sample HVE-UT which was recorded from 182 to 356°C. The maximum mass loss rate for this stage was at the temperature of 338.17°C with a total mass loss of 28%. The second stage happened at a temperature range of 356 to 474°C with the temperature at the maximum mass loss rate at 437.61°C and the mass loss was accounted 59%. In both stages, the decomposition of HVE-NaOH became slowed by reason of the NaOH treatment on the WHF. Hence in the first stage, the NaOH which remains intact with the woven hemp fibres, absorbs and dissipates the heat thus slowing the decomposition of the hemicellulose and cellulose compounds.

The incorporation of NaOH in the hemp fibre made it capable of expelling water vapour while burning. Therefore, it was able to barricade the oxygen accesses and acting as a dehydrating flame retardant agent. This situation is similar to the several flame retardants that generate inert gasses such as CO_2, SO_2, H2O, NH_3, etc. during thermal decomposition thus complicating fuel gas such as oxygen accesses into the flammable volatiles of the combustion product [140]. This situation creates flame retardancy and this mechanism is known as ‘gas dilution theory’ [141]. Consequently, slow degradation of vinyl ester in the second stage was caused by an inadequate gas

fuel supply on the combustion due to the water vapour barricade which was expelled by the NaOH in hemp fibre.

In terms of sample HVE-FR, the first stage of decomposition was later than the sample HVE-NaOH, yet earlier than untreated sample (HVE-UT), and was from 213 to 297°C. However, the stage offset was earlier than HVE-NaOH and this made the mass loss of HVE-FR during the first stage 19%, indicating that the dehydration of cellulose occurred rapidly thus the char formed earlier. The second stage of HVE-FR ranged from 297 to 481°C with the temperature at maximum mass loss at 444.37°C with the mass loss at about 61%. Char formation can reduce the mass of volatile combustible degradation fragment evolved by making the carbon and hydrogen stay in the condensed phase [137, 138].

For this sample, since the reactive ingredient in the flame retardant chemical is ammonium polyphosphate, the char formation is attributed to the presence of ammonium polyphosphate, which promotes polyphosphoric acid which phosphorylates the C(6) hydroxyl groups of the glucopyranose units. In addition, they act as acidic catalysts for dehydrating the glucopyranose units [78, 135, 142, 144]. This phosphorylation eventually prevents the formation of flammable volatiles (i.e. L-glucose), thus ensuring that the competitive char-forming reaction is the favoured pyrolysis pathway. In addition, the high dehydrating power of flame retardants such as ammonium polyphosphate justifies their tendency to form more aromatic chars with respect to organophosphorus molecules [135]. Slow degradation on the vinyl ester resin for sample HVE-FR is because of the FR chemical treatment in the WHF. Ammonium polyphosphate may act in the gas phase in polymers. According to Chapple and Anandjiwala [153], phosphorus radicals are released from the polymer at

temperatures below that required for decomposition of the polymer. The radicals terminate the combustion process by reacting with H and OH radicals in the flame. Furthermore, heavy volatiles containing phosphorus may form a vapor-rich phase at the polymer surface that restricts fuel gas access. Thus, the slow decomposition of vinyl ester in the second stage is due to the phosphorus-containing volatile on the resin surfaces which act as a barrier to the fuel gas releases by the vinyl ester to reach with the flame radicals. This phosphorus-containing volatiles is released from the first stage decomposition (lower temperature than the polymer decomposition) because the ammonium polyphosphate is applied to the WHF.

As for sample HVE-NaOH+FR, the first stage of decomposition was also commenced earlier than the sample HVE-UT and was recorded 160 to 289°C and this was also observed earlier than other treated HVE samples (HVE-NaOH and HVE-FR). The mass loss at the first stage was 28% and the maximum mass loss at this stage was happened at 270.95°C. The second stage ranged from 289 to 486°C in which the maximum mass loss temperature was at 440.34°C with a mass loss of 46.7%.This suggests that the combination of both NaOH and FR treatments increases the dehydration of cellulose even faster.

The char yield percentages for all HVEs were also extracted from the thermogravimetric curves and are shown in Table 6.8 at the char reaction onset temperature (at the end temperature of second stage) and 800°C. The char yield percentages at the char reaction onset temperature in high-to-low order were HVE-NaOH+FR, HVE-FR, HVE-NaOH and HVE-UT with the value of 25.30, 20.48, 13.21 and 9.86% respectively. Whereas, at the end of themogravimetry tests (800°C), a similar trend of char yield for all samples in high-to-low order was found with the

value of 19.85, 15.72, 5.68 and 5.71% correspondingly. The highest char yield possessed by WHF-NaOH+FR sample is due to the synergistic between NaOH and FR which surpasses the effect of NaOH and FR alone on the WHF. Xu et al. [78] suggested that the fire retardant properties increased with the increases in char yield. Thus, in terms of thermogravimetric analyses, a combination of NaOH and fire retardant treatment could give the highest fire retardancy for the HVE as well as char yield, suggesting that it has the best fire retardant properties in comparison to all other HVEs. This is followed by sample HVE-FR, and lastly HVE-NaOH. Overall, it can be implied that all the treatments, not only enhance the fire reatardant properties of WHF, but also the whole system of the HVE.

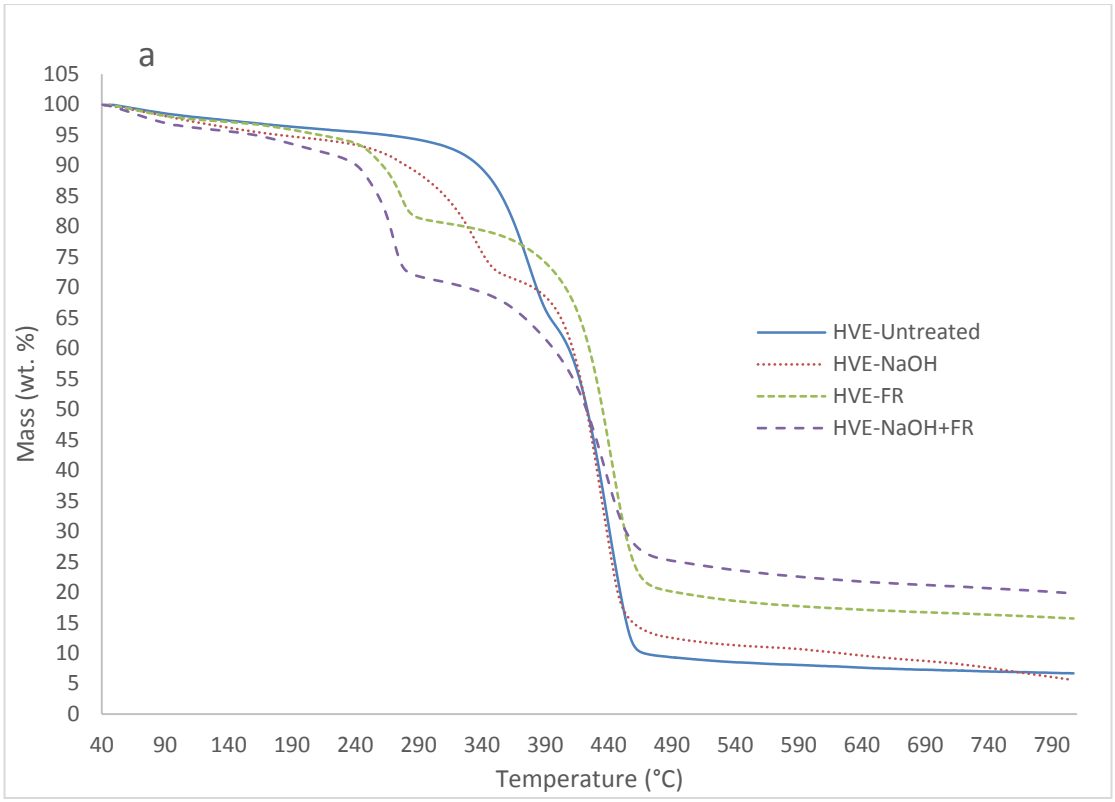

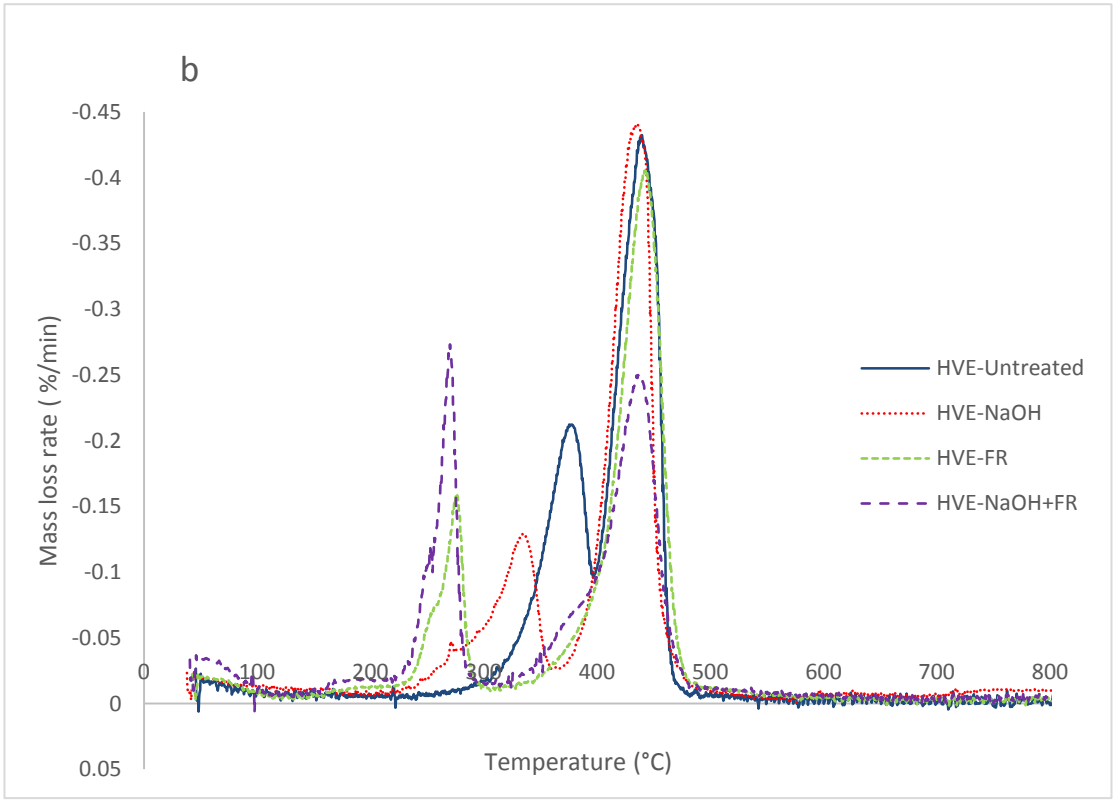

Figure 6.8 (a) TG and (b) DTG curves of untreated and treated WHF samples.

Table 6.8 Data of thermal analysis extracted from TG and DTG curves.

Samples	1st stage (°C)	Max. temp. of mass loss rate (°C)	2nd stage (°C)	Max. temperature of mass loss rate (°C)	Char Yield (%)	
					Charring reaction onset temp.	800 °C
HVE-UT	255 - 395	376.91	395 – 470	440.17	9.86	5.71
HVE-NaOH	182 – 356	338.17	356 - 474	437.61	13.21	5.68
HVE-FR	213 – 297	277.39	297 – 481	444.37	20.48	15.72
HVE-NaOH+FR	160 – 289	270.951	289 - 486	440.34	25.30	19.85

6.3.6 Limiting Oxygen Index Results of HVEs

Limiting oxygen Index (LOI) measurement test is widely used to evaluate the flammability of materials. It shows the minimum amount of oxygen in the oxygen–nitrogen mixture required to support complete combustion of a vertically held sample that burns downward from the top. The higher the LOI value, the more effective the flame-retardant treatment [77, 78]. It is worth mentioning that ASTM D2683 gives no indications of the level of fire retardant based on the LOI value. However, according to Kamath et al. [79] LOI value more than 28 is generally classified as fire retardant. In accordance to GB50222-1995 standard method (which is equivalent to ASTM D2683), 1) the value < 24 indicates the material is flammable; 2) the value ≥ 24 and < 27 indicates the material is combustible, and; 3) the value ≥ 28 indicates the material is fire retardant.

The LOI results shown in Table 6.9 can explain the fire retardant phenomenon discussed in Section 6.3.4. The highest LOI value was shown by sample HVE-NaOH+FR which was a bit higher than the sample HVE-FR due to the advantages from the combination of NaOH and FR treatments on the WHFs. The significant reduction in the LOI values was recorded for the sample HVE-NaOH in comparison

with the two other treated HVE samples and the untreated sample (HVE-UT), possessing the lowest value among all samples.

The LOI value for HVE-UT was lower than 24, thus this HVE type is classified as a flammable material. That is why the whole of the untreated fabric was burnt and minimal residue was left in burning test. Treatment with NaOH on the hemp fabric increased the LOI value of sample HVE-NaOH to 24.1 and this is clustered under combustible material. When the sample HVE-NaOH was subjected to burning test, the ignition of fire produced a yellow flame. Even though the flame can be self-extinguished, the smoulder was produced and kept burning the char residue into ash (refer Section 6.3.4 and Figure 6.7(b)). Thus, it still can be burnt by the exaggeration of other fire sources.

Sample HVE-FR's LOI value was more than 28, thus this sample is clustered as a fire retardant. During burning test, there was no ignition or smoulder produced but, there was char after the flame was removed. The LOI of kenaf reinforced polylactic acid composite made by Shukor et al. [77] increased from 27.6 to 31.6 with the incorporation of ammonium polyphosphate. Similar results were found with the ramie reinforced polylactic acid made by Shumao et al. [147] where the LOI increased ranging from 28.1 to 35.6. Therefore, it can be assumed that the ammonium polyphosphate content compound in the fire retardant chemical contributed to the higher LOI value of the HVE in this work.

In the case of HVE-NaOH+FR, the increment of LOI value might due to the synergistic effect between phosphorus-containing volatiles [153], and expelled water vapour by the NaOH release during the first stage of decomposition suggesting the fire retardant properties of this sample were increased. However, in terms of physical

burning characteristics, there was no difference observed between samples HVE-NaOH+FR and WHF-FR.

Table 6.9 LOI results of all HVEs.

Sample	LOI
HVE-UT	22.8
HVE-NaOH	24.1
HVE-FR	29.2
HVE-NaOH+FR	30.6

6.3.7 Assessment of the Applications

All natural based composite materials have properties similar to wood and engineered wood products [35]. A comparison is briefly presented here, focusing on properties of several woods commonly used as building infrastructure materials; namely Douglas Fir (coastal), Western Hemlock and Ponderosa Pine, and also to the engineered wood products of plywood, oriented strand board (OSB) and glue laminated timber (glulam). Table 6.10 shows the mechanical property ranges of all fire retardants treated HVEs (HVE-NaOH, HVE-FR and HVE-NaOH+FR) tested here, and some woods and engineered wood products used in construction. The mechanical properties of these woods and engineered wood products are emphasised on the flexural properties since infrastructure material prone to exposure to flexure or compression load. Thus most of the works' results on the wood and engineered wood products in Table 6.10 do not expose the tensile properties of their products. It is also worth mentioning that the mechanical properties results of wood and engineered wood product are tested in parallel to the grain except for the flexural modulus of plywood.

Flexural strength of all treated HVEs is comparable to the woods and engineered wood products. In terms of flexural modulus, HVE is roughly half or even lower than that of wood parallel to grain. Nevertheless, it is reported by Hurd [119] that the flexural modulus of wood perpendicular to the grain is about 11 to 35 times less than parallel

to grain. Therefore, while the wood examples given in Table 6.10 are stronger and stiffer than all treated HVEs in one direction, these treated HVEs have a more balanced bi-directional strength and stiffness, as expected.

Table 6.11 shows the allowable mechanical properties used for design with the woods considered here in comparison with biocomposites made by Christian and Billington [35] as per ASTM D245 . They expected that their biocomposites would possess higher mechanical properties than the allowable wood design except for the biocomposites' modulus of elasticity. Similar expectation can be made for the case of treated HVEs (fire retardant treated HVEs) fabricated in this study since its mechanical properties were recorded as comparable (refer Table 6.10) to the biocomposites in Table 6.11.

Table 6.10 Mechanical properties of treated HVEs, wood and engineered wood products.

Material	Tensile Strength (MPa)	Tensile Modulus (GPa)	Shear Strength (MPa)	Flexural Strength (MPa)	Flexural Modulus (GPa)	Density (kg/m^3)
Fire retardant treated HVE	46.61 – 56.30	5.81-6.19	-	77.13 – 90.54	4.28 – 5.07	1140 - 1210
Woods						
Douglas-Fir (Coast) [121]	-	-	7.8	85	13.4	480
Western Hemplock [121]	-	-	8.6	78	11.3	450
Ponderosa Pine [121]	-	-	7.8	65	8.9	400
Engineered woods						
Plywood (B-B Class 1) [35, 119]	27	10.3	1	27	10.3[a]	400-810
Oriented Strand Board [122]			1.2	21.2	5.25	490-810
Glulam [121, 123]	-	-	-	26-72	10.6	320-720

[a] Modulus for ply parallel to grain.

Table 6.11 Allowable design properties of several woods used in construction [35]

	Material	Flexural modulus of rupture (MPa)	Flexural modulus of elasticity (MPa)	Shear strength (MPa)
Clear green properties	Douglas-Fir (Coast)	53	10,800	6.2
	Western Hemplock	46	9000	5.9
	Ponderosa Pine	35	6900	4.8
Strength ratio/quality factor		4%-98%	80%-100%	-
Adjustment factor		2.1	0.94	2.1
Properties adjusted for defects	Douglas-Fir (Coast)	2.1-51.9	8640-10,800	6.3
	Western Hemplock	1.9-41.2	7200-9000	5.9
	Ponderosa Pine	1.5-34.2	5520-6900	4.8
Allowable properties	Douglas-Fir (Coast)	1.0-24.7	9190-11,490	3.0
	Western Hemplock	0.9-21.5	7660-9575	2.8
	Ponderosa Pine	0.7-16.3	5870-7340	2.3
Biocomposite properties	Hemp/CA	95	6560	12.3
	Hemp/PHB	65	5050	9.9

From the Table 6.10, all treated HVEs fabricated in this study show a higher mechanical strength compared to the properties measured for the engineered wood products. However, the flexural modulus of HVEs is only comparable to the oriented strand board but lower than glulam. The flexural modulus of plywood stated in Table 6.10 is for a ply parallel to the grain. However, in practice, the plies are always in a combination of parallel and perpendicular to the grain thus making the modulus 35 times smaller than parallel to grain. Therefore, the modulus of treated HVEs can be considered to be comparable to plywood.

With the assessment shown in Table 6.10, the HVE fabricated in this study can be used as an alternative to engineered wood products and woods. Christian and Billington [35] suggested that in order for these treated HVEs to be used in

nonstructural and structural components, increasing the moment inertia is the most priority, so this material is comparable to wood since the actual stiffness is a combination of the modulus of elasticity, *E*, and the moment of inertia, *I*. Some other advantages of these treated HVEs are that it is easy to tailor its properties and it can be moulded into structural shapes (including hollow sections). The only significant problem with the HVE is its greater densities (1000-1100 kg/m^3) as compared to the woods and engineered wood products (320-810 kg/m^3). In order to replace wood products, a composite should be engineered to be lighter weight.

6.4 Conclusions

Several HVEs were fabricated utilising WHF treated with NaOH, FR and combination of both chemicals to reinforced vinyl ester resin. Characterisations of the physical and mechanical properties were undertaken to analyse the effect of the treatments on the WHF as well as HVEs. All the treatments increased fabric weight, yarn crimp, fabric thickness and density of fabric and fibre density due to the swollen of hemp fibres, deposition of FR particles and salts on the hemp fibre surfaces. The treatments also decreased the mechanical properties of the WHF by the elimination of hemicellulose and lignin during NaOH treatment and dissolution or hydrolisation of some amount of cellulose during FR treatment. The changes of the WHFs's physical properties influenced the physical and constituent contents of the HVEs due to the changes in the WHF properties especially on the increment of fibre density after the treatments.

SEM micrographs confirm the mode of failure that while the fibres within the yarn ruptured, the yarn is pulled-out from the matrix at the failure surface. The mechanical properties of HVEs decreased after the treatments for several reasons: the decrement of WHFs' mechanical properties and the incompatibility or poor adhesion between the

fibre and vinyl ester resin due to the treatments imparted. The NaOH treatment thickened the cell wall of hemp fibre and the presence of ammonium polyphosphate on the fibre surface led to poor adhesion with the vinyl ester. However, the treatments increased the fire retardant properties of HVEs and this was proven by the enhancement of their fire retardant properties and the increment on their limiting oxygen index values compared to the untreated HVE. In terms of the feasibility and readiness on the application in the building infrastructure industry, the assessment by matching its mechanical properties with those of the common woods products revealed that all treated HVEs were comparable and can be used as an alternative to woods and engineered wood products.

Among all of the treated HVEs fabricated in this work, sample HVE-FR can be said the best. Even though it possessed lower mechanical properties in comparison with samples HVE-UT and HVE-NaOH, its mechanical properties were still suitable for use as an alternative to woods and engineered wood products. Furthermore, it exhibited good properties against fire in comparison with other samples in terms of char yield. Therefore, sample HVE-FR will be used for further analysis in the next chapter (Chapter 7).

Chapter 7 Degradability of HVE Properties

7.1 Introduction

The degradation of natural fibre reinforced polymer resin occurs through the degradation of its individual constituents as well as with the loss of interfacial strength between them. Some factors leading to this degradation are heat, moisture/water, ultraviolet light and microorganisms [38, 71, 146, 154-156]. However, the most critical issue that being emphasised by researchers is moisture or water absorption by the composite materials. This issue was also raised in Section 2.6.2 which discussed chemical treatment and water absorption. Water affects the properties of composite materials by infiltrating natural fibre composite and reducing the adhesion among the composite elements. Hemp fibre is hydrophilic, that is, it absorbs moisture and water [49, 64, 94]. Similar to other natural fibre composites, hemp fibre composites are expected to absorb moisture and water, degrading its properties. Therefore, it is important to understand the effects of water absorption on the mechanical properties as well as on the fire retardant treatment applied to the WHFs in HVE.

In this chapter, the two types out of HVE fabricated and mentioned in the previous chapter have been selected for use in this study. Sample fire retardant (FR) treated WHF reinforced vinyl ester composite (HVE-FR) has been chosen based on its good performance in fire retardancy and also its acceptable mechanical properties. HVE-UT been used as a comparison. Both HVEs have gone through water absorption testing in accordance with the nominal standard method. Water absorption testing was selected rather than moisture exposure to study the degradation of composite properties at the worst scenario, thus the measured degradation of HVE properties can be considered to be an extreme level. Periodically, within a specific period of time,

samples were taken out and subjected to tensile, flexural and burning tests. The main purposes of this chapter are to investigate the effects of water absorption on the mechanical properties and to identify the fastness of the FR chemical on the composite materials.

7.2 Materials and Methods

7.2.1 Materials

Similar WHF, resin and a catalyst (hardener) were used in this work, and the detail can be seen in Section 6.2.1. The physical properties of WHF can be seen or referred from Table 6.1. A commercial flame retardant (FR) chemical was supplied by Cyndan Chemicals, Australia. It is worth mentioning that the main active ingredient in this flame retardant is ammonium polyphosphate. This is the only ingredient revealed by the supplier who keeps the other ingredients secret. Information from the technical and material datasheet says that the chemical is water-based, environmentally friendly and not classified as hazardous.

7.2.2 Chemical Treatments of WHF

The WHF was treated with the FR chemical. According to the supplier, the FR can be applied by spraying or dipping, and drying is not necessary. However, in this work, the ‘dips and nips’ method was employed to treat the fabrics. The nipping process was set carefully so that the wet pick-up was consistently maintained at the range of 100-105%. The treated fabric was then left to dry at room temperature for eight hours.

7.2.3 Composite Fabrication

The fabrication process of HVE was elaborated in detail in Section 6.2.2. Two types of composites were fabricated and then reinforced with untreated WHF and WHF treated with FR as shown in Table 7.1**.** The image in Figure 7.1 shows the samples fabricated for this work.

Table 7.1 List of manufactured composite samples and its abbreviation.

Sample Abbreviation	Treatment
HVE-UT	Untreated
HVE-FR	Commercial FR chemical

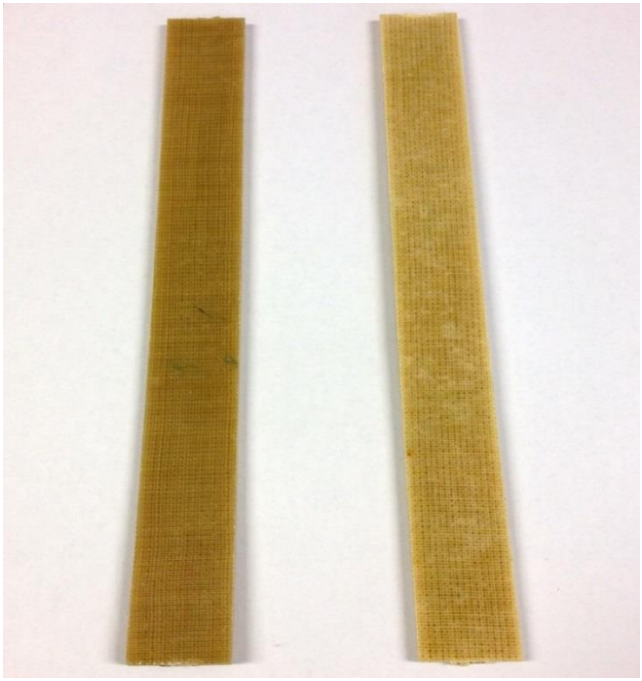

(a) (b)

Figure 7.1 Image of samples; (a) HVE-UT and (b) HVE-FR

7.2.4 Water Absorption Test

The effect of water absorption on the HVEs were investigated in accordance with BS EN ISO 62:1999 [80]. The samples were cut into dimensions similar to those for

tensile and flexural testing. In order to get an initial weight (m_d), the specimens were dried in an oven at 100°C for an hour to remove the moisture trapped in the samples and were then allowed to cool to room temperature before being weighed [38]. The samples were then immediately immersed in a distilled water bath at 23°C. The water content for each specimen was determined by measuring the mass, m, of each specimen periodically until saturation was reached. When specimens were removed from the water bath for measurement (sample weighing), all surface water was removed with a clean dry cloth. Upon completion of mass measurements, the specimens were returned to the water bath.

Measurements were completed more frequently (every 24 hours for the first five days) at the beginning of the test because of the initial high rate of change of mass. The percent of water uptake, *M*, was calculated for each mass measurement as follows:

$$M = \frac{m_i - m_d}{m_d} \times 100 \qquad \textbf{(7.1)}$$

where *m* is the mass of the specimen, the subscript *i* refers the *i*th measurement, and the subscript d refers to the dry state prior to water immersion.

The moisture absorption was calculated by the weight difference. The percentage weight gain of the samples was measured at different time intervals and the moisture content versus square root of time was plotted [38]. Samples were taken for mechanical and burning tests after 168, 840 and 2688 hr of water immersion. Thickness of sample was also measured until the water immersion process was completed. This determines the dimension of stability of the HVE when exposed to the water.

7.2.5 Mechanical Tests

Tensile and flexural tests were completed in accordance with ASTM D638 and ASTM D790 respectively,s and were explained in detail in Section 6.2.5.

7.2.6 Fire Retardant Tests

Burning tests were carried out in accordance to ASTM D635 and limiting oxygen index. The process was explained in Section 6.2.4. Figure 7.2 shows a schematic illustration of the flame retardant test fixture.

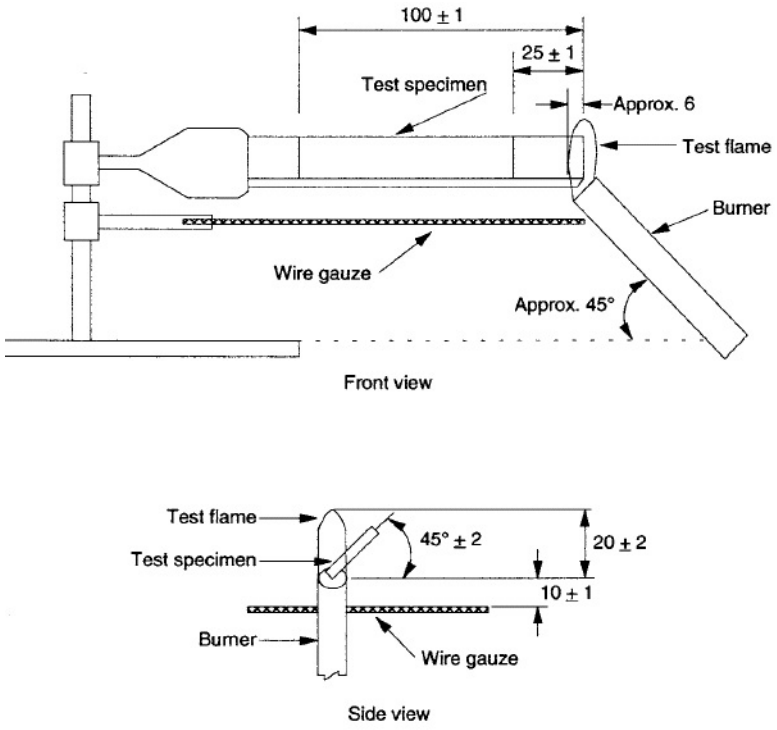

Figure 7.2 Test fixture for burning test in accordance with ASTM D635

7.2.7 Fatigue Test

Fatigue testing was performed in accordance with BS ISO 13003:2003 (Fiber-Reinforced Plastics-Determination of Fatigue Properties Under Cyclic Loading Conditions). They were performed using pneumatic fatigue machines at a frequency

of 3 Hz and a stress ratio (R value) of 0.1 for tension–tension fatigue. The choice of frequency ensured that the heating effect due to hysteresis was minimal. The R value of 0.1 in tension–tension was chosen to maximize the cyclic effects without invoking the complications of compressive stresses and the likely variations in failure mechanisms. Three specimens with dimensions similar to tensile specimens were tested to failure at a minimum of four levels of maximum stress (80, 70, 60 and 50%). The maximum stresses during cyclic loading were recorded as stress level of fatigue. The number of cycles to failure were recorded for each specimen, and these data were plotted in the form of S-N (Wohler) curves [43]. After plotting S-N diagrams, the power-law regression equation were determined for each material to obtain the fatigue strength coefficient.

7.3 Results and Discussion

7.3.1 Water Absorption

Water absorption behaviour of woven hemp composites over 2700 hr of immersion in water curves is shown in Figure 7.3, and Table 7.2 shows the water absorption properties for both samples extracted from the curves. For both samples, the water uptake was quite rapid initially and this happened precisely from 24 hr up to 96 hr immersion in the water and then continued to increase until saturation was reached. It is worth mentioning that the hemp fibres were highly exposed at the edge surfaces rather than the face of the composite, where the cross-section of fibres were exposed to the water. When the woven hemp composites are immersed in the water, hydrogen bonds are formed between the hydroxyl group of the cellulose molecules and the water. This water uptake in the cell walls causes the fibres to swell and the swelling of fibres is found to be directional with the maximum swelling happening in the lateral

but minimum in the longitudinal direction. The high cellulose content of hemp fibres, in this case 65-68% (refer Table 3.6), is responsible for more water to penetrating the composite system [38, 80, 98].

Coming back to the both samples, generally, the water uptake of HVE-UT was slower than for the HVE-FR sample. Based on Figure 7.3, the steeper slope of the HVE-FR graph indicates the faster rate of water diffusion and a higher diffusion coefficient as compared to the HVE-UT sample. In terms of HVE-UT, at 96 hr of water immersion the water uptake was recorded at 1.08%. Further immersion increased the weight to about 2.79% after 744 hr and in this phase the water uptake became slower. The weight was continued to increase to 3.43% after 1848 hr immersion. At this point, the sample continued to maintain the water uptake percentage up to and beyond 2352 hr indicating that saturation was reached. The weight after this point had fallen to 3.36% at 2688 hr of water immersion.

In terms of HVE-FR, the water uptake was recorded at 2.27% after 96 hr immersion and then continued to increase up to 2.8% after 192 hr immersion and at this point the water uptake was still quite rapid. The water uptake after this phase become slower until after 552 hr immersion the water uptake was recorded at the highest point of 3.27%. This sample reached equilibrium at this point and it maintained its weight until after 744 hr immersion before the weight continued to decrease after 840 hr up to 2700 hr immersion. The optimum water uptake percentage for both samples are similar, however, equilibrium is reached at different point in time. The time that HVE-FR sample reaches the equilibrium state was measured 70% lower (at 552 hr) than HVE-UT which reached equilibrium at 1848 hr.

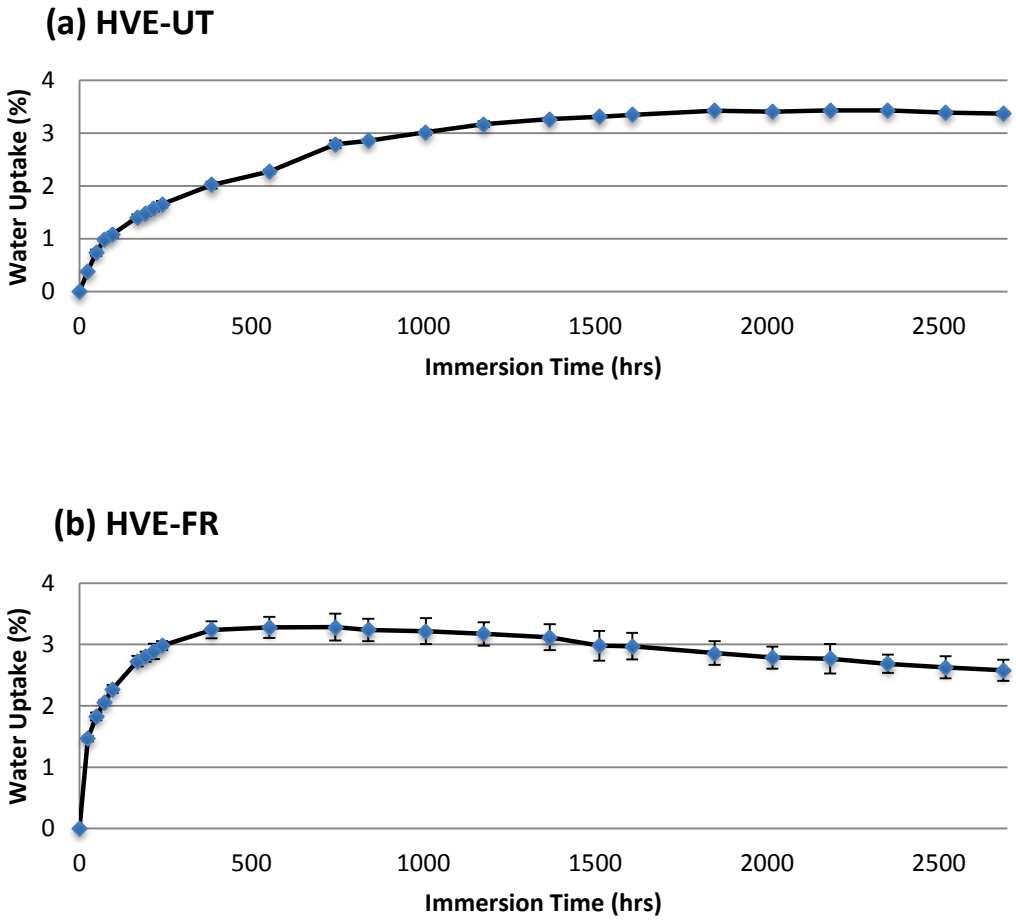

Figure 7.3 Water absorption behaviour of WHF composite.

In order to analyse the different water absorption behaviour of HVE-UT and HVE-FR, the diffusion of water into the composite samples was measured by using the diffusion coefficient which is commonly described by Fick's law [38, 41, 80, 157]. The value of the Fickian diffusion coefficient, D can be obtained from the slope of water uptake gain versus square root time curve using the following equation:

$$D = \pi \left[\frac{kh}{4M_m}\right]^2 \quad \textbf{(7.2)}$$

where k is the slope of the linear portion of the water uptake versus square root of time curves, h is the sample thickness and M_m is the maximum water uptake.

Table 7.2 shows the moisture absorption properties of both composite samples. The steeper slope of sample HVE-FR which indicates the faster (4.71E-06 mm^2/s) water uptake or diffusion into the sample, leads to the higher diffusion coefficient in comparison with sample HVE-UT (1.45E-06 mm^2/s). This situation occurred due to dimensional changes during the FR treatment on the WHF which affects the thickness of the sample and also the compatibility between the treated woven fabric and the vinyl ester.

Table 7.2 Water absorption properties of HVE-UT and HVE-FR samples.

Sample	Time to saturate (hr)	Sample Thickness (mm)	Maximum water uptake, Mm (%)	Diffusion Coefficient, D (mm^2/s)
HVE-UT	1848	5.17	3.43	1.45 E-06
HVE-FR	552	5.36	3.28	4.71 E-06

When the WHF was treated with the FR chemical, the fibre's cross-section changed from lenticular to become rounder (refer Figure 5.2(c) in Section 5.3.1) indicating that the fibres are swollen. Due to the swollen fibres, the interlacement between warp and weft yarn restricts the movement of the fibres and, as a consequence, the contraction acts on the warp and weft yarn making the fabric shrink (refer Table 5.2 in Section 5.3.1). This shrinking fabric makes the fabric a little bit thicker than the untreated fabric thus increasing composite thickness a little bit. When comparing both samples, sample HVE-FR possessed higher thickness (edge) and this made the area exposed to the water, bigger. According to Christian and Billington [41], water flow rate at the edge (at the cut or thickness part) is higher than that through the faces because fibres are exposed more at the edge. Therefore, the water diffusion and the diffusion

coefficient of HVE-FR become faster and higher than the HVE-UT sample due to higher thickness of HVE-FR sample.

Another factor that could lead to higher water uptake properties is the compatibility between the treated WHF and vinyl ester resin which was discussed in the previous chapter (Section 6.3.3). Figure 7.4 shows a scanning electron microscope image of the fracture surface for each sample. The red circle in Figure 7.4(a) shows a bunch of fibres which are actually a yarn in the hemp fabric. Examining the adhesion between the yarn and vinyl ester, there are less gaps appearing, indicating that adhesion is good. However, for sample HVE-FR, lots of gaps appear, indicating the incompatibility in between the yarn surface and the vinyl ester (Figure 7.4(b)). This is due to the ammonium polyphosphate content in the FR chemical which affects the adhesion in the composites [77, 147]. Therefore, with respect to water absorption, the water molecules are not only diffused via the fibre surfaces, but also permeated via the gaps between the fibres and resin. This is the other reason of faster water diffusion and higher diffusion coefficient of sample HVE-FR in comparison with HVE-UT.

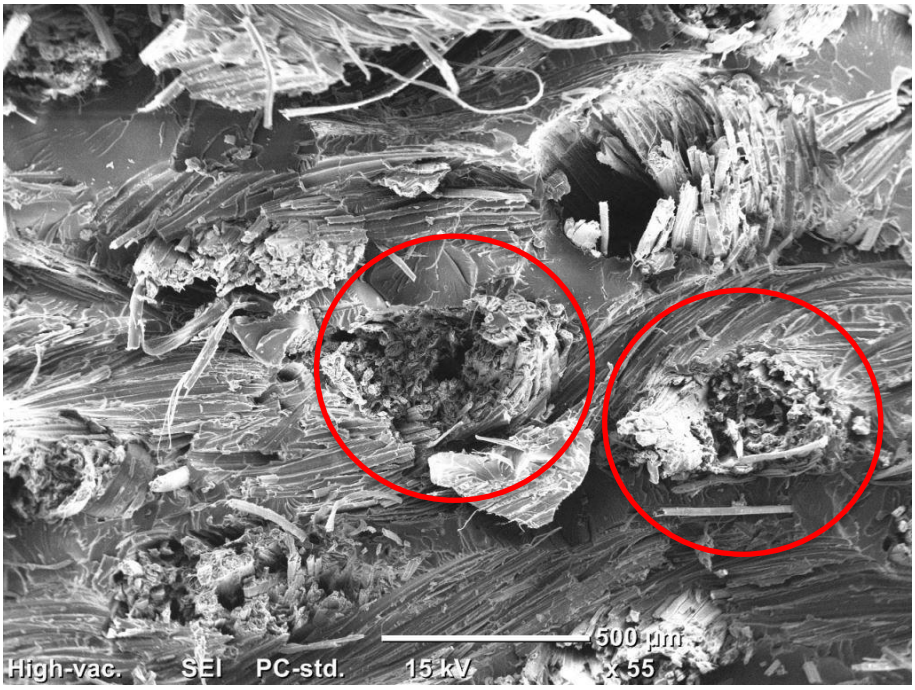

(a)

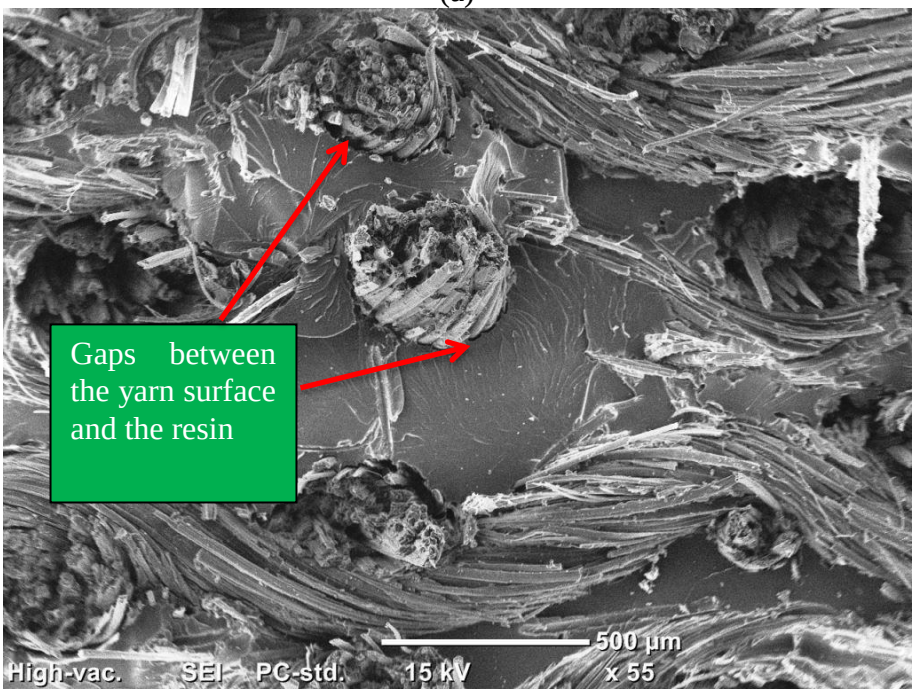

(b)

Figure 7.4 SEM micrographs of tensile fracture surface; (a) HVE-UT and (b) HVE-FR

Shahzad [80] immersed non-woven hemp/unsaturated polyester resin composite in the water (at 23°C.). The diffusion coefficient of his sample was recorded at 8.7E-07 mm2/s with the maximum water uptake of 16% and saturation at 400 hr. Dhakal et al.

[38] also fabricated non-woven hemp/unsaturated polyester for which their diffusion coefficient were recorded at 1.551E-06 to 4.367E-06 for water immersion in room temperature, and much higher in boiling temperature at 48E-03 to 67E-03. Christian and Billington [41] using woven hemp fabric to reinforced natural resin cellulose acetate and poly-hydroxybutyrate (PHB). The diffusion coefficients of their composite ranged from 1.14E-05 to 9.57E-05 depending on the temperature. According to them, samples made of cellulose acetate were higher than PHB because PBH is hydrophobic and more crystalline than cellulose acetate which absorbs less water. The hybrid composite of epoxy/kenaf /PET made by Dan-mallam et al. [157] possessed diffusion coefficient ranging from 1.1E-06 to 6.0E-06. From the other researchers' works mentioned above, the diffusions of water or moisture varies depending on many factors such as fibre type, resin, manufacturing method and test condition. Thus, a direct comparison with other studies can be complicated.

Christian and Billington [41], in their work, also mentioned that the diffusion coefficient for wood is in the range of 0.00001– 0.0001 mm^2/s and the moisture content is about 12% for dry wood and greater than 20% for green wood. They also inferred that the diffusion coefficients and moisture content for engineered wood products would likely be lower than those for wood because in engineered wood, the wood is usually mixed with hydrophobic polymer matrices to form the engineered products. Lastly, they found that their manufactured biobased composites have diffusion properties comparable to wood and most likely higher than engineered wood products [41]. This situation can also be applied to the present samples because they possess lower water diffusion and water uptake than wood products.

It is worth mentioning again that both samples, HVE-UT and HVE-FR, absorbed water about 3 to 3.5%. The diffusion coefficient for HVE-UT is slower than HVE-FR which were recorded at 1.45E-06 and 4.71E-06 respectively. Sample HVE-UT took a longer time to reach saturation as compared to HVE-FR which were 1848 and 552 hr respectively.

When comparing the thickness of both samples at the last hour of water immersion, it was found that the increment in thickness of HVE-FR and HVE-UT were recorded at 1.442 and 2.142% respectively (refer Table 7.3). Therefore, in terms of dimensional stability, sample HVE-FR was better than HVE-UT because its thickness swelling was lower. Thickness swelling of hemp fibres/polypropylene composites made by Hargitai et al. [158] ranged 6 – 8%, values higher than HVE in this study. Some other wood products also show higher than HVE. Examples of these are particleboard (5 – 30%) [159], oriented strand board (4.3 – 22.1%) [160] and woods in general (4 – 6% radial wood swelling) [161]. This shows that the HVE possesses a better dimensional stability in comparison with some other composites, woods and engineered wood products.

Table 7.3 Results of thickness swelling for HVE-UT and HVE-FR samples.

Sample	Thickness Swelling (%)	
	At the saturation point	At the last hour
HVE-UT	[a]1.693 (0.629)	[c]2.142 (0.514)
HVE-FR	[b]0.689 (0.287)	[c]1.442 (0.284)

[a] - 1848 hrs water immersion
[b] - 552 hrs water immersion
[c] - 2688 hrs water immersion
* Figures in bracket indicate standard deviation

7.3.2 Effect of Water Diffusion on the Mechanical Properties

7.3.2.1 Tensile Properties

Figure 7.5 shows the typical tensile stress-strain response for samples HVE-UT and HVE-FR. Tensile properties were obtained for both samples at 168, 850 and 268 hr. During 0 to 168 hr, water immersion for both sample was at the highest rate. The immersion rate slowed from 168 hr up to 2688 hr. Thus, at the slower phase tensile properties were obtained as well as at 840 hr and lastly 2688 hr. For both samples, before saturation, the specimens tended to fail at the cross-section perpendicular to loading with all fibres failing in the same plane (Figure 7.6(a)). However, for both samples, after the saturation (more than 2000 hr immersion), not only the fibre but the yarn protruded from the fracture surface due to the weak fibre-resin interface caused by the water immersion (Figure 7.6(b)). More protruded yarns were noticed for sample HVE-FR than for HVE-UT and this shows that the adhesion/interface in between fibre and resin is weaker for HVE-FR than HVE-UT. The failure mode can be seen from the Figures 7.8 and 7.9 for HVE-UT and HVE-FR respectively, with ruptured protruding yarn as well as pulled-out yarn from the surface indicating that, as the yarn pulled-out from the matrix at the failure surface, the fibres within the yarn ruptured.

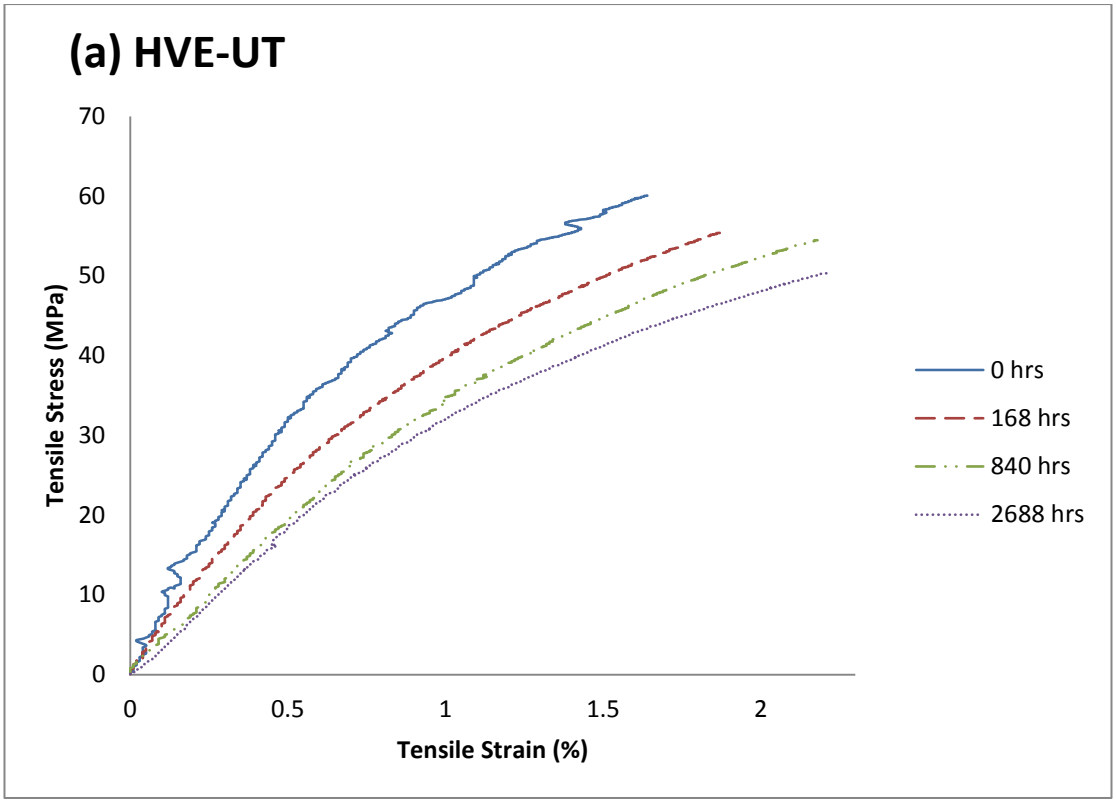

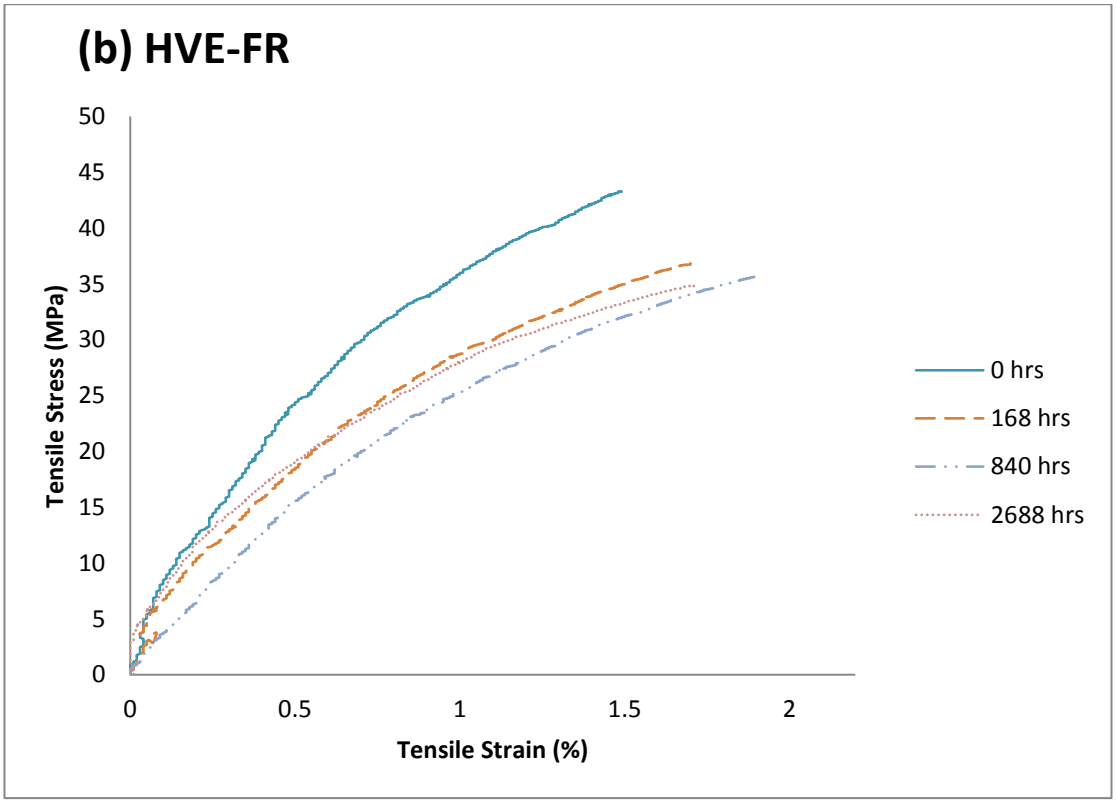

Figure 7.5 Typical tensile stress-strain curves for sample HVE-UT and HVE-FR.

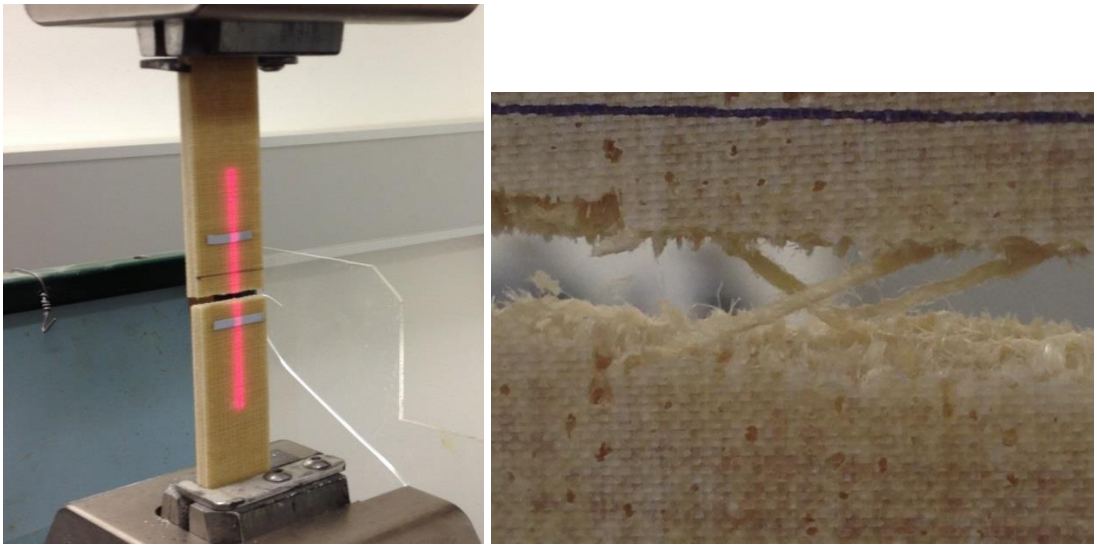

(a) **(b)**

Figure 7.6 Failure of (a) Typical of all samples after immersion before reaching saturation and (b) Typical of all samples after reaching saturation (2688 water immersion).

Table 7.4 shows the mechanical properties of HVE-UT and HVE-FR with respect to water absorption. Generally, the tensile properties of HVE-FR are lower in comparison to HVE-UT. This is due to the deposition of ammonium polyphosphate that leads to poor adhesion between the hemp fibres and vinyl ester resin [77, 147]. The adhesion between fibres and resin was weakened due to the immersion of HVE-FR sample in water.

Table 7.4 Results of tensile properties of sample HVE-UT and HVE-FR with respect to water immersion times.

Tensile Properties	Time (Hrs)			
HVE-UT	0	168	840	2688
Tensile Strength	60.897 (0.933)	55.309 (1.479)	53.589 (1.106)	48.341 (1.756)
Tensile Strain	1.78 (0.283)	1.924 (0.124)	2.222 (0.138)	1.932 (0.203)
Tensile Modulus	6.073 (0.803)	5.391 (0.811)	3.734 (1.593)	3.8432 (0.745)
HVE-FR				
Tensile Strength	46.479 (2.930)	36.232 (1.300)	35.613 (0.31)	35.191 (1.63)
Tensile Strain	1.643 (0.130)	1.752 (0.168)	1.87 (0.0628)	1.844 (0.270)
Tensile Modulus	4.690 (0.742)	3.812 (0.154)	3.179 (0.245)	3.378 (0.367)

The effects of water immersion on the normalized tensile properties of the composites are shown in Figure 7.7. The normalized values were obtained by dividing the tensile properties following immersion in water by the properties of dry composites. In terms of tensile strength (Figure 7.7(a)), the loss of sample HVE-UT was only about 9% of the original strength after 168 hr immersion and it continued to lose the strength up to 21% by the end of the immersion time. Figure 7.8(a), (b) and (c) shows the SEM images of HVE-UT fractured specimens after 0, 840 and 2688 hr respectively. The ruptured protruding yarns for 840 hr (Figure 7.8(b)) are a bit longer than 0 hr (Figure 7.8(a)). This is because of the weak adhesion between the fibres and matrix, thus letting the tensile loading act on the fibres with less or weaker adhesion with matrix [41, 157]. As for the 2688 hr (Figure 7.8(c)) water immersion specimen, we can see not only the ruptured and pulled-out yarns but also a lot of pulled-out yarns perpendicular to the loading directions (either warp or weft yarn). This indicates that the adhesion between the fibres and matrix is weaker in comparison to the specimen immersed for 840 hr [41, 80]. A similar thing was reported by Christian and Billington [41]. When their saturated sample was subjected to tensile loading, long protruded fibres (yarns) from the perpendicular to loading direction appeared and this was because of the weakened fibres and matrix interface.

Sample HVE-FR shows a similar trend but the reduction of the strengths are higher than for sample HVE-UT (Figure 7.7(a)). After 168 hr immersion the tensile strength of HVE-FR was reduced 22% from the original strength. The strength continued to decline but the difference was insignificant. At 2688 hr water immersion, the reduction in tensile was recorded at 24% which is only 2% lower than the sample immersed for 168 hr. Figure 7.9(a), (b) and (c) show SEM images of the fractured surfaces of the HVE-FR specimens immersed in the water for 0, 840 and 2688 hr

respectively. As we can see from the Figure 7.9(a), pulled-out protruded yarn only appeared on the surface. However, unlike the HVE-UT sample after 840 hr water immersion, for HVE-FR there are much longer pulled-out protruded yarn as well as the pulled-out yarn from the perpendicular direction to tensile loading that appeared after 840 hr of water immersion (Figure 7.9(b)). This situation is expected to happen because sample HVE-FR reached the saturation point at 552 hr (refer Table 7.2) which was earlier than when the sample was tested (840 hr). Thus, those yarns protruding from the perpendicular direction and tensile loading direction pulled-out due to weakened adhesion between fibres and resin. As for Figure 7.9(c), more fibres and yarns appeared on the fractured surface because it was immersed in the water for so long after reaching saturation point.

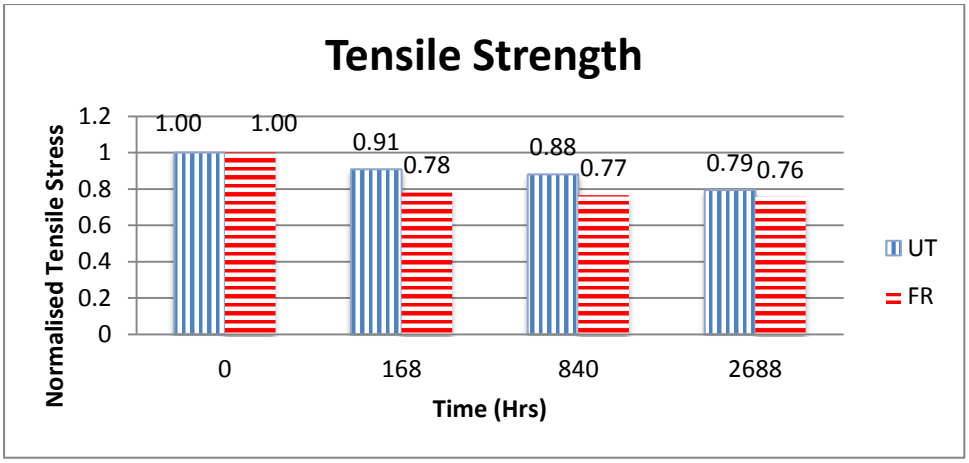

(a)

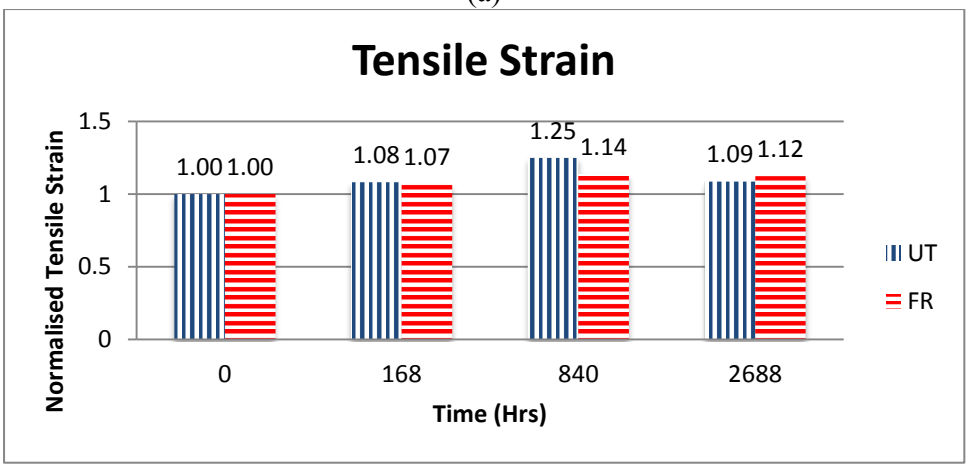

(b)

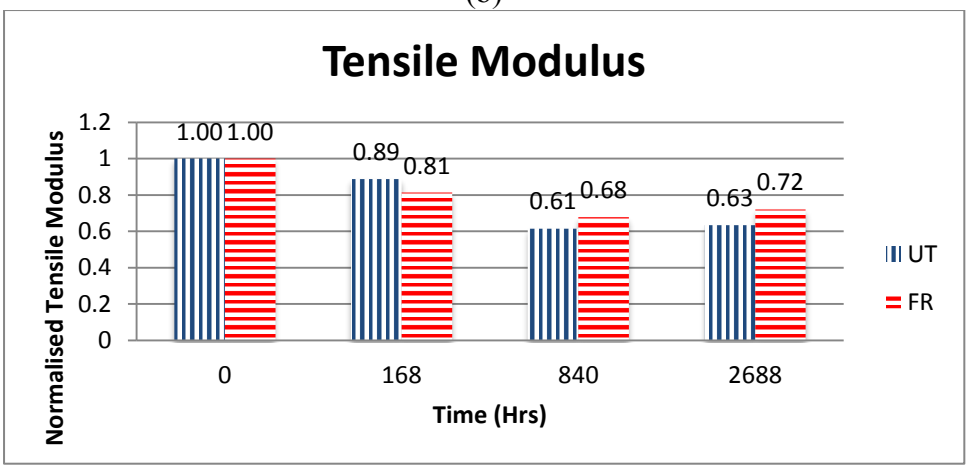

(c)

Figure 7.7 Effect of water absorption on the normalized tensile properties of the composites; (a) Tensile Strength, (b) Tensile Strain and (c) Tensile Modulus.

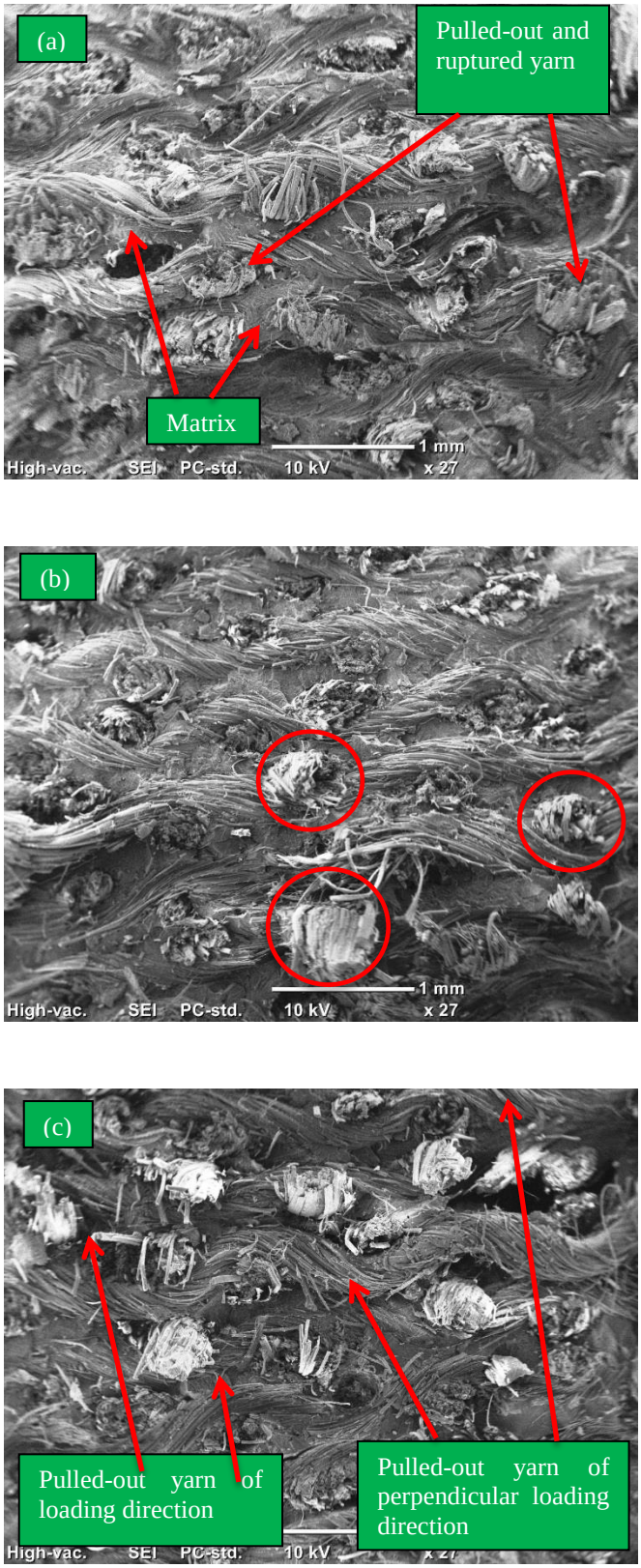

Figure 7.8 Scanning electron image of sample HVE-UT; (a) 0 hr, (b) 840 hr and (c) 2688 hr water immersion.

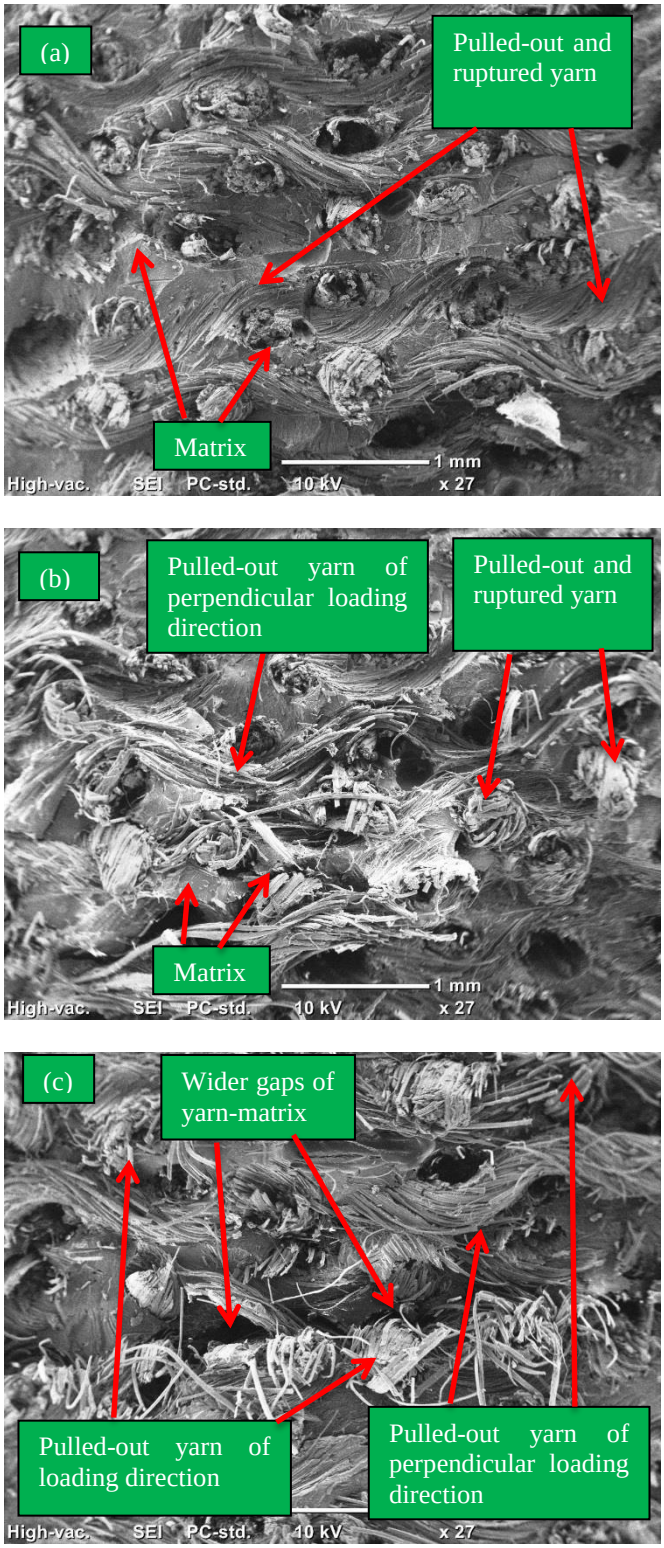

Figure 7.9 Scanning electron image of sample HVE-FR; (a) 0 hr, (b) 840 hr and (c) 2688 hr water immersion.

Figure 7.7(b) shows tensile strain for both samples with respects to water absorption. Tensile strain for sample HVE-UT increased with the increase of immersion time and the increment was up to 25% at 840 hr immersion before it reduced a bit after 2688 hr immersion. Similarly for sample HVE-FR, the strain also showed an increment of 7% after 168 hr immersion and then continued to increase to 14% after 840 hr immersion before decreasing towards the end of water immersion period.

The effect of water immersion on the tensile modulus is shown in Figure 7.7(c). Tensile modulus for sample HVE-UT is obviously reduced when the water permeates the composite system. The modulus reduced 11% after 168 hr water immersion and kept continuing declined to 39% after 840 hr immersion. However, the modulus increased a little bit after immersion in the water for 2688 hr. For sample HVE-FR, the reduction was a little bit lower than HVE-UT which was 19% after 168 hr water immersion. However the reduction continued after 840 hr immersion before it increased at the end of the immersion period.

Some other research which used hemp fabric (non-woven) to reinforce polymers were Shahzad [80] and Dhakal et al. [38]. After their composites were immersed in water and reached saturation point, they found that their composites also experienced a reduction in the mechanical properties after saturation. Both works agree that the decline in tensile properties was because of the weakening of adhesion between the fibre and resin, as discussed in previous section. The reduction in tensile modulus for samples HVE-UT and HVE-FR is due to the water absorbed in the composite system which weakened the adhesion between the woven hemp fibres and vinyl ester resin.

Another thing that should be pointed out in this work is the greater decline in tensile modulus in comparison with tensile strength for both the HVE-UT and HVE-FR

samples. This phenomenon also occurred in the other workers [38, 43]. What happened here can be explained by analysing the tensile strains and modulus of the samples. The increase in strain and the reduction in tensile modulus shows that the samples became softer and ductile due to the plasticisation by water. Water can act as a plasticiser as the water permeates between hemp fibres and vinyl ester. The composite material stiffness is reduced as plasticisers infiltrate between the polymer chains and push the chains apart, effectively lowering the glass transition temperature for the resin making it softer [41]. Not only to the resin, water also plasticised the hemp fibres using a similar mechanism [38, 41, 80].

7.3.2.2 Flexural Properties

Figure 7.10 shows typical flexural stress - strain curves of samples HVE-UT and HVE-FR at different water immersion times, and Table 7.5 shows the flexural properties for both samples extracted from the flexural test. The observations made earlier for the effect of water absorption on tensile properties are also relevant for flexural properties. Overall, the flexural properties of both samples decreased gradually with the longer time of water immersion. This is due to the weakened interface between fibre and matrix caused by water infiltration. Comparing the two samples, HVE-FR initially possessed lower flexural properties than HVE-UT. Again, as for tensile properties, this is because the ammonium polyphosphate deposition leads to poor adhesion between the hemp fibres and vinyl ester resin. The degradation of both samples worsens with immersion and the reason is similar to that discussed in tensile properties.

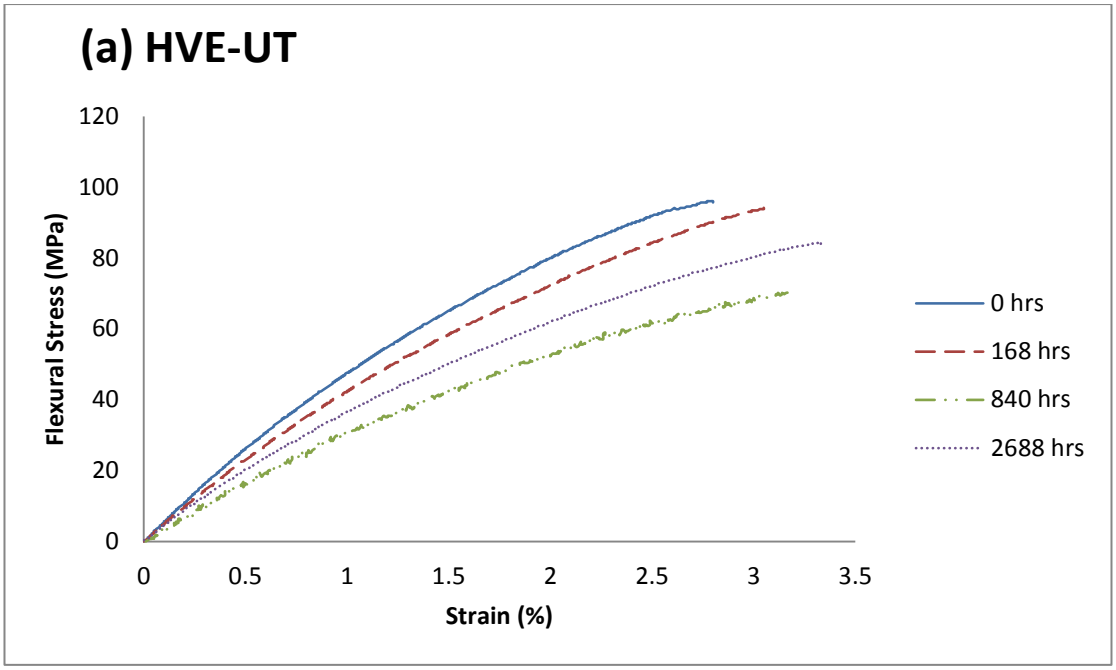

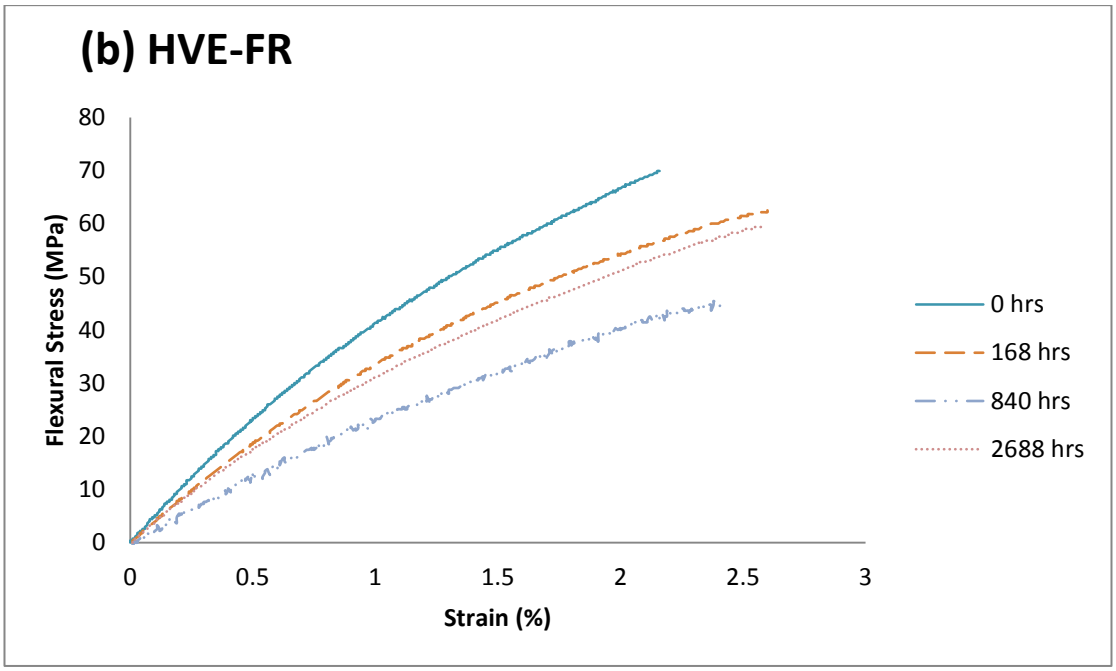

Figure 7.10 Typical flexural stress-strain curves for samples HVE-UT and HVE-FR.

Table 7.5 Results of flexural properties of samples HVE-UT and HVE-FR with respect to water immersion times.

Flexural Properties	Time (Hrs)			
HVE-UT	**0**	**168**	**840**	**2688**
Flexural Strength	95.390 (4.906)	95.099 (1.243)	70.768 (1.756)	85.3461 (3.571)
Flexural Strain	2.746 (0.253)	3.092 (0.066)	3.204 (0.191)	3.554 (0.329)
Flexural Modulus	5.428 (0.087)	4.825 (0.095)	3.463 (0.176)	4.301 (0.029)
HVE-FR				
Flexural Strength	70.238 (2.000)	60.120 (3.821)	44.371 (3.270)	59.787 (1.524)
Flexural Strain	2.214 (0.086)	2.500 (0.224)	2.446 (0.127)	2.704 (0.082)
Flexural Modulus	4.809 (0.050)	3.997 (0.059)	2.636 (0.112)	3.737 (0.079)

Figure 7.11 shows the effects of water immersion on the normalized flexural properties of the composites. 168 hr immersion of the HVE-UT sample did not affect its flexural strength but after 840 hr immersion the strength dropped significantly; as much as 26%. However, it is interesting to note that the flexural strength for HVE-UT immersed for 2688 hr is higher (reduced 15% only) than the sample immersed for 840 hr. A similar trend is shown for sample HVE-FR but the reduction in flexural strengths is higher than sample HV-UT. Again, the reduction in flexural strength after 2688 hr recorded as less (only 15%) in comparison with the sample after 840 hr immersion (37%). This is due to the fact that high amounts of water causes swelling of the fibres, which fill the gaps between the fibre and the matrix thus increasing the friction between them, eventually leading to an increase in the flexural properties of the composites [38, 80, 155].

In term of flexural strain, both samples show the increment after immersion and the percentage becomes higher as the time of immersion increases. Flexural strain for sample HVE-UT increased up to 29% while sample HVE-FR recorded an increase up

to 22% at the end of water immersion test at 2688 hr. The reason is similar to the tensile strain which has been discussed previously.

Flexural modulus for both samples possessed a similar trend to flexural strength. Again, the reduction in flexural modulus is higher than flexural strength for both samples, HVE-FR than HVE-UT. Again, the reason for this is that the water acts as a plasticiser which penetrates the samples softening the resin and hemp fibres. The increase in flexural strain and decrease in flexural modulus are the evidence for this phenomenon.

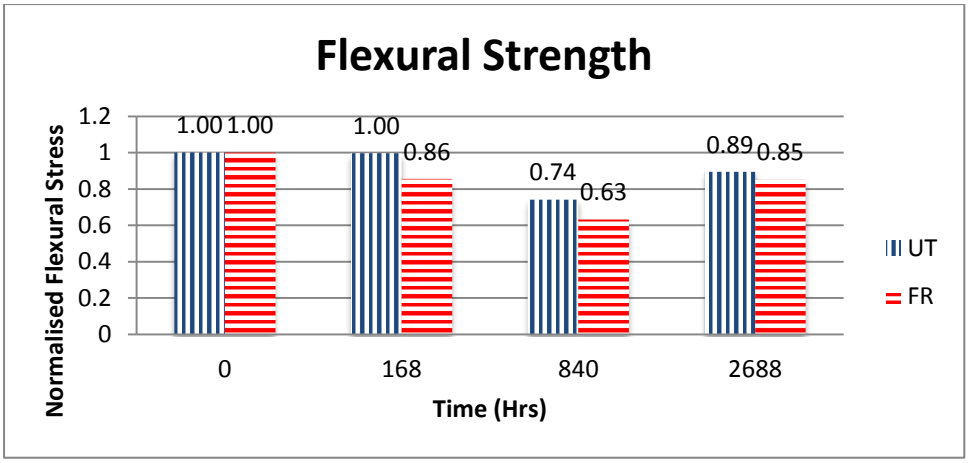

(a)

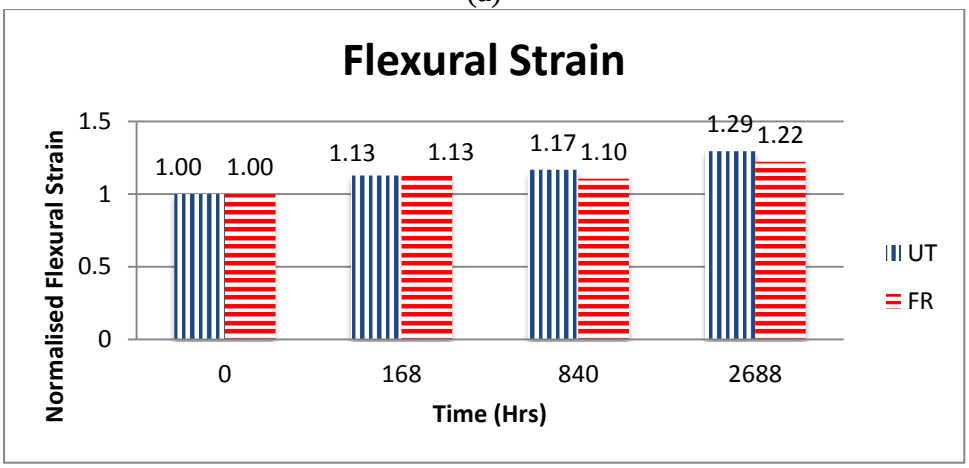

(b)

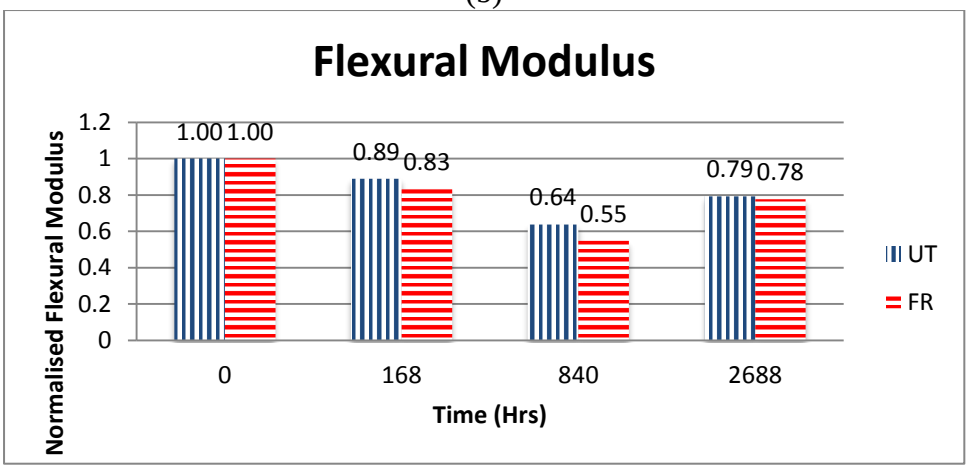

(c)

Figure 7.11 Effect of water absorption on the normalized flexural properties of the composites; (a) Flexural Strength, (b) Flexural Strain and (c) Flexural Modulus.

7.3.3 Effect of Water Absorption on the Fire Retardant Properties

7.3.3.1 Burning Test Results

The effects of FRs treated HVE were discussed in Chapter 6 and the HVE-FR sample was found to be the best in in terms of FR performances, thus it was chosen for further analyses in this chapter. Table 7.6 shows the results of a burning test in accordance with ASTM D635. The burning test was carried out after the samples were immersed in the water for 168, 840 and 1512 hr. Water immersions ended at 1512 hr because the fire retardant performance of both samples were greatly reduced and this was observed through burning test.

In terms of sample HVE-UT, all samples were burned to the second mark (100 mm) but the total burning time reduced from 627.2 s to 463.4 s with the increment of water immersion times. This means that the burning time is gets faster and the FR performance of sample HVE-UT becomes poorer as immersion time increases. All the HVE-UT burnt to ashes as shown in Figure 7.12(a).

As for HVE-FR, the specimen without water immersion did not burn even to the first mark and this proved its good FR performance (Figure 7.12(b). During the flame exposure, charring processes occurred in the area reached by the flame. It is also worth mention that during the test, both HVE-FR specimens released black smoke, an intense smell mixed with burnt plastic, burning in a yellow flame and a hard residue. Since the active ingredient of the FR is ammonium polyphosphate, the hard residue product (char) is actually due to the ammonium polyphosphate which promotes char formation reducing the mass of volatile combustible degradation fragments evolved by making the carbon and hydrogen remain in the condensed phase. This subject was discussed in Section 6.3.5. Figure 7.12(c) shows the burnt specimen after 168 hr of immersion.

The sample was burnt for 171 s but the affected area did not reach, and was even far from the second mark. However, after 840 hr of immersion, the specimen was burnt to the second mark and the time taken was recorded at 650.67 s (Figure 7.12(d)) indicating that its FR performance was reduced. The residue was observed slightly fragile as compare to the residue of sample immersed for 168 hr. The specimen which was immersed in the water for 1512 hr shows a drop in total burning time which was recorded at 544.33 s. Here the sample totally lost its resistance to the fire and the residue was burn to ash (Figure 7.12(e)). Thus, it can be said that the HVE-FR sample had actually lost its resistance to fire after 840 hr of immersion.

Table 7.6 Results of burning test for HVE-UT and HVE-FR.

Sample	Water immersion time (hr)	1st mark (25 mm) (s)	2nd mark (100 mm) (s)	Total burning (s)	Burning rate (mm/min)
UT	0	37.8 (1.924)	624.4 (24.582)	627.2 (23.026)	7.183 (0.268)
	168	37.4 (1.817)	516.4 (14.775)	517.8 (16.146)	8.697 (0.272)
	840	36.8 (0.447)	428.8 (16.962)	465.6 (17.242)	9.675 (0.353)
	1512	37.2 (1.483)	426.2 (12.317)	463.4 (12.857)	9.716 (0.268)
FR	0	x	x	x	x
	168	36.667 (1.528)	134.333 (7.371)	171 (7.550)	2.074 (0.252)
	840	36.6 (0.548)	624 (19.545)	650.667 (19.296)	6.920 (0.208)
	1512	36.6 (1.140)	533.4 (16.471)	544.333 (31.086)	7.90 (0.239)

x – Indicates that the expected event did not occur.

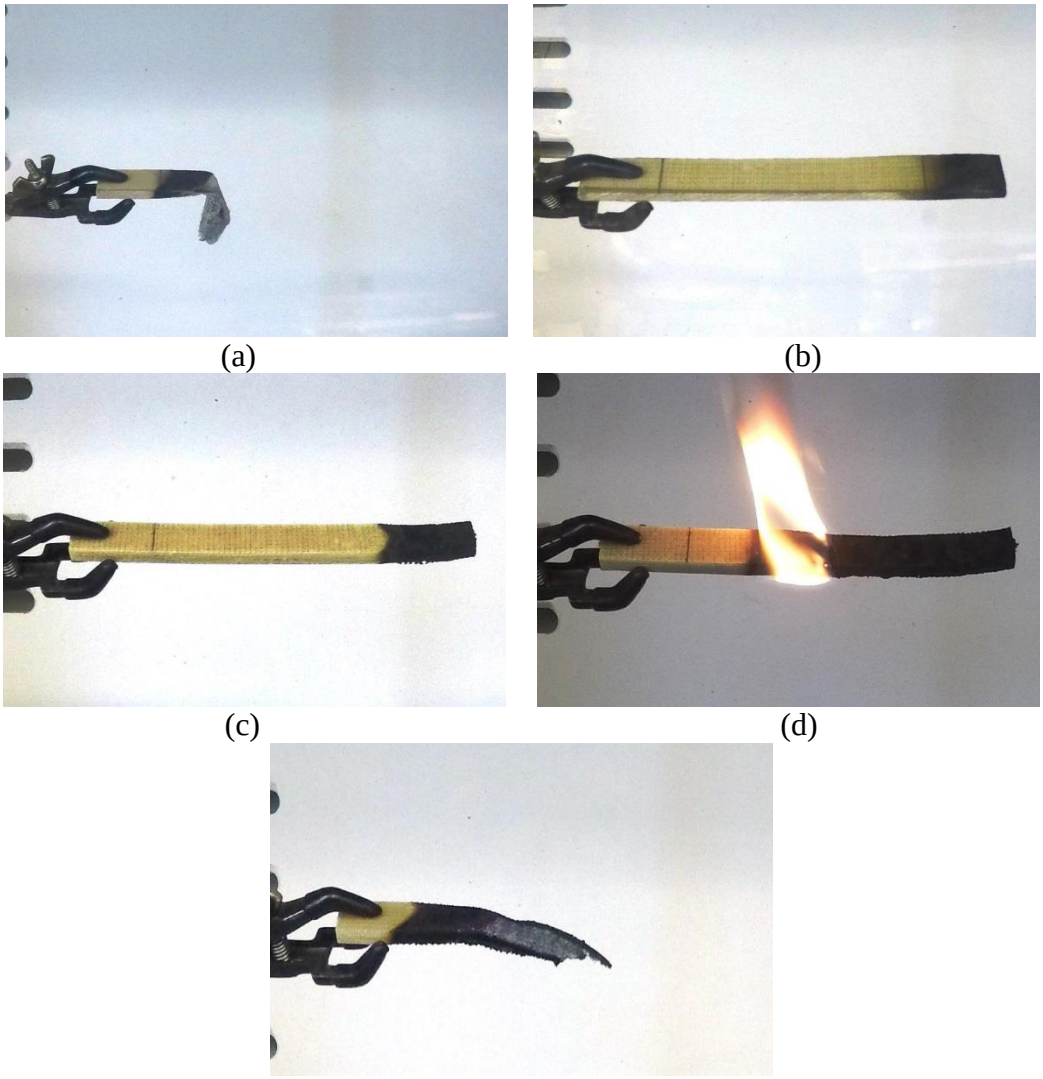

Figure 7.12 Images of specimens subjected to burning test; (a) HVE-UT, (b) HVE-FR without water immersion (0 hr), (c) HVE-FR after 168 hr water immersion, (d) HVE-FR after 840 hr water immersion and (e) HVE-FR after 1512 hr water immersion

Figure 7.13 shows the burning rate of both samples versus water immersion time extracted from Table 7.6, and the burning rates for both samples are consistent with their burning times. In the case of sample HVE-UT, burning rates were increased with the increased period of immersion. Although the sample not immersed was burnt completely, the existence of water had worsened its FR properties from 7.18 to 9.72 mm/min and this is about a 35% increase.

In terms of sample HVE-FR, we can see in Figure 7.13 that the sample did not burn initially. However, the burning rate was increased to 2.1 mm/min after 168 hr water immersion. The burning rates kept increasing rapidly to 6.92 mm/min and lastly 7.9 mm/min after the specimen was immersed for 840 and 1512 hr respectively. Thus, the water immersion not only decreased the FR performances but also increased the burning rate of HVE-FR sample.

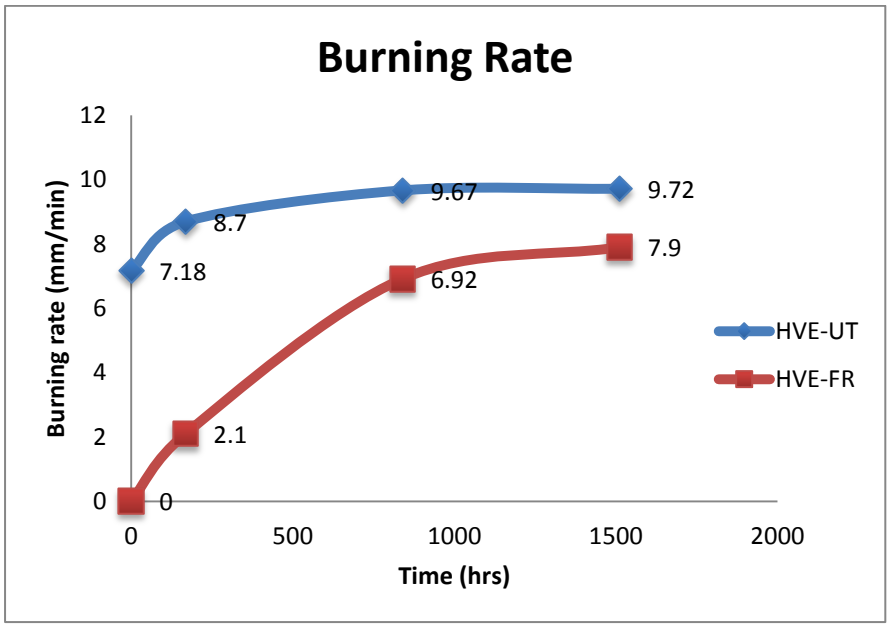

Figure 7.13 Burning rates of sample HVE-UT and HVE-FR.

7.3.3.2 Limiting Oxygen Index

The value of the Limiting Oxygen Index (LOI) measurement test shows the minimum amount of oxygen in an oxygen–nitrogen mixture required to support complete combustion of a vertically held sample that burns downward from the top. A LOI value more than 28 is generally classified as fire retardant [79]. The GB50222-1995 standard method (which is equivalent to ASTM D2683) states that, 1) the value < 24 indicates that the material is flammable; 2) the value ≥ 24 and < 27 indicates that the

material is combustible, and; 3) the value ≥ 28 indicates that the material is fire retardant.

The LOI results shown in Table 7.7 confirmed the fire retardant properties above. In the case of HVE-UT, none of them can be classified as FR material because all the values were recorded lower than 27, which means that they were flammable material. However, the values were reduced as period of immersion increased which explained why the burning times were getting faster.

As for the HVE-FR sample, the value above 27 only shown by the sample immersed in the water after 168 hr (LOI of 28.7) and sample without water immersion possessed the highest value of 29.4 indicating that both samples are fire retardant material. Nevertheless, the LOI values for specimens HVE-FR immersed for 840 and 1512 hr were recorded lower than 27, 23.7 and 23.1 respectively indicating that both specimen are flammable material. Hence, the LOI confirms that HVE-UT sample is still be able to retain its fire retardant performance after 168 hr of water immersion.

Table 7.7 Results of LOI for sample HVE-UT and HVE-FR.

Water Immersion Time (hr)	LOI value	
	HVE-UT	HVE-FR
0	22.3	29.4
168	21.8	28.7
840	21.5	23.7
1512	21.7	23.1

7.3.3.3 The Fastness of Fire Retardant Treatment on the HVE.

In order to explain how long the effectiveness of FR treatment can be retained on the sample, a scanning electron microscope image is used to analyse the surface of substances in the fabricated composites. The analysis conducted from the scope of fibres or yarns. It is worth mentioning that the method of applying FR chemical on the WHF was by the 'dips and nips' method and the wet pick-up was consistently maintained around 100-105% (refer Section 7.2.2). The chemical pick-up (after drying) was recorded at 24.94% out of the total weight of WHF (refer Chapter 5, Section 5.3.1).

Figure 7.14(a) shows the SEM images of WHF fibres before FR treatments which were clean unless some hemicelluloses appeared on the surface of the fibres. Figure 7.14(b) shows the woven hemp fibres after FR treatment. There were obviously FR particles of sizes ranging from several micro to nanometres deposited evenly on the yarn or fabric surface. The only particles that can be presumed are the ammonium polyphosphate which the FR manufacturer reveals as the fire retardant's active ingredient. Other particles cannot be clarify and justify as the manufacturer has not revealed these. Thus the image from Figure 7.14(b) confirmed the deposition of the FR chemical in the WHF and this has been discussed is Chapter 5, Section 5.3.2.

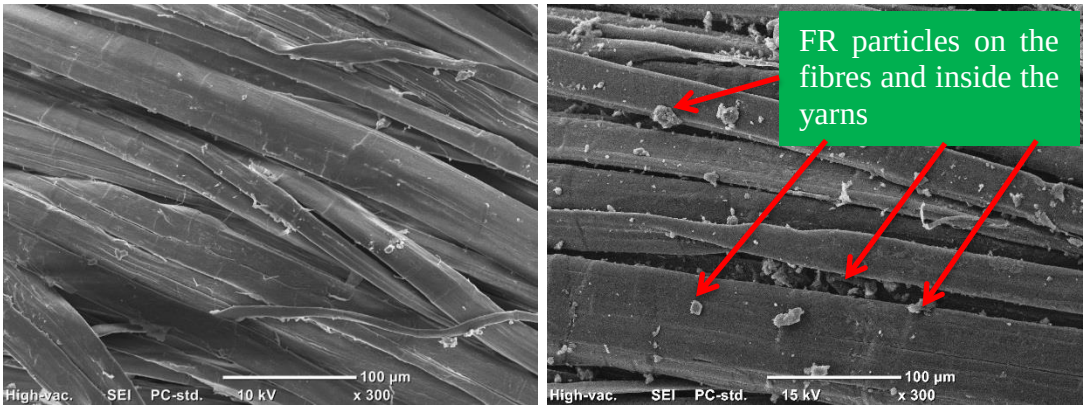

(a) (b)

Figure 7.14 SEM images of woven hemp fibre; (a) before FR treatment and (b) after FR treatment of WHF.

Figure 7.15 shows images of fracture surfaces of specimens HVE-UT and HVE-FR before immersion. The images of the pulled-out protruded yarn were magnified to analyse the surface of the fibres. The image of the specimen in Figure 7.15(a) shows that the surface of protruded fibre was clean and smooth. When analysing the surface of fibres from the HVE-FR specimen, it was observed that the surface of the fibres was covered by the sputter which was believed to be FR chemical deposition (Figure 7.15(b)). Since the FR composition is unknown except for the ammonium polyphosphate, only speculation can be made about the possibility of fire retardant chemical which could react with the resin or natural fibres.

According to the FR technical data sheets, this chemical is intended for curtain, carpet and soft upholstery and is specially made for natural fibres as well as a mixture of natural and synthetic fibres. Retreatment is recommended after 9 – 12 months after treatment suggesting that this FR is a semi-durable to durable formulation [144, 162-164]. Therefore, the deposition of this FR chemical on the WHF can be said to be strong. This FR was proven to increase FR performance of WHF as has been discussed in Chapter 5. Not only that, utilisation of WHF treated with this FR chemical in vinyl

ester composites also greatly improved its fire retardant performance (refer Chapter 6). Hence, the sputter on the fibre surfaces shown in Figure 7.15(b) is strongly believed to be the product of the FR chemical which is responsible for the HVE-FR's good fire retardant performances.

All the HVE-FR specimens' fracture surfaces with respect to different time water absorption are shown in Figure 7.16. For specimens immersed in the water for 168 hr in Figure 7.16(a), the sputters can still be observed from the surface of the fibres. This image explains why the sample can still retard fire the burning test. In the cases of specimen HVE-FR immersed in the water for 840 and 1512 hr in Figure 7.16(b) and (c) respectively, it can be seen that the sputter were no longer seen on the fibres' surfaces. This is the reason that the specimens no longer retarded the fire during the burning test. The disappearance of the sputter from the fibre surfaces is due to a leaching out or migration of the FR chemical from the sample during immersion [163, 165-167].

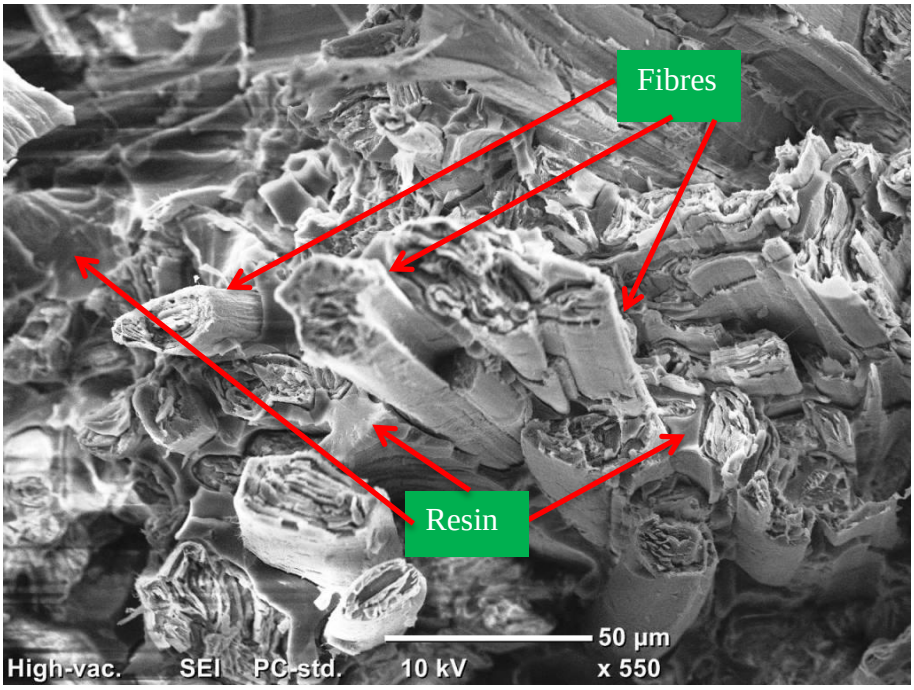

(a)

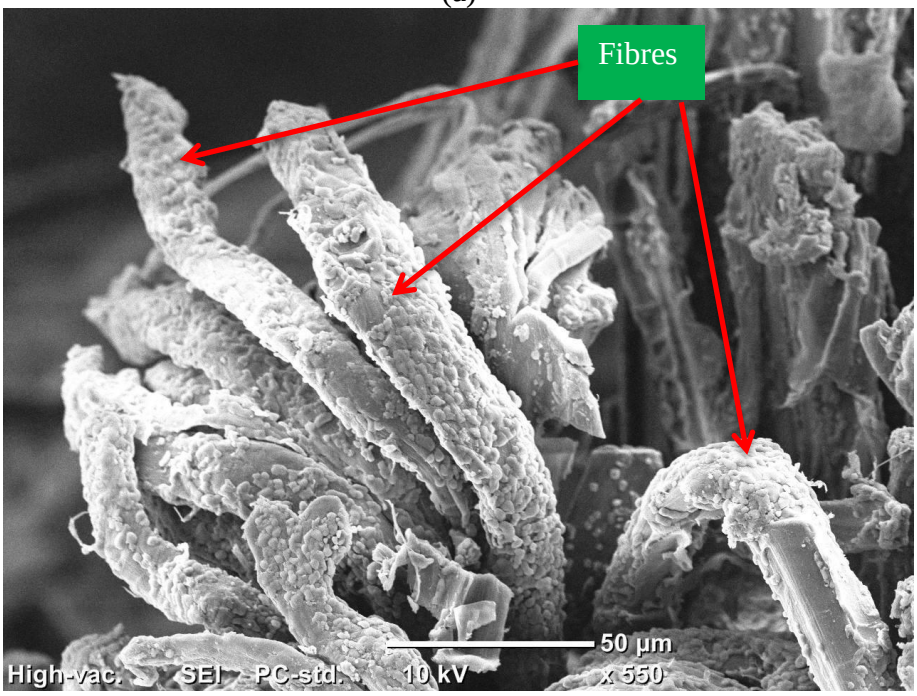

(b)

Figure 7.15 SEM images of fracture surfaces for sample HVEs; (a) HVE-UT and (b) HVE-FR

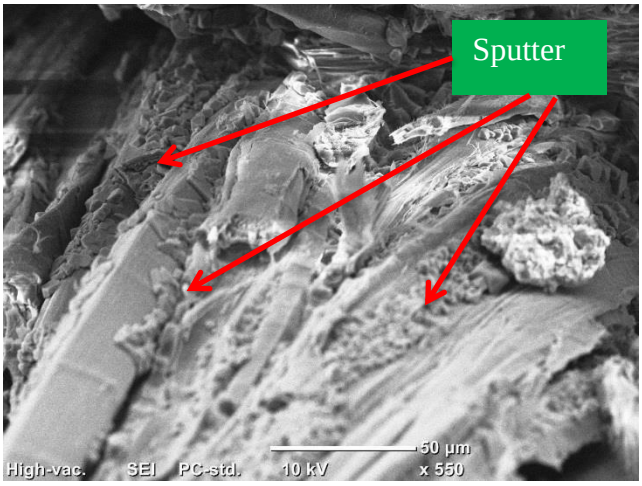

(a)

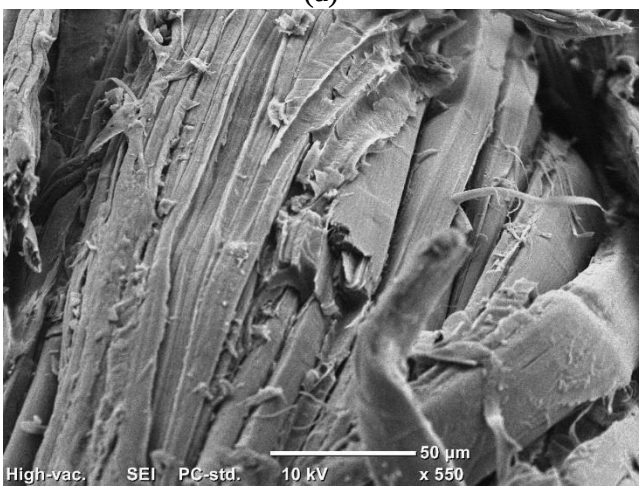

(b)

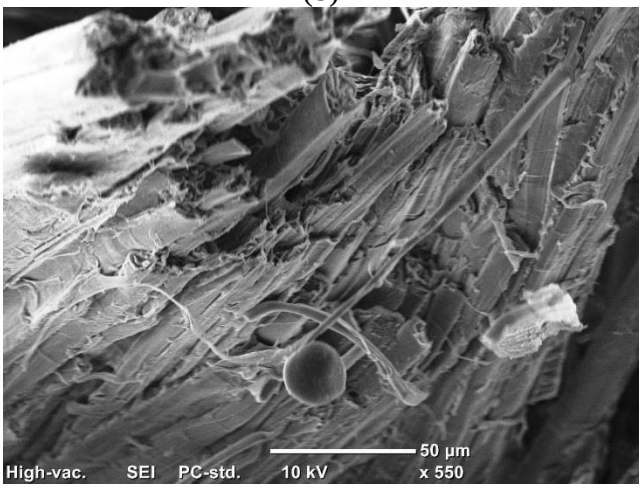

(c)

Figure 7.16 SEM images of fracture surfacs of HVE-FR specimen; (a) after 168 hr, (b) 840 hr and (c) 1512 hr or water immersion.

Overall, for the effect of water absorption on fire retardant properties, the immersion of HVE-UT and HVE-FR in the water could degrade its fire retardant properties and increase the burning rates. This was proven by the LOI results for both samples. The LOI results also confirmed that only HVE-FR is classified as a fire retardant material up to 168 hr of immersion. However, it lost its fire retardant properties after 840 hr of immersion. Therefore, the fastness of fire retardant chemical treatment on the HVE-FR sample is between 168 hr to 840 hr of water immersion.

The regression and correlation was done and several relationships were established which involved the relationship between the mechanical, burning and fire retardant properties of fabricated composites to the water absorption. The results are presented in Section 7.5.4 as a guide to material selection.

7.3.4 Fatigue Analysis

Fatigue tests for samples HVE-UT and HVE-FR wereconducted in tension-tension mode at a stress ratio *(R*) of 0.1 for the stress levels of 50, 60, 70 and 80% of the fabricated composite tensile stress. Table 7.8 shows the combinations of fatigue testing parameters (% stress level, S_{max} and S_{min}) for samples HVE-UT and HVE-FR. The results of fatigue tests are presented by plotting Wohler stress-life (S-N) diagrams. The fatigue strength coefficient is very useful parameter to determined fatigue degradation [44]. The higher b values infer slower degradation of fatigue strength for every decade of cycles [43, 44, 81]. It was obtained by Power–law regression equations and given by:

$$S_{max} = S_0 N^b \tag{7.3}$$

Where S_{max} is the maximum stress applied, N is the number of cycles to failure, S_0 is the single cycle (static) ultimate strength of the material, and b is the material fatigue strength coefficient.

Table 7.8 Values of S_{max}/S_{min} and stress levels (% of tensile strength) for sample HVE-UT and HVE-FR.

Sample	Tensile Stress (TS) (Mpa)	S_{max}/S_{min} (Mpa/Mpa)			
		0.8 TS	0.7 TS	0.6 TS	0.5 TS
HVE-UT	60.9	48.72/4.87	42.63/4.26	36.54/3.65	30.45/3.04
HVE-FR	46.48	37.18/3.72	32.54/3.25	27.89/2.79	23.24/2.32

Figures 7.17 and 7.18 shows S–N and normalised S-N fatigue data for the present samples. A gradual decrement in fatigue strength with an increasing number of fatigue cycles was observed. It was observed that the power–law model of Equation [44] is a fit with the experimental fatigue data. All regressions have an R^2 value > 0.95 which is generally characteristic of composites whose lifetime is matrix crack growth and inter-laminar cracking domination [44, 168]. The type of final failure observation in specimens tested in static tensile tests and tension–tension fatigue tests was similar; which is that specimens fail catastrophically starting from the matrix crack, with the short ruptured protruding yarns and pulled-out from the fracture surface (refer Figure 7.8). From the S–N diagram in Figures 7.17 and 7.18, it is observed that even though the static strength of sample HVE-UT is greater than HVE-FR, their fatigue strength coefficient can be said to be similar; 0.12 and 0.128 respectively. Thus, it can be said that the fire retardant treatment imparted on the WHF composites did not affect the fatigue strength of the materials.

Hemp composites fabricated by other works tested under a stress ratio R = 0.1, did not fail after 10^6 which suggests that the endurance limit for hemp composites is 10^6 [42-45]. de Vasconcellos et al. [45] fabricated composite made of WHF and epoxy resin. This is the closest comparison in terms of substances utilised in the present work. However, their woven hemp fabric/epoxy's ultimate strength was far superior to the HVE-FR. This is most probably due to the epoxy resin used which commonly possesses higher mechanical properties than vinyl ester since the woven hemp fabric used was quite similar in terms of weight yet their endurance limit was reported as 10^6. Since the HVE-FR was tested under low cycle with the higher stress level (50-80%), it can be projected that this sample can reached up to of at least 10^5 cycles with lower stress levels based on extrapolating the curves in Figures 7.17 and 7.18.

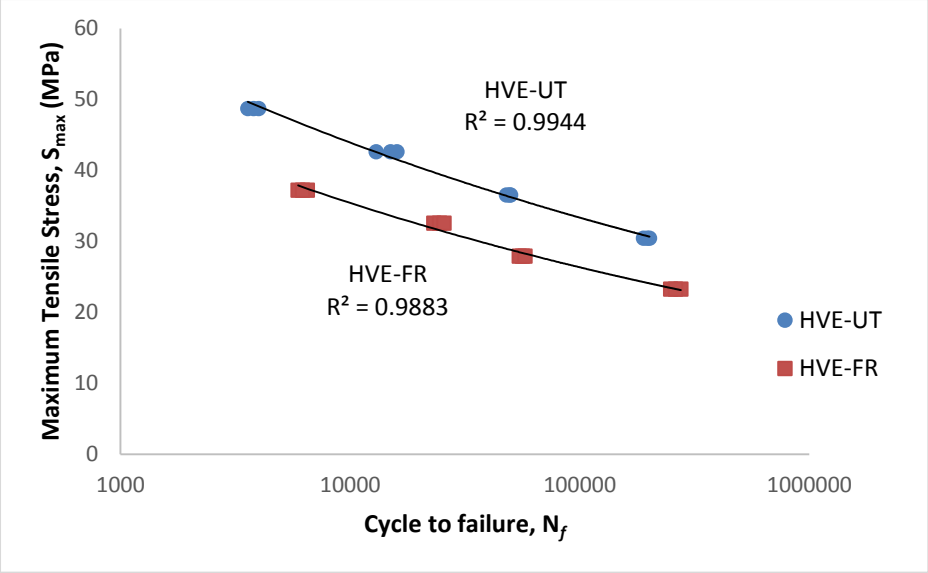

Figure 7.17 Lifetime S–N diagram for samples HVE-UT and HVE-FR.

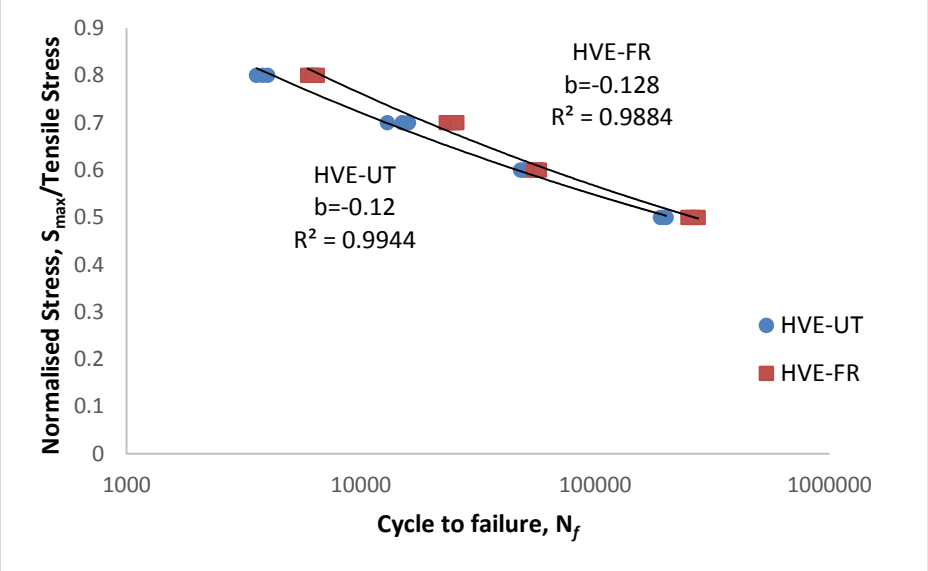

Figure 7.18 Normalised S–N diagram of HVE-UT and HVE-FR.

The reliability for safety, insurance risk, life cycle costs and high longitudinal stiffness of the material can be estimated from the low cycle fatigue [169, 170]. For this purpose, Harik et al. [169] defined taking the low cycle fatigue at 10^4 cycles and 50% ultimate strength of the materials. Therefore, the fatigue strength of the present samples' (HVE-UT and HVE-FR) values which were tested under low cycle fatigue (at 50% tensile strength) can be used as a safety limit for the end products' application.

In this work the safety limit strength utilisation for sample HVE-UT and HVE-FR are about 30 and 24MPa respectively.

Figure 7.19(a) and (b) shows the images of fracture surfaces after fatigue tests for samples HVE-UT and HVE-FR respectively at 50% stress level. For both samples, there were a lot of protruded, pulled-out and ruptured yarn on the surface. The matrix cracks were observed from the fracture surface as was observed by de Vasconcellos et al. [45] in their hemp/epoxy composites. According to Harik et al. [169], the mode of failure for fatigue always shows progressive matrix cracking and this is true for the high cycle fatigue. However, in low cycle fatigue, the damage mode involves more failed fibres as opposed to the high cycle fatigue. Therefore, for the present samples there were no consistent matrix cracks but only the protruded, pulled-out and ruptured yarns were observed from the fracture surfaces because the test were done at low cycle fatigue for 50% stress level.

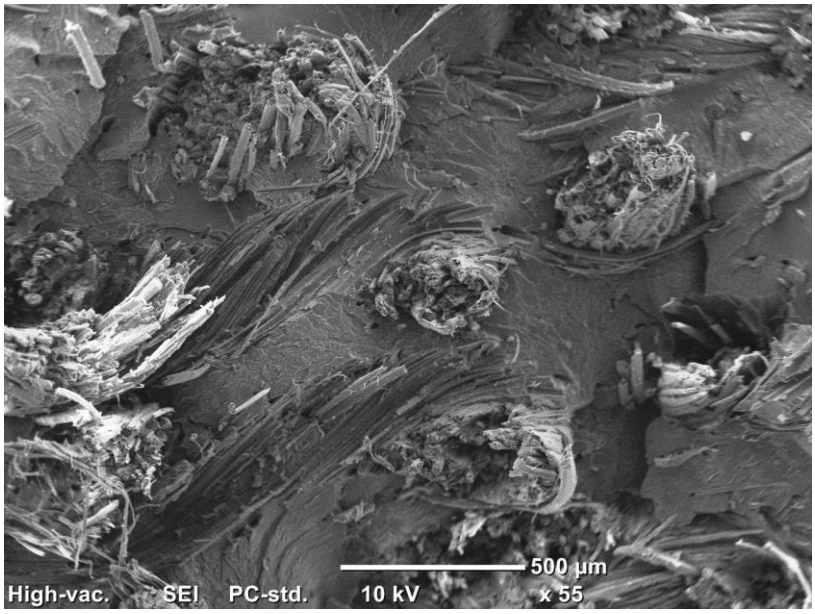

(a)

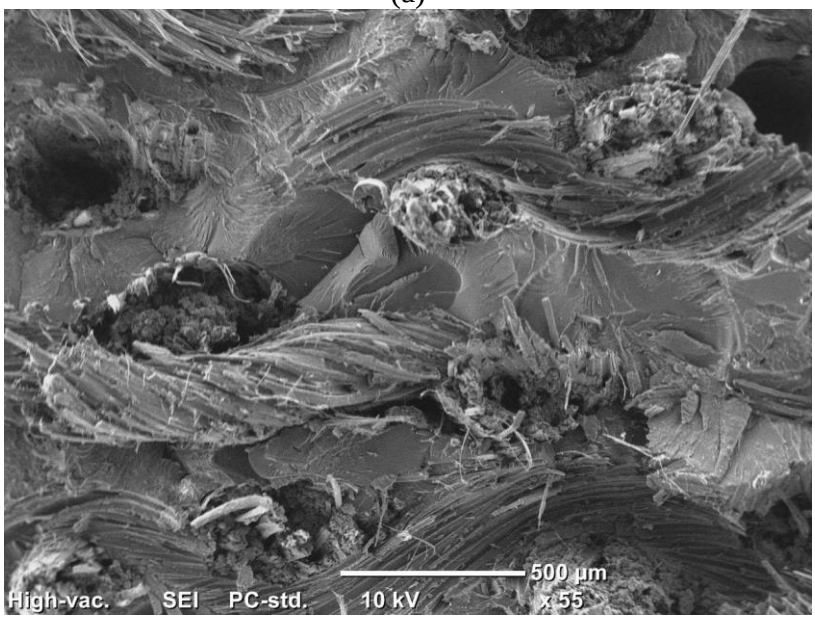

(b)

Figure 7.19 SEM images of fracture surfaces after fatigue test for; (a) HVE-UT and (b) HVE-FR

7.4 Material Selection Guide

Based on the results in previous chapters, a ‘material selection guide’ was established for the use of relevant stakeholders when producing HVEs. All the characteristics provided in this sections are measured using several standard methods while others were measured using the method introduced in the relevant section from the previous chapter.

7.4.1 Woven Hemp Fabric (WHF)

The fabric for selection is WHF with a weave structure of ‘plain weave’ or ‘taffeta’. The fabric is classified as ‘heavy fabric’ by the textile industry, made of 100% hemp fibres which are usually utilized for technical purposes such as furniture and upholstery; not for apparel and garment purposes. The fibres are spun withw 430 twists per metre. The physical properties of the fabric are as follows in the Table 7.9. WHF chemical composition is given in Table 7.10 which was identified by thermogravimetric analysis.

Table 7.11 shows the thermal properties of WHF which was determined from the thermogravimetric analysis. Table 7.12 shows the mechanical properties of the WHF. All of these properties are important in order to clarify the behaviour of the fabricated composites.

Looking at all the physical properties, WHF was designed to be balanced so it should have similar weight on warp and weft yarn which reflects its fibre distribution in both directions. Thus, it is expected that there should not be a significant difference in mechanical properties of the composites reinforced with this fabric by changing its layering orientation.

Table 7.9 Physical properties of WHF (heavy fabric)

Fabric Types			**Standard Methods/ References**
Weave Structure		Plain/Taffeta	
Fabric Density (per 2cm)	Warp	25	ASTM D3775 [83]
	Weft	23	
Total Fabric Weight (Reading) (g/m^2)		228.520	ASTM D3776 [84]
Total yarn weight (measured) (g/m^2)	Warp	119.813	Section 3.3.2
	Weft	116.859	Section 3.3.2
Total Fabric Weight (Total weight of warp + weft)		236.67	Section 3.3.2
Thickness (mm)		0.417	ASTM D1777 [85]
Yarn Size (Tex)	Warp	90.459	ASTM D1907 [86]
	Weft	92.970	
Yarn Crimp (%)	Warp	6.0	ASTM D3883 [87]
	Weft	9.3	
Density of Fibre (g/cm^3)		1.473	Section 3.3.5
Total Fabric Cover, K		0.663	Section 3.3.6

*Warp – direction of yarn in lengthwise
*Weft – direction of yarn in widthwise

Table 7.10 Chemical composition of WHFs.

WHF composition (%)		**Standard Methods/ References**
Moisture	4.31	Section 3.2.2 Section 3.3.4
Hemicellulose	5.95	
Cellulose	64.77	
Lignin	2.92	
Ash	22.05	

Table 7.11 Thermal properties of woven hemp fibres,

TG Stages	Temperature range (°C)	Weight loss (%)	Major component lost	Maximum mass loss rate (%/°C)	Standard Methods/ References
1st Stage	Room Temp – 120	4.26	Moisture	-	Section 3.2.2
2nd Stage	220 - 400	67.93	Hemicellulose and Cellulose	1.38	
3rd Stage	400 - 458	5.80	Lignin	-	

Table 7.12 Mechanical properties of WHF.

WHF	Peak Load (N)	Tensile Strength (MPa)	Tensile Strain	Tensile Modulus (GPa)	Standard Methods/ References
Warp	415.3±21	21.975±1.11	0.093±0.026	0.530±0.041	ASTM D5034 Section 3.2.5
Weft	469.3±38	24.833±1.99	0.112±0.006	0.493±0.044	

*Warp – direction of yarn in lengthwise
*Weft – direction of yarn in widthwise

7.4.2 Fire Retardant of WHF

The fire retardant chemical applied on the WHF is a commercial flame retardant (FR) grade supplied by Cyndan Chemicals, Australia. This chemical is water-based, not classified as hazardous, and environmental friendly. The FR chemical was applied to the WHF by the dips and nips method.

Tables 7.13 and 7.14 show the burning test (flame spreading under 12 s flame exposure) and thermal properties of untreated (WHF-UT) and FR treated WHF (WHF-FR). These tables shows the differences effect of FR chemical utilisation on the WHF. Since, the FR treated WHF do not burn in the spreading flame test, it is advisable to see the effect of burning under prolonged flame exposure. Table 7.15 shows the characteristic of FR treated WHF under 120 s flame exposure and thus the char formation can be measured.

Table 7.16 shows the limiting oxygen index for both WHF. It is widely used to evaluate the flammability of materials. It shows the minimum amount of oxygen in oxygen–nitrogen mixture required to support complete combustion. The higher the LOI value, the more effective the flame-retardant treatment. Lastly, the mechanical properties of untreated and FR treated WHF are given in Table 7.17. All of tables provided and mentioned above show the effectiveness of FR chemical treatment on

the WHF. Based on all the tables provided, FR chemical treatment is shown to enhance the fire retardant properties of WHF.

Table 7.13 Flame spreading properties of untreated and FR treated WHF.

Sample	1st mark (300 mm)		2nd mark (600 mm)		Horizontal		Burning Rate (cm s^{-1})	Standard Methods/ References
	warp	weft	warp	weft	warp	weft	Vertical	ISO 6491
WHF-UT	22.33 (1.53)	22.25 (1.09)	46.17 (1.04)	50.43 (1.50)	77.08 (1.01)	73.17 (1.04)	1.2-1.3	
WHF-FR	X	X	X	X	X	X	X	

X – Indicates the expected event had not happened.

Table 7.14 Thermal properties of untreated and FR treated WHF.

Sample	Max. temperature of mass loss rate (°C)	Mass loss rate (%/min)	Onset temperature of charring reaction (°C)	Char Yield (%)		Standard Methods/ References
				Charring reaction onset temp.	800°C	
WHF-UT	378.667	0.54	400	19	11	Section 5.2.5
WHF-FR	273.219	0.55	285	53	35	

Table 7.15 Spreading of burnt or char formation for FR treated WHF.

Burnt/Char formation (mm) at 120 s		Char Formation Rate for 120 s (cm s^{-1})	Standard Methods/ References
Width	Height		Section 5.3.4
38 (1.52)	98 (0.91)	0.082	

Table 7.16 Limiting oxygen index.

Samples	LOI	Standard Methods/ References
WHF-UT	18.6	ASTM D2863
WHF-FR	51.0	

Table 7.17 Mechanical properties of treated and FR treated WHF.

Sample		Peak Load (N)	Tensile Strength (MPa)	Tensile Strain at Peak (%)	Tensile Modulus (GPa)	Standard Methods/ References
WHF-UT	Warp	444.440 (13.65)	23.515 (0.72)	6.459 (0.389)	0.590 (0.0098)	ASTM D5034 Section 3.2.5
	Weft	510.88 (8.396)	27.031 (0.448)	11.187 (0.37)	0.621 (0.026)	
WHF-FR	Warp	365.740 (6.395)	19.351 (0.338)	8.323 (0.417)	0.398 (0.026)	
	Weft	394.26 (33.61)	20.860 (1.778)	11.048 (0.647)	0.41263 (0.0100)	

*Figures in bracket indicate standard deviation

7.4.3 WHF Reinforced Vinyl Ester

Composite materials are made of untreated and FR treated WHF which are known in this section as HVE-UT and HVE-FR. Commercial grade vinyl ester resin, SPV 1356 PROM THIX and the catalyst methyl ethyl ketone peroxide (MEKP), NOROX 925H supplied by Nuplex® Composite Industry (Australia) was used in the fabrication.

The ratio of vinyl ester to catalyst is 44:1 by weight. The prepared resin is applied to the WHF ($[0,90]_n$ fabric layering orientation) depends on the desired thickness by employing the hand lay-up technique. A roller is used to gently squeeze out the air trapped after pouring the resin on the fibre. This mixture (wet fabrics) should then laid in between of thick glass plates which are coated with a polymer mould release agent. This assemblage was compressed with a weight placed on top of the mixture to stabilize and remove the excess resin. The entire process should be completed within 40 minutes because the mixture ratio above will take 40 minutes room temperature before the resin starts to solidify. This mixture is then left to cure under room temperature for 24 hours before being post-cured in an oven for four hours at 80°C.

Tables 7.18, 7.19 and 7.20 provide the physical, tensile strength and flexural strength properties of the fabricated composite of HVE-UT and HVE-FR. Whilst Table 7.21, 7.22 and 7.23 provide the burning, thermal and limiting oxygen index properties of the composite made from untreated and FR treated HVE respectively.

Table 7.18 Physical properties of HVE.

Sample	Density (g/cm^3)	Fibres content (wt.%)	Matrix content (wt.%)	Fibres content (vol.%)	Matrix content (vol.%)	Standard Methods/ References
HVE - Untreated	1.10	43.6461	56.36	32.65	60.36	ASTM D3171 test method II
HVE – FR treated	1.21	46.02	53.98	36.3	63.83	

Table 7.19 Tensile Strength Properties.

Composite Types	Tensile Strength (MPa)	Tensile Strain (%)	Tensile Modulus (GPa)	Standard Methods/ References
HVE-UT	61.68 (±1.00)	1.82 (±0.06)	6.20 (±0.23)	ASTM D638
HVE-FR	51.51 (±0.75)	1.59 (±0.07)	5.96 (±0.34)	

Table 7.20 Flexural Strength Properties.

Composite Types	Flexural Strength (MPa)	Flexural Strain (%)	Flexural Modulus (GPa)	Standard Methods/ References
HVE-UT	93.65 (±2.62)	3.00 (±0.20)	5.62 (±0.18)	ASTM D790
HVE-FR	85.20 (±2.14)	3.16 (±0.26)	5.07 (±0.18)	

Table 7.21 Burning characteristic.

Sample Types	1^{st} mark (25 cm) (s)	2^{nd} mark (100 cm) (s)	Smoulder (s)	Total burning (s)	Burning rate (mm/min)	Standard Methods/ References
HVE-UT	38.00	591.33	354.33	983.66	9.53	ASTM D635
HVE-FR	x	x	x	x	x	

X – Indicates that expected event did not occur.

Table 7.22 Thermal properties of HVE-UT and HVE-FR composite.

Samples	1st stage (°C)	Max. temp. of mass loss rate (°C)	2nd stage (°C)	Max. temperature of mass loss rate (°C)	Char Yield (%)		Standard Methods/ References
					Charring reaction onset temp.	800°C	
HVE-UT	255 - 395	376.91	395 – 470	440.17	9.86	5.71	Section 6.3.6
HVE-FR	213 – 297	277.39	297 – 481	444.37	20.48	15.72	

Table 7.23 Limiting oxygen index properties.

Sample	LOI value	Standard Methods/ References
HVE-UT	22.8	ASTM D2863
HVE-FR	29.2	

7.4.4 Properties Degradation to Water of HVE

Degradation on the properties of untreated and FR treated reinforced vinyl ester composite (HVE-UT and HVE-FR) can be evaluated by water absorption and the test was carried out in accordance to BS EN ISO 62:1999. The test specimen's dimension for water absorption should follow the requirements stated in ASTM D638, ASTM D790 and ASTM D635 and then test for their tensile, flexural and burning properties periodically. Tables 7.24 and 7.25 provide the water absorption properties and thickness swelling data for both samples. The relationships between tensile, flexural and burning properties to water absorption percentage are established by regression analysis.

As a guideline for 'regression analysis', it is a type of statistical modelling process for estimating the relationship among the variables. It helps one to understand how the typical value of the dependent variable changes when any one of the independent variables is changed. R-squared (R^2) or in the statistical terminology pronounced as 'coefficient of determination' is a key output of regression analysis. Generally, R^2 is

interpreted as the proportion of the variance in the dependent variable that is predictable from the independent variable and the value ranges from 0 to 1. For instance, the R^2 value of 0.5 means that 50% of the variance in y (from the relationship) is predictable from x. It is common that in linear regression, the R^2 value lower than 0.5 indicates that the model or equation does not possess a good fit. The R^2 value of the 0.5 indicates that the model has a good level of acceptance. Therefore, the higher of R^2 value, the better the data fits the model.

Figure 7.20 to Figure 7.21 and Table 7.26 to Table 7.27 provide the relationships of mechanical properties to water absorption of the HVE-UT and HVE-FR samples. Based on the figures and table, all the mechanical properties are indirectly proportional to water absorption. All the R^2 values are more than 0.5 which indicate that all data have good fit with the each equation.

Figure 7.22 and Figure 7.23 provide the graphical representation of burning rate and limiting oxygen index to water absorption which reflect their relationship in Table 7.28 for HVE-UT and HVE-FR composite materials. Only the burning rate is directly proportional with water absorption. Nevertheless, all the R^2 values are more than 0.5 which indicates that all data have good fit to the each equation. All of these relationships can be used as a guidelines and prediction for the composite material produced from the WHF and vinyl ester.

Table 7.24 Water absorption properties of HVE-UT and HVE-FR.

Sample	Time to saturate (hr)	Sample thickness (mm)	Maximum water uptake, M_m (%)	Diffusion coefficient, D (mm^2/s)
HVE-UT	1848	5.17	3.43	1.45 E-06
HVE-FR	552	5.36	3.28	4.71 E-06

Table 7.25 Results of thickness swelling for HVE-UT and HVE-FR samples.

Sample	Thickness Swelling (%)	
	At the saturation point	At the 2688 hr water immersion
HVE-UT	[a]1.693 (0.629)	[c]2.142 (0.514)
HVE-FR	[b]0.689 (0.287)	[c]1.442 (0.284)

[a] - 1848 hr water immersion
[b] - 552 hr water immersion
* Figures in bracket indicate standard deviation

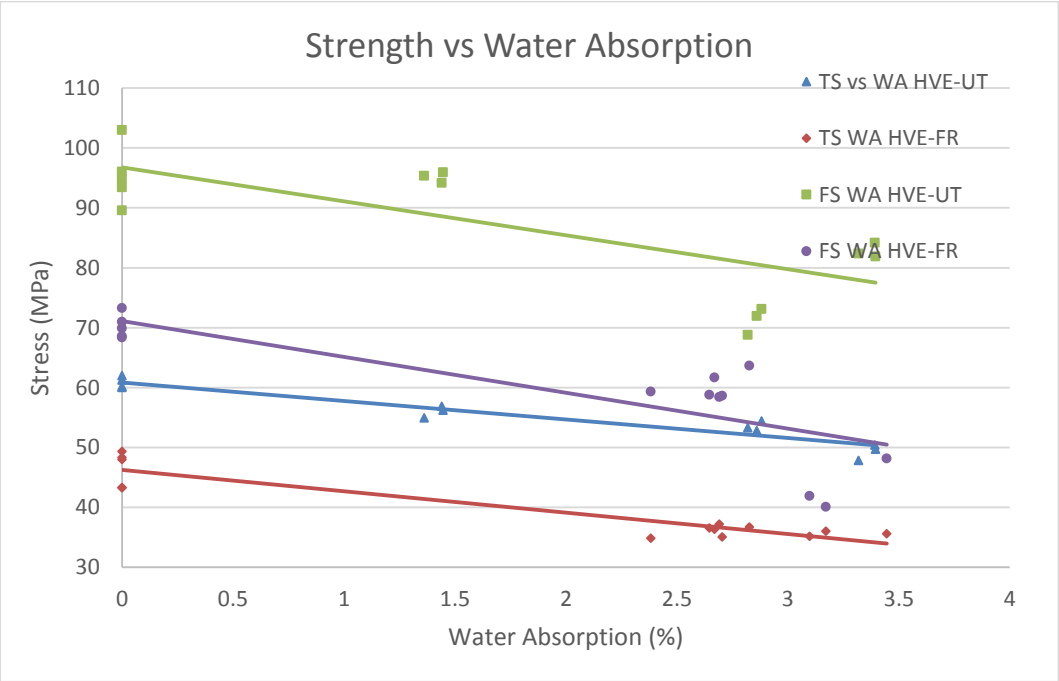

*TS – Tensile strength, FS – Flexural strength, WA – Water absorption

Figure 7.20 Tensile and flexural strengths vs water absorption.

Table 7.26 The relationship of tensile and flexural strength to water absorption of HVE-UT and HVE-FR.

	Sample	Equation	R^2
TS vs WA	HVE-UT	TS = -3.0895WA + 60.859	0.9135
	HVE-FR	TS = -3.5745WA + 46.274	0.873
FS vs WA	HVE-UT	FS = -5.6603WA + 96.762	0.5964
	HVE-FR	FS = -5.9788WA + 71.101	0.6765

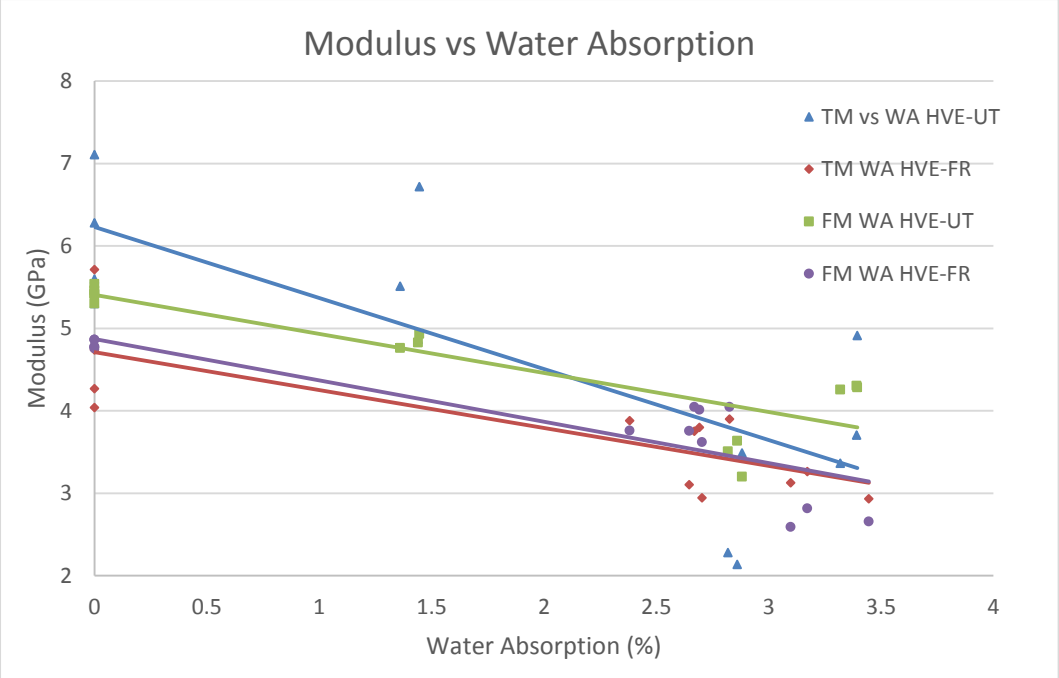

*TM – Tensile Modulus, FM – Flexural Modulus, WA – Water absorption

Figure 7.21 Tensile and flexural modulus vs. Water Absorption

Table 7.27 The relationship of tensile and flexural modulus to water absorption of HVE-UT and HVE-FR.

	Sample	Equation	R^2
TM vs WA	HVE-UT	TM = -0.8616WA + 6.2327	0.5782
	HVE-FR	TM = -0.4592WA + 4.7106	0.6518
FM vs WA	HVE-UT	FM = -0.4738WA + 5.4086	0.7562
	HVE-FR	FM = -0.5016WA + 4.8724	0.7785

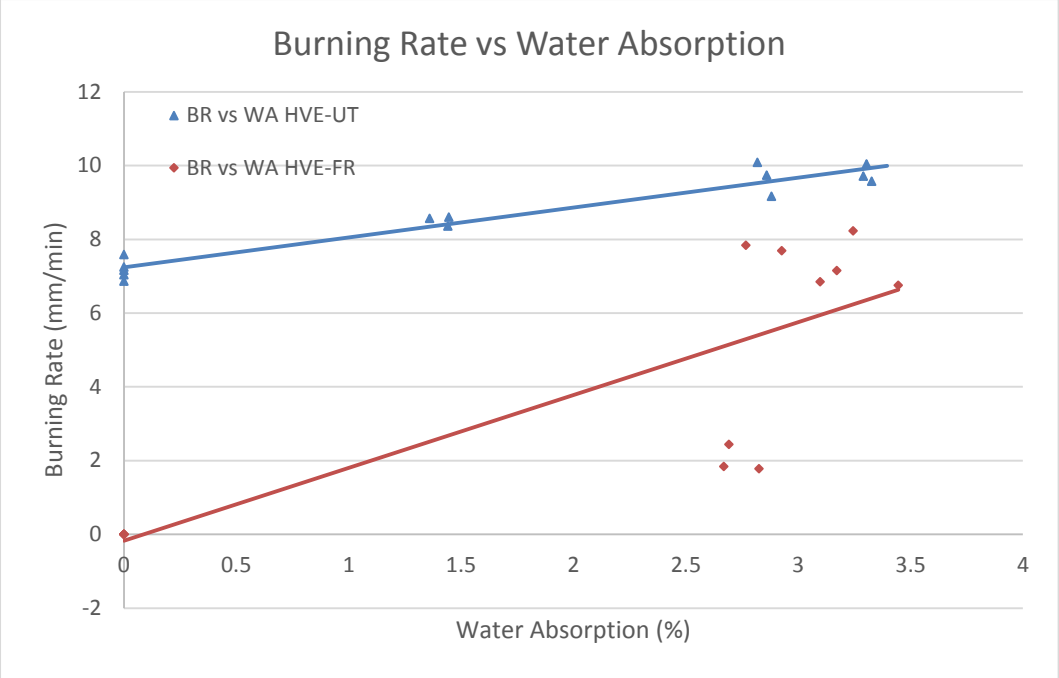

*BR – Burning Rate, WA – Water absorption

Figure 7.22 Burning rate vs. water absorption

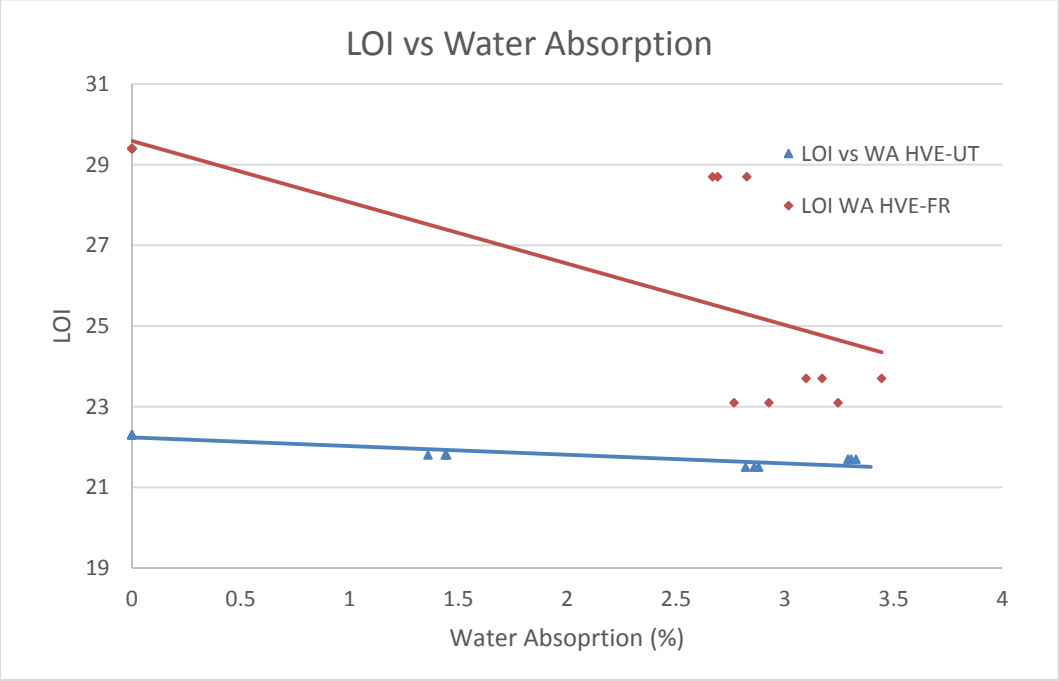

*LOI – Limiting Oxygen Index, WA – Water absorption

Figure 7.23 Limiting Oxygen Index vs. water absorption

Table 7.28 The relationship of burning rate and limiting oxygen index to water absorption of HVE-UT and HVE-FR.

	Sample	Equation	R^2
BR vs WA	HVE-UT	BR = 0.8123WA + 7.2373	0.9407
	HVE-FR	BR = 1.9753WA - 0.1739	0.7037
LOI vs WA	HVE-UT	LOI = -0.2151WA + 22.242	0.8536
	HVE-FR	LOI = -1.5208WA + 29.594	0.5903

7.4.5 Durability

Figure 7.24 and Figure 7.25 provide fatigue strength and normalised stress characteristics of HVE-UT and HVE-FR respectively. Fatigue test for sample HVE-UT and HVE-FR were conducted in accordance with BS ISO 13003:2003, in low cycle tension-tension mode at the stress ratio *(R*) of 0.1 for different stress levels of 50, 60, 70 and 80% of the fabricated composite tensile stress. Data distribution of fatigue stress fit to the power-law model of equation with R^2 value of more than 0.9 (Figure 7.24). The coefficient of fatigue strength, b, provided for both samples in Figure 7.25 shows that the fatigue strength of HVE-UT is similar to HVE-FR.

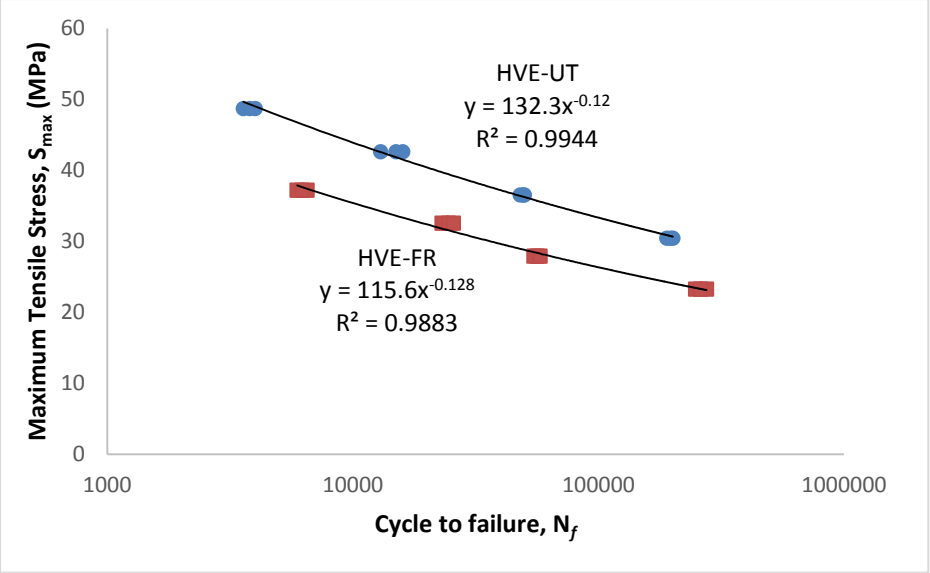

Figure 7.24 Lifetime S–N diagram for samples HVE-UT and HVE-FR.

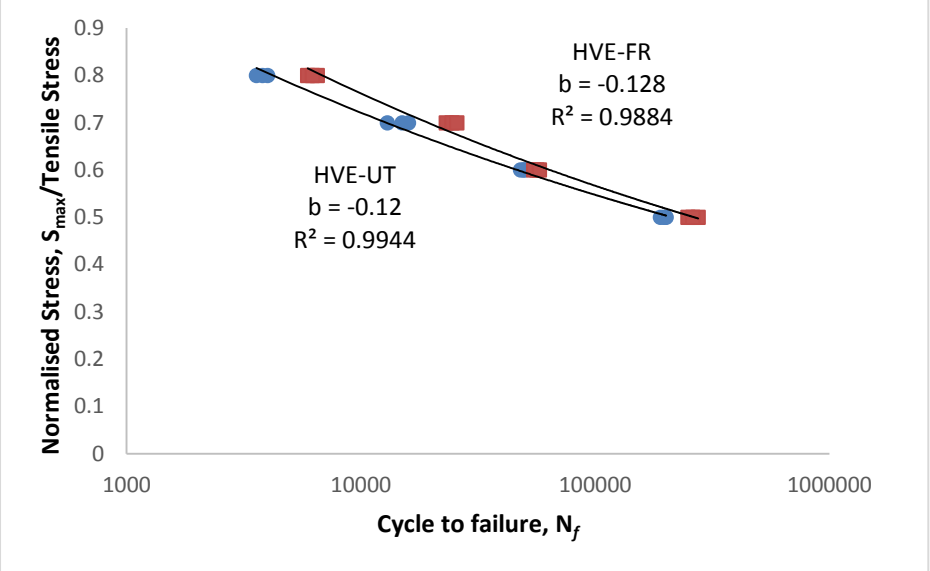

Figure 7.25 Normalised S–N diagram of HVE-UT and HVE-FR.

7.5 Conclusions

The main purpose of this chapter is to investigate the degradation properties of HVE when subjected to water absorption and to analyse the degradation (fastness) of the FR chemical treated WHF composite with the presence of water. In terms of water absorption properties, the maximum water uptake for both HVE-UT and HVE-FR upon the saturation point are 3.43% and 3.27% respectively. The water uptake for both samples can be said to be similar yet the time to reach saturation point for HVE-UT was far longer in comparison with HVE-FR; 848 hr and 552 hr respectively. This is due to several factors in the HVE-FR which are; 1) the swelling of the fibre effects from the FR treatment on the WHF which increased penetration of water via bigger hemp fibre cross-section, and 2) the incompatibility between the hemp fibre treated with FR chemical and vinyl ester resin which creates gaps between fibre and resin, thus increasing the rate of water penetration into the composites. The different rate of water penetration for both samples can be expressed using the diffusion coefficient calculated using Fick's Law which is 4.71E-06 mm^2/s for HVE-FR, far higher than HVE-UT which is 1.45E-06 mm^2/s. The water uptake and diffusion coefficient figures for both samples are lower than wood products. The dimensional stability of HVEs are also better than some natural fibre composites, woods and engineered wood products.

In terms of mechanical properties, for both samples, the presence of water reduced the tensile strength and modulus up to 24% and 39% respectively. The reduction in these properties is due to the penetration of water which weakened the adhesion between the fibres and resin. Another point worth addressing is the greater decline in tensile modulus than tensile strength is due to the plasticisation of water on the vinyl ester and hemp fibres. Similar reasons can be applied on the flexural properties for both

samples since the trend in the cases of flexural and tensile properties is similar. However, the increase in flexural properties after 2688 hr water immersion is due to the swelling of fibres caused by a high amount of water which fill the gaps between the fibre and the matrix. This situation increases the friction between them and eventually increases the resistance of both samples to resist flexural load.

The presence of water in the fabricated composites increases their burning rates thus reducing the Limiting Oxygen Index. The fire retardant properties of sample HVE-FR is reduced as the time of water immersion increases. Using a scanning electron micrograph image, it is proven that the FR sputter on the hemp fibre decreases after 168 hr of immersion and the sputter totally disappears after 840 hr of immersion. The disappearance of sputter from the fibre is due to the migration of the FR chemical from the sample during water immersion. Since the HVE-FR sample has totally lost its fire retardant properties after 840 hr of immersion, it can be said that the durability or fastness of fire retardant chemical treatment on the HVE-FR sample is between 168 hr to 840 hr of water immersion.

In terms of fatigue strength, both samples show a similar fatigue strength coefficient b of 0.12 and 0.128 for HVE-UT and HVE-FR respectively which implies that the fire retardant treatment imparted on the WHF composites did not affect the fatigue strength of the materials. These samples were tested under low load cycle with higher stress level ranging from 50% up to 80%. As suggested by other work that employs low cycle fatigue (at 10^4 cycles) and 50% ultimate strength of the materials, the safety limits for sample HVE-UT and HVE-FR are defined to be 30 and 24MPa respectively.

A ‘material selection guide’ was established for the use of relevant stakeholder when producing WHF to reinforce vinyl ester. The data provided are the characteristics and

properties of WHF, woven hemp `fabric treated with fire retardant chemical, composite made of untreated and FR treated WHF and vinyl ester, degradation of fabricated composites due to water absorption as well as the durability (fatigue) of the fabricated composites. This selection guide is important which can also be related to determination of product life cycle, cost and energy, identification of suitable applications etc.

Chapter 8 Conclusions and Recommendations

8.1 Conclusions

This research has been structured so that it meets several criteria in developing a potential material for infrastructure and building construction material and also answers the objectives of this research. A greater understanding of the effects of fire retardant chemical treatments on woven hemp fabric (WHF) and its composite (HVE) properties have also been achieved in this study.

8.1.1 WHF Characterisation

The WHF characterisation should be done to obtain or verify the data given by the supplier. The methods of characterisation (more accurate and reliable) can also be used to differentiate between two batches of WHF. The measured fabric properties were fabric density, warp and weft yarn size and yarn crimp percentage. From these properties, the weight of fabric can be measured accurately. The weight of WHF was found heavier (ranging from 234.796 to 236.672g/m^2) than the figure given by the supplier (271g/m^2).

Some major chemical composition of hemp fibre were determined using thermogravimetric analysis. The content of cellulose ranged from 64.77 to 67.47%, hemicellulose ranged from 5.95 to 8.46% and lignin ranged from 2.92 to 3.52%. The amount of cellulose and lignin can be used to analyse the densities and mechanical properties between the fabric batches. The yarn crimp percentages ranged from 5.4 to 9.3% depending on the yarn direction and this can be used to explain the tensile strain of the WHF. The total cover factor for the WHF used in this study is 0.66 which means that 66% of the fabric sheets are covered by yarn and it is presumed that the resin could

penetrate the whole fabric system. All these properties are useful in explaining the mechanical behaviour of composites reinforced with WHF.

8.1.2 Effect of the Layering Orientation on the Composite Properties

The utilisation of WHF and its layering orientation do affect its composites due to the slight difference in the properties between warp and weft yarns. The density and fibre volume fraction (1.1g/cm^3 and 33% respectively) are consistent for all HVE samples due to the good fibre distribution in the fabric which can be determined by the weight of the warp (ranging from 118.083g/m^2 to 119.813g/m^2) and weft (ranging from 116.712g/m^2 to 116.859g/m^2) yarns. A composite which has all fabrics layered in the warp direction will have higher tensile properties and the reduction of layer fabric in warp direction will lead to reduce tensile strength due to slightly higher fabric strength in warp rather than weft direction. The flexural strength and modulus for composites also show similar trends with tensile properties. Impact energy is mostly dissipated by the vinyl ester since its volume fraction (60%) is higher than WHF in the composites. Impact strength of fabricated composites is influenced by the loose fibres rather than yarn crimps. The slight difference in weight consequently made the warp have higher loose fibre than weft direction thus energy can be dissipated more effectively in the 0° than 90° direction.

Inferential statistical analyses confirm that the fabric layering orientations affects the tensile, flexural and impact properties, yet the influence of the fabric layering orientation in composite is small and the differences among all the mechanical properties are less than 10%. Therefore, when using this kind of WHF, the fabric can be layered in any orientation. Composites fabricated by $[0, 90]_n$ layer orientation

exhibited better results than the others in terms of balanced mechanical properties in x and y direction.

When comparing WHF to some of woods and engineered wood products properties, shear strength and flexural strength of the fabricated composites were found to be higher and their balanced mechanical properties made the composite even better, much more consistent and stable. This predicts that they can be used as a potential alternative materials for wood products.

8.1.3 Effect of Fire Retardant Treatments on the Fabrics

Utilisation of NaOH, FR chemical and a combination of both (NaOH+FR) improved the fire retardant properties of WHFs, yet the treatments affected the physical properties of the WHFs. The fibre densities increased from 1.47 to 1.53g/cm^3 depending on the treatments and they also shrank within the range of 1.67 to 5% and 0.67 to 3% for warp and weft, respectively. These changes are attributed to the changing physical properties of the fibre. From the fibres' appearance, the fibre cross-section changed from elliptical to a rounder and cleaner surface by NaOH, deposition of particle by FR on the fibre surfaces and salt deposition by the NaOH+FR treatments.

Under the burning test, all the treatments increased fire retardant properties of the WHF. Impregnation of treatments improves the thermal stability (thermogravimetric analysis) of the WHF where the onset of main pyrolysis changed from 220°C to much earlier which is 140°C indicated faster cellulose dehydration and char forming promotion. The char yield at 800°C showed that the treated WHFs possessed higher (ranging from 21 to 40%) char residue than untreated WHF (11%). In terms of LOI, the sample treated with the FR chemical showed the highest value (51) of all the

samples which suggests that this is fire retardant material, followed by sample treated with NaOH+FR (49.4). The lowest value (24.2) was possessed by sample treated with NaOH which was clustered under combustible material.

The treatments reduced the tensile strength of the WHF ranging from 18 to 32% and 23 to 39% for warp and weft respectively due to the elimination and hydrolisation of hemicellulose and lignin during NaOH and FR treatments. The treatments affect the physical properties of WHF by increasing fibre densities and fabric shrinkage. Although the treatments improves the fire retardant properties of WHFs, it can reduce mechanical properties of WHF.

8.1.4 Effect of Fire Retardant Treated WHFs on the Fire Retardant of Their Composites

HVE materials were fabricated utilising WHF (using [0,90] layering orientation) treated with NaOH, FR and a combination of both chemicals (NaOH+FR) to reinforced vinyl ester resin. Characterisations of the physical and mechanical properties were done in order to analyse the effect of the treatments on the fabricated HVEs. The changes of the WHF physical properties especially on the increment of fibre density after treatments influenced the physical and constituent contents of the fabricated HVEs.

SEM micrographs confirmed the mode of failure of HVE that, while the fibres within the yarn ruptured, the yarn pulled-out from the matrix at the failure surface. The mechanical properties of HVEs are decreased after the treatments for several reasons;

(1) the decrement of WHF mechanical properties due to the treatments, and (2) the incompatibility or poor adhesion between the treated fibres and vinyl ester resin.

In the other perspective, the utilisation of treated WHFs increased the fire retardant properties of its composites and this was proven by the enhancement of their thermal stability and the increase in their limiting oxygen index values. The assessment by matching their mechanical properties with common wood products revealed that all treated HVEs were comparable and can be used as a potential alternatives to woods and engineered wood products. HVE sample made of FR treated (FR chemical only) WHF can be said to be the best among all samples considering its good fire retardant ability and acceptable mechanical properties. It is also proven that utilising FR treated WHF as reinforcement in vinyl ester can enhance the fire retardant properties of this composite. This can be an alternative method for producing fire retardant composite materials.

8.1.5 Properties Degradation of HVE to Water Absorption and Fatigue Loading

The water absorption test was selected rather than moisture exposure to imitate the worst scenario for HVE, thus degradation was measured at an extreme level. The comparison is emphasized on the HVE made of untreated (HVE-UT) and FR chemical treated WHF composites (HVE-FR). The maximum water uptake for HVE upon the saturation ranged from 3.27% to 3.43%. However, the time to reach saturation point for HVE-UT was far longer in comparison with HVE-FR due to several factors in HVE-FR which are; (1) the swelling of the fibre effects from the FR treatment on the WHF which increased penetration of water via bigger hemp fibre cross-sections, and (2) the incompatibility between the hemp fibre treated with FR chemical and vinyl

ester resin which creates gaps between fire and resin. The diffusion coefficient calculated using Fick's Law which is 4.71E-06 mm^2/s for HVE-FR far higher than HVE-UT which is 1.45E-06 mm^2/s. However, the water uptake percentage and diffusion coefficient, D, for wood products are higher than present composites which are in the range of 12 to 20% and 0.00001 to 0.0001 mm^2/s respectively.

In terms of mechanical properties, the presence of water reduced the tensile strength and modulus up to 24% and 39% respectively due to the penetration of water which weakened the adhesion between the fibres and the resin. The greater decline in tensile modulus than tensile strength is due to the plasticisation of water on the vinyl ester and hemp fibres. Also, similar factors can be applied to the flexural properties for both samples since its shows quite similar behaviour as tensile properties.

The presence of water in the fabricated composites increased their burning rates thus reduced the Limiting Oxygen Index. The fire retardant properties of sample HVE-FR was reduced as the time of water immersion increased. Since the HVE-FR sample totally lost its fire retardant properties after 840 hr of water immersion, it can be said that the durability or fastness of the fire retardant chemical treatment on the HVE-FR sample is between 168 hr to 840 hr of water immersion.

In terms of fatigue properties, the FR treatment applied to the WHF composites did not affect the fatigue strength of the materials. The fatigue strength coefficient, b, for HVEs are 0.12 and 0.128 for HVE-UT and HVE-FR respectively. As specified by Harik et al. [169], safety limits were defined at the low cycle fatigue at 10^4 cycles and 50% ultimate strength of the HVE-UT and HVE-FR which were 30 and 24MPa respectively. A 'material selection guide' was established and provided for the use of

relevant stakeholders when producing HVE which can be referred to determine the product life cycle, cost and energy, identification of suitable application etc.

In conclusion, it can be highlighted that the mechanical properties of the composite made of vinyl ester and fire retardant treated WHF are comparable and matching with the current properties of woods and engineered wood products and it has the potential to be used in infrastructure and building material. Since the material is a woven fabric, this material can be produced consistently and persistently because the fibres are distributed evenly throughout the fabric. Fire retardant chemical treatment on the fabric not only enhances fire retardant properties of the fabric itself but also its composites. This can be considered as a new and alternative method to produce a fire retardant composite, which is easier and cheaper (using commercial fire retardant chemical). Without any water influence, this material can be categorised as fire retardant material. This material also possesses good fatigue properties at low cycle and it is presumed that it can reach at least 10^5 with extrapolation. The degradation of its properties to water absorption shows that the water uptake is just 3.5% at most. A 'material selection guide' is also provided to facilitate the stakeholders in deciding the suitable applications of this material. Emerging research on natural fibres has been gradually replacing the traditional materials with these ones in many industries such as automotive and building construction. Findings of this research have resulted another competitive replacement for particularly traditional building construction materials.

8.2 Recommendations

The following aspects need to be studied in more detail to further improve the properties of WHF reinforced vinyl ester composites. Some recommendations for future work are proposed:

- It is proven, in this work, that the commercial FR enhances the fire retardant properties of WHF and it composites. However, the appropriate amount of FR chemical imparted on the fabric needs to be detailed so it provides the optimum effect on the mechanical, and fire retardant properties as well as for effective cost
- Since the adhesion between the FR treated WHF with the vinyl ester can be said to be incompatible, a study should be carried out to enhance the compatibility between this treated fabric and resin
- The durability or fastness of the FR treatment on the WHF reinforced vinyl ester were found between 168 hr and 840 hr water immersion. There is a need to study water absorption in detail to reduce the variation of total degradation time for fire retardant properties in this kind of composites
- There should be more study on the environmental degradation behaviours of WHF reinforced vinyl ester such as through outdoor weathering tests. The effect of environmental factors on interface bonding strength needs to be understood through mechanical property analysis. Such environmental factors include moisture resistance, UV index and sunlight
- Properties degradation with respect to moisture absorption should also be undertaken to analyse the degradation level as compared to the water absorption.

References

[1] Bahari SA, Ahmad M, Jamaludin MA, Nordin K, Arifin MI. Potential of Bamboo as an Alternative Raw Material Through Production of Bio-Composite Panelboard for Light Weight Interior Construction Uses. Proceeding, International Panel Products Symposium 2007 (IPPS 2007), United Kingdom. 2007:319-26.
[2] Bahari SA, Ahmad M, Jamaludin MA. Characterization on Bending Bending Strength of Binderless Bamboo Fibreboard (BBF). Proceeding,9th Pacific Rim Bio-Based Composites Symposium 2008. New Zealand: CSIRO and SCION; 2008. p. 238 – 46.
[3] Pandey A, Soccol CR, Nigam P, Soccol VT. Biotechnological potential of agro-industrial residues. I: sugarcane bagasse. Bioresource Technology. 2000;74:69-80.
[4] MTIB. Malaysia Major Import and Export of Timber Products. Malaysian Timber Industry Board; 2015.
[5] Mishra S, Tripathy SS, Misra M, Mohanty AK, Nayak SK. Novel Eco-Friendly Biocomposites: Biofiber Reinforced Biodegradable Polyester Amide Composites—Fabrication and Properties Evaluation. J Reinf Plast Compos. 2002;21:55-70.
[6] Mohanty AK, Khan MA, Hinrichsen G. Surface modification of jute and its influence on performance of biodegradable jute-fabric/Biopol composites. Compos Sci Technol. 2000;60:1115-24.
[7] Nishino T, Hirao K, Kotera M, Nakamae K, Inagaki H. Kenaf reinforced biodegradable composite. Compos Sci Technol. 2003;63:1281-6.
[8] Dhakal HN, Zhang ZY, Bennett N. Influence of fibre treatment and glass fibre hybridisation on thermal degradation and surface energy characteristics of hemp/unsaturated polyester composites. Composites Part B. 2012;43:2757-61.
[9] Satyanarayana KG, Arizaga GGC, Wypych F. Biodegradable composites based on lignocellulosic fibers—An overview. Prog, Polym Sci. 2009;34:982-1021.
[10] Dittenber DB, GangaRao HVS. Critical review of recent publications on use of natural composites in infrastructure. Composites Part A. 2012;43:1419-29.
[11] Misnon MI, Bahari SA, Wan Ahmad WY, Ab Kadir MI, Anuar M. Reinforcement of Textile Fabric in Agricultural Waste Particleboard. in Proceeding 87th Textile Institute World Conference 2010. 2011:408-52.
[12] Misnon MI. Cotton waste for composite reinforcement. Universiti Tekologi MARA, Shah Alam, Selangor, Malaysia: Universiti Teknologi MARA; 2007.
[13] Barkoula NM, Garkhail SK, Peijs T. Biodegradable composites based on flax/polyhydroxybutyrate and its copolymer with hydroxyvalerate. Industrial Crops and Products. 2010;31:34-42.
[14] Bodros E, Pillin I, Montrelay N, Baley C. Could biopolymers reinforced by randomly scattered flax fibre be used in structural applications? Compos Sci Technol. 2007;67:462-70.
[15] Ouagne P, Bizet L, Baley C, Bréard J. Analysis of the Film-stacking Processing Parameters for PLLA/Flax Fiber Biocomposites. J Compos Mater. 2010;44:1201-15.
[16] Goriparthi BK, Suman KNS, Mohan Rao N. Effect of fiber surface treatments on mechanical and abrasive wear performance of polylactide/jute composites. Composites Part A. 2012;43:1800-8.
[17] Ma H, Joo CW. Structure and mechanical properties of jute—polylactic acid biodegradable composites. J Compos Mater. 2011;45:1451-60.
[18] Reddy N, Yang Y. Completely biodegradable soyprotein–jute biocomposites developed using water without any chemicals as plasticizer. Industrial Crops and Products. 2011;33:35-41.

[19] Cyras VP, Vallo C, Kenny JM, Vazquez A. Effect of chemical treatment on the mechanical properties of starch-based blends reinforced with sisal fibre. J Compos Mater. 2004;38:1387-99.
[20] Hu R, Lim J-K. Fabrication and Mechanical Properties of Completely Biodegradable Hemp Fiber Reinforced Polylactic Acid Composites. J Compos Mater. 2007;41:1655-69.
[21] Lopez JP, Vilaseca F, Barberà L, Bayer RJ, Pèlach MA, Mutjé P. Processing and properties of biodegradable composites based on Mater-Bi® and hemp core fibres. Resources, Conservation and Recycling. 2012;59:38-42.
[22] Nam TH, Ogihara S, Tung NH, Kobayashi S. Effect of alkali treatment on interfacial and mechanical properties of coir fiber reinforced poly(butylene succinate) biodegradable composites. Composites Part B. 2011;42:1648-56.
[23] Ibrahim NA, Yunus WMZW, Othman M, Abdan K, Hadithon KA. Poly(Lactic Acid) (PLA)-reinforced Kenaf Bast Fiber Composites: The Effect of Triacetin. J Reinf Plast Compos. 2010;29:1099-111.
[24] Cao Y, Shibata S, Fukumoto I. Mechanical properties of biodegradable composites reinforced with bagasse fibre before and after alkali treatments. Composites Part A. 2006;37:423-9.
[25] Angelov I, Wiedmer S, Evstatiev M, Friedrich K, Mennig G. Pultrusion of a flax/polypropylene yarn. Composites Part A. 2007;38:1431-8.
[26] Huang X, Netravali A. Characterization of flax fiber reinforced soy protein resin based green composites modified with nano-clay particles. Compos Sci Technol. 2007;67:2005-14.
[27] Zhang L, Miao M. Commingled natural fibre/polypropylene wrap spun yarns for structured thermoplastic composites. Compos Sci Technol. 2010;70:130-5.
[28] Kim JT, Netravali AN. Development of aligned-hemp yarn-reinforced green composites with soy protein resin: Effect of pH on mechanical and interfacial properties. Compos Sci Technol. 2011;71:541-7.
[29] George G, Tomlal Jose E, Jayanarayanan K, Nagarajan ER, Skrifvars M, Joseph K. Novel bio-commingled composites based on jute/polypropylene yarns: Effect of chemical treatments on the mechanical properties. Composites Part A. 2012;43:219-30.
[30] Khondker OA, Ishiaku US, Nakai A, Hamada H. A novel processing technique for thermoplastic manufacturing of unidirectional composites reinforced with jute yarns. Composites Part A. 2006;37:2274-84.
[31] Akovali G, Uyanik N. Introduction. In: Akovali G, editor. Handbook of Composite Fabrication. Shropshire, U.K: Rapra Technology Limited; 2001. p. 1-19.
[32] Scardino F. An Introduction to Textile Structures and their Behaviour. Textile Structural Composite. 1989;3:1-26.
[33] Song YS, Lee JT, Ji DS, Kim MW, Lee SH, Youn JR. Viscoelastic and thermal behavior of woven hemp fiber reinforced poly(lactic acid) composites. Composites Part B. 2012;43:856-60.
[34] Misnon MI, Islam MM, Epaarachchi JA, Lau K-t. Potentiality of utilising natural textile materials for engineering composites applications. Mat Des. 2014;59:359-68.
[35] Christian SJ, Billington SL. Mechanical response of PHB- and cellulose acetate natural fiber-reinforced composites for construction applications. Composites Part B. 2011;42:1920-8.
[36] Kabir MM, Wang H, Lau KT, Cardona F, Aravinthan T. Mechanical properties of chemically-treated hemp fibre reinforced sandwich composites. Composites Part B. 2012;43:159-69.

[37] Michel AT, Billington SL. Characterization of poly-hydroxybutyrate films and hemp fiber reinforced composites exposed to accelerated weathering. Polymer Degradation and Stability. 2012;97:870-8.
[38] Dhakal HN, Zhang ZY, Richardson MOW. Effect of water absorption on the mechanical properties of hemp fibre reinforced unsaturated polyester composites. Compos Sci Technol. 2007;67:1674-83.
[39] Akovali G, Kaynak C. Constituent Materials. In: Akovali G, editor. Handbook of Composite Fabrication. Shropshire, U.K: Rapra Technology Limited; 2001. p. 21-57.
[40] Ramezani Kakroodi A, Kazemi Y, Rodrigue D. Mechanical, rheological, morphological and water absorption properties of maleated polyethylene/hemp composites: Effect of ground tire rubber addition. Composites Part B. 2013;51:337-44.
[41] Christian SJ, Billington SL. Moisture diffusion and its impact on uniaxial tensile response of biobased composites. Composites Part B. 2012;43:2303-12.
[42] Yuanjian T, Isaac DH. Impact and fatigue behaviour of hemp fibre composites. Compos Sci Technol. 2007;67:3300-7.
[43] Shahzad A. Effects of alkalization on tensile, impact, and fatigue properties of hemp fiber composites. Polymer Composites. 2012;33:1129-40.
[44] Shah DU, Schubel PJ, Clifford MJ, Licence P. Fatigue life evaluation of aligned plant fibre composites through S–N curves and constant-life diagrams. Compos Sci Technol. 2013;74:139-49.
[45] de Vasconcellos DS, Touchard F, Chocinski-Arnault L. Tension–tension fatigue behaviour of woven hemp fibre reinforced epoxy composite: A multi-instrumented damage analysis. Int J Fatigue. 2013.
[46] Britnell D, Cain R, Tucker N. What are composites? In: Tucker N, Lindsey K, editors. An introduction to automotive composites. United Kingdom: Rapra Technology Ltd.; 2002. p. 9-21.
[47] Rowell RM. Material science of lignocelluosics. In: Caulfield DF, Passaretti JD, Sobczynski SF, editors. Materials interactions relevant to the pulp, paper, and wood industries. Pittsburgh: PA: Material Research Society; 1990. p. 3-9.
[48] Burgueño R, Quagliata MJ, Mohanty AK, Mehta G, Drzal LT, Misra M. Load-bearing natural fiber composite cellular beams and panels. Composites Part A. 2004;35:645-56.
[49] Faruk O, Bledzki AK, Fink H-P, Sain M. Biocomposites reinforced with natural fibers: 2000–2010. Prog, Polym Sci. 2012;37:1552-96.
[50] Wambua P, Ivens J, Verpoest I. Natural fibres: can they replace glass in fibre reinforced plastics? Compos Sci Technol. 2003;63:1259-64.
[51] Long AC. Introduction. In: Long AC, editor. Desgin and manufacture of textile composites. England: CRC Press, Woodhead Publishing Ltd, Cambridge; 2005.
[52] Lomov SV, Verpoest I, Robitaille F. Manufacturing and internal geometry of textiles. In: Long AC, editor. Design and Manufacture of Textile Composites CRC Press, Woodhead Publishing Ltd, Cambridge, England; 2005. p. 1-61.
[53] Kadolph SJ, Langford AL. Textiles. 9th ed. New Jersey:: Prentice Hall; 2001.
[54] Anonymous. Textile Handbook. Hong Kong: The Hong Kong Cotton Spinners Association and 2001.
[55] Reddy N, Yang Y. Novel green composites using zein as matrix and jute fibers as reinforcement. Biomass and Bioenergy. 2011;35:3496-503.
[56] Di Bella G, Fiore V, Valenza A. Effect of areal weight and chemical treatment on the mechanical properties of bidirectional flax fabrics reinforced composites. Mat Des. 2010;31:4098-103.

[57] Jawaid M, Abdul Khalil HPS, Hassan A, Dungani R, Hadiyane A. Effect of jute fibre loading on tensile and dynamic mechanical properties of oil palm epoxy composites. Composites Part B. 2013;45:619-24.
[58] Sever K, Sarikanat M, Seki Y, Erkan G, Erdoğan ÜH, Erden S. Surface treatments of jute fabric: The influence of surface characteristics on jute fabrics and mechanical properties of jute/polyester composites. Industrial Crops and Products. 2012;35:22-30.
[59] Behera AK, Avancha S, Basak RK, Sen R, Adhikari B. Fabrication and characterizations of biodegradable jute reinforced soy based green composites. Carbohydrate Polymers. 2012;88:329-35.
[60] Lei W, Lei W-g, Ren C. Effect of volume fraction of ramie cloth on physical and mechanical properties of ramie cloth/UP resin composite. Transactions of Nonferrous Metals Society of China. 2006;16, Supplement 2:s474-s7.
[61] Porras A, Maranon A. Development and characterization of a laminate composite material from polylactic acid (PLA) and woven bamboo fabric. Composites Part B. 2012;43:2782-8.
[62] Asumani OML, Reid RG, Paskaramoorthy R. The effects of alkali–silane treatment on the tensile and flexural properties of short fibre non-woven kenaf reinforced polypropylene composites. Composites Part A. 2012;43:1431-40.
[63] Ogin LS. Textile-reinforced composite materials. In: Horrocks AR, Anand SC, editors. Handbook of Technical Textiles. North and South America: Woodhead Publishing Limited, The Textile Institute; 2000. p. 264-81.
[64] Bledzki AK, Gassan J. Composites reinforced with cellulose based fibres. Prog, Polym Sci. 1999;24:221-74.
[65] John MJ, Thomas S. Biofibres and biocomposites. Carbohydrate Polymers. 2008;71:343-64.
[66] Abdul Khalil HPS, Bhat AH, Ireana Yusra AF. Green composites from sustainable cellulose nanofibrils: A review. Carbohydrate Polymers. 2012;87:963-79.
[67] Azwa ZN, Yousif BF, Manalo AC, Karunasena W. A review on the degradability of polymeric composites based on natural fibres. Mat Des. 2013;47:424-42.
[68] Stankovich S, Dikin DA, Dommett GHB, Kohlhaas KM, Zimney EJ, Stach EA, et al. Graphene-based composite materials. Nature. 2006;442:282-6.
[69] Bledzki AK, Mamun AA, Volk J. Barley husk and coconut shell reinforced polypropylene composites: The effect of fibre physical, chemical and surface properties. Compos Sci Technol. 2010;70:840-6.
[70] Chilton J, Velasco R. Applications of textile composites in the construction industry. In: Long AC, editor. Design and manufacture of textile composites. England: CRC Press, Woodhead Publishing Ltd Cambridge; 2005. p. 424-35.
[71] Hollaway LC. A review of the present and future utilisation of FRP composites in the civil infrastructure with reference to their important in-service properties. Construction and Building Materials. 2010;24:2419-45.
[72] Netravali AN, Huang X, Mizuta K. Advanced 'green' composites. Adv Compos Mater. 2007;16:269-82.
[73] Kretschmann DE. Mechanical properties of wood. wood handbook: Forests Product Laboratory; 2010. p. 1-46.
[74] Dorez G, Taguet A, Ferry L, Lopez-Cuesta JM. Thermal and fire behavior of natural fibers/PBS biocomposites. Polymer Degradation and Stability. 2013;98:87-95.
[75] Kandare E, Luangtriratana P, Kandola BK. Fire reaction properties of flax/epoxy laminates and their balsa-core sandwich composites with or without fire protection. Composites Part B. 2014;56:602-10.

[76] Lazko J, Landercy N, Laoutid F, Dangreau L, Huguet MH, Talon O. Flame retardant treatments of insulating agro-materials from flax short fibres. Polymer Degradation and Stability. 2013;98:1043-51.
[77] Shukor F, Hassan A, Saiful Islam M, Mokhtar M, Hasan M. Effect of ammonium polyphosphate on flame retardancy, thermal stability and mechanical properties of alkali treated kenaf fiber filled PLA biocomposites. Mat Des. 2014;54:425-9.
[78] Xu JZ, Gao M, Guo HZ, Liu XL, Li Z, Wang H, et al. Study on the Thermal Degradation of Cellulosic Fibers Treated with Flame Retardants. Journal of Fire Sciences. 2002;20:227-35.
[79] Kamath MG, Bhat GS, Parikh DV, Condon BD. Processing and Characterization of Flame Retardant Cotton Blend Nonwovens for Soft Furnishings to Meet Federal Flammability Standards. Journal of Industrial Textiles. 2009;38:251-62.
[80] Shahzad A. Effects of water absorption on mechanical properties of hemp fiber composites. Polymer Composites. 2012;33:120-8.
[81] Liang S, Gning PB, Guillaumat L. A comparative study of fatigue behaviour of flax/epoxy and glass/epoxy composites. Compos Sci Technol. 2012;72:535-43.
[82] Sondhelm WS. Technical fabric structures – 1. Woven fabrics. In: Horrocks AR, Anand SC, editors. Handbook of Technical Textiles. North and South America: Woodhead Publishing Limited & The Textile Institute; 2000.
[83] ASTM D3775-12. Standard Test Method for Warp (End) and Filling (Pick) Count of Woven Fabrics. ASTM International, West Conshohocken, PA; 2012.
[84] ASTM D3776 / D3776M-09a(2013). Standard Test Methods for Mass Per Unit Area (Weight) of Fabric. ASTM International, West Conshohocken, PA; 2013.
[85] ASTM D1777-96(2011)e1. Standard Test Method for Thickness of Textile Materials. ASTM International, West Conshohocken, PA; 2011.
[86] ASTM D1907 / D1907M-12. Standard Test Method for Linear Density of Yarn (Yarn Number) by the Skein Method. ASTM International, West Conshohocken, PA; 2012.
[87] ASTM D3883-04(2012). Standard Test Method for Yarn Crimp and Yarn Take-up in Woven Fabrics. ASTM International, West Conshohocken, PA; 2012.
[88] Yahya MF, Salleh J, Ahmad WYW. Uniaxial failure resistance of square-isotropic 3D woven fabric modelled with finite element analysis. Business, Engineering and Industrial Applications (ISBEIA), 2011 IEEE Symposium on2011. p. 16-21.
[89] Süle G. Investigation of bending and drape properties of woven fabrics and the effects of fabric constructional parameters and warp tension on these properties. Textile Research Journal. 2012;82:810-9.
[90] Chen X, Leaf GAV. Engineering Design of Woven Fabrics for Specific Properties. Textile Research Journal. 2000;70:437-42.
[91] Ishak MR, Sapuan SM, Leman Z, Rahman MZA, Anwar UMK. Characterization of sugar palm (Arenga pinnata) fibres. J Therm Anal Calorim. 2012;109:981-9.
[92] Yang H, Yan R, Chen H, Lee DH, Zheng C. Characteristics of hemicellulose, cellulose and lignin pyrolysis. Fuel. 2007;86:1781-8.
[93] Madsen B, Hoffmeyer P, Thomsen AB, Lilholt H. Hemp yarn reinforced composites – I. Yarn characteristics. Composites Part A. 2007;38:2194-203.
[94] Kabir MM, Wang H, Lau KT, Cardona F. Effects of chemical treatments on hemp fibre structure. Applied Surface Science. 2013;276:13-23.
[95] Hakamy A, Shaikh FUA, Low IM. Thermal and mechanical properties of hemp fabric-reinforced nanoclay–cement nanocomposites. J Mater Sci. 2014;49:1684-94.

[96] Wang HM, Postle R, Kessler RW, Kessler W. Removing Pectin and Lignin During Chemical Processing of Hemp for Textile Applications. Textile Research Journal. 2003;73:664-9.
[97] Le Troedec M, Sedan D, Peyratout C, Bonnet JP, Smith A, Guinebretiere R, et al. Influence of various chemical treatments on the composition and structure of hemp fibres. Composites Part A. 2008;39:514-22.
[98] Bismarck A, Aranberri-Askargorta I, Springer J, Lampke T, Wielage B, Stamboulis A, et al. Surface characterization of flax, hemp and cellulose fibers; Surface properties and the water uptake behavior. Polymer Composites. 2002;23:872-94.
[99] Sedan D, Pagnoux C, Smith A, Chotard T. Mechanical properties of hemp fibre reinforced cement: Influence of the fibre/matrix interaction. Journal of the European Ceramic Society. 2008;28:183-92.
[100] Ambroziak A, Kłosowski P. Mechanical testing of technical woven fabrics. J Reinf Plast Compos. 2013;32:726-39.
[101] ASTM D792-13. Standard Test Methods for Density and Specific Gravity (Relative Density) of Plastics by Displacement. ASTM International, West Conshohocken, PA; 2013.
[102] ASTM D3171-11. Standard Test Methods for Constituent Content of Composite Materials. ASTM International, West Conshohocken, PA; 2011.
[103] ASTM D638-10. Standard Test Method for Tensile Properties of Plastics. 2010.
[104] ASTM D790-10. Standard Test Methods for Flexural Properties of Unreinforced and Reinforced Plastics and Electrical Insulating Materials. ASTM International, West Conshohocken, PA; 2010.
[105] ASTM D256-10. Standard Test Methods for Determining the Izod Pendulum Impact Resistance of Plastics. ASTM International, West Conshohocken, PA; 2010.
[106] Albdiry MT, Ku H, Yousif BF. Impact fracture behaviour of silane-treated halloysite nanotubes-reinforced unsaturated polyester. Eng Fail Anal. 2013;35:718-25.
[107] Misnon MI, Islam MM, Epaarachchi JA, Lau KT. Analyses of woven hemp fabric characteristics for composite reinforcement. Mat Des. 2015;66, Part A:82-92.
[108] Khalfallah M, Abbès B, Abbès F, Guo YQ, Marcel V, Duval A, et al. Innovative flax tapes reinforced Acrodur biocomposites: A new alternative for automotive applications. Mat Des. 2014;64:116-26.
[109] Madsen B, Hoffmeyer P, Lilholt H. Hemp yarn reinforced composites – II. Tensile properties. Composites Part A. 2007;38:2204-15.
[110] Summerscales J, Dissanayake N, Virk A, Hall W. A review of bast fibres and their composites. Part 2 – Composites. Composites Part A. 2010;41:1336-44.
[111] Santhosh J, Balanarasimman N, Chandrasekar R, Raja S. STUDY OF PROPERTIES OF BANANA FIBER REINFORCED COMPOSITES. 2014.
[112] Kim HJ, Seo DW. Effect of water absorption fatigue on mechanical properties of sisal textile-reinforced composites. Int J Fatigue. 2006;28:1307-14.
[113] Rassmann S, Paskaramoorthy R, Reid RG. Effect of resin system on the mechanical properties and water absorption of kenaf fibre reinforced laminates. Mat Des. 2011;32:1399-406.
[114] Muralidhar B, Giridev V, Raghunathan K. Flexural and impact properties of flax woven, knitted and sequentially stacked knitted/woven preform reinforced epoxy composites. J Reinf Plast Compos. 2012;31:379-88.

[115] Rodriguez ES, Stefani PM, Vazquez A. Effects of Fibers' Alkali Treatment on the Resin Transfer Molding Processing and Mechanical Properties of Jute—Vinylester Composites. J Compos Mater. 2007;41:1729-41.
[116] Misnon MI, Bahari SA, Wan Ahmad WY, Ab Kadir MI, Atiyyah M. The mechanical properties of textile fabrics reinforced hybrid composites. Science and Social Research (CSSR), 2010 International Conference: IEEE; 2010. p. 809-14.
[117] Bax B, Müssig J. Impact and tensile properties of PLA/Cordenka and PLA/flax composites. Compos Sci Technol. 2008;68:1601-7.
[118] Mishra S, Mohanty AK, Drzal LT, Misra M, Parija S, Nayak SK, et al. Studied on Mechanical Performance of Biofibre/Glass reinforced Polyester Hybrid Composites. Compos Sci Technol. 2003;63:1377-85.
[119] Hurd MK. Formwork for concrete. American Concrete Institute; 2005.
[120] ASTM D245-06(2011). Standard Practice for Establishing Structural Grades and Related Allowable Properties for Visually Graded Lumber. ASTM International, West Conshohocken, PA; 2011.
[121] Green DW, Winandy JE, Kretschmann DE. Wood handbook—Wood as an engineering material. Gen Tech Rep FPL–GTR–113. Madison, WI: U.S. Department of Agriculture, Forest Service, Forest Products Laboratory; 1999.
[122] Thomas W. Concentrated Load Capacity and Stiffness of Oriented Strand Board: Calculation versus Test. Journal of Structural Engineering. 2002;128:908-12.
[123] Issa CA, Kmeid Z. Advanced wood engineering: glulam beams. Construction and Building Materials. 2005;19:99-106.
[124] Shafizadeh F, Chin PS, DeGroot WF. Mechanistic Evaluation of Flame Retardants. Fire Retardant Chemistry. 1975;2:195-203.
[125] Mostashari SM, Nia YK, Fayyaz F. Thermogravimetry of deposited caustic soda used as a flame-retardant for cotton fabric. J Therm Anal Calorim. 2008;91:237-41.
[126] Chen Y, Frendi A, Tewari SS, Sibulkin M. Effects of fire retardant addition on the combustion properties of a charring fuel. Fire Safety Sciences. 1991;3:527-36.
[127] Zhu P, Sui S, Wang B, Sun K, Sun G. A study of pyrolysis and pyrolysis products of flame-retardant cotton fabrics by DSC, TGA, and PY–GC–MS. Journal of Analytical and Applied Pyrolysis. 2004;71:645-55.
[128] Brancatelli G, Colleoni C, Massafra MR, Rosace G. Effect of hybrid phosphorus-doped silica thin films produced by sol-gel method on the thermal behavior of cotton fabrics. Polymer Degradation and Stability. 2011;96:483-90.
[129] Försth M, Modin H, Sundström B. A comparative study of test methods for assessment of fire safety performance of bus interior materials. Fire and Materials. 2013;37:350-7.
[130] Rossi RM, Bruggmann G, Stämpfli R. Comparison of flame spread of textiles and burn injury prediction with a manikin. Fire and Materials. 2005;29:395-406.
[131] Grgac SF, Lozo B, Banić D. Flame retardancy of paper obtained with environmentally friendly agents. Fibres & Textiles in Eastern Europe. 2009;17:74.
[132] Cireli A, Onar N, Ebeoglugil MF, Kayatekin I, Kutlu B, Culha O, et al. Development of flame retardancy properties of new halogen-free phosphorous doped SiO2 thin films on fabrics. Journal of Applied Polymer Science. 2007;105:3748-56.
[133] Hu J. Structure and mechanics of woven fabrics. North America: Published by Woodhead Publishing Limited in association with The Textile Institute, Woodhead Publishing Ltd; 2004.
[134] Zugenmaier P. Cellulose. Crystalline Cellulose and Derivatives: Characterization and Structures. 2008:101-74.

[135] Alongi J, Carosio F, Malucelli G. Influence of ammonium polyphosphate-/poly(acrylic acid)-based layer by layer architectures on the char formation in cotton, polyester and their blends. Polymer Degradation and Stability. 2012;97:1644-53.
[136] Lam YL, Kan CW, Yuen CWM. Flame-retardant finishing in cotton fabrics using zinc oxide co-catalyst. Journal of Applied Polymer Science. 2011;121:612-21.
[137] Anderson CE, Ketchum DE, Mountain WP. Thermal conductivity of intumescent chars. Journal of Fire Sciences. 1988;6:390-410.
[138] Camino G, Costa L, Casorati E, Bertelli G, Locatelli R. The oxygen index method in fire retardance studies of polymeric materials. Journal of Applied Polymer Science. 1988;35:1863-76.
[139] De AK. A text book of inorganic chemistry: New Age International; 2007.
[140] Uppal R, Bhat G, Akato K, Parikh DV, Nam S, Condon B. Flame retardant antibacterial cotton high-loft nonwoven fabrics. Journal of Industrial Textiles. 2012;41:281-91.
[141] Troitzsch JH. Overview of flame retardants. Chemistry today. 1998;16.
[142] Kandola B, Horrocks A, Price D, Coleman G. Flame-retardant treatments of cellulose and their influence on the mechanism of cellulose pyrolysis. Journal of Macromolecular Science, Part C: Polymer Reviews. 1996;36:721-94.
[143] Yang CQ, Weishu Wei, Lickfield GC. Mechanical Strength of Durable Press Finished Cotton Fabric: Part III: Change in Cellulose Molecular Weight. Textile Research Journal. 2000;70:910-5.
[144] Horrocks AR. Flame retardant challenges for textiles and fibres: New chemistry versus innovatory solutions. Polymer Degradation and Stability. 2011;96:377-92.
[145] Zhang J, Zhang J, Lin L, Chen T, Zhang J, Liu S, et al. Dissolution of microcrystalline cellulose in phosphoric acid—Molecular changes and kinetics. Molecules. 2009;14:5027-41.
[146] Mwaikambo LY, Ansell MP. Chemical modification of hemp, sisal, jute, and kapok fibers by alkalization. Journal of Applied Polymer Science. 2002;84:2222-34.
[147] Shumao L, Jie R, Hua Y, Tao Y, Weizhong Y. Influence of ammonium polyphosphate on the flame retardancy and mechanical properties of ramie fiber-reinforced poly (lactic acid) biocomposites. Polymer International. 2010;59:242-8.
[148] Jeencham R, Suppakarn N, Jarukumjorn K. Effect of flame retardants on flame retardant, mechanical, and thermal properties of sisal fiber/polypropylene composites. Composites Part B. 2014;56:249-53.
[149] Duquesne S, Samyn F, Ouagne P, Bourbigot S. Flame retardancy and mechanical properties of flax reinforced woven for composite applications. Journal of Industrial Textiles. 2015;44:665-81.
[150] Zhang K, Gong Y, Niu P, Wang X, Yang J. Properties of polypropylene/hemp fibers flame retardant composites: Effects of different processing methods. J Reinf Plast Compos. 2013.
[151] Ehsani M, Khonakdar HA, Ghadami A. Assessment of morphological, thermal, and viscoelastic properties of epoxy vinyl ester coating composites: Role of glass flake and mixing method. Progress in Organic Coatings. 2013;76:238-43.
[152] Alhuthali A, Low IM, Dong C. Characterisation of the water absorption, mechanical and thermal properties of recycled cellulose fibre reinforced vinyl-ester eco-nanocomposites. Composites Part B. 2012;43:2772-81.
[153] Chapple S, Anandjiwala R. Flammability of Natural Fiber-reinforced Composites and Strategies for Fire Retardancy: A Review. Journal of Thermoplastic Composite Materials. 2010;23:871-93.

[154] Azwa ZN, Yousif BF, Manalo AC, Karunasena W. A review on the degradability of polymeric composites based on natural fibres. Mat Des. 2013;47:424-42.
[155] Karmaker AC, Hoffmann A, Hinrichsen G. Influence of water uptake on the mechanical properties of jute fiber-reinforced polypropylene. Journal of Applied Polymer Science. 1994;54:1803-7.
[156] Suriyamongkol P, Weselake R, Narine S, Moloney M, Shah S. Biotechnological approaches for the production of polyhydroxyalkanoates in microorganisms and plants — A review. Biotechnology Advances. 2007;25:148-75.
[157] Dan-mallam Y, Hong TW, Abdul Majid MS. Mechanical Characterization and Water Absorption Behaviour of Interwoven Kenaf/PET Fibre Reinforced Epoxy Hybrid Composite. International Journal of Polymer Science. 2015;2015.
[158] Hargitai H, Rácz I, Anandjiwala RD. Development of HEMP Fiber Reinforced Polypropylene Composites. Journal of Thermoplastic Composite Materials. 2008;21:165-74.
[159] Medved S, Diporovic-Momcilovic M, Popovic M, Antonovic A, Jembrekovic V. Dimensional stability of particleboards. First Serbian Forestry Congress-Future with Forests2011. p. 1538.
[160] Papadopoulos NA, Traboulay E. Dimensional stability of OSB made from acetylated Fir strands. Holz als Roh- und Werkstoff.60:84-7.
[161] Zhang Y, Zhang SY, Yang DQ, Wan H. Dimensional stability of wood–polymer composites. Journal of Applied Polymer Science. 2006;102:5085-94.
[162] Horrocks AR, Kandola BK, Davies PJ, Zhang S, Padbury SA. Developments in flame retardant textiles – a review. Polymer Degradation and Stability. 2005;88:3-12.
[163] Wu W, Yang CQ. Comparison of different reactive organophosphorus flame retardant agents for cotton. Part II: Fabric flame resistant performance and physical properties. Polymer Degradation and Stability. 2007;92:363-9.
[164] Wu W, Yang CQ. Comparison of different reactive organophosphorus flame retardant agents for cotton: Part I. The bonding of the flame retardant agents to cotton. Polymer Degradation and Stability. 2006;91:2541-8.
[165] Baysal E, Sonmez A, Colak M, Toker H. Amount of leachant and water absorption levels of wood treated with borates and water repellents. Bioresource technology. 2006;97:2271-9.
[166] Yew MC, Ramli Sulong NH, Yew MK, Amalina MA, Johan MR. Fire Propagation Performance of Intumescent Fire Protective Coatings Using Eggshells as a Novel Biofiller. The Scientific World Journal. 2014;2014:9.
[167] Gérard C, Fontaine G, Bourbigot S. New trends in reaction and resistance to fire of fire-retardant epoxies. Materials. 2010;3:4476-99.
[168] Baets J, Plastria D, Ivens J, Verpoest I. Determination of the optimal flax fibre preparation for use in UD flax-epoxy composites. 2011.
[169] Harik VM, Klinger JR, Bogetti TA. Low-cycle fatigue of unidirectional composites:: Bi-linear S–N curves. Int J Fatigue. 2002;24:455-62.
[170] Abdullah AH, Alias SK, Jenal N, Abdan K, Ali A. Fatigue behavior of kenaf fibre reinforced epoxy composites. Engineering Journal. 2012;16:105-14.

Appendix

Appendix A

Fabric Parameter Results

The details of fabric parameter results which were discussed in Chapter 3 are given here as an example of measurement executions for all fabric characterisation in this research.

Fabric Density

Density of warp or weft yarns in 2 cm.

Fabric A

Specimen	Warp	Weft
1	25	22
2	26	23
3	25	23
4	25	23
5	26	23
6	26	23
7	26	23
8	25	23
9	25	23
10		
Average	25.444	22.888
Stdev	0.527	0.333

Fabric B

Specimen	Warp	Weft
1	25	23
2	26	23
3	25	23
4	25	23
5	26	23
6	25	23
7	25	23
8	25	23
9	25	23
10	25	23
Average	25.2	23

Stdev	0.421637021	0

Fabric Weight

The weight of fabric in g/m^2.

Fabric A

Specimen	Fabric Weight (g/m^2)
1	231.86
2	234.74
3	229.41
4	230.6
5	230.43
Average	231.408
Stdev	2.056

Fabric B

Specimen	Fabric Weight (g/m2)
1	228.3
2	227.64
3	229.2
4	229.15
5	228.33
Average	228.524
Stdev	0.655

Yarn Crimp

The result in the table below shows the value after stretching in centimeter.

Fabric A

Specimen	Warp	Weft
1	21	22
2	21	21.6
3	21.2	21.8
4	21	21.9
5	21	21.8
6	21.1	21.9
7	21	21.8
8	21.22	21.9
9	21.1	21.9
10	21.1	21.9
Average	21.072	21.85
Stdev	0.0859	0.108

Fabric B

Specimen	Warp	Weft
1	21.22	21.8
2	21.3	21.7
3	21.2	21.9
4	21.3	21.9
5	21.4	21.8
6	21.2	21.8
7	21.1	21.9
8	21.1	21.8
9	21	21.9
10	21.1	22.1
Average	21.192	21.86
Stdev	0.120	0.107

Fabric Strength

The details of the fabric strength results discussed in Chapter 3 are presented here as an example for fabric tensile test execution done in all respective chapters.

Fabric A

Warp

Specimen	Load (N)	Stress (MPa)	Strain (%)	Ten. Modulus (GPa)
1	398.200	21.069	0.068	0.533
2	408.400	21.608	0.069	0.523
3	442.800	23.429	0.073	0.532
4	423.400	22.402	0.079	0.506
5	443.100	23.444	0.075	0.536
6	494.100	26.143	0.077	0.594
7	447.000	23.651	0.076	0.530
8	432.600	22.889	0.075	0.542
9	472.800	25.016	0.076	0.556
10	458.600	24.265	0.072	0.549
Average	442.100	23.392	0.074	0.540
Stdev	28.765	1.522	0.004	0.023

Weft

Specimen	Load (N)	Stress (MPa)	Strain (%)	Ten. Modulus (GPa)
1	361.300	19.116	0.109	0.445
2	468.000	24.762	0.112	0.511
3	465.600	24.635	0.118	0.523
4	526.400	27.852	0.140	0.541
5	521.900	27.614	0.120	0.537
6	503.500	26.640	0.120	0.513
7	545.000	28.836	0.121	0.509
8	562.400	29.757	0.119	0.553
9	502.400	26.582	0.122	0.497

10	515.000	27.249	0.126	0.476
Average	497.150	26.304	0.121	0.510
Stdev	56.472	2.988	0.008	0.032

Fabric B

Warp

Specimen	Load (N)	Stress (MPa)	Strain (%)	Ten. Modulus (GPa)
1	423.000	22.381	0.077	0.473
2	403.500	21.349	0.074	0.485
3	425.700	22.524	0.073	0.506
4	428.300	22.661	0.071	0.568
5	409.900	21.688	0.069	0.541
6	404.400	21.397	0.066	0.553
7	429.900	22.746	0.120	0.566
8	423.300	22.397	0.111	0.561
9	442.600	23.418	0.120	0.588
10	414.900	21.952	0.138	0.473
11	363.100	19.212	0.107	0.52
AVERAGE	415.327	21.975	0.093	0.530
STDEV	20.907	1.106	0.026	0.041

Weft

Specimen	Load (N)	Stress (MPa)	Strain (%)	Ten. Modulus (GPa)
1	499.700	26.439	0.112	0.527
2	467.200	24.720	0.107	0.518
3	523.600	27.704	0.116	0.494
4	482.900	25.550	0.102	0.535
5	502.800	26.603	0.122	0.529
6	409.600	21.672	0.115	0.416
7	421.300	22.291	0.113	0.424
8	453.600	24.000	0.113	0.505
9	463.400	24.519	0.109	0.491

Average	469.344	24.833	0.112	0.493
Stdev	37.639	1.991	0.006	0.044

Appendix B

Detail results on hemp fabric reinforced vinyl ester tensile, flexural, impact and selected shear strengths discussed in Chapter 4, as an example for tensile test execution for all related chapters in this research.

Tensile Strength Results

HVE[0]

Sample	Peak Load (N)	Tensile Strain (%)	Tensile Strength (Mpa)	Tensile Modulus (Gpa)
1	8469.200	2.080	71.670	7.310
2	8124.200	1.700	68.806	7.668
3	8683.700	2.210	73.545	6.335
4	8356.3	2.11	67.988	6.381
5	8350.7	2.09	68.246	6.475
6	6851.500	1.930	58.024	6.319
7	8027.500	1.930	67.960	6.242
8	6998.900	1.890	58.571	7.411
9	8610.300	2.050	72.771	7.086
10	8469.200	2.080	71.670	7.310
Average	8029.313	2.054	68.892	6.960
Stdev	718.209	0.123	5.512	0.571

HVE[90]

Sample	Peak Load (N)	Tensile Strain (%)	Tensile Strength (Mpa)	Tensile Modulus (Gpa)
1	7395.100	2.190	62.606	6.463
2	7382.300	2.290	61.580	5.624
3	7693.600	2.610	64.411	5.490
4	7687.700	2.230	62.548	5.217
5	6851.500	1.930	58.024	6.319
6	7963.200	2.760	66.887	6.872
7	7822.900	2.400	66.036	6.582
8	7660.300	2.250	64.581	6.222

9	7235.000	2.410	62.235	6.301
10	7748.800	2.180	64.051	6.731
Average	7593.200	2.416	64.048	6.222
Stdev	263.399	0.204	1.995	0.502

HVE[0,90]

Sample	Peak Load (N)	Tensile Strain (%)	Tensile Strength (Mpa)	Tensile Modulus (Gpa)
1	8278.500	2.120	67.247	6.163
2	8070.000	2.070	66.518	6.848
3	8143.000	2.170	66.927	6.553
4	8304.600	2.150	68.228	6.255
5	8081.500	1.930	65.382	6.712
6	8197.700	2.130	67.214	6.051
7	8356.300	2.110	67.989	6.381
8	8350.700	2.090	68.247	6.475
9	8449.000	2.140	68.967	6.545
10	8683.700	2.210	73.545	6.335
Average	8247.922	2.101	67.413	6.443
Stdev	132.180	0.071	1.080	0.258

HVE[S]

Sample	Peak Load (N)	Tensile Strain (%)	Tensile Strength (Mpa)	Tensile Modulus (Gpa)
1	7715.500	2.130	64.250	6.664
2	7924.200	2.360	65.772	6.366
3	7748.800	2.180	64.051	6.731
4	8022.500	2.380	65.298	6.308
5	7687.700	2.230	62.548	5.217
6	7889.900	2.210	64.402	6.052
7	7847.100	2.570	63.819	5.621

8	7951.300	2.220	64.929	6.652
9	7976.300	2.140	65.264	7.192
10	7693.600	2.610	64.411	5.490
Average	7862.589	2.269	64.482	6.311
Stdev	120.583	0.143	0.973	0.606

Flexural Strength Results

HVE[0]

Sample	Load (N)	Flexural Strain (%)	Flexural Stress (MPa)	Flexural Modulus (GPa)
1	243.000	2.720	102.649	6.082
2	236.000	3.030	108.005	6.251
3	238.000	3.010	109.013	6.323
4	251.000	2.960	106.463	5.974
5	236.000	2.860	107.097	6.268
6	244.000	3.010	109.242	6.335
7	252.000	3.150	112.352	6.363
8	241.000	2.860	107.539	6.363
9	246.000	2.990	109.405	6.340
10	254.000	3.100	112.112	6.213
Average	243.375	3.001	109.346	6.307
Stdev	6.948	0.102	1.961	0.056

HVE[90]

Sample	Load (N)	Flexural Strain (%)	Flexural Stress (MPa)	Flexural Modulus (GPa)
1	226.000	3.200	100.584	5.335
2	235.000	2.700	98.605	5.686
3	226.000	3.140	100.247	5.442
4	235.000	3.270	103.542	5.653
5	240.000	3.400	105.128	5.471
6	234.000	3.200	101.649	5.367

7	236.000	3.160	102.945	5.627
8	242.000	3.350	105.386	5.587
9	232.000	3.110	100.195	5.606
10	235.000	3.260	102.354	5.513
Average	234.000	3.232	102.448	5.511
Stdev	5.454	0.097	1.978	0.115

HVE[0,90]

Sample	Load (N)	Flexural Strain (%)	Flexural Stress (MPa)	Flexural Modulus (GPa)
1	241.000	2.840	102.827	5.800
2	251.000	2.960	106.463	5.974
3	261.000	3.220	109.698	5.897
4	254.000	3.050	107.025	5.994
5	231.000	2.610	97.744	5.827
6	241.000	2.790	101.377	5.914
7	257.000	3.190	108.471	5.958
8	243.000	2.720	102.649	6.082
9	256.000	3.060	107.767	5.930
10	235.000	2.700	98.605	5.686
Average	247.000	2.914	104.263	5.906
Stdev	10.165	0.213	4.210	0.112

HVE[S]

Sample	Load (N)	Flexural Strain (%)	Flexural Stress (MPa)	Flexural Modulus (GPa)
1	227.000	2.950	93.801	5.263
2	242.000	3.140	99.248	5.173
3	242.000	3.070	101.535	5.374
4	228.000	2.800	94.071	5.269
5	224.000	2.660	93.583	5.396

6	236.000	2.970	97.998	5.219
7	229.000	2.790	95.026	5.207
8	240.000	2.970	99.340	5.333
9	234.000	3.200	101.649	5.367
10	232.000	2.800	95.853	5.341
Average	233.333	2.906	96.717	5.286
Stdev	6.874	0.153	2.895	0.079

Impact Strength Results

HVE[0]

Test no.	Energy to failure-1 (J)	Total energy-1 (J)	Impact Strength (kJ/m2)
1	1.722	1.724	17.822
2	1.663	1.666	17.294
3	1.789	1.792	18.660
4	1.571	1.574	16.478
5	1.631	1.636	16.986
6	1.721	1.725	17.750
7	1.664	1.667	17.253
8	1.687	1.690	17.593
9	1.902	1.907	19.906
10	1.908	1.911	19.937
Average	1.726	1.729	17.968
Median	1.704	1.707	17.671
Minimum	1.571	1.574	16.478
Maximum	1.908	1.911	19.937
Std.Dev	0.111	0.111	1.177

HVE[90]

Test no	Energy to failure-1 (J)	Total energy-1 (J)	Impact Strength (kJ/m2)
1	1.485	1.740	18.160
2	1.609	1.610	16.828
3	1.581	1.585	16.482
4	1.348	1.352	14.284

5	1.469	1.471	15.524
6	1.485	1.488	15.504
7	1.476	1.479	15.396
8	1.478	1.734	17.932
9	1.273	1.502	15.652
10	1.581	1.584	16.557
Average	1.478	1.554	16.232
Median	1.482	1.543	16.067
Minimum	1.273	1.352	14.284
Maximum	1.609	1.740	18.160
Std.Dev	0.104	0.121	1.201

HVE[0,90]

Test no	Energy to failure-1 (J)	Total energy-1 (J)	Impact Strength (kJ/m2)
1	1.275	1.500	15.691
2	1.305	1.307	13.521
3	1.460	1.462	14.974
4	1.342	1.345	13.896
5	1.282	1.514	15.689
6	1.408	1.411	14.485
7	1.621	1.623	16.778
8	1.285	1.288	13.301
9	1.473	1.476	15.139
10	1.575	1.577	16.218
Average	1.402	1.450	14.969
Median	1.375	1.469	15.057
Minimum	1.275	1.288	13.301
Maximum	1.621	1.623	16.778
Std.Dev	0.126	0.112	1.163

HVE[S]

Test no	Total energy-1 (J)	Impact energy-1 (J)	Impact Strength (kJ/m2)
1	1.103	13.738	11.319
2	1.414	13.687	14.504
3	1.375	13.214	14.009
4	1.275	13.715	12.992

5	1.211	13.123	12.406
6	1.124	13.422	11.492
7	1.145	13.513	11.706
8	1.212	13.852	12.367
9	1.273	13.215	13.123
10	1.241	13.243	12.794
Average	1.237	13.472	12.671
Median	1.227	13.467	12.600
Minimum	1.103	13.123	11.319
Maximum	1.414	13.852	14.504
Std.Dev	0.102	0.265	1.043

Shear Strength Results

HVE[0]

Specimen #	Peak Load	Peak Stress	Modulus of Elasticity	Poisson's Ratio	Shear Strength
	N	MPa	MPa	mm/mm	Mpa
1	6650.000	54.740	4983.000	0.423	27.370
2	6898.000	56.380	4953.000	0.452	28.190
3	6803.000	55.530	4995.000	0.447	27.765
4	6760.000	55.240	5050.000	0.439	27.620
5	6416.000	52.290	4935.000	0.436	26.145
6	6867.000	56.160	5006.000	0.454	28.080
7	6858.000	56.000	4970.000	0.446	28.000
8	6643.000	54.360	4905.000	0.443	27.180
9	6475.000	53.130	4954.000	0.433	26.565
10	6623.000	54.930	4981.000	0.451	27.465
Mean	6699.300	54.876	4973.200	0.442	27.438
Std Dev	166.406	1.323	40.144	0.010	0.662

HVE[0,90]

Specimen #	Peak Load	Peak Stress	Modulus of Elasticity	Poisson's Ratio	Shear Strength
	N	MPa	MPa	mm/mm	Mpa
1	6901.000	56.560	5101.000	0.443	28.280
2	6760.000	55.070	4939.000	0.429	27.535
3	6788.000	55.070	5048.000	0.428	27.535

4	6896.000	55.570	4947.000	0.431	27.785
5	7097.000	57.550	5013.000	0.423	28.775
6	6753.000	54.940	5013.000	0.429	27.470
7	7038.000	57.370	5088.000	0.432	28.685
8	7051.000	57.390	5024.000	0.436	28.695
9	6963.000	56.650	5004.000	0.432	28.325
10	6913.000	56.840	5076.000	0.425	28.420
Mean	6916.000	56.301	5026.667	0.432	28.151
Std Dev	122.928	1.043	58.004	0.005	0.521